DOE/CE/40936--T2
(DE96006558)

Energy CONSERVATION

SODIUM AND SULFUR RELEASE AND RECAPTURE DURING BLACK LIQUOR BURNING

By
W.J. Frederick
K. Iisa
K. Wag
V.V. Reis
L. Boonsongsup
M. Forssen
and M. Hupa

August 1995

Work Performed Under Contract No. FG02-90CE40936

For
U.S. Department of Energy
Office of Industrial Programs
Washington, D.C.

By
Oregon State University
Corvallis, OR

DISCLAIMER

DOE/CE/40936--T2
(DE96006558)
Distribution Category UC-1400

SODIUM AND SULFUR RELEASE AND RECAPTURE DURING BLACK LIQUOR BURNING

Report for the Following Project Activities

at Oregon State University, Corvallis, Oregon, USA
"Black Liquor Combustion–Validated Recovery Boiler Modeling"
Under Contract No. DE-FG02-90CE40936

and

at Åbo Akademi University, FIN-20520, Turku, Finland
Project LIEKKI 2-24
"Release of Inorganic Constituents During Black Liquor Pyrolysis and Combustion"
co-funded by Tampella Power and the Ministry of Trade and Industry of Finland

This Project is also Part of the
Combustion and Gasification Research Program LIEKKI in Finland

Prepared by
W.J. Frederick, K. Iisa, K. Wåg, V.V. Reis, L. Boonsongsup,
M. Forssén, and M. Hupa

Prepared for
Office of Industrial Programs
Conservation and Renewable Energy
Washington, DC 20585
USA

and

Ministry of Trade and Industry
Energy Department
P.O. Box 37
FIN-00131 Helsinki
Finland

August 1995

TABLE OF CONTENTS

LIST OF FIGURES

LIST OF TABLES

I. PREFACE

The efforts toward understanding the process of black liquor combustion through steady-state process modeling have increased markedly in the past five years. An international consortium of research groups from Canada, Finland, and the U.S. are currently developing a new steady-state model for recovery boilers.

A key component of such models is a sufficiently detailed description of the in-flight combustion behavior of black liquor droplets. Previous reports by the present research groups described the overall combustion behavior including rate expressions for the duration of the three stages, drying, devolatilization and char oxidation, respectively, and a quantitative description of the onset of the pyrolysis and the concurrent rapid swelling of the burning liquor particles. (Frederick, W.J., *"Combustion processes in black liquor recovery: analysis and interpretation of combustion rate data and an engineering design model,"* U.S. DOE Report DOE/CE/40637-T8 (DE90012712), March 1990, and, Frederick, W.J., Hupa, M., *"Combustion properties of kraft black liquors,"* published simultaneously as an Åbo Akademi University, Combustion Chemistry Research Group Report 93-3, 1993, Turku, Finland, and a U.S. DOE Report DOE/CE/40936-T1.

The present report extends the previous studies to also include the fate of the key cooking chemicals, sodium and sulfur, during black liquor droplet combustion. This information is of crucial importance, when the steady state recovery furnace process models are extended to predict also the amount of fume and sulphurous gases at the exit of the furnace and in the flue gases.

The experimental studies in this report have been conducted both at the Åbo Akademi University in Turku, Finland, and at the Oregon State University in Corvallis, Oregon, USA. The study has been co-sponsored by Tampella Power Inc., the Finnish Ministry of Trade and Industry through the Combustion and Gasification Research Program LIEKKI, and the U.S. Department of Energy. Funding for travel to Finland and for the Fourier-Transform Infrared spectrometer used at OSU was provided by the National Science Foundation under NSF Award Numbers INT-9200224 and CTS-9213028, respectively.

Many people have contributed to the success of this project. Jarkko Nurmi and Chris Verrill helped in designing and building the experimental system at Åbo Akademi University and Kirsi Laaksonen in obtaining the experimental data. Rainer Backman at Åbo Akademi University gave a number of useful comments on sodium and sulfur chemistry issues. Scott Sinquefield designed and built the laminar entrained-flow reactor used in the work at Oregon State University. Paavo Hyöty, Kauko Janka, Jussi Mäntyniemi, and Pekka Siiskonen, all with Tampella Power Inc., provided valuable input during planning the program and interpreting the data.

This report is simultaneously published as an Åbo Akademi University Report in Finland and as a U.S. Department of Energy Report in the United States.

Corvallis - Turku, August 1995

The authors

II. EXECUTIVE SUMMARY

The release of sodium and sulfur during black liquor burning play a key role in the fouling and plugging of heat transfer surfaces and gas passages, and in emissions of sulfur gases and particulates from recovery boilers. In 1990, a project was begun, under the sponsorship of Tampella Power Inc. and the U.S. Department of Energy, to investigate the processes by which sodium and sulfur are volatilized during black liquor burning, and by which sulfur gases are recaptured by fume and carry-over particles, and deposits. Most of this work was carried out at the Combustion Chemistry Laboratory, Åbo Akademi University, in Turku, Finland.

One objective of the work reported here was to provide experimental data on sulfur and sodium volatilization during black liquor burning, and on SO_2 capture by solid Na_2CO_3 and NaCl. A second was to interpret the data, and to put it into the form of rate models which could be used in computational models for recovery boilers.

The specific topics to be investigated were

- sodium release from black liquor droplets during the devolatilization and char burning stages,
- sulfur release during pyrolysis of single black liquor droplets,
- sulfur release during char burning,
- SO_2 capture by solid Na_2CO_3 at kraft recovery boiler conditions, and
- sulfation of solid NaCl at combustion conditions.

The results of the experimental investigations of these three areas are presented in Sections IV.B - IV.E of this report. A separate subsection that contains a rate model for each of these processes is also included.

II.A SUMMARY OF KEY RESULTS

II.A.1 Sodium Release

Significant quantities of sodium are volatilized during burning of black liquor droplets and char. Sodium release occurs during black liquor burning occurs during all of the final three stages of burning: devolatilization, char combustion, and smelt reactions. The data from this and other studies indicate that during devolatilization, relatively little sodium is volatilized as vapor species (e.g., Na, NaCl) while most of the sodium is released as small ($\approx$ 10-100 μm) liquor or char fragments that are shed or ejected from the larger droplets. Additional work is needed to clarify the mechanisms of sodium species vapor and small particle release.

During char burning and gasification, sodium release is primarily the result of the reduction of Na_2CO_3 with carbon, producing elemental sodium. The reaction is extremely temperature dependent and only occurs to a significant extent above 800°C at the conditions encountered in recovery boilers. For black liquor droplets of the size fired in recovery boilers, both chemical kinetics and film mass transfer are important in determining the overall rate of sodium release by this mechanism. At high temperatures, film mass transfer apparently limits the overall rate of sodium volatilization, accounting for the lower temperature sensitivity of sodium volatilization observed in recovery boilers.

Sodium volatilization during char burning both in flight and on the char bed accounts for most of the sub-micron sodium fume formed during black liquor combustion.

II.A.2 Sulfur Release During Pyrolysis of Single Black Liquor Droplets

Sulfur release is a decomposition reaction that starts when decomposition of the organic fraction of black liquor begins. The rate is dependent on the temperature of the furnace in which the droplets are devolatilized. It is not greatly affected by the initial droplet mass in the range studied (10-70 mg).

The rate of sulfur release is influenced by both chemical kinetics and the rate of heat transfer to the black liquor droplet. Heat transfer becomes more important as temperature increases, and dominates above 700°C. In most regions of a recovery boiler, therefore, the rate of sulfur release will be controlled by the rate of heat transfer.

The amount of sulfur released during pyrolysis has been shown earlier to go through a maximum with furnace temperature. Our data indicates that the amount released is not strongly dependent on initial droplet size. The maximum in release rate with furnace temperature can be explained qualitatively in terms of competing release and recapture mechanisms. However, this concept remains to be tested quantitatively.

An empirical model for predicting the rate and total amount of sulfur released during devolatilization of black liquor droplets has been developed based on experimental data from this and other studies. In this model, the rate of sulfur release is proportional to the rate of carbon release, while the total amount of sulfur released is a fraction of the total sulfur in black liquor and depends only on furnace temperature.

II.A.3 Sulfur Release During Char Burning

Less sulfur is volatilized during char burning than during devolatilization, but the amount volatilized from char can still be significant. The mechanism of sulfur release during char burning is the reaction Na_2S with CO_2 and water vapor to form H_2S and COS. When water vapor is present, the rate of H_2S formation is much faster than that of COS. Under conditions

of interest in recovery boilers, H_2S formation during char burning is much more important than COS formation.

H_2S and COS formation are both strongly affected by chemical equilibrium. The equilibria for both reactions favor more sulfur release at lower furnace temperatures and less at high temperatures. At conditions typical in recovery boilers, conversion of char sulfur to gases would not be complete but would be greater in colder regions. By contrast, in low temperature gasification of black liquor, all of the Na_2S in the char may be converted to H_2S.

The rate of conversion of char sulfur to gases is controlled by both equilibrium and mass transport effects at temperatures of interest in recovery boilers. The reactions of Na_2S with water vapor and CO_2 are rapid, and within a char particle, H_2S and COS are at their equilibrium partial pressures. Because the equilibria increasingly favor Na_2S rather than H_2S and COS as furnace temperature increases, the partial pressure of these gases within the char particle decreases as temperature increases. For a given H_2S or COS partial pressure within the particle, the overall rate of sulfur gas release is then dependent on the rate at which it diffuses from the particle and is transported away from it.

The rate of H_2S release is also apparently influenced by the rate of sulfate reduction as well as reactions of H_2S with other gas species, forming, e.g., SO_2 or CS_2. Sulfate reduction is slow relative to H_2S formation and can limit the availability of Na_2S, thereby limiting the rate of H_2S production. Reactions of H_2S with other gas species can increase the H_2S concentration gradient, thereby increasing the rate of transport of H_2S and the overall rate of sulfur release. Further work is needed to confirm and quantify these effects.

II.A.4 SO_2 Capture by Solid Na_2CO_3 at Kraft Recovery Boiler Conditions

The reaction of SO_2 with Na_2CO_3 is important in the capture of sulfur gases in black liquor combustion. Published data on the sulfation of solid Na_2CO_3 are available but no data were found on the reactions of molten Na_2CO_3 with SO_2. The data for sulfation of solid Na_2CO_3 were fitted with appropriate gas-solid reaction models. The rate of sulfation of Na_2CO_3 is mainly controlled by intraparticle diffusion in the temperature range 120-700°C and the diffusion process is probably solid-state diffusion. Based on the intraparticle diffusion rate, the residence time of solid fume particles in a recovery furnace is too short for any substantial sulfation to take place. Thus almost all of the sulfation of Na_2CO_3 has to take place in the molten phase.

The rates of sulfation of both Na_2CO_3 and NaCl in solid particles is too slow at conditions in the boiler and generator banks to account for significant SO_2 capture. This implies that nearly all of the sulfation of fume particles in recovery boilers occurs as reactions in the gas phase or before the particles solidify. This conclusion is supported by experimental data obtained from operating recovery boiler. The rates are fast enough, however, to account for significant sulfation of Na_2CO_3 and NaCl in boiler tube deposits.

II.A.5 Sulfation of Solid NaCl at Combustion Conditions

The sulfation of NaCl was studied in a fixed bed reactor in the temperature range 400-600°C where NaCl, Na_2SO_4, and their mixtures are solids. Under the experimental conditions employed, diffusion and mass transfer did not influence the overall rate and true kinetic data were obtained. The rate of sulfation of NaCl was very slow for solid NaCl, with only 0.5-1.0% of the NaCl converted to HCl in three hours at the experimental conditions employed. The rate was not strongly temperature dependent, with an activation energy of 17.3 kJ/mol. The rate of reaction depends on the partial pressure of SO_2 but not in the partial pressure of O_2 and H_2O for the range of conditions of $0.3\% < P_{SO2} < 1.1\%$, $3\% < P_{O2} < 11\%$, $0.5\% < P_{H2O} < 20\%$ and $400°C < T < 600°C$. The adsorption of SO_2 (g) on the surface of NaCl was determined to be the rate limiting step of this reaction.

The rate of sulfation of NaCl in solid particles is too slow at conditions in the boiler and generator banks to account for significant SO_2 capture and HCl release in that part of the boiler. The rate is fast enough, however, to account for significant sulfation of NaCl in boiler tube deposits.

III. INTRODUCTION

Black liquors contain much more alkali metal salts than any other fuel, typically 17-22% Na and 0.5-2% K, and their sulfur content is higher than many high sulfur coals. Part of these elements are volatilized during combustion, forming fume and contributing to fouling of heat transfer surfaces, plugging of gas passages, corrosion, and emissions of particulates and acid gases. The reactions between sulfur and sodium compounds provide an important trap for sulfur gases which results in their recycle within the process.

Neither the mechanism of fume formation in kraft recovery boilers nor the relative amounts formed during the various stages of black liquor combustion are well understood. A critical observation regarding the fume content of the gases in recovery boilers is its relatively low sensitivity to temperature. This lack of temperature sensitivity is not consistent with any of the mechanisms previously proposed for fume formation. Nearly all of the previous experimental work on fume formation has focused on sodium release from smelt or during char burning. There has been relatively little consideration given to sodium release during devolatilization of black liquor prior to char combustion.

Sulfur release from black liquor during pyrolysis has been studied more extensively by several research groups using a variety of different experimental methods. While the information on sulfur release during black liquor pyrolysis and is extensive, it is not adequate for modeling of sulfur release during black liquor droplet combustion or gasification. Also, although much of the sulfur release during black liquor combustion or gasification occurs during devolatilization sulfur release continues to occur from char during char burning, gasification, and even during heating in non-reactive gases.

Capture of sulfur gases by sodium salts, forming Na_2SO_4 in fume, carry-over particles, and deposits, is very important in the operation of recovery boilers. Limited data is available on the capture of SO_2 by solid Na_2CO_3 or NaCl, and no data is available on reactions in the molten or vapor phase.

In 1990, a project was begun, under the sponsorship of Tampella Power Inc. and the U.S. Department of Energy, to investigate the processes by which sodium and sulfur are volatilized during black liquor burning, and by which sulfur gases are recaptured by fume and carry-over particles, and deposits. One of the main objectives of this work were to provide a fundamental understanding of the processes of sodium and sulfur volatilization during black liquor burning, and to begin to understand the recapture mechanisms for the sulfur gases produced. The other main objective was to develop rate models for these processes that could be used in the on-going work on modeling of recovery boilers. Most of this work was carried out at the Combustion Chemistry Laboratory, Åbo Akademi University in Turku, Finland. Additional work on sodium volatilization and SO_2-NaCl reactions was carried out at Oregon State University.

A variety of experimental procedures were used in the various studies that were conducted as part of this project. They are described in Sections IV.A and V.A of this report. The results

of the experimental work and interpretation of the data are presented in Sections IV.B, IV.C, V.B, and V.C. The computational models developed are presented in Sections IV.D and V.D.

IV.A EXPERIMENTAL METHODS

IV.A.1 Single Droplet Techniques

Pyrolysis, gasification, and combustion experiments were performed at Åbo Akademi University with single black liquor droplets in two different experimental apparatuses. The apparatuses are referred to as the single droplet/stagnant-gas reactor (SD/S reactor) and the single droplet/flow reactor (SD/F reactor). The equipment and experimental procedures are described as follows.

Experiments in the Single Droplet/Stagnant Gas (SD/S Reactor)

Combustion experiments were conducted by suspending single droplets of spent pulping liquors in a stagnant gas within laboratory muffle furnaces (Figure IV.A-1), using a method developed earlier by Hupa and co-workers (Hupa et al., 1987; Noopila and Hupa, 1988). The furnace per se was placed in an enclosure, and a gas mixture of controlled composition flowed through the enclosure to isolate the furnace from the ambient environment. The thermal event for each droplet was recorded using a video camera. The elapsed times for each combustion stage were read from the video recordings. Droplet dimension versus time data were also obtained from the recordings.

The gas mixing system, not shown in Figure IV.A.1-1, consisted of rotameters for N_2, O_2, CO_2 and CO to obtain a desired gas composition. Water vapor was added to the dry gases through a vaporizator connected to a rotameter calibrated for water flow rate. The vaporizer consisted of a stainless steel tube wrapped with a heating element. The tube was filled with small copper pieces to achieve a high heating area. The vaporizer was heated to 200°C. The vapors produced are immediately mixed with the gas mixture that is preheated to 150-200°C. Water vapor contents as high as 33% (wet gas basis) were used in the experiments.

The gas mixture was fed into an isolation chamber in which the muffle furnace was enclosed. The container was preheated (~150°C) when mixtures with water vapor was used. Prior to insertion of droplets into the furnace, the gas mixture also flowed into the furnace cavity per se through a small port low in the rear wall, but that part of the gas flow was diverted to the isolation chamber during the droplet burning events. The feed of the gas mixtures into the isolation chamber was started 30 minutes before experiments were performed, and a flow rate of 200 l/h was fed into the approx 0.1 m^3 container. A vent on the top of the container led the exhaust gases to the vent duct.

A specially designed nitrogen purge chamber was placed on top of the furnace/isolation chamber at the insertion point of the droplet. The purge chamber allowed the droplets to be cooled in a non-oxidizing environment as they were removed from the furnace per se.

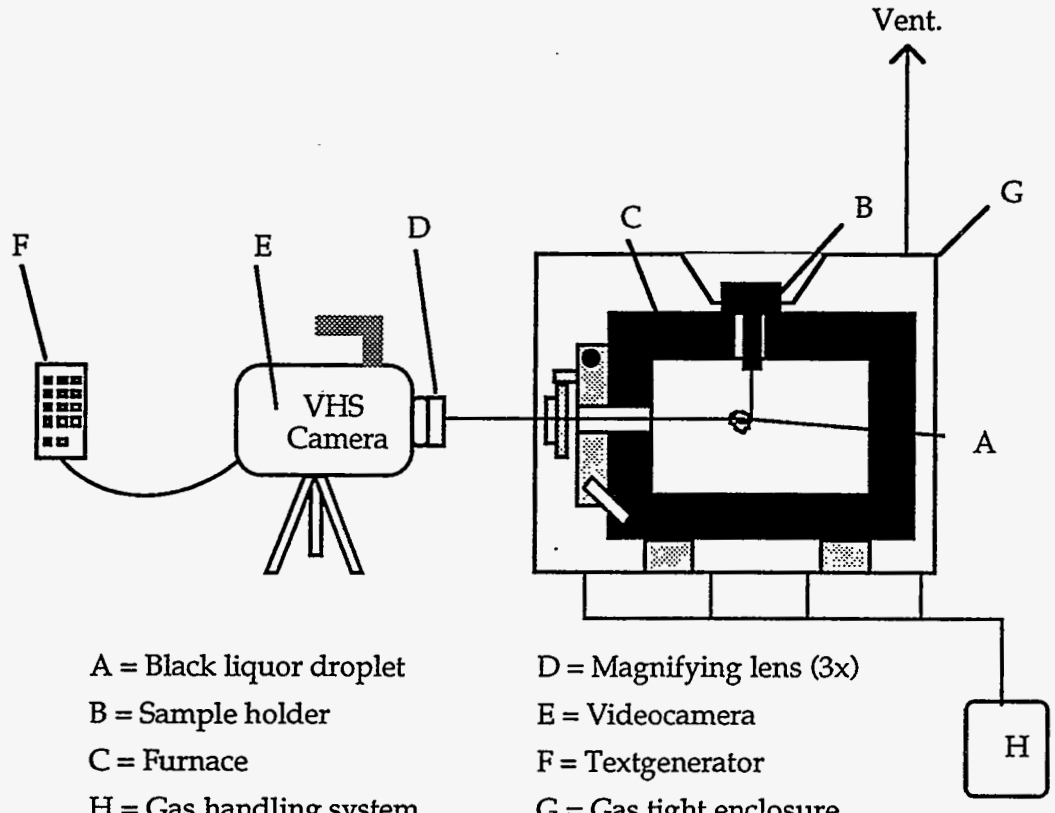

Figure IV.A.1-1. Diagram of the Åbo Akademi single droplet/stagnant gas reactor.

In the experiments, droplets of black liquor at solids contents of 60% or greater and weighing 5-20 mg were suspended on a platinum hook and weighed, lowered into the furnace through a hole on the top and allowed to remain in the furnace for the desired time. The pyrolyzed droplets were then removed and cooled in the nitrogen purge chamber at the exit to the furnace, weighed, and analyzed for sulfur, carbon and sodium content.

The experiments were conducted at furnace temperatures of 700-1000°C with 14 different liquors. The dry solids content and elemental analysis of the liquors are given in Table IV.A.1-1. Gas mixtures containing CO, CO_2, O_2 or H_2O in N_2 were used. All experiments conducted are listed in Appendix _____.

Table IV.A.1-1. Elemental analysis of black liquors used in this work

Liquor	Dry Solids (DS)	Na % of DS	S % of DS	C % of DS	Liquor Type
A	76.10% (82.30%)	19.1%	6.4%	31.4%	Pine/birch
B	74.20%	19.7%	6.5%	33.0%	Pine kraft (virgin)
C	78.60%	21.6%	8.5%	27.3%	(as fired)
D	76.40%	19.2%	6.5%	31.2%	Pine kraft
E	67.70%	18.9%	9.7%	30.1%	Pine kraft
F	64.40%	19.6%	4.6%	35.8%	Pine kraft
G	68.90%	19.0%	4.9%	35.4%	Pine kraft
H	60.00%	21.7%	3.3%	41.7%	Birch kraft

Experiments in the Single Droplet/Flow (SD/F Reactor)

The single droplet/flow (SD/F) reactor consisted of a gas preheater, a pyrolysis reactor, oxidizer, gas sampling pump, SO_2 and CO_2 analyzers (all shown in Figure IV.A.1-2) and a computer for data collection.

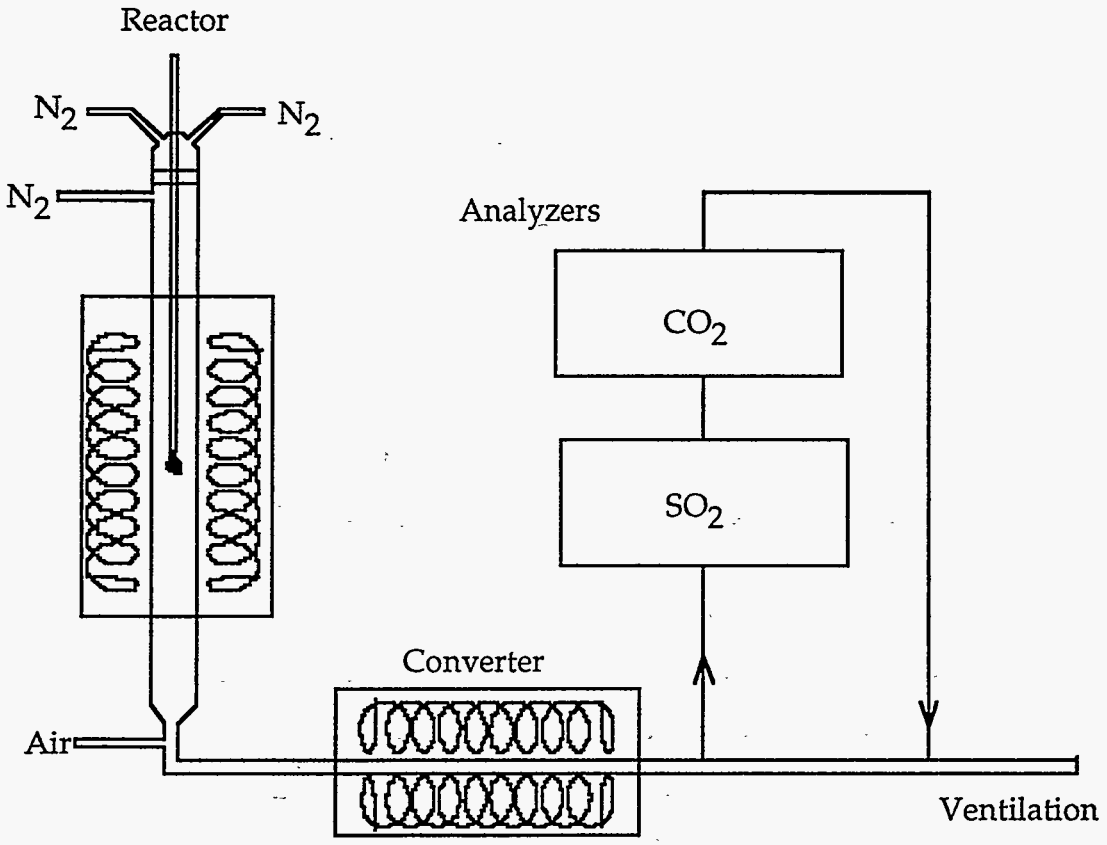

Figure IV.A.1-2. Diagram of the Åbo Akademi single droplet/flow reactor.

Droplets of black liquor were pyrolyzed/pyrolyzed and gasified in the reactor. The quartz reactor was purged with desired gas composition and in that way isolated from the ambient gas environment. The gas mixture leaving the pyrolysis zone was mixed with air downstream of the tube furnace. The mixture then passed through an oxidizer where the sulfur and carbon gases were converted to SO_2 and CO_2, respectively. SO_2 and CO_2 where analyzed with gas UV and IR analyzers. The char was lifted up in a nitrogen purge, weighed and analyzed for sodium, sulfur and carbon.

The droplet reactor consists of a quartz tube, 25 mm in diameter, in a tube furnace. There were two gas inlets at the top of the reactor as shown in Figure IV.A.1-2. The inlet highest up is used for purging and cooling the black liquor droplet before insertion, and the char after the experiment. The second inlet below that is used for feeding the gas, of the composition used in the experiments and preheated to 200°C, into the reactor. The temperature of the furnace was controlled in the experiments between 350°C and 1050°C. A typical temperature profile with a gas flow of 200 l/h through the reactor, measured with a thermocouple inserted into the quartz reactor is shown in Figure IV.A.1-3.

Steady-State Particle Temperature Estimation

To estimate the steady-state temperature of black liquor particles suspended in the hot furnace, we assumed that the gas was completely heated to 200°C before entering the actual reactor. The volume flow increased from 200 to 317 l/h upon preheating. The length of the duct is actually longer than 0.45 m furnace length, and this was taken into consideration in estimating the gas temperature at the particle elevation.

Three different Nusselt number correlations were tested.

1. Fully developed laminar flow in long ducts
2. Laminar flow in short ducts
3. Laminar flow in intermediate ducts

The calculations were made assuming using the following parameters:

- distance from gas entry to particle: 0.45 m
- particle diameter: 2 cm
- Pr = 0.7
- inlet gas temperature: 200°C

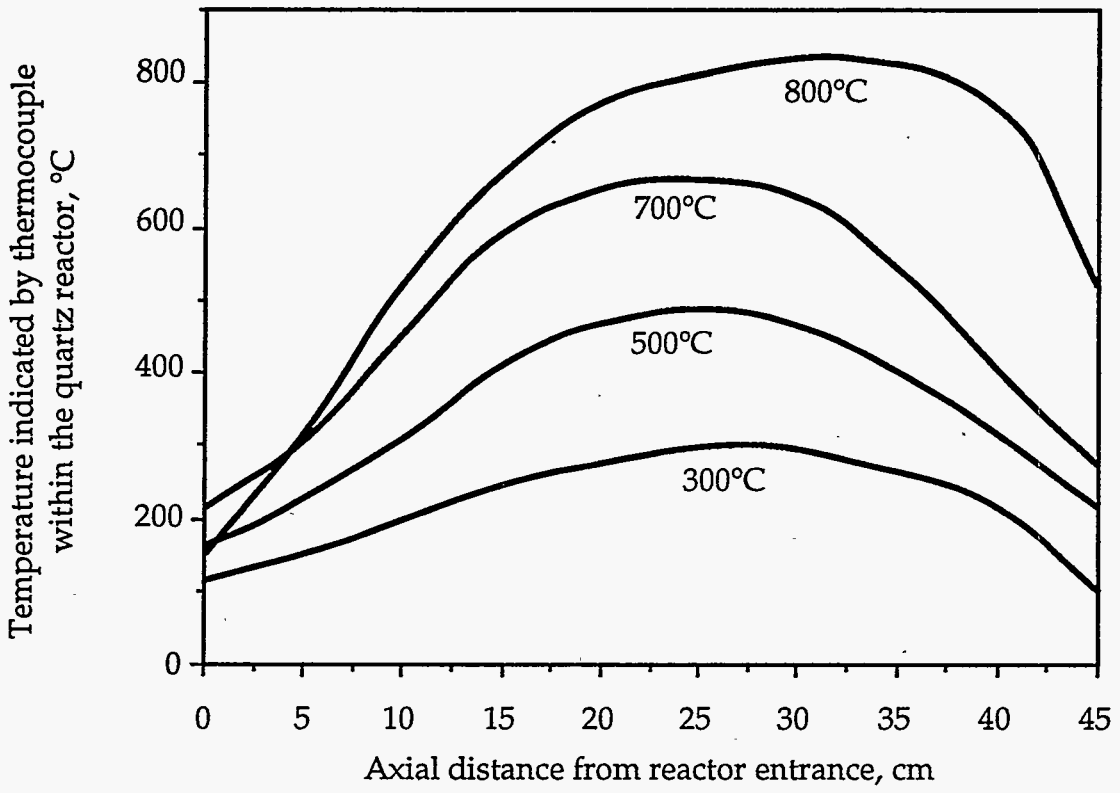

Figure IV.A.1-3. Temperature within reactor versus axial distance from the reactor entrance as measured by a bare wire thermocouple at the furnace temperature settings indicated. The gas temperature entering the reactor during these measurements was 200°C.

- actual volumetric flow rate = 317 l/h,
- mass fraction inorganic in char particle: 0.5

For fully developed laminar flow the following equation applies:

$$Nu = 3.66 \left[\frac{T}{T_{wall}} \right]^{0.25}$$

This equation accounts for the property variations for a gas heated in a tube. The results for fully developed laminar flow are given in Table IV.A.1-2.

Table IV.A.1-2. Estimated particle temperature for fully developed flow

Furnace temperature, °C	T_{gas}, °C	T_{part}, °C	$T_{furnace}$-T_{part}
700	601.0	659.3	40.7
800	685.4	761.3	38.7
900	770.6	864.0	36.0
1000	856.5	967.1	32.9

The Hausen equation applies for laminar flow in short ducts.

$$Nu = 3.66 + \frac{0.0668\, Re\, Pr\, D/L}{1 + 0.045\, (Re\, Pr\, D/L)^{0.66}} \left[\frac{\mu_{bulk}}{\mu_{wall}} \right]^{0.14}$$

when $100 < (Re\ Pr\ D/L) < 1500$

For this case the deviation from the region of validity was large. The results for laminar flow in short ducts are given in Table IV.A.1-3.

Table IV.A.1-3. Estimated particle temperature for laminar flow in short ducts

Furnace temperature, °C	T_{gas}, °C	T_{part}, °C	$T_{furnace}$-T_{part}
700	613.2	664.5	35.5
800	699.7	766.3	33.7
900	786.9	868.7	31.3
1000	874.7	971.4	28.6

The following equation for ducts of intermediate lengths is given by Sieder and Tate:

$$Nu = 1.86 \times \left[\frac{Re\,Pr\,D}{L}\right]^{0.33} \left[\frac{\mu_{bulk}}{\mu_{wall}}\right]^{0.14}$$

when $(Re\ Pr\ D/L)^{0.33}\ (\mu_{bulk}/\mu m_{wall})^{0.14} > 2$ and $0.0044 < (\mu_{bulk}/\mu_{wall})^{0.14} < 9.75$ and $0.48 < Pr < 16700$.

These conditions were met except for the first, which was about 1.5. The results for laminar flow in intermediate length ducts are given in Table IV.A.1-4.

Table IV.A.1-4. Estimated particle temperature for laminar flow in intermediate length ducts

Furnace temperature, °C	T_{gas}, °C	T_{part}, °C	$T_{furnace}$-T_{part}
700	559.3	640.8	59.2
800	633.9	742.5	57.5
900	709.1	845.7	54.3
1000	784.9	949.7	50.3

The gas temperature profile calculation was done with a FORTRAN program using the Runge-Kutta method for solving the differential heat transfer equation. Three different Nusselt number equations were tested. 100% N_2 was assumed and curve fits were made for viscosity, heat capacity, and thermal conductivity data for the entire temperature range of interest. The calculated gas temperature at the sample elevation are given in the previous tables. The FORTRAN program is given in Appendix 1.

The particle temperature calculation was done with the TK Solver program given in Appendix 2. The calculations shown were done for a gas mixture containing 10% CO_2, 5% H_2O, and 85% N_2. The effect of gas composition was tested. The difference in the calculated temperatures were negligible when water vapor was also included. The calculations were sensitive to the apparent thermal conductivity of the droplet.

The results from the work with Nusselt number equations show that the flow is close to fully developed and that the gas temperature is roughly 100-200 degrees lower at the sample elevation of the fixed-bed flow reactor. Consequently, the particle temperature is estimated to be 30-40 degrees below the furnace temperature, with smaller differences at higher furnace temperatures.

Thermocouple temperature calculation

To validate the droplet temperature calculation procedure, we also calculated the temperature of a bare wire thermocouple inserted at the same position as the droplet in the reactor tube. A modification of Ranz and Marshall's Nusselt equation for spheres was used in the thermocouple temperature calculation:

$$Nu = 2 + \left(0.4\,Re^{1/2} + 0.06\,Re^{2/3}\right) Pr^{0.4} \left[\frac{\mu_{bulk}}{\mu_{surface}}\right]^{1/4}$$

A 1 cm length of the tip of the thermocouple was considered. The area for this part of the thermocouple was calculated. Using this area the equivalent diameter of a sphere with the same volume was calculated as 2.7 mm.

Depending on if the thermocouple is oxidized or polished and whether it is in an inert or reacting atmosphere, the value can vary between 0.7 to 0.95. A grey body emissivity of 0.85 at 700 and 800°C was recommended by the Omega Company, and this value was used at all temperatures. The thermocouple temperature calculation program is given in Appendix 3.

The results for gases preheated to 200°C before entering the reactor are given in the Table IV.A.1-5.

Table IV.A.1-5. Estimated thermocouple temperatures for preheated and non-preheated gas entering the reactor

D = 2.7 mm	200 l/h		317 l/h	
	25°C inlet	ε = 0.85	200°C inlet	ε = 0.85
$Tf_{ur,}$ .C	T_{gas}, °C	T_{fur}-T_{tc}	T_{gas}, °C	T_{fur}-T_{tc}
300	223.5	49.7	269.4	19.6
500	384.7	53.8	412.3	40.7
700	553.1	47.4	559.3	45.4
800	638.9	43.2	633.9	44.6

It was observed that the results were more sensitive to the diameter of the sphere than the emissivity, i.e. the bigger the sphere, the lower the temperature difference. The calculated thermocouple temperatures at 20 cm into the reactor agree very well with the experimental data at all reactor temperatures (see Figure IV.A.1-4).

Gases were fed into the quartz reactor through a gas mixing and preheating system. The gas mixing consisted of rotameters for N_2, O_2, CO_2 and CO to mix a desired gas composition. H_2O was fed into the gases through a vaporizator connected to a rotameter calibrated for water. The vaporizator consists of a stainless steel tube wrapped with a heating element. The tube is filled with copper pieces to achieve a high heating area. The vaporizer was heated to 200°C. The vapors produced are immediately mixed with the gas mixture, preheated to 200°C and led into the top of the reactor. H_2O contents of 33% where the highest used in the experiments. A nitrogen purge was fed to the top part of the quartz reactor. The flow rate through the reactor was kept at approximately 400 l/h (20°C) in all experiments of which the purge was 60 l/h.

The gases exiting the bottom of the quartz droplet reactor were fed to the oxidizer which consisted of a quartz tube 60 cm long and 13 mm in diameter located within a second tube furnace. Air was premixed with the gases from the droplet reactor just upstream of the oxidizer. The air input rate to the oxidizer was 30 l/h. This input rate was chosen to provide approximately 1.5% O_2 in oxidizer. The temperature of the oxidizer was kept at 800°C. Conditions were selected to yield at least 90% conversion to SO_2 and to minimize further oxidation of SO_2 to SO_3 which would not be detected by the SO_2 analyzer.

From the oxidizer a gas sample was pumped continuously to a UV-visible SO_2 analyzer and a CO_2 analyzer connected in series. The humidity and impurities in the gases were removed by a gas handling system where the gases were cooled to 4°C and pumped through a 5 μm fiberglass filter.

The SO_2 analyzer was a Leybold UV-visible analyzer operating at 200 nm. It had two detection ranges, 0-100 ppm SO_2 and 0-1000 ppm SO_2.

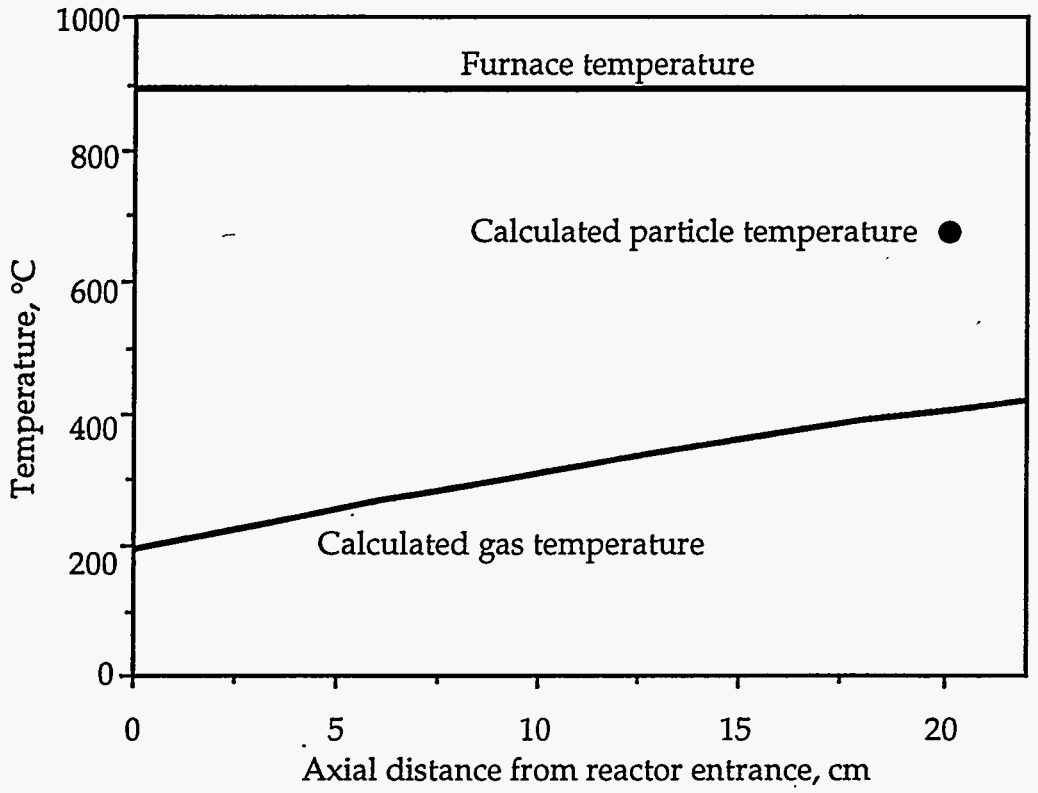

Figure IV.A.1-4. Measured (small symbols) and calculated (large symbols) temperatures indicated by a bare wire thermocouple inserted into the single droplet/flow reactor.

The CO_2 analyzer was a Hartmann-Brown infrared analyzer. It could detect CO_2 concentrations to 200 ppm.

The signals from the analyzers were recorded by a Mikro Mikko 4m 326 computer with a Data Translation data acquisition card. A program in Quick Basic was written to read data from the data acquisition card.

In each experiment, a single droplet of black liquor was inserted on the end of a hook into the down-flowing gas from a port in the top of the reactor. The droplet was held at about 0.4 m below the point of introduction. The gas mixture leaving the pyrolysis zone was mixed with air downstream of the tube furnace. The mixture, containing about 1.5% O_2, then passed through an oxidizer where the sulfur gases were converted to SO_2 at 800°C. From the oxidizer a sample was pumped continuously to a UV-visible SO_2 analyzer and a CO_2 analyzer and the output signals were recorded by computer. The SO_2 versus time curves were integrated numerically to determine the total sulfur released.

The droplets used in the experiments were formed outside the reactor, weighed, and inserted into the reactor through a port at the top on a quartz glass rod. All droplets were prepared from black liquors at least 60% dry solids content. The insertion of the glass rod was not totally gas tight. However, the leakage of gases was in outward direction, thus preventing air from entering the reactor. The range of droplet sizes used was 10-70 mg initial mass (wet basis) which corresponds to initial diameters of 2.3-4.5 mm.

Black Liquors Used

Black liquors used in these experiments were from Finnish pulp mills. They were analyzed for dry solids, carbon, sodium, sulfur, and sulfur species. The data for each liquor is included in Tables IV.A.1.1. and IV.A.1.6. The black liquors with code names B and C were obtained from the same mill at approximately the same time. Liquor B was obtained as "virgin liquor" (concentrator product) and liquor C was the corresponding "as fired" liquor to which the precipitator and ash hopper dust has been added. Mass balance calculations for the different species (carbon, sulfur and sodium) indicate that approximately 14.6% of liquor C is precipitator dust.

Analysis Procedures

Dry solids measurement were made at Åbo Akademi University with Tappi standard methods. Elemental analysis of the black liquors were performed by Analytische Laboratorien, Gummersbach, Germany. The following procedures were used (see Appendix IV.B for more details).

Table IV.A.1-6. Distribution of sulfur species for liquor E used in this study

Specie	% of black liquor solids		% of total sulfur
	as specie	as sulfur	
Sulfide (S^{2-})	0.70	0.70	10.7
Sulfate (SO_4^{2-})	0.93	0.31	4.7
Thiosulfate ($S_2O_3^{2-}$)	4.10	2.34	35.7
Sulfite (SO_3^{2-})	2.17	0.87	13.2
Organic sulfur (S)[1]	2.34	2.34	35.7
Total sulfur		6.56	

[1]by difference

Dry solids: Tappi test method T650 om-89. Weighing of sample in a glass jar together with quartz sand, dilution to ~40% with distilled water. Drying in 105°C for 12 h (until dry). Dry solids calculated as weight difference.

Carbon: Method "Carhomat 12 ADG" by Fa.Wösthoff oHG, Bochum was used. The sample was combusted in oxygen at 1350°C. The combustion gases were absorbed in a sodium hydroxide solution. The change in the electrical conductivity was measured and converted ted to amount of carbon from a calibration curve.

Sulfur: Method "Sulmhomat 12 ADG" by Fa.Wösthoff oHG, Bochum was used. The sample was combusted in oxygen at 1350°C, V_2O_5 was added to catalyze the oxidation. The gases were passed through a weak sulfuric acid solution with H_2O_2 added. The change in the electrical conductivity was measured and converted ted to amount of sulfur from a calibration curve.

Sodium: Extracted in sulfuric/phosphoric acid solution, detected with flame photometry, DIN 51729.

Reproducibility of Experimental Results

Figures IV.A.1-5 – IV.A.1-8 show the reproducibility of droplet burning runs made at various conditions in the Åbo Akademi single particle reactors. The char yields in the single particle/flow reactor were very reproducible, with the range of variations less than 5% (with one exception) of the initial black liquor solids mass (Figures IV.A.1-5 – IV.A.1-7). Char yield in the single particle/stagnant gas reactor were lower and varied by about twice as much. The sodium retained in the char varied more (Figure IV.A.1-7), over a range of 20% of the Na in the black liquor for seven replicate samples.

Figure IV.A.1-8 shows the reproducibility obtained for char residue, carbon, sulfur, and sodium on sets of experiments run on separate days. Each data point shown represents the average of eight measurements. The reproducibility is very good on these data sets, with less than 5% difference between the averages for each data pair.

The data on which Figures IV.A.1-5 – IV.A.1-8 are based are included in Tables IV.A.1-7 – IV.A.1-10.

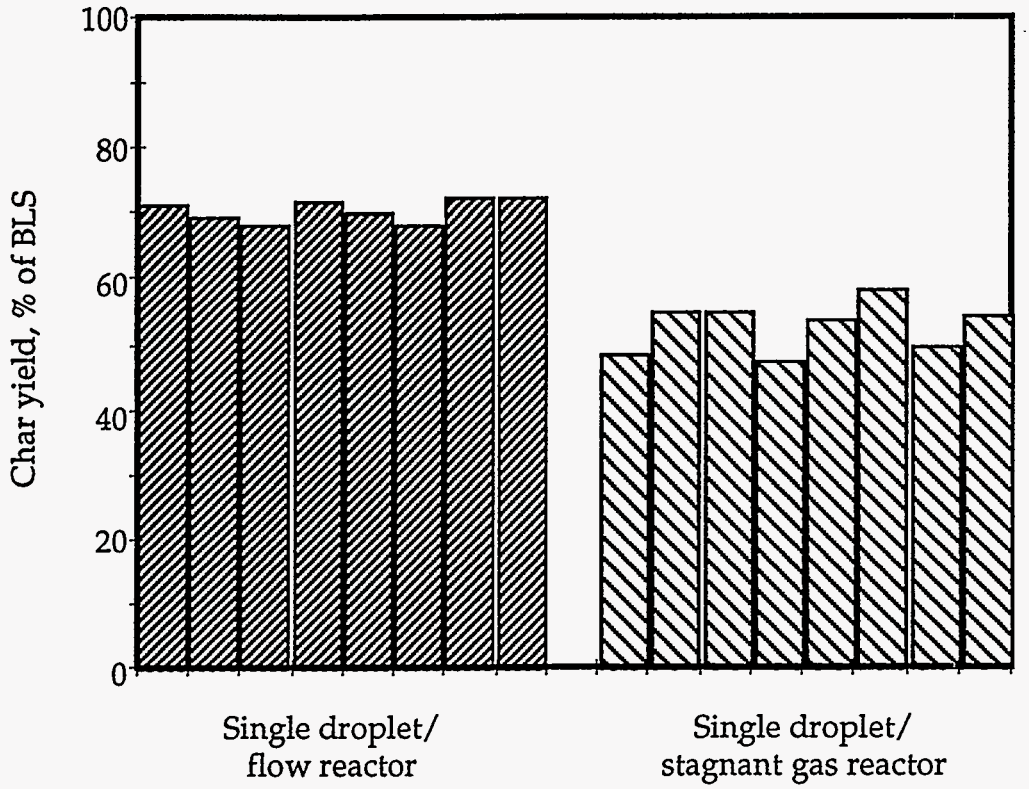

Figure IV.A.1-5. Reproducibility of char yields for liquor A after 15 seconds exposure to a 5% CO, 95% N_2 atmosphere in a 900°C furnace. Data are for replicate samples in each of the Åbo Akademi single particle reactors.

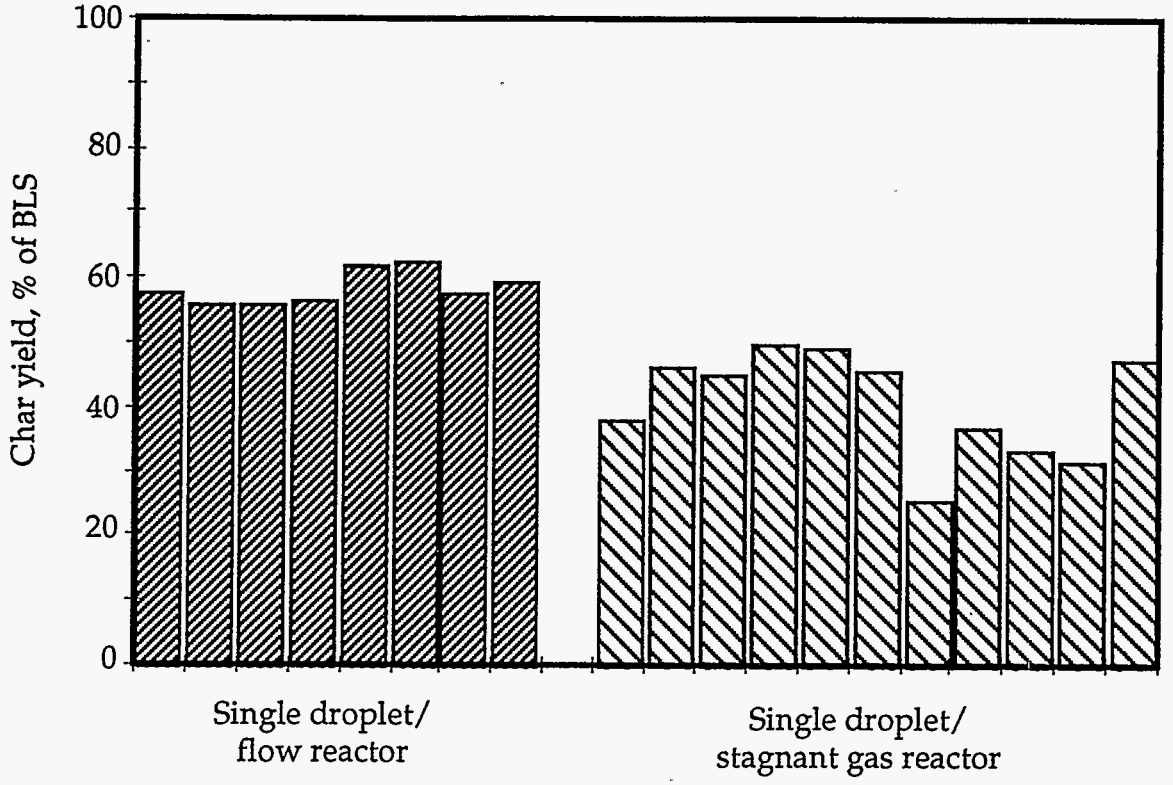

Figure IV.A.1-6. Reproducibility of char yields for liquor A after 15 seconds exposure to a 10% CO_2, 10% CO, 10% water vapor, 70% N_2 atmosphere in a 900°C furnace. Data are for replicate samples in each of the Åbo Akademi single particle reactors.

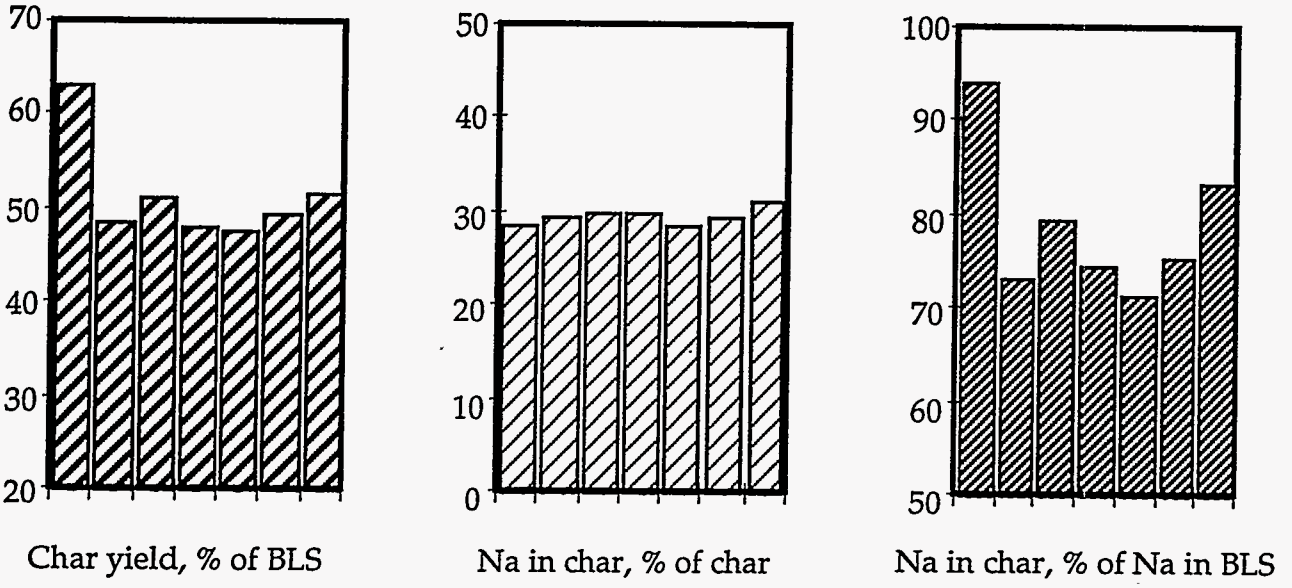

Figure IV.A.1-7. Reproducibility of char and sodium yields for liquor D after 8 seconds exposure to a 5% CO_2, 95% N_2 atmosphere in a 750°C furnace. Data are for replicate samples in the Åbo Akademi single particle/flow reactor.

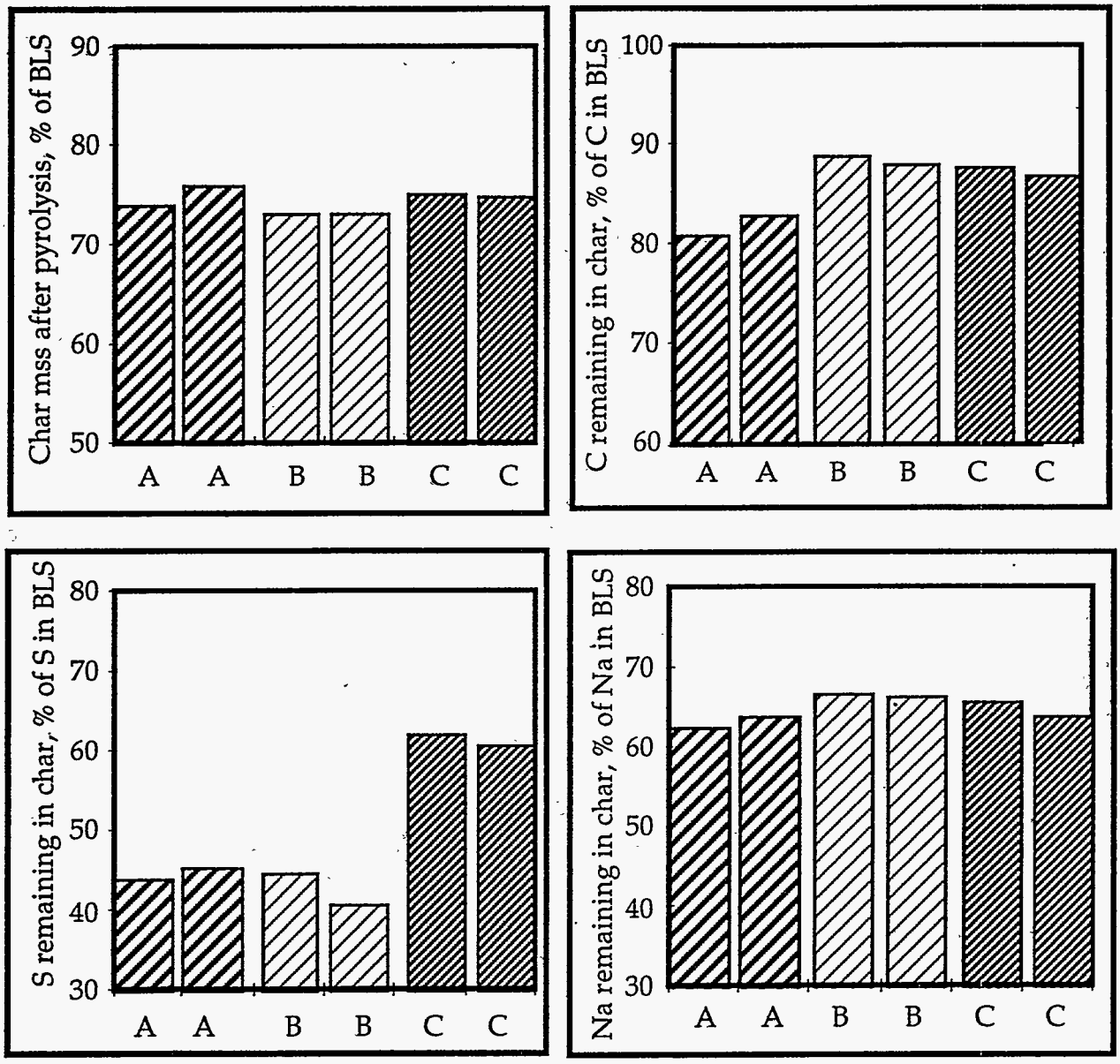

Figure IV.A.1-8. Comparison of replicate char, carbon, sulfur, and sodium yields for three different liquors. Conditions were pyrolysis in nitrogen on separate days for each sample of each liquor. Data are for replicate samples in the Åbo Akademi single particle/flow reactor.

Table IV.A.1-7. Reproducibility of char yields for liquor A after 15 seconds exposure to a 5% CO, 95% N_2 atmosphere in a 900°C furnace. Data are for replicate samples in each of the Åbo Akademi single particle reactors.

Sample	Single Particle/ Flow Reactor	Single Particle/ Stagnant Gas Reactor
1	71.3	48.3
2	69.6	55.0
3	68.3	55.2
4	72.0	47.5
5	70.4	53.5
6	68.6	58.2
7	72.5	49.5
8	72.5	54.6
Average	70.7	52.7
Standard Deviation	1.7	3.8
Coefficient of Variation, %	2.4	7.3

Table IV.A.1-8. Reproducibility of char yields for liquor A after 15 seconds exposure to a 10% CO_2, 10% CO, 10% water vapor, 70% N_2 atmosphere in a 900°C furnace. Data are for replicate samples in each of the Åbo Akademi single particle reactors.

Sample	Single Particle/ Flow Reactor	Single Particle/ Stagnant Gas Reactor
1	57.6	38.2
2	55.8	46.2
3	55.9	45.2
4	56.6	50.3
5	61.7	49.1
6	62.8	45.8
7	57.8	25.7
8	59.7	37.0
9		33.6
10		31.7
11		47.8
Average	58.5	41.0
Standard Deviation	2.6	8.2
Coefficient of Variation, %	4.5	19.9

Table IV.A.1-9. Reproducibility of char and sodium yields for liquor D after 8 seconds exposure to a 5% CO_2, 95% N_2 atmosphere in a 750°C furnace. Data are for replicate samples in the Åbo Akademi single particle/flow reactor.

Sample	Char Yield % of BLS	Na in Char % of Char	Na in Char % of Na in BLS	Initial Mass mg	Char Mass mg
1	63.0	29.0	94.0	20.30	9.8
2	48.5	29.0	73.4	19.7	7.3
3	51.2	29.6	79.1	18.9	7.4
4	47.7	29.9	74.4	15.9	5.8
5	47.5	28.9	71.5	17.9	6.5
6	49.2	29.6	75.8	18.9	7.1
7	51.7	31.1	83.8	17.2	6.8
Average	51.3	29.5	78.8	18.4	7.2
Standard Deviation	5.5	0.8	7.8	1.5	1.3
Coefficient of Variation, %	10.7	2.9	9.9	8.2	17.3

Table IV.A.1-10. Comparison of replicate char, carbon, sulfur, and sodium yields for three different liquors. Conditions were pyrolysis in nitrogen on separate days for each sample of each liquor. Data are for replicate samples in the Åbo Akademi single particle/flow reactor.

Black Liquor	Char Remaining % BLS			Na Remaining in Char % Na in BLS			Sulfur Remaining in Char % S in BLS			Carbon Remaining in Char % C in BLS		
A	74%			81%			44%			62%		
A	76%			83%			45%			64%		
B		73%			89%			45%			67%	
B		73%			88%			41%			67%	
C			75%			87%			62%			66%
C			75%			87%			61%			64%

IV.A.2 Fume Reactor Experiments

Experimental System

In the single droplet experiments, the sodium retained in the black liquor droplet residue was measured, and the amount of sub-micron fume produced was assumed to be some fraction of the sodium lost. To obtain a direct measurement of the amount of fume formed, a separate experimental system, in which both the fume and char residue were collected and measured, was designed and constructed. This experimental facility allowed a check on sodium material balance closure as well as separate measurements of the fume generated and the sodium retained in the char.

The experimental apparatus as initially designed is shown schematically in Figure IV.A.2-1. It consisted of a semibatch reactor in which stationary char particles are contacted with a hot, flowing gas. The temperature of the combustion zone was maintained up to 1000°C by an electric furnace. A 22 mm i.d. alumina tube protected the steel reactor shell from corrosion. Char particles or liquor droplets were supported on a stainless steel screen which was protected by woven zirconia cloth.

Combustion gas is preheated as it enters the furnace though a coil of stainless steel tubing. The flows of carrier gas and oxidizer were controlled by rotameters, a maximum combustion gas flow rate of 800 l_n/h is possible.* The gas mixing and control system is shown in Figure IV.A.2-2.

In the initial design, combustion products were cooled and transported to the filter chamber through the flush zone. Nitrogen was transpired radially through a 15 mm ID porous ceramic tube enclosed in the lower part of the reactor shell. A nominal flow of 200 l_n/h was maintained to prevent deposition of particulate on tube walls.

Millipore Mitex filters with a 5.0 mm pore size were chosen as the initial filtration media, these filters are made of polytetrafluoroethylene (PTFE). In order to quench the combustion gas temperature below the filter melting point of 260°C, up to 680 l_n/h N_2 can be introduced through two ports located between the porous tube and the filter chamber.

Fume Reactor Experimental Procedure

The procedure developed for the first phase of study applies to combustion of pyrolyzed black liquor char particles. The aerosol captured will necessarily be from the char burning and smelt oxidation stages. It may be possible to burn black liquor as a film on the zirconia cloth or modify the equipment to allow insertion of single droplets. Modification to the equipment

*Gas flow at normal conditions (0°C, 101.3 kPa) when meter is operated at 20°C and 101.3 kPa.

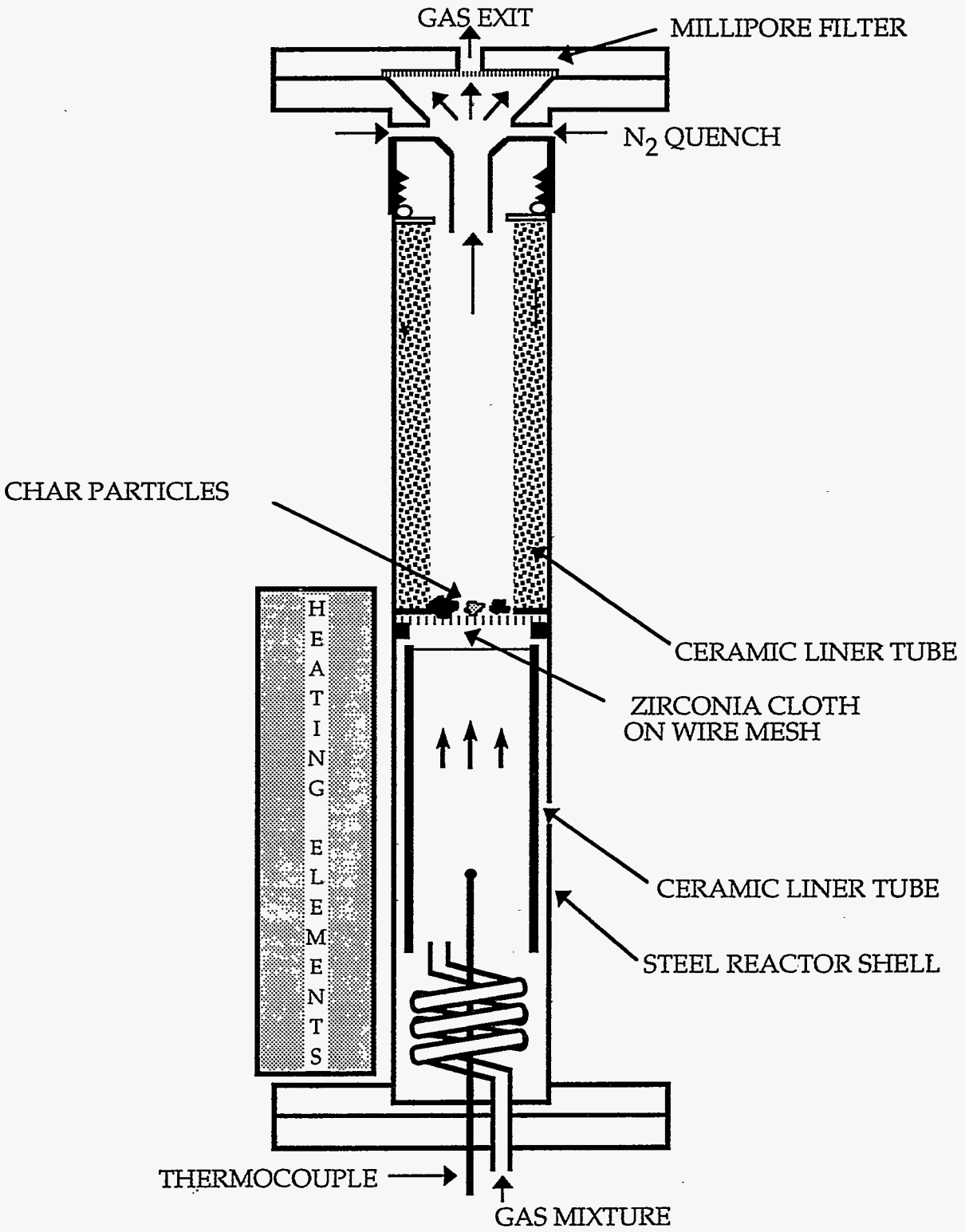

Figure IV.A.2-1. Schematic of char combustion furnace

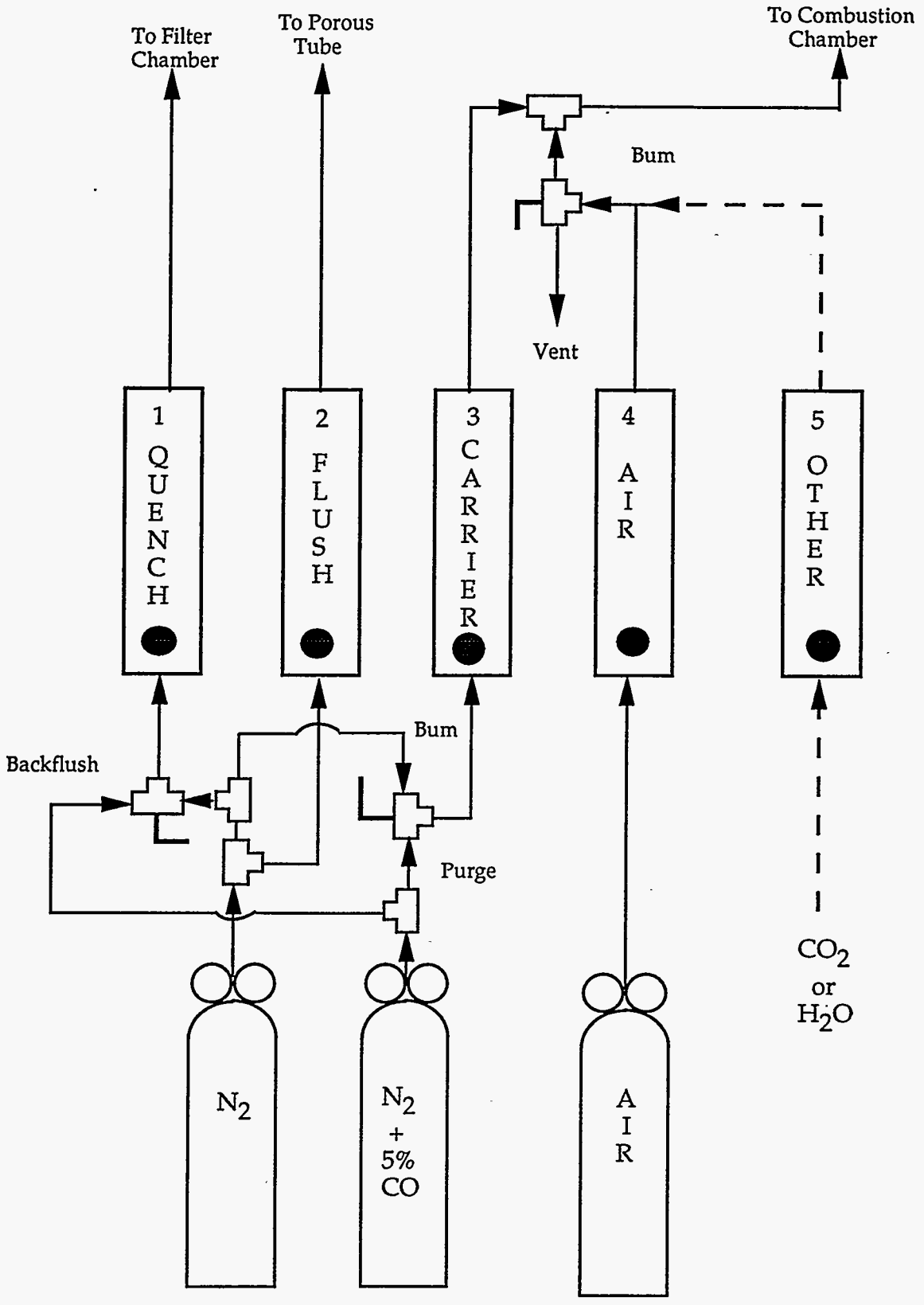

Figure IV.A.2-2. Gas flow control and mixing system

or procedure will have to be devised to measure the fume formation rate during the individual stages of kraft black liquor combustion.

As originally designed, the furnace was heated with nominal levels of nitrogen flowing through the combustion chamber and flush zone. A combustion cartridge was prepared by attaching a stainless steel screen and zirconia cloth to an alumina tube. The cartridge is placed in the combustion zone and allowed to reach furnace temperature. Before inserting char particles, the furnace is purged with a backflow of 5% CO in N_2 to scavenge any oxygen that may be in the system. Dried char particles were weighed and placed in the combustion chamber. After the char was added, the reactor shell was sealed and the N_2/CO mixture is introduced through the preheater coil. An appropriate flow rate of quench gas was set and a weighed filter is placed in the holder.

Just prior to combustion the carrier gas is changed to pure nitrogen, the flows of carrier and oxidizer are adjusted, and the oxidizer (air, O_2, CO_2, or H_2O) is added. When combustion is complete the oxidizer flow is stopped and the filter is removed. The reactor shell is opened and the combustion cartridge containing the char residue is removed.

The mass of the Millipore filter and captured particulate is recorded then the filter is stirred in 100 ml of reverse osmosis purified water. After the ionic strength of the solution is adjusted, the electrical potential is measured by a Na^+ ion-selective electrode. Sodium concentration is determined by comparison of the indicated potential with a calibration curve. The range of concentration measurement is 10^{-6} mol/l to 1 mol/l with an accuracy of $\pm$ 4%.

Modifications to the Fume Reactor and Experimental Procedure

The experimental apparatus was initially designed so that a combustion cartridge was prepared by attaching a stainless steel screen and zirconia cloth to an alumina tube. The cartridge was then inserted into the preheated reactor and allowed to reach furnace temperature. Several problems were noted in the experiments conducted with the initial design:

- when particles were loaded, some combustion and possibly fume loss occurred before reactor could be closed,
- it was difficult to unload the combustion cartridge quickly while hot.
- poor closure of Na material balance was obtained.

Because of these problems, the equipment was modified. This report describes the original data, the modifications to the reactor, and the initial data with the modified reactor.

Data with the Initial Reactor Design

The original fume reactor (Figure IV.A.2-1) was designed on the following basis

- a downflow of gas past hot char particles,
- transport of sodium vapor released from the particles with the gas,
- gas flow radially inward through a porous tube to prevent fume particles from migrating to and collecting on the reactor walls,
- gas injection for cooling, and
- a Millipore filter to collect the fume particles.

Table IV.A.2-1 shows the data for the runs made by this method. As these were the first runs made with the equipment, some problems in sodium recovery were expected. However, we were concerned about the high percentage of the sodium input which was retained in the porous zirconia support pad for the particles. This may have indicated that the sodium fume had already condensed and that the particles were being filtered by the zirconia pad rather than passing through it. The lack of any sodium reaching the filter supports this conclusion. At this point we decided to change to a gas up-flow design.

Table IV.A.2-1. Data for runs 1-3. 800°C, 9% O_2, 5 minutes duration, 199 l/h carrier gas, 200 l/h flush, 200 l/h quench.

Run	1	2	3
Char, mg	100.6	100.0	200.9
Na recovered, % of input			
Filter	0.04	0.0	0.0
Char residue	—	—	28.4
Support fabric	—	—	56.8
Char + support fabric	—	21.8	—
Total recovered	.04	21.8	85.2

Data with the First Gas Up-Flow Design

Conversion to a gas up-flow design was accomplished by inverting the reactor. In a few runs, the char particles were fed from the top, with the filter placed in position after the char particles were dropped into the reactor. This was not a satisfactory method as combustion began before the filter was in place. To solve this problem, char particles were placed into one of the nitrogen lines for the quench gas with flow shut off. The particles were injected by turning the quench gas on. This feed method worked better, although particles did not always fall to the zirconia cloth.

Table IV.A.2-2 shows typical data for the runs using the first gas up-flow reactor design. With this design, some sodium was collected on the filter. However, the material balance closure was poor, averaging 31% but varying widely.

We suspected that the porous tube through which the flush gas passed to prevent fume deposition may have been collecting either particles or that sodium vapor was deposition by condensation on it. The tubes were very permeable and were always broken during the experiments. We felt that the flush gas was not flowing uniformly radially through the tube. This would have allowed the fume particles to reach the tube wall.

- In two of the runs, the tube were removed from the upper half of the reactor, leached, and the leachate analyzed for sodium. The sodium content was high, and accounted for 15-30% of the sodium input. However, a blank analysis on an unused tube showed that the tubes originally contained a large amount of sodium.

Table IV.A.2-2. Data for runs with the first gas up-flow reactor design. 800°C, 9% O_2, 5 minutes duration, 199 l/h carrier gas, 200 l/h flush (runs 4, 5, 7) or 400 l/h (runs 9, 10), 200 l/h quench.

Run	4	5	7	9	10	Avg	St Dev
Char input, mg	200.5	199.5	204.1	206.3	201.7	202.4	2.8
Na input, mg	40.4	40.2	41.1	41.6	40.6	40.8	0.6
Na recovered, %							
Filter	4.0	0.9	3.4	1.9	2.1	2.4	1.2
Char residue	21.6	16.3	20.1	53.5	32.9	28.9	15.1
Total recovered	25.6	17.2	23.5	55.3	35.1	31.3	14.9

Second Gas Up-Flow Design

To solve the flush flow tube problems, we decided to eliminate the porous tube altogether. It was replaced by a non-porous ceramic liner with no detectable sodium content. Instead of flushing with gas, it was decided to keep the liner hot by placing that part of the fume reactor entirely within the furnace. The filter assembly was modified so that cooler metal surface downstream of the ceramic liner could be a collection site for fume. The feeder was also modified so that particles would drop to the zirconia pad directly from above it. The modified reactor is shown in Figure IV.A.2-2.

With this design, we found fume in the tubing leading to the filter assembly, on the surface of the ceramic liner, and a little on the filter itself. We counted all of these as fume in the material balances. We also analyzed the residue on the zirconia support as well as the residue in the particle feeder. We calculated the input as the difference between the sodium in the char input and the residue in the feeder.

Table IV.A.2-3 shows the results of the runs with the second gas up-flow design. The sodium counted as fume collected mainly in the ceramic liner in the tubing leading to the filter assembly; almost none reached the filter. This accounted for only a few percent of the total fume. The majority of the sodium was in the droplet residue and the support pad.

In these runs, the material balances closed quite well. Most of the unaccounted sodium was found in the bottom of the reactor when it was opened after these and a few additional runs were made. The sodium shown as fume in Table IV.A.2-3 is, therefore, a good estimate of the total sodium released as fume during the experiments. There is, however, a large variation in the amount of fume collected in the different runs.

Table IV.A.2-3. Data for runs with the second gas up-flow reactor design. 800°C, in N_2, 5 minutes duration, 199 l/h carrier gas, 200 l/h quench.

Run	14	16	17	18	Avg	St. Dev.
Char mass, mg	200.7	201.9	200.1	203.3	201.5	1.4
Na in char, mg	40.4	40.7	40.3	41.0	40.6	0.3
Na in feeder, mg	1.5	0.3	0.0	1.3	0.8	0.7
Net Na input, mg	38.9	40.4	40.3	39.6	39.8	0.7
Na as fume, %	6.6	1.5	2.2	10.4	5.2	4.2
Na as residue, %	84.6	97.3	93.0	82.2	89.3	7.1
Balance close, %	91.1	98.9	95.2	92.7	94.5	3.4

IV.A.3 Laminar Entrained-Flow Reactor

The pyrolysis and combustion experiments with black liquor were conducted in a laboratory scale laminar entrained-flow reactor (LEFR). Laminar entrained-flow reactors are commonly used to measure the pyrolysis and combustion characteristics of coal and other solid fuels (e.g., Quann et al., 1982; Hurt and Mitchell, 1992). These reactors have two features that are important when obtaining fundamental pyrolysis and combustion data: they provide very rapid heating, and use particles that are small enough so that temperature gradients within the particles are small. Another important advantage is that all aspects of pyrolysis or combustion, e.g., carbon volatilization, char formation, sulfur release, sulfate reduction, and volatilization of sodium, potassium, and chloride, and the formation and destruction of nitrogen species, can be studied in a single experiment.

A schematic of the OSU laminar entrained-flow reactor used in the experiments reported here is shown in Figure IV.A.3-1. The LEFR consists of a vertical 3-zone high temperature electrical furnace with two mullite tubes inside. It operates with a downward flowing gas stream at high temperatures and laminar conditions. The primary flow, a low temperature gas stream, is injected at the center of the reactor. The secondary flow, a high temperature gas stream, is injected coaxially with the primary flow. The annular space between the tubes is used to preheat the secondary flow. When traveling upward through this space, the gas reaches the operating temperature and then turns and flows downward through the smaller of the tubes after passing through a flow straightener to eliminate any turbulence or rotational flow. The primary and secondary flows merge to form a single laminar flow with uniform temperature.

The particles are initially entrained in the low temperature gas stream to prevent changes from occurring before reaching the reaction zone of the reactor. The particles, injected near the top of the unit, travel downward along the centerline of the reactor in a narrow, laminar column. At the moment when the particles enter the reactor, they are simultaneously exposed to the high temperature secondary gas and the hot walls of the reactor. The small particle size and primary flow result in a rapid heat transfer rate. It can be assumed that the laminar gas velocity and particle velocity are the same for small particles. When particles and gases reach the collector, they are quenched with nitrogen to stop the chemical reactions. Most of the quench gas is fed into the first 2 cm of the collector to provide a rapid quench, and the rest flows through the porous wall of the collector to avoid deposition of the aerosol particles on the cooler walls. The residence time is set by moving the collector up or down or by changing the gas velocities. After the quench, the products of reaction are separated. The particles larger than 3 μm in diameter (char) are removed by a cyclone and the fine particles (fume) are collected on a nylon membrane filter (0.5 μm pore size) located before the exhaust duct. The cyclone/filter setup is shown in Figure IV.A.3-2.

The length of the heated zone is 80 cm and the inside diameter of the smaller tube is 70 mm. The electrical heater can operate at temperatures up to 1200°C. The temperature of the reactor wall and the secondary flow are expected to be about the same. The heating zones of the reactor are controlled with a Omega CN 76000 microprocessor based temperature/process controller capable of ramping to its set point temperature at a maximum heating rate of

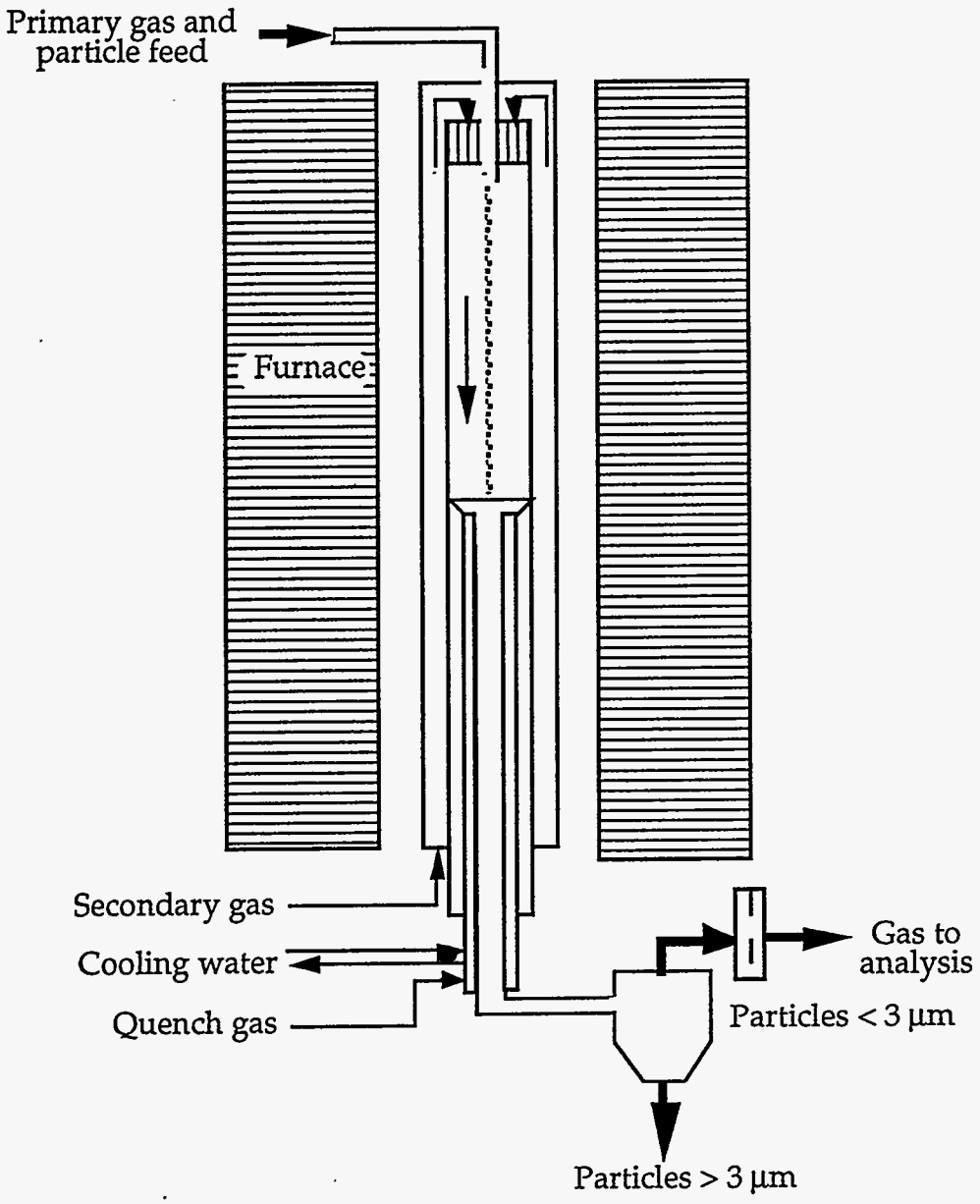

Figure IV.A.3-1. Schematic of the OSU laminar-entrained flow reactor.

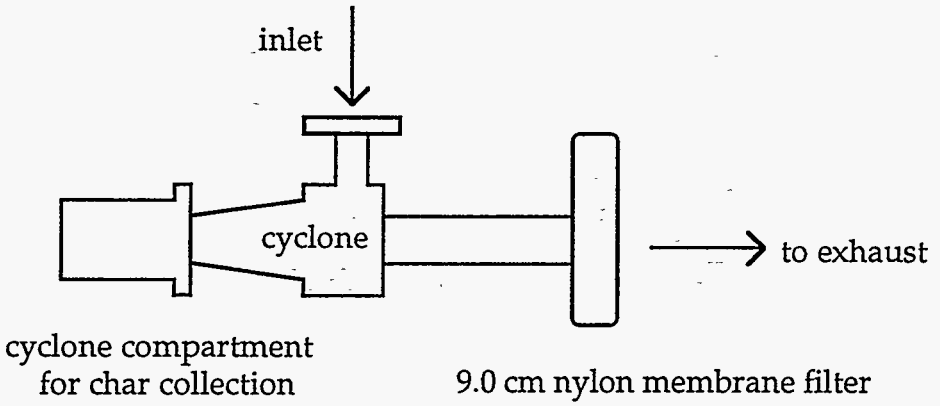

Figure IV.A.3-2. Schematic of cyclone/filter set-up.

300°C/hour. All gas flows are controlled by Omega FMA 5600 Electronic Mass Flowmeters (MFM).

In each LEFR run, the reactor was preheated with nitrogen flowing through the reactor at the desired secondary gas flow rate. At the beginning of each run, the particle feeder was started so that the primary gas and particles began to flow through the reactor. The duration of each run was 3-5 minutes to ensure that steady state had been achieved. At the termination of each run, the cyclone was removed to a nitrogen-purged glove bag where its contents were weighed and part of the contents were placed in a volumetric flask for extraction with water and analysis of the dissolved inorganic ions. Other portions of the char were sent to the Weyerhaeuser Company analytical laboratory in Tacoma, Washington, for carbon analysis. The fine particle samples collected on the filter downstream of the cyclone were weighed and a portion of each was extracted and analyzed for water-soluble inorganic ion content.

Ion Analysis by Capillary Electrophoresis

A Dionex model CES-1 Capillary Electrophoresis System (CES) with a conventional fused-silica capillary was used to analyze the inorganic species in the black liquors used and chars and fine particles produced in the LEFR experiments. Capillary electrophoresis is a simple, high resolution technique which separates ions based on their relative velocity in an applied electric field. Ions with high charge-to-mass rations have the greatest migrational velocity in an electric field, and these are detected first. Ions with lower charge-to-mass ratios have a lower migrational velocity and are detected later.

Sodium, potassium and chloride as well as most of the inorganic cations and anions have no optical absorbance. In order to detect them, indirect photometric detection is used. When using indirect absorbance method with capillary electrophoresis, an absorbing ion is incorporated in the electrolyte to provide a background signal. Ions present in the sample will displace an absorbing ion in the electrolyte and result is a negative peak. The negative peaks are then inverted to positive signals on the screen for better visualization.

In the CES measurements, samples were first extracted with diluted acid. All the sample injections were hydrostatic and performed by raising the sample vial 100 mm above the level of the destination vial for 30 seconds. Dionex cation and anion electrolyte buffers were used in the analyses. Operating parameters for the CES for each group of ions are shown in Table IV.A.3-1. More detailed descriptions of the analytical procedures are provided by Reis (1994).

Table IV.A.3-1. Operating parameters for capillary electrophoresis analyses

Ions	Na^+, K^+	Cl^-	$CO_3^=$, sulfur anions
Capillary ID, μm	50	50	50
Capillary length, cm	50	50	60
Separation voltage, kv	20	30	30
Detection wavelength, nm	215	250	210

Ion Analysis By Ion-Selective Electrodes

Analysis using Ion-Selective Electrode (ISE) is a fairly quick, accurate and economical way to determine ion concentrations in aqueous solutions when systems like atomic absorption (AA) or ion chromatograph (IC) are not available.

The electrical potential of an ion-selective electrode is a function of the logarithm of the activity of the ion to be measured. The relationship is given by the Nernst equation:

$$E = E^o - 2303\ R\ T \log a_{ion} \qquad \text{(IV.A.3-1)}$$

where

Eo = Constant characteristic of the electrode

R = universal gas constant

T = Absolute temperature

F = Faraday constant

a_{ion} = activity of the ion

This equation can be simplified to

$$E = \text{Constant} - S \log a_{ion} \qquad \text{(IV.A.3-2)}$$

where S is the slope of the calibration curve. The measured potential E can only be measured against a reference electrode placed in the same solution. A reference electrode is an ion-selective electrode whose potential is held constant by fixing the composition of the internal filling solution.

For potassium analysis, an Orion Model 93-19 potassium electrode was used. To determine chloride concentration, we used a Corning 476126 chloride electrode. Whenever necessary, the Corning double junction 476067 reference electrode was used. A sodium combination electrode, Corning 476138, was the electrode used for sodium ion analysis.

In a few runs, analyses were made with both the CES and ion-selective electrodes. The agreement between the two methods was acceptable as indicated by the data in Table IV.A.3.2.

References

Hupa, M., Solin, P., and Hyöty, P. (1987), "Combustion Behavior of Black Liquor Droplets" *JPPS*, 13(2):J67-72.

Hurt, R.H. and Mitchell, R.E. (1992), On the combustion kinetics of heterogeneous char particle populations, Twenty-fourth Symp. (Intl.) on Combustion/The Combustion Institute, pp. 1233-1241.

Kreith, F. and Bohn, M.S. (1986), *Principles of Heat Transfer*, Harper Collins, 4th ed.

Olson, A.T. and Shelstad, K.A. (1987), *Introduction to Fluid Flow and the Transfer of Heat and Mass*, Prentice-Hall.

Quann R.J., Neville, M., Janghorbani, M., Mims, C.A., and Sarofim, A.F. (1982), "Mineral Matter and Trace-Element Vaporization in a Laboratory-Pulverized Coal Combustion System" *Environ. Sci. Technol.*, 16:776-781.

Reis, V.V. (1994), "Potassium and Chloride Release During Black Liquor Combustion," M.S. thesis, Oregon State University (October, 1994).

IV.B Sodium Release

Summary

Sodium release from black liquor droplets during black liquor burning is known to occur during all of the final three stages, devolatilization, char combustion, and smelt reactions. The data currently available indicate that during devolatilization, relatively little sodium is volatilized as vapor species (e.g., Na, NaCl) while most of the sodium may be released as small ($\approx$ 10-100 μm) liquor or char fragments that are shed or ejected from the larger droplets. Additional work is needed to clarify the mechanisms of sodium species vapor and small particle release.

During char burning and gasification, sodium release is primarily the result of the reduction of Na_2CO_3 with carbon, producing elemental sodium. The reaction is extremely temperature dependent and only occurs to a significant extent above 800°C at the conditions encountered in recovery boilers. For black liquor droplets of the size fired in recovery boilers, both chemical kinetics and film mass transfer are important in determining the overall rate of sodium release by this mechanism. At high temperatures, film mass transfer limits the overall rate of sodium volatilization, accounting for the lower temperature sensitivity of sodium volatilization observed in recovery boilers.

Sodium volatilization during char burning both in flight and on the char bed accounts for most of the sub-micron sodium fume formed during black liquor combustion.

Introduction

Spent pulping liquor typically contains 4-7% sulfur, 17-20% Na and 0.5-2% K. Part of these elements are volatilized during combustion, forming fume and contributing to fouling of heat transfer surfaces, plugging of gas passages, corrosion, and emissions of particulates and acid gases. The reactions between sulfur and sodium compounds provide an important trap for sulfur gases which results in their recycle within the process.

An important area is the volatilization of alkali metals during gasification. The formation of sub-micron alkali metal fume particles is a serious potential problem in gasification processes because these materials deposit readily on cooled surfaces and create serious clean-up problems in integrated gasification combined-cycle power generation. Another key question involves the subsequent reactions of the alkali metals with volatile sulfur compounds formed during gasification and the constraints this may impose on separate recovery of alkali and sulfur.

Neither the mechanism of fume formation in kraft recovery boilers nor the relative amounts formed during the various stages of black liquor combustion are well understood. Various researchers have attempted to describe the mechanism of sodium volatilization which leads to fume formation, or to predict the amount of fume formed. Borg et al. (1974) and Pejryd and Hupa (1984) used a chemical equilibrium approach to estimate the fume content of gases in the lower furnace. Cameron (1988) showed that sodium can be volatilized by a mechanism involving the oxidation of Na_2S in the smelt.

A critical observation regarding the fume content of the gases in recovery boilers is its relatively low sensitivity to temperature (Hyöty et al., 1989). This lack of temperature sensitivity is not consistent with any of the mechanisms proposed for fume formation. For example, thermodynamic equilibrium predicts a nearly exponential increase in fume content with increasing temperature (Borg et al., 1974; Pejryd and Hupa, 1984). The data of Cameron (1988) for inorganic melts indicates that the rate of fume formation doubles with a temperature increase of 110°C for smelt temperatures near 1000°C. Both are higher than the observed increase in fume content with temperature in recovery boilers.

Nearly all of the experimental work on fume formation has focused on sodium release from smelt or during char burning. There has been relatively little consideration given to sodium release during devolatilization of black liquor prior to char combustion. In those studies where measurements were made during devolatilization there is evidence that some sodium may be released during devolatilization (Volkov et al., 1980; Verrill, 1992; Verrill et al., 1994).

This section of the report deals with sodium release during three stages of black liquor burning: devolatilization, char burning, and smelt reactions. We first review the published data on sodium volatilization from black liquor. Then we present new experimental data and evaluate it along with the data published by other researchers. Finally we propose rate models for sodium release during each of the three stages of black liquor burning.

Sodium Release During Black Liquor Burning - Review of Published Data

A. Single Droplet Burning Data

Experimental data on sodium release from black liquor during three types of combustion and gasification experiments has been published. The three types of experiments are compared in Table IV.B-1. The droplet or particle size ranged by more than a factor of 100, from less than 37 μm to 5 mm, and the range of heating rates varies by a factor of 10^4, from 0.33°C/s to 3000°C/s.

Table IV.B-1. Comparison of previously reported experimental methods for sodium loss during black liquor burning and gasification.

Method	Particle Size	Heating Rate, °C/s	Researchers
Single Droplet	2-5 mm	100[1]	Volkov et al. (1980) Verrill et al. (1994)
Thermobalance	< 37 μm	0.33	Li and van Heiningen (1990)
Grid Heater	100 μm	1000	McKeough et al. (1994)

[1]Nominal heating rate; varies with furnace temperature and particle size.

The fist quantitative experimental data on sodium release during black liquor burning was reported by Volkov et al. (1980). They measured the residual sodium in droplets that had been exposed to temperatures of 900°C, 1000°C, and 1100°C in air and at 1000°C in gas atmospheres created by burning methane in air at various air factors.* The gas compositions, estimated from the air factors, are shown in Table IV.B-2. Their data at 1000°C, air/methane = 1.4 are plotted in Figure IV.B-1. It shows that the sodium content of black liquor droplets burned at these conditions decreases continuously with time, and the sodium retained in the char usually decreased linearly with burning time. Also plotted in Figure IV.B-1 is the approximate boundary between the devolatilization and char burning stages, calculated using the droplet combustion models of Frederick (1990). In these calculations it was assumed that there was no overlap between these stages and that the black liquor used was a typical swelling liquor. The rate of decrease of the sodium in each droplet, indicated by the slope of each data set in Figure IV.B-1, did not change from devolatilization to char burning. Similar calculations for char burning times indicated that the experiments were terminated before char burning was complete.

Table IV.B-2. Approximate gas compositions used by Volkov et al. (1980) in their sodium loss experiments with black liquor. Combustion products in substoichiometric air are assumed to be equilibrated according to the water gas shift reaction at 1000°C.

Air Factor*	0.88	1.2	1.4	air
O_2, %	0.0	3.2	5.6	21.0
CO_2, %	8.7	8.1	7.0	0.0
CO, %	1.6	0.0	0.0	0.0
H_2O, %	18.6	16.1	14.0	0.0
H_2, %	2.2	0.0	0.0	0.0
N_2, %	68.8	72.6	73.5	79.0

Figure IV.B-2 is a plot of sodium remaining in 3 mm droplets versus time when burned at 1000°C in different gas atmospheres. Sodium was lost more rapidly from the droplet burned in air than from those burned in lower oxygen content gases, but there is no trend of sodium loss rate with oxygen content of the gas phase. The Volkov et al. data for other droplet sizes was similar.

*Air factor is defined as the ratio of air used to the stoichiometric air required for complete combustion of methane in the gases that were first burned and then flowed past the suspended black liquor droplets.

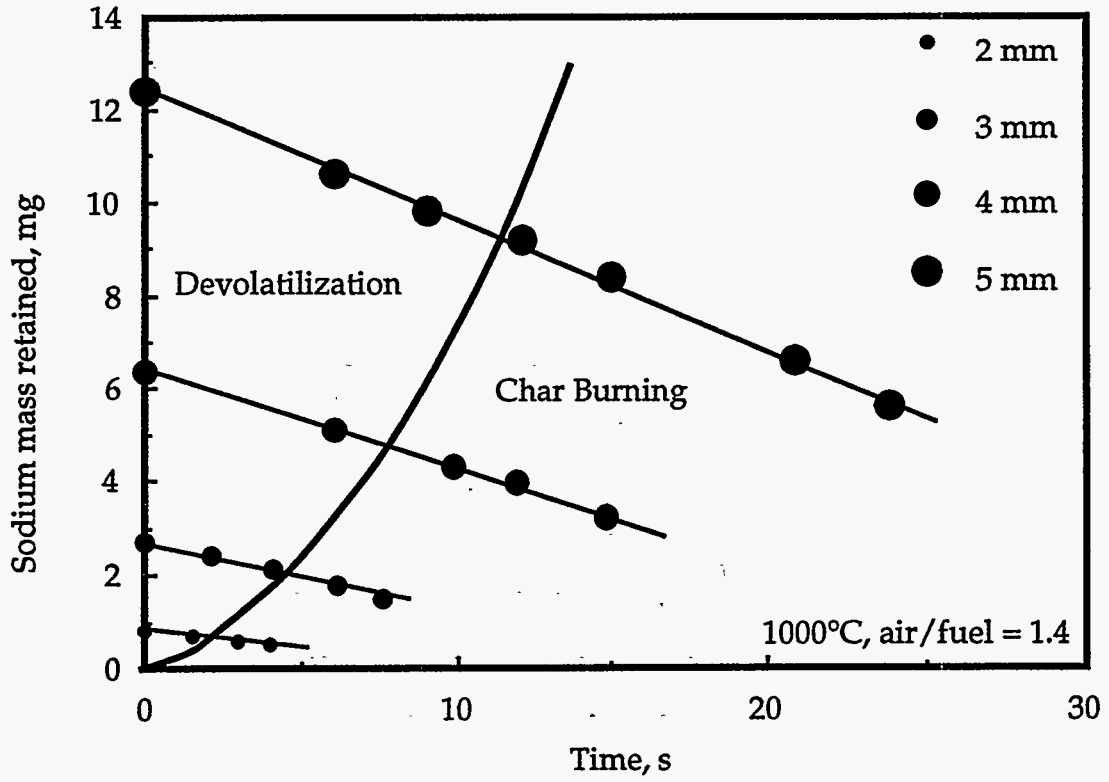

Figure IV.B.1. Typical droplet sodium content versus time for black liquor droplets of different size burned at 1000°C in 5.6% O_2, 7% CO_2, 14% H_2O, rest N_2. Data are from Volkov et al. (1980). The parabolic curve indicates the transition from devolatilization to char burning as estimated with Frederick's model (1990).

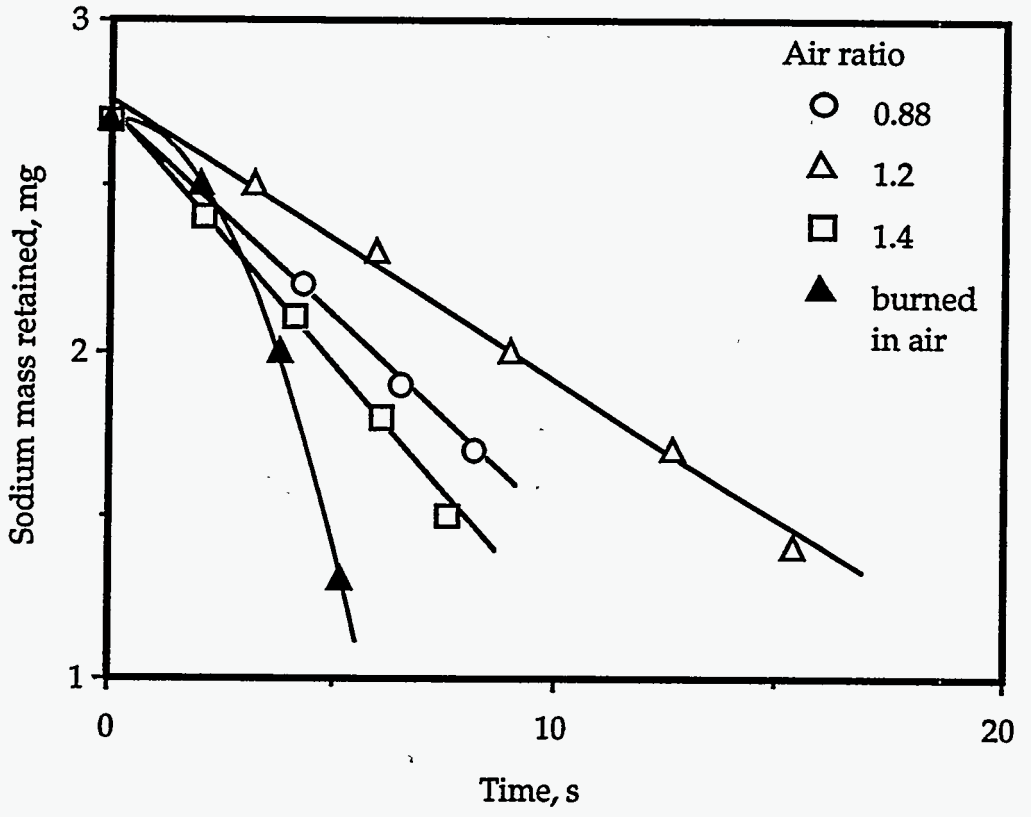

Figure IV.B.2. Typical droplet sodium content versus time for 3 mm diameter black liquor droplets at 1000°C in gases of different composition. Data are from Volkov et al. (1980).

The more rapid loss of sodium for droplets burned in air probably resulted from the higher droplet temperatures which occur under these conditions (Frederick et al., 1994). The lack of correlation of the sodium loss rate with gas composition in the other experiments may be related to a tradeoff between higher droplet temperatures and lower swelling as the oxygen content of the gas phase increased (Frederick et al., 1994a; Frederick et al., 1994b)). Volkov et al. did not report swelling data for their droplets.

The slopes from plots similar to Figure IV.B-1 for the droplets burned in air were plotted in an Arrhenius plot (Figure IV.B-3) to estimate the apparent activation energy for sodium volatilization. The apparent activation energies are shown in Table I.V.3. The apparent activation energy shows no trend with droplet size, and, based on all data, is about 80 kJ/mole.

Table IV.B-3. Apparent activation energies for sodium volatilization based on the data of Volkov et al. (1980).

Droplet Diameter	E_a, kJ/mole
2 mm	94
3 mm	63
4 mm	85
5 mm	77
average	80

In a more recent study, Verrill et al. (1994) burned or pyrolyzed single black liquor droplets in a flowing gas stream and collected the fume particles produced on moving silver membrane filters downstream of the burning particles. Figures IV.B-4 and IV.B-5 show, respectively, their rate of fume particle collection for two droplets of nearly the same size burned at 750°C in 7.5% oxygen and the cumulative percentage of the total fume particles collected, both as a function of time. The dashed line in each figure marks the end of the devolatilization stage and the onset of char burning as reported by Verrill et al. These data suggest that sodium release is faster during char burning and that more but not all of the fume particles collected were generated during the char burning stage. In Verrill and Nichols' (1994) experimental system, the non-plug flow of gases and finite width of the filter section exposed to the particle-laden gases meant that the fume collected at any location on the filter represented an integration of fume released over several seconds of char burning. This made it difficult to distinguish clearly between the devolatilization and char burning stages. The maximum particle temperature during char burning in these experiments, based on the data of Frederick et al. (1994) would have been at least 830°C.

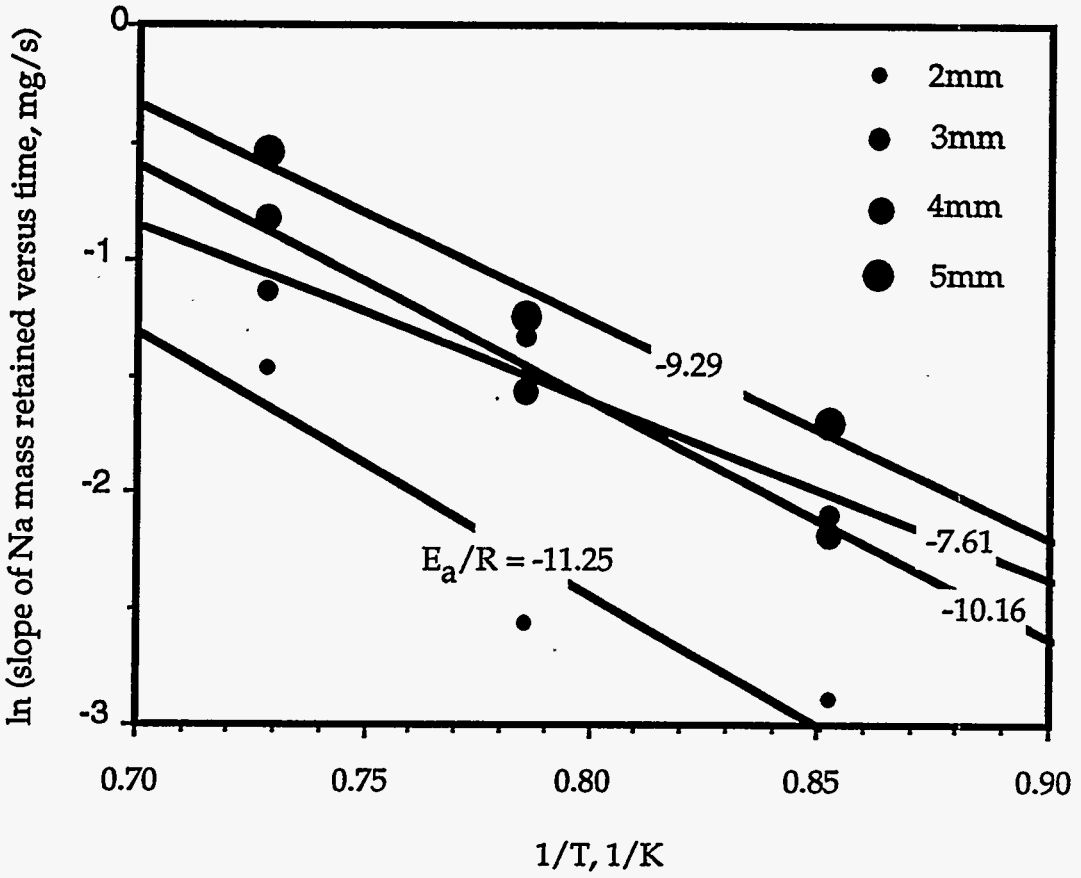

Figure IV.B.3. Apparent activation energy plot for Volkov's sodium mass versus time data for droplets burned in air.

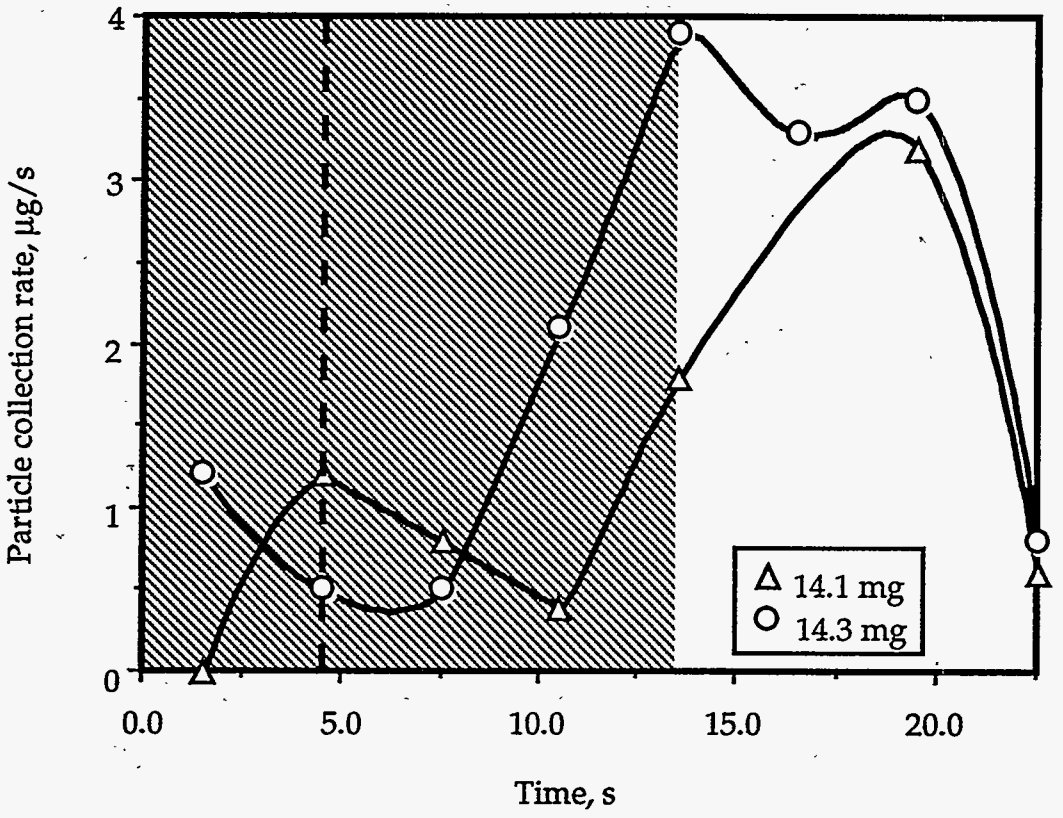

Figure IV.B.4. The rate of collection of fume particles from gases flowing past single black liquor droplets burned at 750°C in 7.5% O_2, 92.5% N_2. The dashed line indicates the observed end of devolatilization and the shaded area represents the uncertainty interval (due to gas mixing) in the time at which the particles were actually collected. Data are from Verrill et al. (1994).

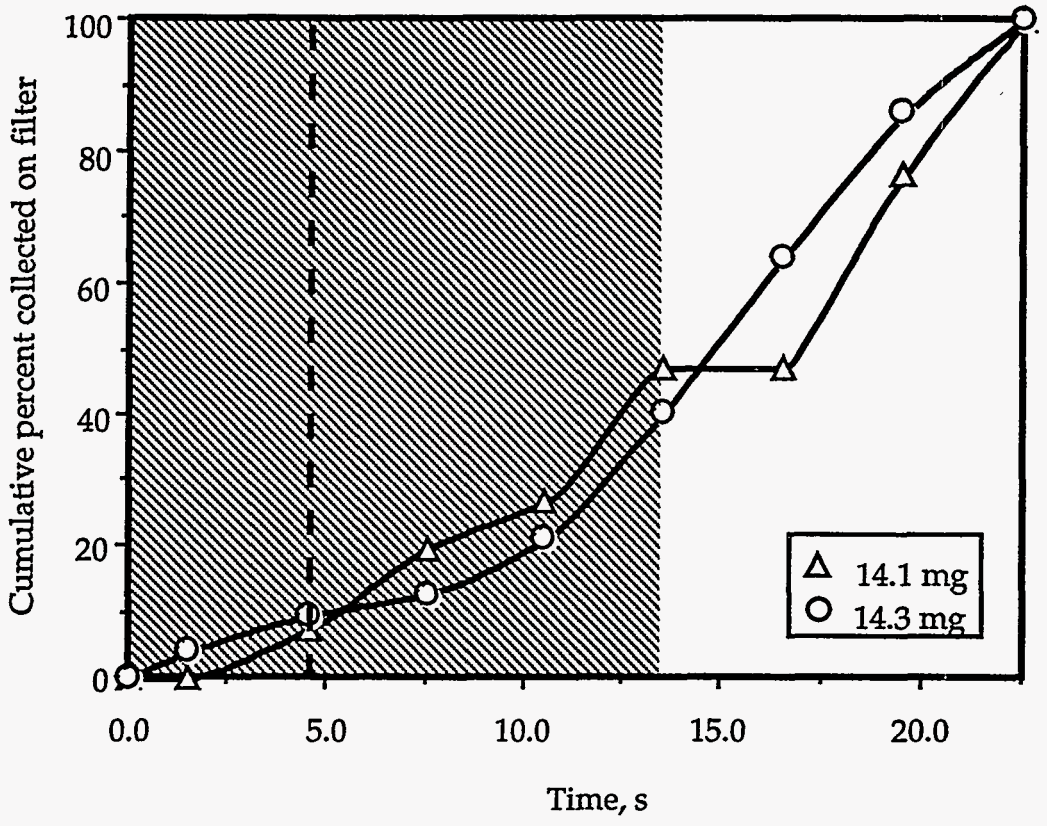

Figure IV.B.5. Cumulative percentage of fume particles collected from gases flowing past single black liquor droplets burned at 750°C in 7.5% O_2, 92.5% N_2. The dashed line indicates the observed end of devolatilization and the shaded area represents the uncertainty interval (due to gas mixing) in the time at which the particles were actually collected. Based on the data of Verrill et al. (1994).

B. Thermobalance Data

Li and van Heiningen (1990) measured the rate of reduction of Na_2CO_3 and sodium losses during slow heating of black liquor solids in a thermobalance. In some of their experiments, the black liquor solids were heated at 20°C/min in an inert (He) atmosphere to a final temperature between 675 and 800°C and then removed and analyzed. In other experiments, the samples were held at the final temperature until the rate of mass loss became negligible. The length of the constant temperature periods were of the order of an hour, but the actual times were not reported. The mass versus time curves from these experiments indicated that devolatilization was complete when the black liquor residue had reached 600°C. The sodium loss data for the final temperatures employed are shown in Table IV.B-4. These data show clearly that sodium loss from black liquor char can exceed 50% of the sodium initially in the black liquor solids. For the samples heated to their final temperature and immediately removed, the sodium loss from the sample heated to 800°C is substantially greater than from those heated to lower final temperatures. Also, the sodium loss increased when the samples were held at their final temperature, with greater sodium losses at higher final temperatures. Sodium loss may have continued in all of the experiments at the point that they were terminated, but at a slow rate.

Table IV.B-4. Sodium release from black liquor char heated in helium. Data are from Li and van Heiningen (1990)

Final Temperature °C	Sodium Loss, % of Sodium in Black Liquor Solids	
	Heated to Final Temperature[1]	Held at Final Temperature[2]
675	6.8	9.5
700	13.4	30.1
725	17.9	48.7
750	18.1	72.4
775	22.9	79.0
800	47.2	81.9

[1]Black liquor solids samples were heated in He to the final temperature indicated and then removed and analyzed for sodium content.
[2]Black liquor solids samples were heated in He to the final temperature indicated, held at that temperature until the rate of mass loss was negligible (below 0.015 mg/min for 10-40 mg samples) and then removed and analyzed for sodium content.

The changes in sodium, carbonate, and carbon in some of Li and van Heiningen's experiments are summarized in Table IV.B-5. The sodium loss during heating to 675°C was about 10% of the sodium in black liquor. The losses of sodium, carbonate, and carbon from 675°C to the end of the experiments that they reported, reproduced in Table IV.B-5, are shown as the *incremental* change during this part of the experiments. From this data it is clear that sodium loss can be significant from char after devolatilization is complete. The ratio of $CO_3^=/Na_2$ lost supports the argument that sodium carbonate reduction is the mechanism of sodium loss. The ratio of non-carbonate (fixed) carbon/Na_2 lost is consistent with carbonate reduction according to the stoichiometry indicated in reactions 1 and 2:

$$Na_2CO_3 + C \rightarrow 2Na + CO + CO_2 \quad (1)$$

$$Na_2CO_3 + 2C \rightarrow 2Na + 3CO \quad (2)$$

Table IV.B-5. Changes in the sodium, carbonate, and fixed carbon content of black liquor char upon heating in He from 675°C to the final temperature indicated and maintained at the final temperature until the rate of mass loss became negligible. The data are from Li and van Heiningen (1990).

Temperature Range, °C	675 → 750	675 → 775	675 → 800
Total Mass Loss, mg	34.1	37.9	40.6
Sodium Loss			
Mass, mg	12.4	14.0	14.5
Molar, mmole	0.54	0.60	0.63
Change in Carbonate			
Mass, mg	15.8	19.8	20.4
Molar, mmole	0.26	0.33	0.34
Fixed Carbon Loss			
Mass, mg	5.9	4.1	5.7
Molar, mmole	0.49	0.34	0.48
$CO_3^=/Na_2$ mole Ratio Lost	0.96	1.10	1.08
Fixed C/Na_2 mole Ratio Lost	1.8	1.1	1.5

Li and van Heiningen also reported that the rate of Na_2CO_3 reduction by carbon is first order in Na_2CO_3 and increases rapidly with temperature, doubling every 23°C over the temperature range of their experiments. The effect of carbon content or Na_2CO_3/C ratio was not determined. An equation that describes the rate of Na_2CO_3 reduction in their black liquor char is

$$\frac{d[Na_2CO_3]}{dt} = 10^9 [Na_2CO_3] \exp(-244000/RT) \quad (1)$$

In Eq. 1, t is in seconds, R is 8.314 J/mol K, and T is in degrees Kelvin.

In their experiments, Li and van Heiningen (1990) observed that, below 800°C, both CO and CO_2 suppressed the rate of sodium loss from black liquor char. Table IV.B-6 shows Li and van Heiningen's data for black liquor char heated (a) in 12% CO, 88% He at 750°C and 800°C and (b) gasified in 20% CO_2, 10% CO, 70% He at 750°C. The sodium release from Li and van Heiningen's experiments in CO/He mixtures was calculated as the sodium in the char (from their Table IV) as a percentage of the sodium in the char after pyrolysis of black liquor solids to 675°C (from their Figure 4). For their char gasification data, the sodium retained is based on the initial sodium content of the char (from their Table V). Data for char heated at 750°C in He is also included for comparison. At these temperatures, the presence of CO and/or CO_2 nearly completely suppressed sodium volatilization.

Table IV.B-6. Sodium loss during heating of black liquor char at constant temperature in different gas atmospheres. Data are from Li and van Heiningen (1990).

Temperature °C	Gas Atmosphere	Time at Temperature, min	Na Retained in Char, %
750	100% He	30	28.6
750	12% CO, 88% He	30	96.8
800	12% CO, 88% He	30	97.4
750	20% CO_2, 10% CO, 70% He	35	98.1

In pressurized thermobalance experiments, Frederick et al. (1993) observed a similar suppression effect with CO_2. When black liquor char samples were gasified in CO_2 at temperatures of 650-800°C, no sodium was lost from the char. The reaction times in these experiments were 0.5-4 hours.

c. Grid Heater Experiments

McKeough et al. (1994) reported sodium loss during pyrolysis for experiments in which 100 μm diameter particles of dried black liquor solids were heated to temperatures of 600-900°C on an electrically heated grid. Their heating rate of the grid was in the order of 1000°C/s. The char residue was collected and analyzed for sodium. Figure IV.B-6 shows the results of this work. At 600°C, essentially all of the sodium was retained in the char residue, while at 900°C, the sodium content of the residue decreased with time during the entire experiments. McKeough et al. reported that the rate of sodium volatilization was initially faster than predicted by Li and van Heiningen's sodium carbonate reduction rate equation, but then decreased to less than predicted.

Experimental Results from This Work

In our work, three types of experiments were conducted to evaluate sodium release during black liquor burning. The objective of these experiments was to obtain rate and yield data for sodium volatilization from black liquor particles during both devolatilization and char burning.

Much of the data was obtained by the single droplet method discussed in Section IV.A.1. Additional measurements for sodium release from black liquor char were made using a specially designed reactor. These experiments were conducted at Åbo Akademi University. All were made with 2-3 mm black liquor droplets or char particle formed from burning droplets of approximately that size, and heating rates of the order of 100°C/s.

Additional measurements were made with a laminar entrained flow reactor at Oregon State University. These experiments were made with 100 μm particles of dry black liquor solids at heating rates exceeding 10^4 °C/s.

Table IV.B-7 compares the three types of experiments. The experimental procedures for all three types of experiments are described in detail in Section IV.A.

a. Åbo Akademi University Single Droplet/Stagnant Gas Reactor

Experiments to determine the sodium release during devolatilization in inert atmosphere were performed in a furnace with a stagnant gas atmosphere around the particle (ÅA single droplet/stagnant reactor). The experiments were done in either N_2 or in mixture of N_2 and CO. Figures IV.B-7 and IV.B-8 show how the sodium content in the char residue varied with exposure time for single black liquor droplets, 5-15 mg, in a pyrolysis or gasifying environment. The data are for a softwood kraft liquors and represent averages of 3-4 measurements per point. The error bars for the 800°C data in Figure IV.B-6 indicate ± 1 standard deviation and are representative for all of the data. As reference, devolatilization was complete in 6-11 s for droplets pyrolyzed at 700°C, in 4-8 s at 800°C, 3-6 s at 900°C, and 2-4 s at 1000°C, depending

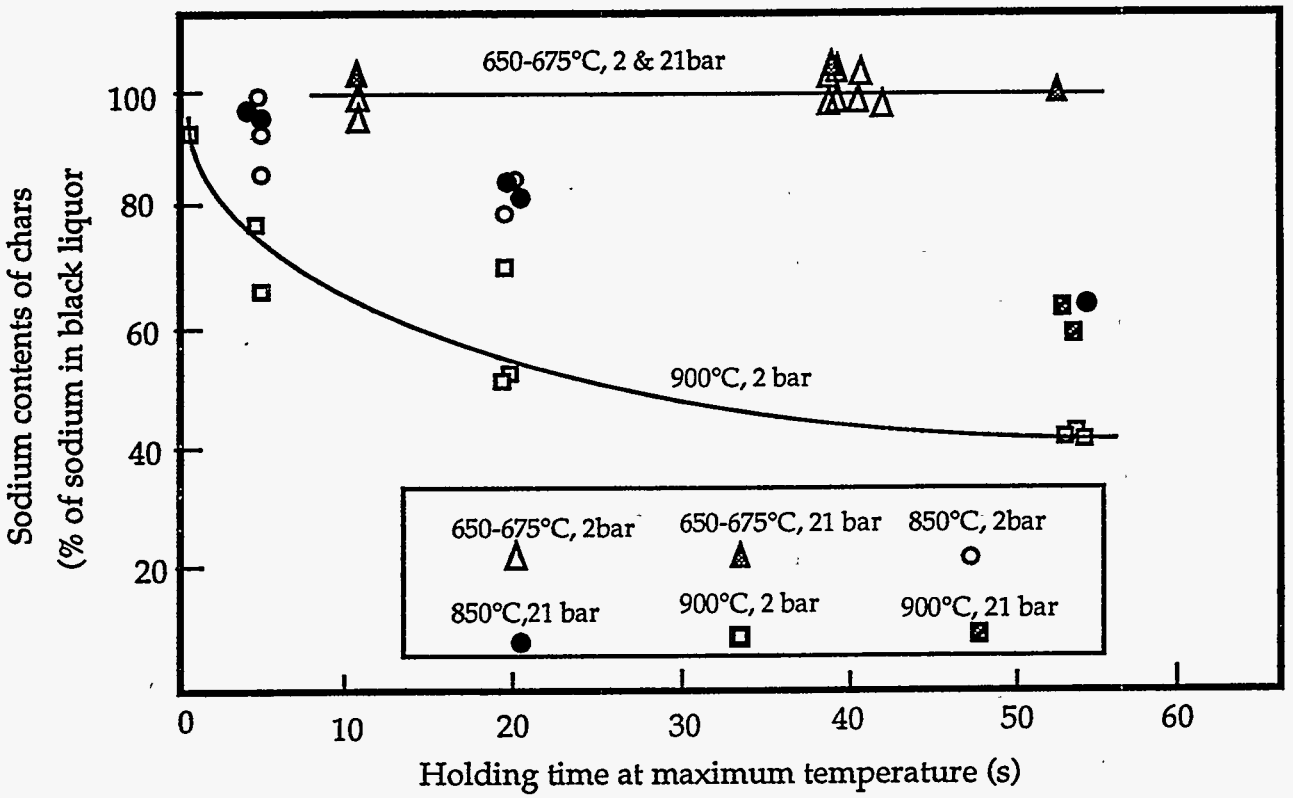

Figure IV.B-6. Sodium release data from 100 micron dry black liquor particles in grid heater experiments. Data are from McKeough et al. (1994).

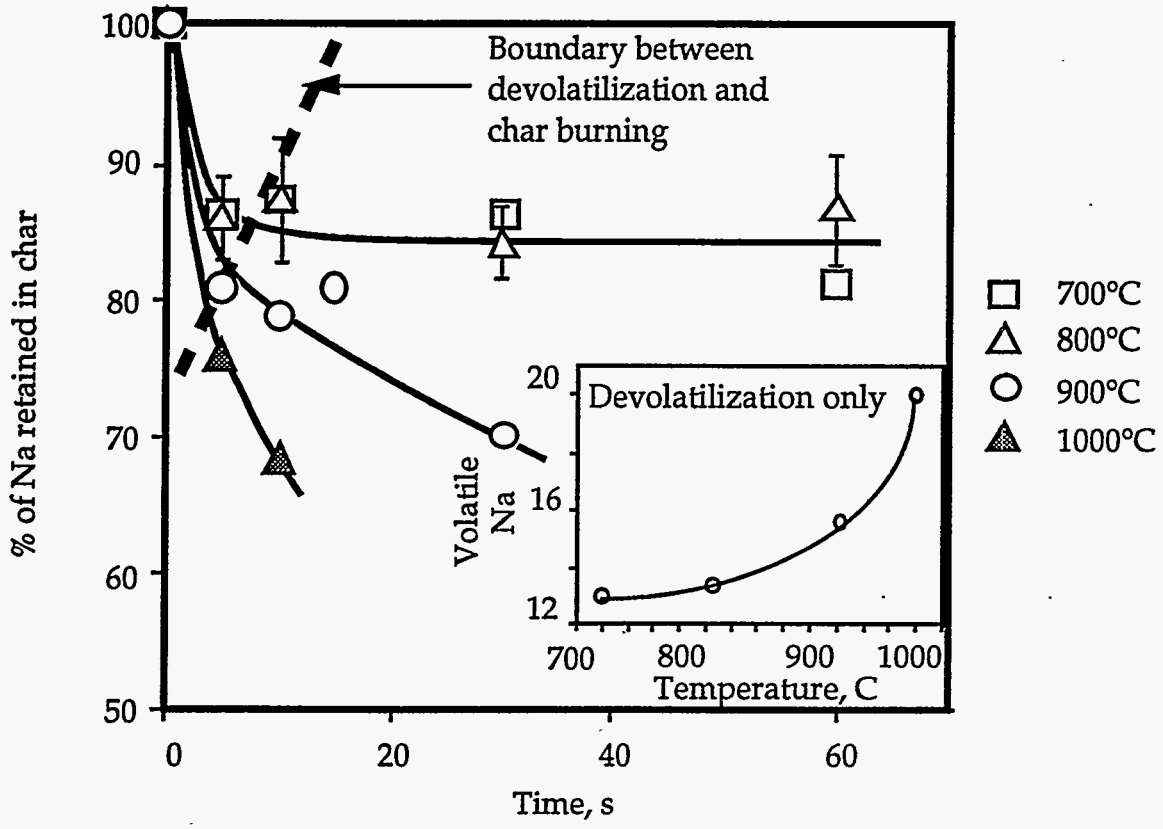

Figure IV.B-7. Sodium retained in the droplets versus time for single black liquor droplets heated for up to 60 seconds in a quiescent gas atmosphere, 5% CO, 95% N_2 at temperatures of 700-1000°°C.

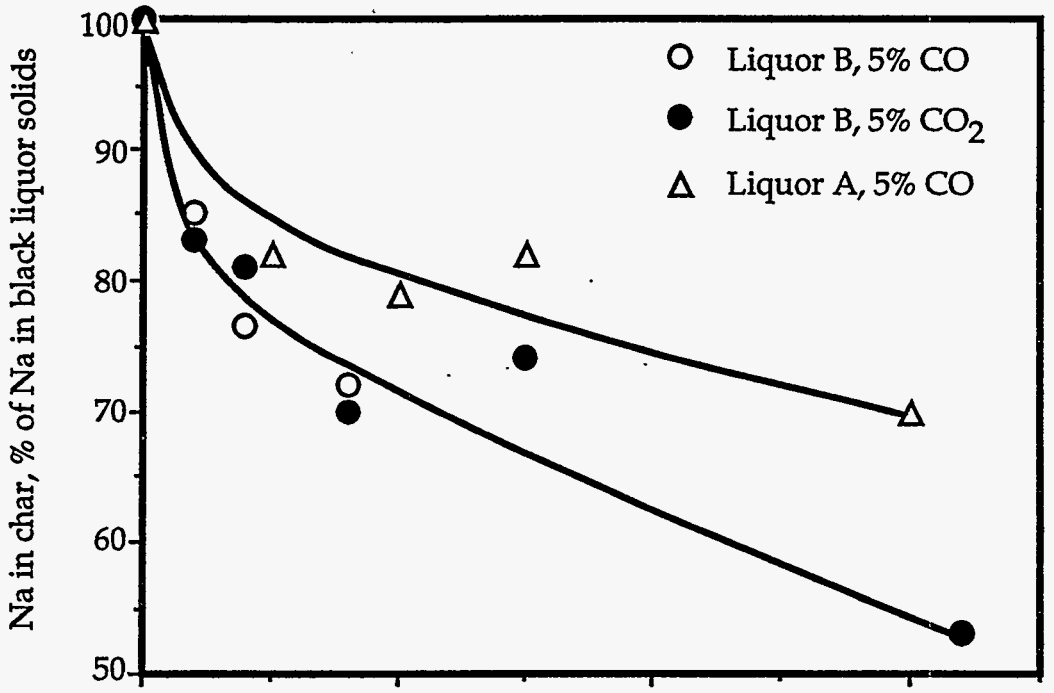

Figure IV.B.8. Sodium retained in the droplets versus time for single black liquor droplets heated for up to 30 seconds in a quiescent gas atmosphere containing 5% CO or 5% CO_2, 95% N_2 at 900°C.

Table IV.B-7. Comparison of experimental methods used in this study to measure sodium loss during black liquor burning and gasification.

Method	Particle Size	Heating Rate °/s[1]	Dry Solids Content, %	Location
Single droplet[2]	2-3 mm	100[1]	60-70	ÅAU
Char reactor	2-3 mm	100[1]	60-70	ÅAU
Laminar entrained-flow reactor	100 μm	30,000[1]	100	OSU

[1]Nominal heating rate; varies with furnace temperature and particle size.
[2]Single droplet experiments were performed in both stagnant and flowing gas atmospheres.

primarily on the droplet mass. The approximate end of the devolatilization stage is indicated in Figure IV.B-6 by a dashed line.

At 700°C and 800°C the sodium content, expressed as a percentage of the initial sodium mass of the droplet, decreased with time to 80-85% of the initial sodium content and then became constant after devolatilization was complete. Pyrolysis occurs rapidly but no combustion reactions occur in a N_2/CO gas environment and reduction of Na_2CO_3 and Na_2SO_4 is too slow to contribute to Na or C loss at these temperatures. This data indicates that 15-20% of the sodium was lost during devolatilization of this liquor at these conditions.

At 900 and 1000°C, the sodium retained continued to decrease with time after devolatilization. This agrees with the results of Volkov et al (17) who reported a monotonically decreasing residual sodium content with time for furnace temperatures 900-1100°C. Their experiments were conducted in air with a larger range of droplet sizes and in post-combustion gases at 1000°C. These results indicate that significant sodium release can continue to occur beyond devolatilization at 900°C and above, but not at 800°C or below in the time scale of these measurements. There was no difference in sodium retained in the char for droplets pyrolyzed in N_2/CO versus N_2/CO_2 gas mixtures (Figure IV.B-8).

The levelling off of sodium content with time at the lower temperatures was also observed by Verrill et al. (1994). It can also be seen in the data of Li and van Heiningen (1990). In their non-isothermal, slow pyrolysis data, the sodium in the liquor residue decreases with time as devolatilization proceeds, then remains constant between 725°C and 750°C, and finally begins to decrease rapidly at higher temperatures. The plateau in sodium retained may occur because devolatilization is complete by 725°C; this temperature is consistent with simultaneous combustion stage observations and droplet temperature measurements during devolatilization (10). The increasing Na loss above 750°C is similar to what we have observed at higher temperatures. It may be due to Na_2CO_3 decomposition after devolatilization is complete; this is discussed in more detail at the end of this section. The amount of sodium

retained in the droplet residue at the end of devolatilization at all four furnace temperatures is indicated by the dashed line in Figure IV.B-7.

The difference in sodium lost from the particles during devolatilization between the extremes in furnace temperature (see Figure IV.B-7 insert) is surprisingly small: 14% of the sodium in the liquor was lost during devolatilization at 700°C, while 18% was lost at 1000°C. However, these relative values are similar to those for total volatiles loss during devolatilization (Frederick et al., 1994c). This suggests that sodium loss during devolatilization is rather weakly dependent on furnace temperature but proportional to the overall volatiles loss.

The sodium loss during pyrolysis was similar for the seven liquors of three different types that we tested. The residual sodium content after 10 seconds exposure at 800°C in the N_2/CO atmosphere is shown in Figure IV.B-9. The data are averages for 4-5 droplets per liquor and the error bars represent the range of sodium contents for the particular liquor. For the six liquors shown in Figure IV.B-9, the average sodium loss during pyrolysis for ten seconds is 23-33% and is not strongly dependent on liquor type. There is no correlation between the sodium loss during pyrolysis and the sodium content of the liquor in these experiments.

The complete data on which Figures IV.B-6 - IV.B-8 are based are included in Appendix IV.A.

Experiments in the Åbo Akademi Single Droplet/Flow Reactor

A second set of experiments to determine the sodium release during devolatilization in an inert atmosphere were performed in a tube furnace with a gas flow past the particle (ÅA single particle/flow reactor). The experiments were done in either N_2 or in mixture of N_2 and CO. Figure IV.B-9 shows the Na release not returned in the droplet residue at different temperatures for two of the liquors. The values are calculated from the char mass and chemical analysis. The composition of the liquors used in these experiments are shown in Table IV.B-7. Black liquor A was used at 600-900°C and black liquors B and C only at 800°C. The release of Na, Figure IV.B-10, ranges between 10% and 20% of the initial Na content for black liquor A. With addition of 5% CO to the gases the release of Na was smaller than without CO. These Na release numbers are slightly smaller than in the experiments in the single droplet/stagnant gas (see Figures IV.B-7 – IV.B-9).

The release of sodium from different black liquors are presented in Figure IV.B-11. Each column is the average sodium release from a set of eight droplets pyrolyzed at 800°C in 100% N_2. The values for two different sets at the same conditions do not vary more than 11% of initial Na. The release from these liquors vary between 11% and 20% of initial sodium in black liquor solids.

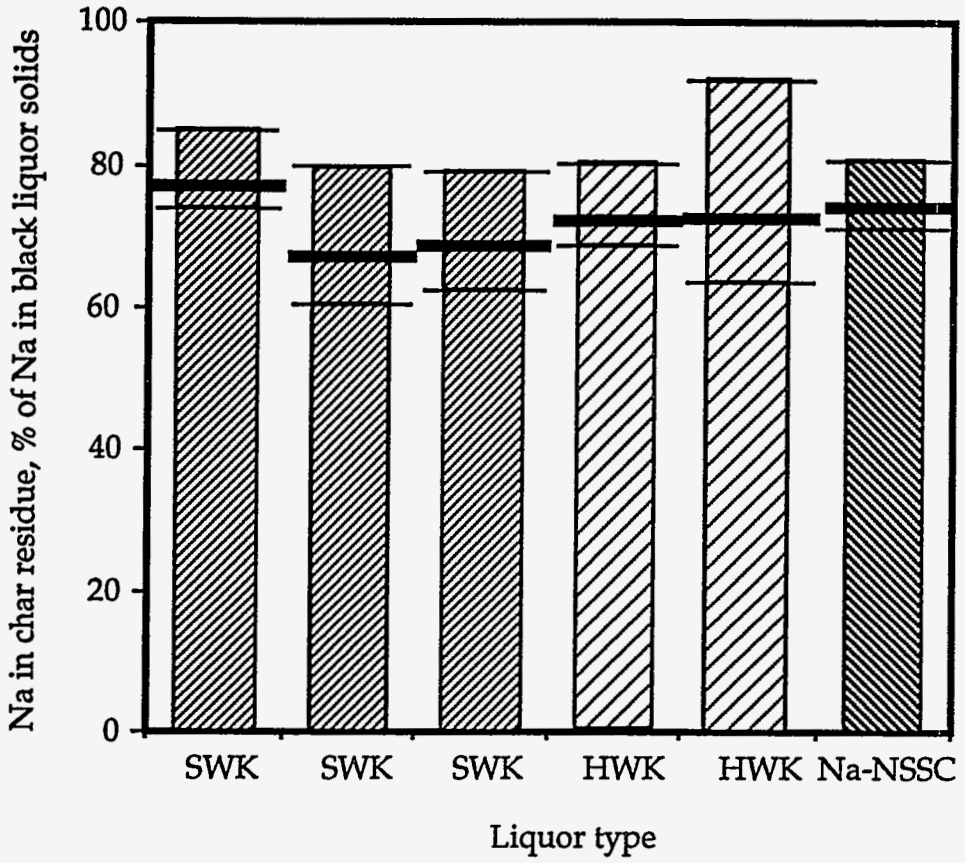

Figure IV.B.9. Sodium in char residue as a percentage of sodium initially in the black liquor solids for six liquors pyrolyzed in 95% nitrogen, 5% CO at 800°C for 10 Seconds. Heavy horizontal lines indicate average values, light lines indicate range of values obtained. SWK denotes softwood kraft liquors, HWK denotes hardwood kraft, and Na-NSSC denotes a sodium-base neutral sulfite semichemical liquor.

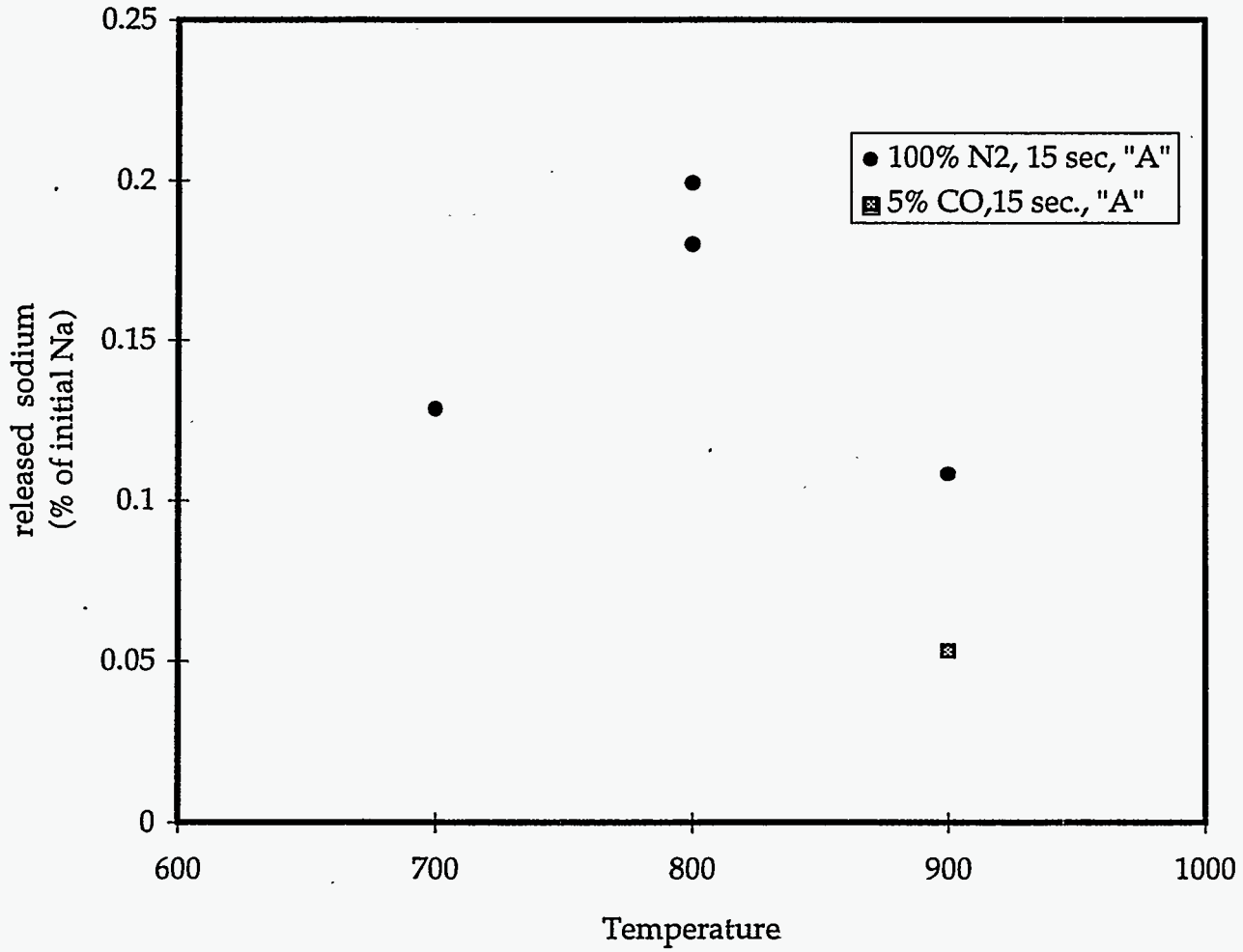

Figure IV.B.10. Na release as function of temperature for liquor A and at 800°C, 15 seconds exposure time.

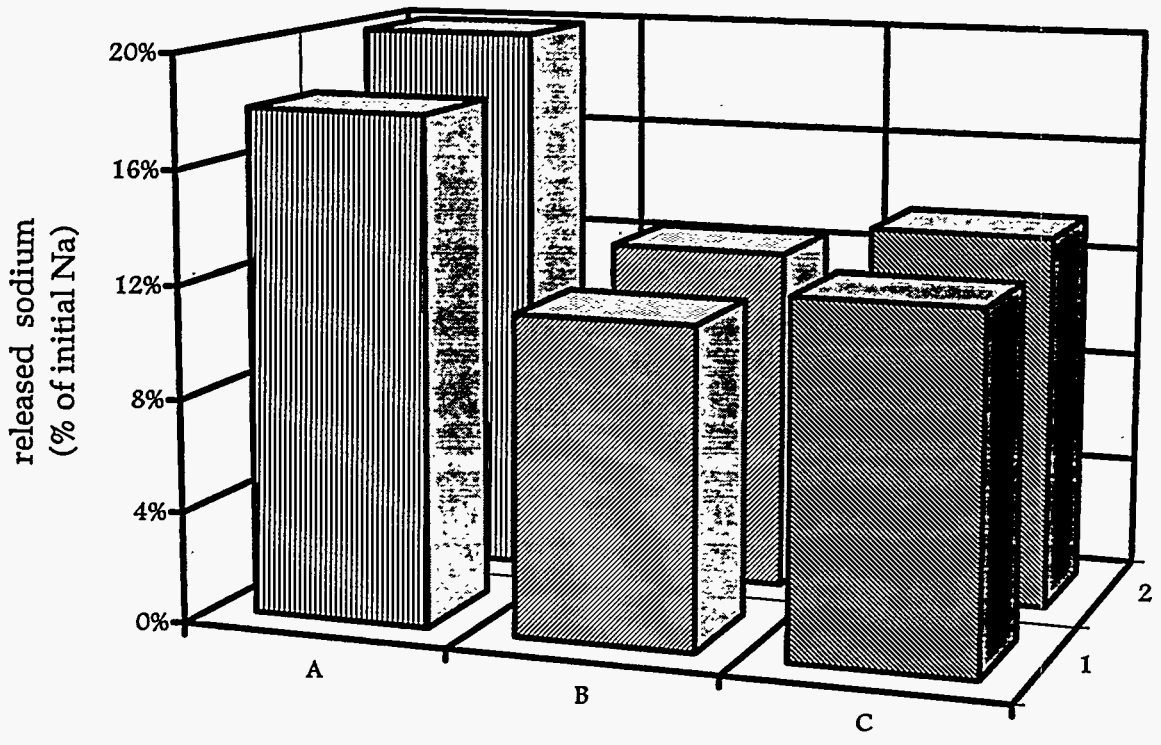

Figure IV.B-11. Release of Na during pyrolysis of different black liquors (A-C) at 800°C in a nitrogen atmosphere. Values are mean values for 8 droplets in each experiment; the two values for each liquor represent replicate sets of runs.

Figure IV.B-12 shows the percentage of sodium released for three different liquors (A, B, and C) versus the percentage of total of released during pyrolysis for 15 seconds. The fraction sodium released ranges from 5% to 20% of the total sodium. By comparison, the total mass released was 25-35% of the initial droplet mass. The experiment with 5% CO, which had the lowest sodium release, had about the same total volatile mass release as did the experiment done in 100% N_2. The total mass released for liquors B and C were equal in these experiments.

The amounts of sodium released in the same experiments are shown in Figure IV.B-13, plotted against the amount of carbon released. The release of carbon from liquor A is about the same for 700 and 800°C, but at 900°C the release increases slightly. For the experiments at 800°C the amount of carbon released from liquor C is lower than for liquor B. This is probably due to the higher inorganic content of liquor C, which is the "as fired" liquor of the "concentrator product" liquor B. No direct relationship between carbon release and sodium release can be seen in Figure IV.B-13.

Figure IV.B-14 shows the molar ratio between sodium and sulfur released. The molar ratio for Na_2SO_4, found in the dust of the recovery boiler, is very nearly 2. Therefore, the sulfur released during pyrolysis is less than the stoichiometric requirement for conversion of sulfur released during pyrolysis. Only at 900°C and longer reaction times does the ratio of Na/S increases over 2, to almost 4. This means that there was a much greater release of sodium compared to sulfur during the first 15 seconds at 900°C. At this temperature, part of the sodium that reacts with sulfur to form fume may have come from char reactions which occur during most of the 15 second period at 900°C.

Effect of Time-Temperature on Sodium Release

Figure IV.B-15 shows the sodium release for different reaction times and temperatures, plotted versus volatile mass released as a percentage of black liquor solids. The points in the lower left corner are for 15 seconds duration and the points in the upper right corner are for 180 seconds duration. The three lines in the figure show the data points that have the duration of 15 and 180 seconds with the same temperature and gas composition. The CO/N_2 data (triangles) shows that, compared to the N_2 experiment (diamonds), there is no difference in Na or total mass released for the 180 s duration time. The data at 700°C (open squares) shows that there is no further release of sodium at 180 seconds duration for that temperature. At 800°C only measurements with 15 seconds duration were made. They showed a slightly higher release of sodium than at 900°C and 700°C. When the char residue after devolatilization was heated for longer times in only nitrogen, no additional release of either Na or C occurred at 700°C or lower temperatures. At 900°C, however, the release of both carbon and sodium increased. This is most likely due to reduction of Na_2CO_3 by char carbon. 12% CO in the gas phase did not inhibit the reaction at 900°C. Li and van Heiningen (1990) reported that the presence of 12% CO in the gas inhibited the release of sodium at 800°C.

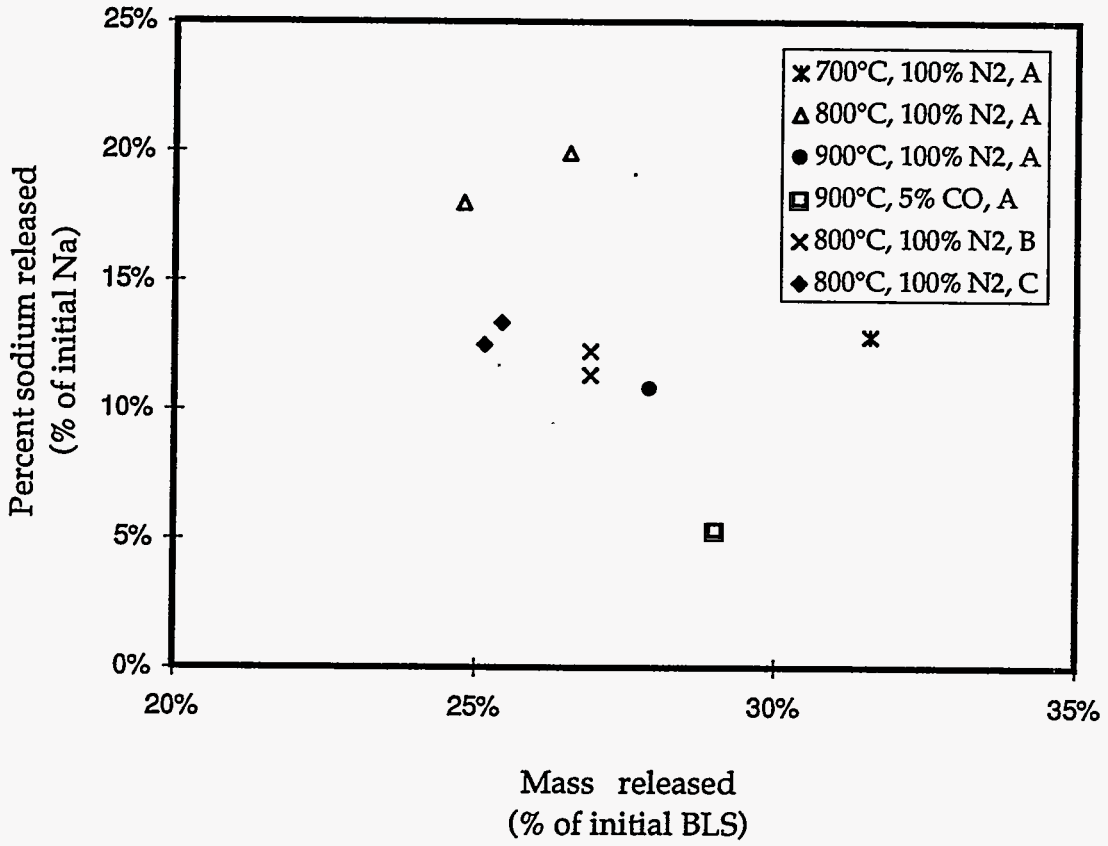

Figure IV.B-12. Sodium released vs total mass released for 15 seconds pyrolysis of black liquors A, B and C in inert atmosphere at 700-900°C.

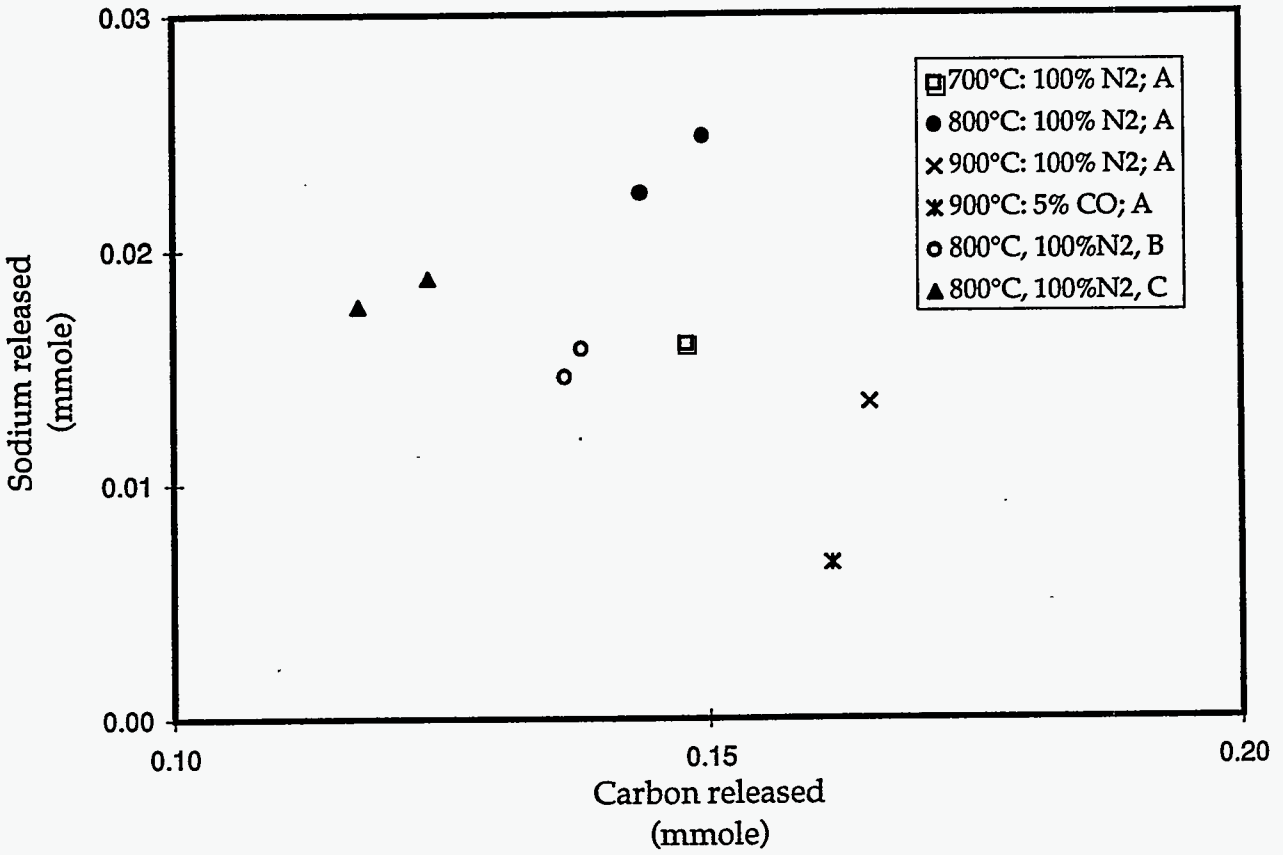

Figure IV.B-13. Amount of sodium released versus amount of carbon released for 15 seconds pyrolysis of black liquors A, B and C in inert atmosphere at 700-900 C.

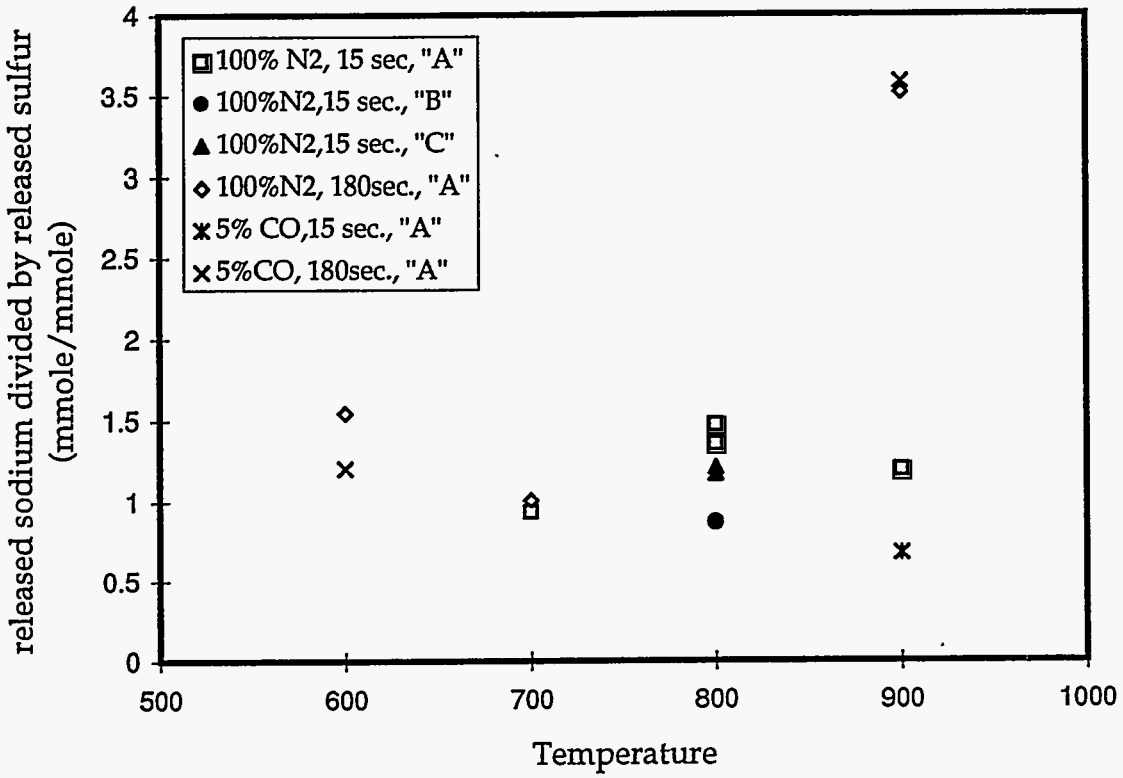

Figure IV.B-14. Molar ratio of sodium to sulfur for pyrolysis of black liquors A, B and C in inert atmosphere for 15 or 180 seconds at 600-900°C.

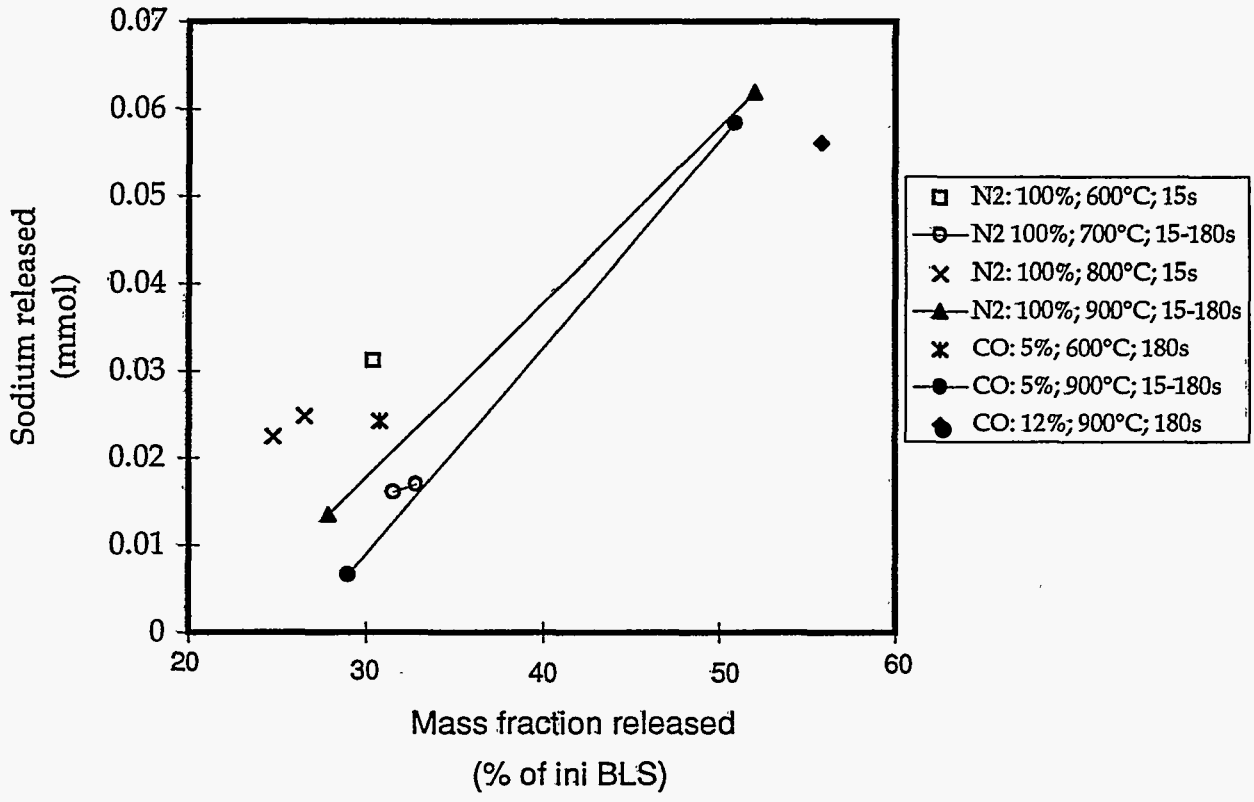

Figure IV.B-15. Sodium released in moles as function of volatile mass released for pyrolysis of black liquor A at 600-900°C in inert gas atmosphere.

In Figure IV.B-16, the sodium release is compared to the carbon release on molar basis. The release of sodium and carbon are similar regardless of the presence or absence of CO. More of the total mass was volatilized in 12% CO than at 5% CO (see Figure IV.B-15) but this was not the case for carbon release which was the same for those experiments.

Figure IV.B-17 shows the molar sodium release against the molar sulfur release during devolatilization or devolatilization plus prolonged heating. For all the 15 seconds experiments there is a trend of increasing sodium release with increasing sulfur release. A regression line through the data below 900°C and at 900°C, 15 seconds has a slope of 1.8, which corresponds to nearly the same ratio of Na/S found in precipitator catch. The points for 180 seconds for the 900°C experiments are well above this line which again indicates that relatively more Na than S had been released for longer heating times after devolatilization was complete. The points for 180 seconds for the 600 and 700°C experiments fall on the same line as do the experiments conducted for 15 seconds.

Na Bound to Sulfur Ions, Carbonate, and Carbon as Free Carbon in Char

Li and van Heiningen (1990) found that all sodium was inorganically bound to ions in black liquor char after slow heating rate devolatilization to temperatures above 675°C in nitrogen atmosphere. They reported that 91% of the sulfur in the form of sulfide and that the amount of sulfur ions in the char didn't vary much over the temperature range 675-800°C. The sulfur content of char after devolatilization at a slow heating rate up to 800°C was constant. They also measured the Na_2CO_3 in the char - it had increased from an initial 10% of BLS to about 22% of BLS at 675°C and then dropped slightly to about 18% of BLS at 800°C. The carbonate decreased to almost zero at 800°C after 50 minutes of heating at 800°C. McKeough et al. measured the Na_2CO_3 in char after devolatilization at 2 bar in an electrically heated grid apparatus. At 675°C and 900°C, over 95% of the Na in the char residue was as Na_2CO_3 after 1 second.

Figures IV.B-18 – IV.B-21 show the calculated values of Na as sulfur salts, Na as carbonate, the amount of free carbon in the char, and the amount of the rest of the species in char as function of temperature. The following assumptions were made in the calculations:

1. The calculations are based on the C, Na and S analyses before and after devolatilization and the total mass of char.

2. All the inorganic sulfur in char is bound as Na_2S, Na_2SO_4 and Na_2SO_3 – none as $Na_2S_2O_3$ – i.e., all inorganic sulfur in the char is bound to sodium at a Na/S mole ratio of 2.0.

3. The rest of the available Na is bound as Na_2CO_3.

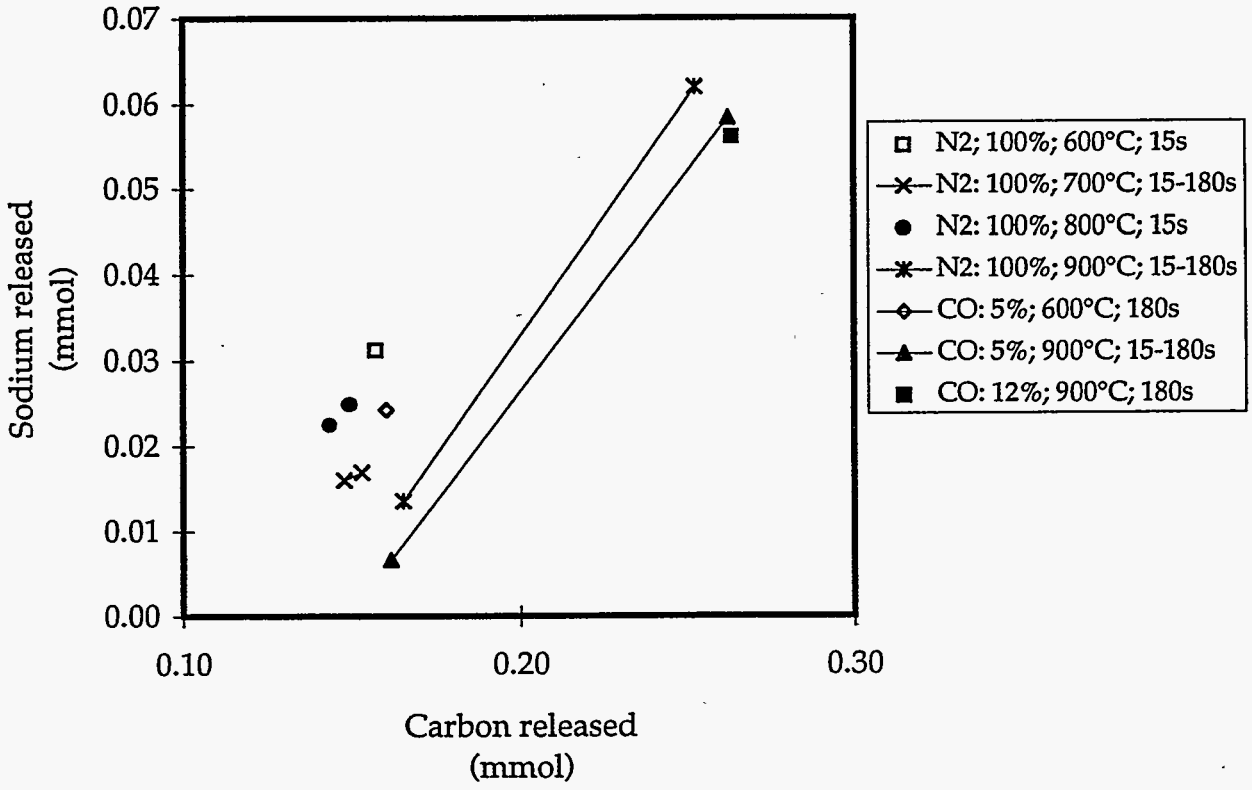

Figure IV.B-16. Sodium released as function of carbon released for pyrolysis of black liquor A at 600-900°C in an inert gas atmosphere.

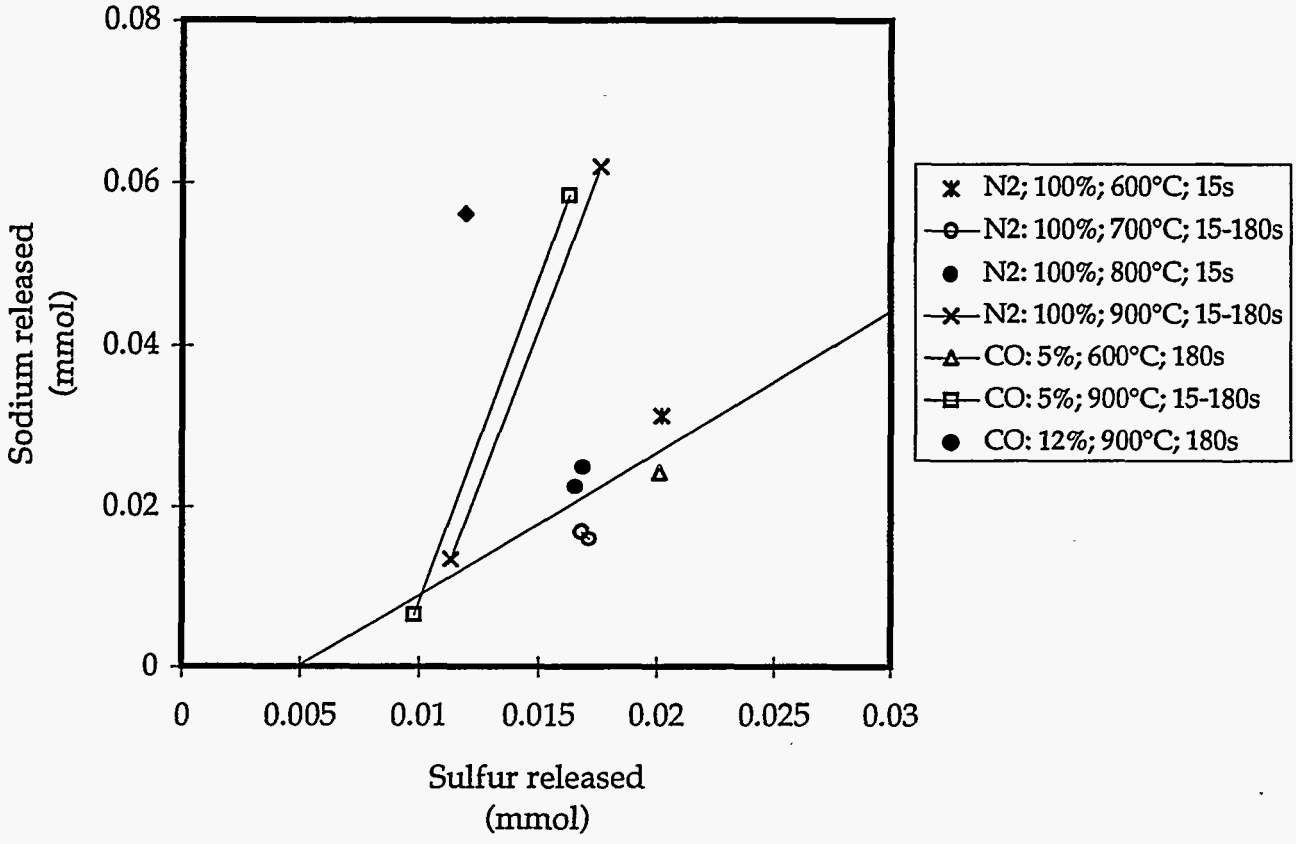

Figure IV.B-17. Sodium released as function of sulfur released for pyrolysis of black liquor A at 600-900°C in inert gas atmosphere.

4. Fixed carbon is the difference between the carbon analyzed and the amount that is included in the Na_2CO_3.

The initial contents of Na_2S and Na_2CO_3 are calculated with the assumptions that, 40% of the sodium initially in the char is inorganic and the rest is organically bound, and 60% of the initial sulfur is inorganic and the rest 40% is organically bound. These values are taken from the analysis of different black liquors made by Söderhjelm et al. (1989). Total Na, S and C in this work was analyzed by Analytische Laboratorien in Germany.

Figure IV.B-18 shows that the Na_2S content in char decreases at lower temperatures during devolatilization. The initial value of Na_2S is calculated as if the organically bound sulfur has been converted to Na_2S. The data in Figure IV.B-18 implies that all the organic sulfur would be released as well as part of the inorganic sulfur and that the organic reactions are important during devolatilization.

Figure IV.B-19 shows the sodium bound as Na_2CO_3 when all the sulfur in char is bound to sodium as Na_2SO_x as stated above. The Na_2CO_3 level increases dramatically at all temperatures, by a factor of 5-6 over the value in black liquor solids. These values are higher than earlier reported by Li and van Heiningen (1990) and McKeough et al. (1994), both of whom reported a increase of about 100% in the Na_2CO_3. The level of Na_2CO_3 stays constant for all the 15 seconds of the devolatilization experiments. At durations of 180 seconds the level of Na_2CO_3 did not decrease at 600 or 700°C. Only at 900°C was the amount of Na_2CO_3 much lower. The addition of CO at levels of 5% or 12% apparently did not hinder the Na_2CO_3 decomposition. Li and van Heiningen found that without the suppressing effect of CO in the carrier gas, the Na_2CO_3 started to decompose by 750°C and Na_2CO_3 decomposition increased greatly at 800°C. Na_2CO_3 had decomposed totally by 800°C in about 100 minute in their experiments. With our much shorter reaction times, a significant decomposition may not be not be observable at 800°C.

Figure IV.B-20 shows the amount of fixed carbon left in char, i.e. all the remaining carbon that is not bound as Na_2CO_3. The amount of fixed carbon decreased to about half of that in black liquor because the loss of carbon during devolatilization. A part of the carbon is converted to Na_2CO_3 as mentioned in the previous paragraph. The amount of fixed carbon in the char is at the same level for all experiments except those at 900°C and 180 seconds exposure time. This implies that the yield of fixed char carbon from devolatilization is independent of temperature. At 900°C the amount of fixed carbon decreases when the droplet residue is kept in the hot environment for 180 seconds. The decrease of fixed carbon is about 0.1 mmole, but the decrease of carbon due to Na_2CO_3 decomposition is, from Figure IV.B-13, only 0.02 mmole. The additional loss of fixed carbon is therefore due to some other reaction, probably by the faster reaction of Na_2SO_4 reduction by carbon in char with formation of Na_2S.

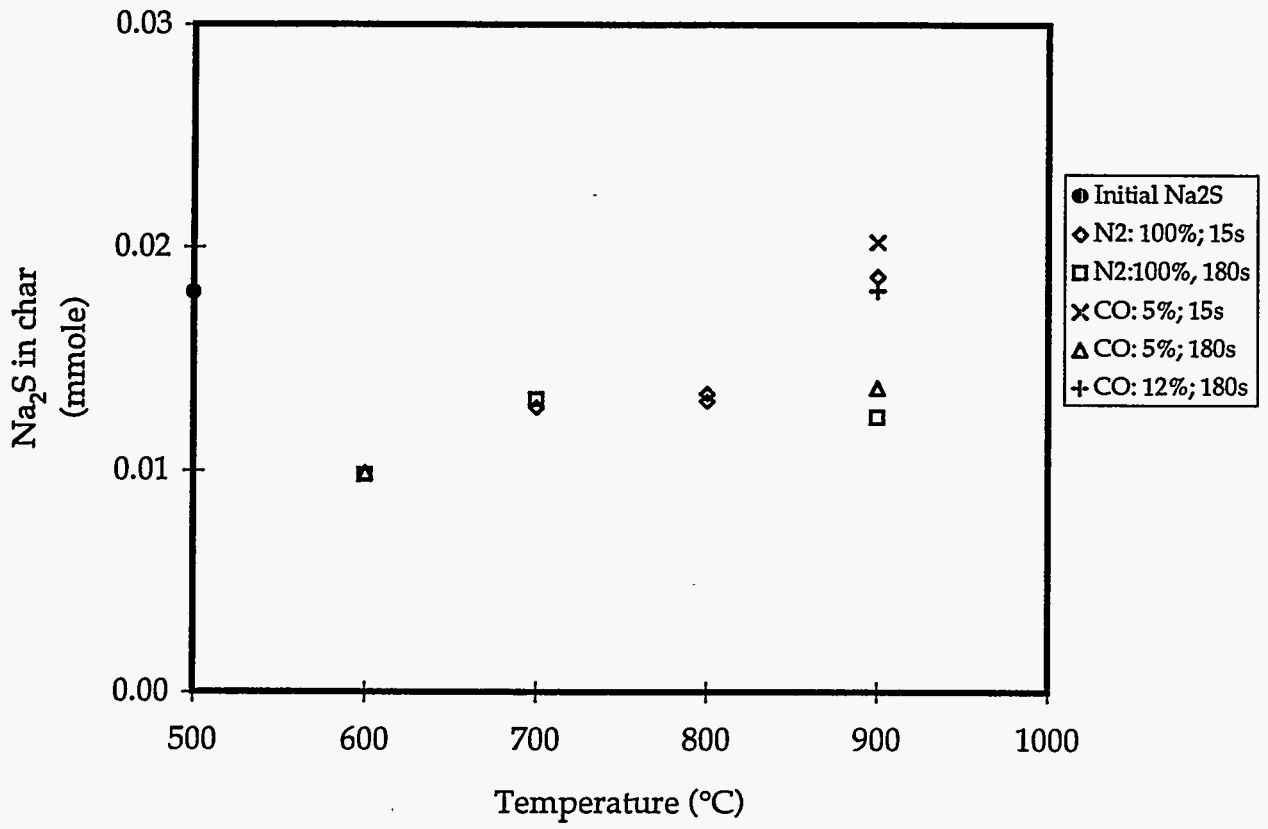

Figure IV.B-18. Sodium bound to sulfur as function of temperature for pyrolysis of black liquor A at 600-900°C in inert gas atmosphere. Sulfur bound as Na_2S, Na_2SO_4 or Na_2SO_3.

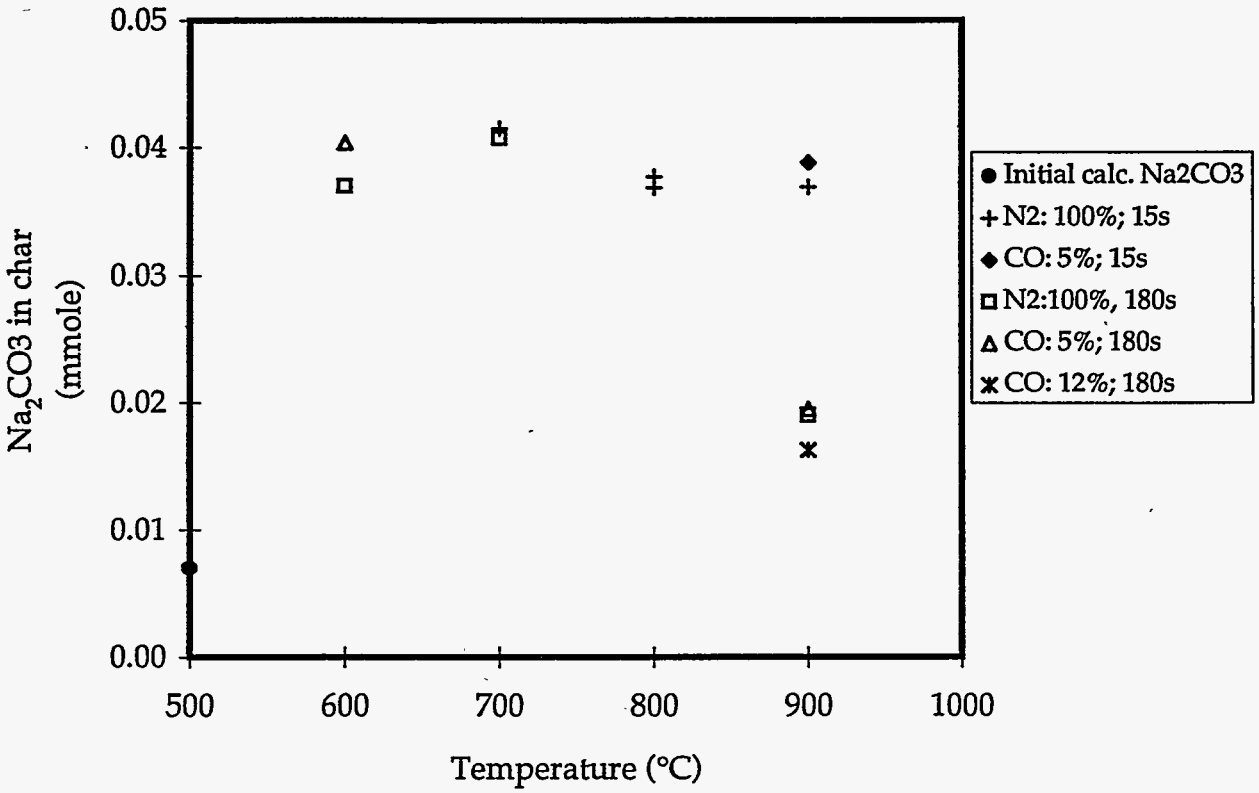

Figure IV.B-19. Sodium as carbonate as function of temperature for pyrolysis of black liquor A at 600-900°C in inert gas atmosphere. Sulfur bound as Na_2S, Na_2SO_4 or Na_2SO_3 in part a and as $Na_2S_2O_3$ in part b.

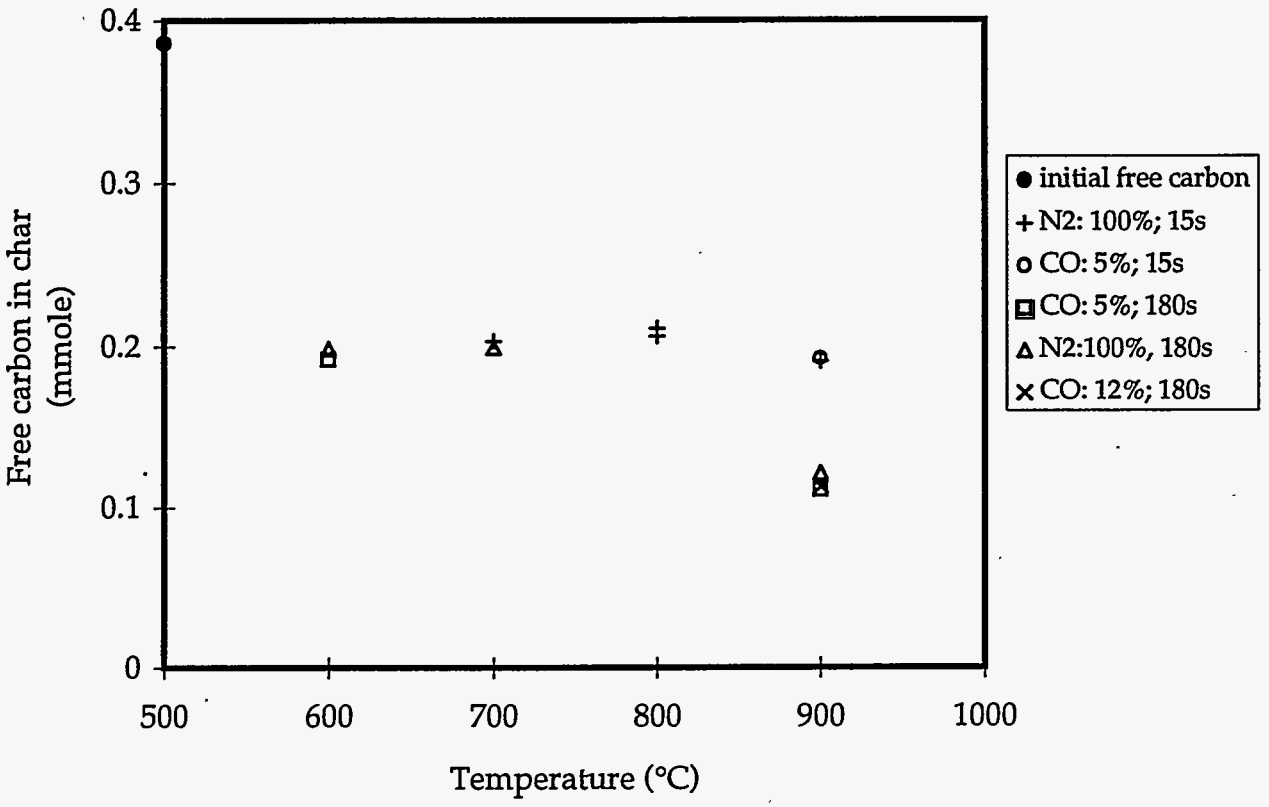

Figure IV.B-20. Fixed carbon as function of temperature for pyrolysis of black liquor A at 600-900°C in inert gas atmosphere. Sulfur bound as Na_2S, Na_2SO_4 or Na_2SO_3.

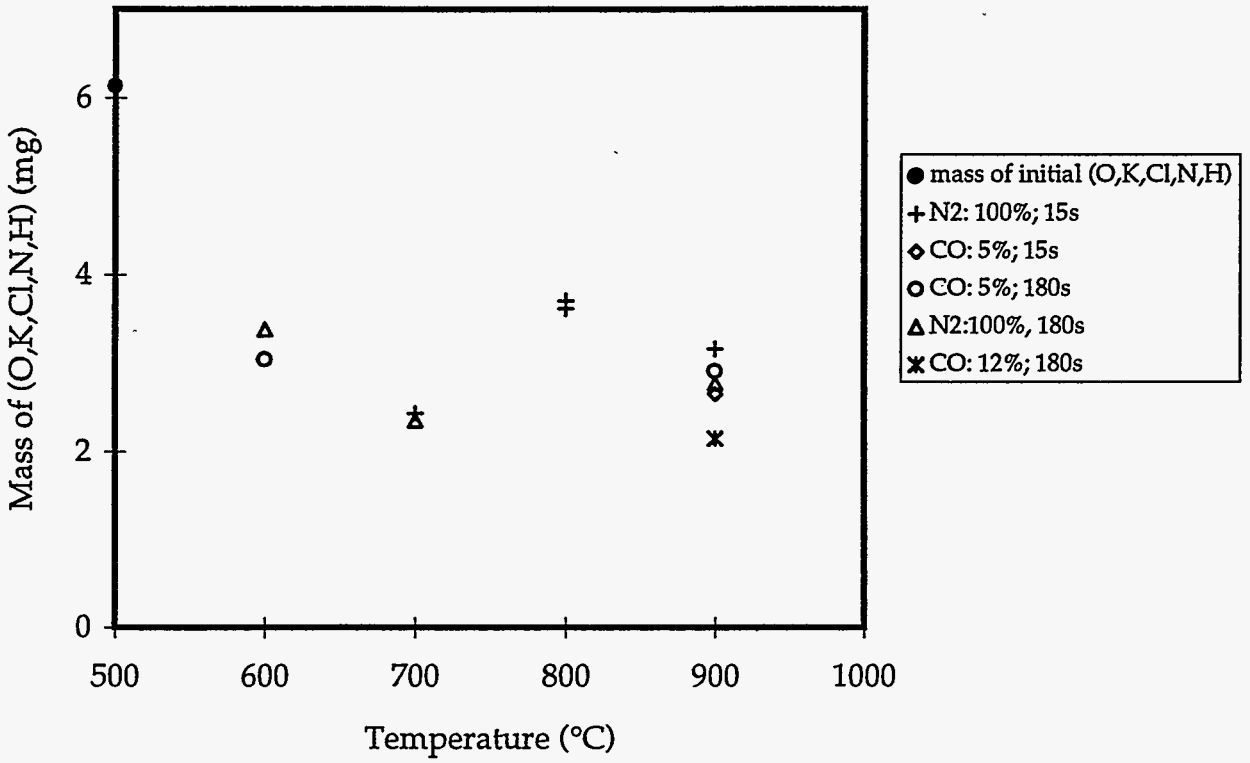

Figure IV.B-21. The rest of the mass as function of temperature for pyrolysis of black liquor A at 600-900°C in inert gas atmosphere. Sulfur bound as Na_2S, Na_2SO_4 or Na_2SO_3.

Comparison of Flow and Stagnant Reactor Data

a. Single Droplet/Flow Reactor Data

Verrill et al. (1994) reported a strong decrease in sodium loss from suspended single droplets as the gas velocity past the droplets increased. Our results fit with that trend (Figure IV.B-22).

b. Åbo Akademi University Fume Reactor Data

The data in Figures IV.B-8 – IV.B-22 show the sodium *retained* in droplets that had been pyrolyzed, but the fate of the sodium released from the droplets was not determined. Additional experiments were conducted in which both the char residue and the sodium volatilized were collected. In these experiments, black liquor char particles were dropped into a hot, cylindrical reactor with an upflowing gas. The char particles fell to and were collected on a porous support plate located near the mid-length of the cylinder. Each experiment was conducted for five minutes. The sodium released was collected on a filter downstream of the reactor. Details of the reactor design and the experimental procedure are given in Section IV.A.2 of this report.

Table IV.B-8 contains the data obtained in these experiments for temperatures of 700°C and 800°C. The mean values for fume yield and the standard deviations at each condition are shown in Figure IV.B-23. In these experiments, the fume yield increased with increasing temperature and was greater when O_2 was present in the gas phase. The presence of CO_2 in the gas phase suppressed fume formation when compared to the results both in N_2 and in 2% O_2.

Closure of the sodium material balance in these experiments was reasonable, averaging between 84 and 94%. The last column in Table IV.B-8 shows how much fume could have been generated if all of the unaccounted sodium were fume. The qualitative conclusions regarding the effect of temperature would not be changed if all of the unaccounted sodium were fume, but the conclusion that CO_2 suppresses fume formation relative to that for particles heated in N_2 would not be valid.

Additional experiments were conducted at 1000°C. Only 20-30% of the sodium was retained in the char residue, suggesting that the rate of fume generation was much higher (Table IV.B-9). In these experiments, fume generation occurred so rapidly that some of the fume escaped through the feed valve as the particles were being injected. Also, fume particles were observed to leak from the reactor at the joint between the main reactor tube and the feeder after the feed valve was closed. Closure of the sodium material balance was poorer in these runs, with about 40% of the sodium input accounted for (Table IV.B-9).

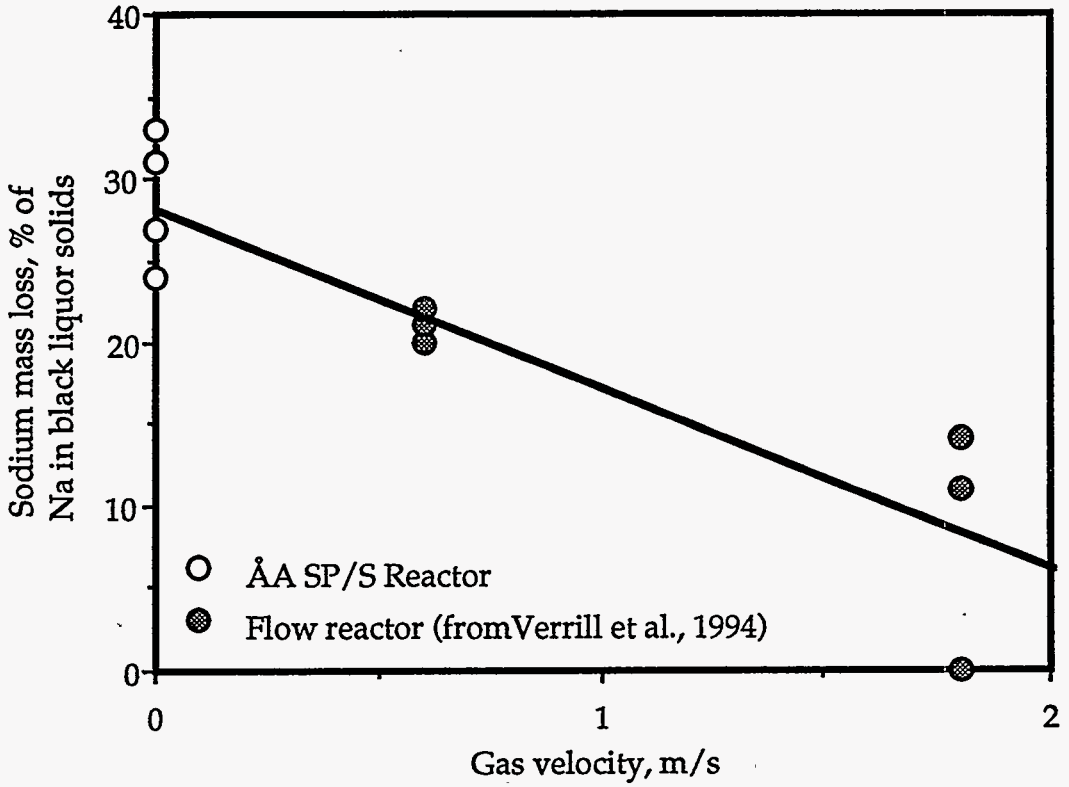

Figure IV.B.22. Effect of gas velocity past pyrolyzing suspended droplets on the sodium loss from the droplet. Experimental temperatures were 700°C (data from this study) and 750°C (Verrill et al., 1994).

Table IV.B-8. Sodium release data for char particles reacted for five minutes at 700°C or 800°C and the gas compositions indicated.

Gases	Temperature °C	Run No.	Sodium, % of Input			Fume Plus Unaccounted Na
			Char Residue	Fume	Total	
N_2	800	14	81.3	7.9	89.2	18.7
		16	96.5	1.8	98.4	3.5
		17	93.0	2.3	95.2	7.0
		18	79.5	13.4	92.9	20.5
		Average	87.6	6.3	93.9	12.4
		St. Dev	8.4	5.4	3.9	8.4
2% O_2	700	36	84.0	2.5	86.5	16.0
		37	82.5	1.9	84.4	17.6
		38	77.7	4.9	82.6	22.3
		Average	81.4	3.1	84.5	18.6
		St. Dev	3.3	1.6	2.0	3.3
2% O_2	800	19	77.3	6.0	83.2	22.7
		20	65.9	19.0	84.9	34.1
		21	66.2	14.2	80.4	33.8
		22	74.6	9.8	84.4	25.4
		Average	71.0	12.2	83.2	29.0
		St. Dev	5.8	5.6	2.0	5.8
2% O_2, 20% CO_2	800	25	82.1	1.6	83.7	18.0
		26	91.6	1.1	92.7	8.4
		27	84.5	1.6	86.1	15.6
		Average	86.0	1.5	87.5	14.0
		St. Dev	5.0	0.3	4.7	5.0

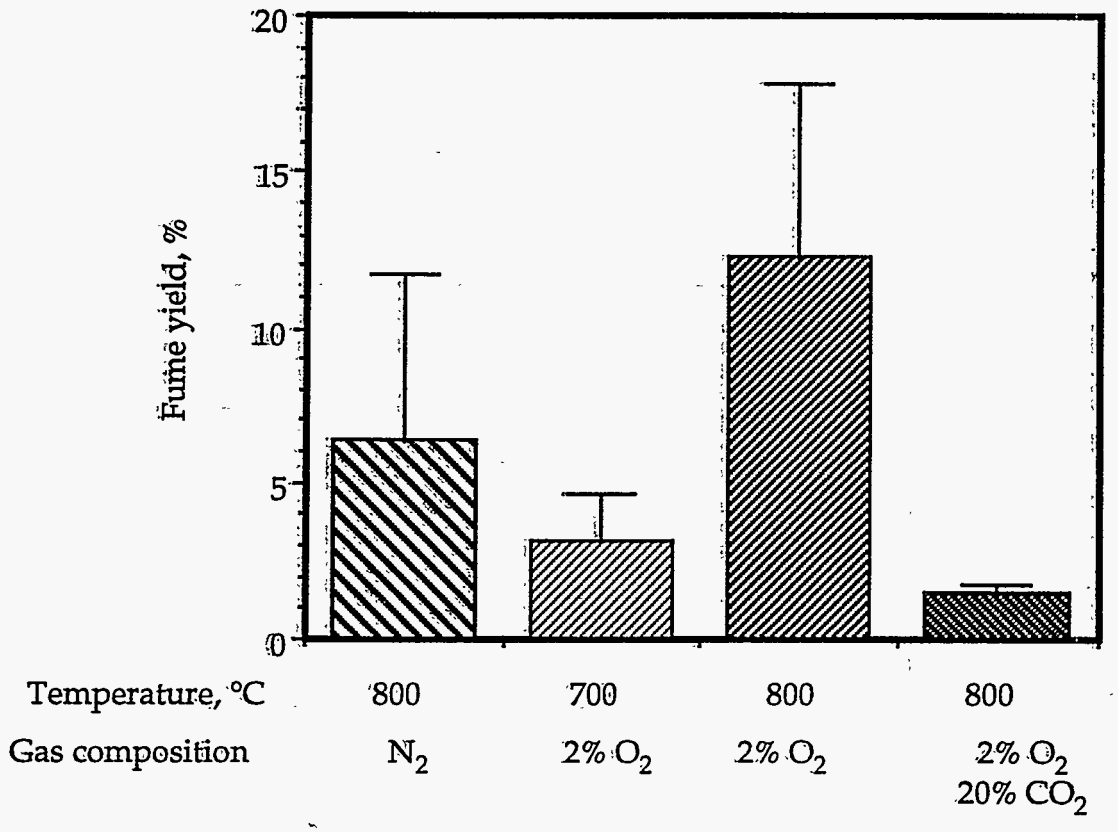

Figure IV.B.23. Summary of sodium release data for char particles reacted for five minutes at the temperatures and gas compositions indicated. The error bars indicate one standard deviation.

Table IV.B-9. Sodium release data for char particles reacted for five minutes at 1000°C and the gas compositions indicated.

Gases	Temperature °C	Run No.	Sodium, % of input		
			Char Residue	Fume	Total
2% O_2	1000	40	28.8	12.1	40.9
		41	19.1	20.2	39.3
		42	22.7	10.8	33.5
		Average	23.5	14.4	37.9
		St. Dev	4.9	5.1	3.9

c. OSU Laminar Entrained Flow Reactor Data

Fume yields were measured during pyrolysis and combustion experiments using the OSU laminar entrained-flow reactor. In these experiments, 100 μm particles of dry black liquor solids were pyrolyzed or burned for 0.6-0.8 s. The composition of the liquor solids used are listed in Table IV.B-10. The experimental procedure is described in detail in Section IV.A.3 of this report. Figures IV.B-24 and IV.B-25 show the amount of material collected on the post-cyclone filter and the sodium in the filter catch as a fraction of the sodium in the black liquor solids. The numerical data are included in Table IV.B-11.

Table IV.B-10. Composition of the liquor solids

Element	Weight %
Carbon	34.90
Hydrogen	3.05
Oxygen[1]	35.10
Sodium	22.65
Sulfur	2.90
Potassium	0.62
Chlorine	0.67
Nitrogen	0.11

% by difference

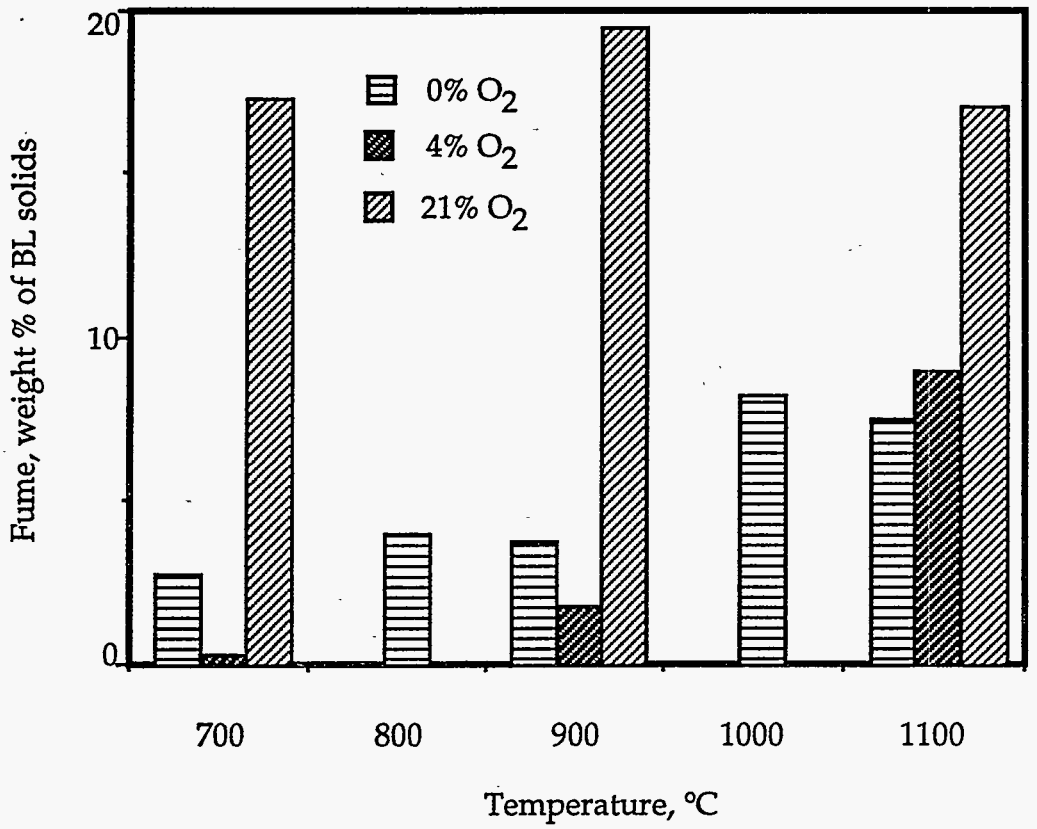

Figure IV.B.24. Fume yield as measured by the post-cycle filter catch versus furnace temperature and furnace oxygen concentration for 100 μm dry black liquor particles pyrolyzed or burned for 0.5 seconds.

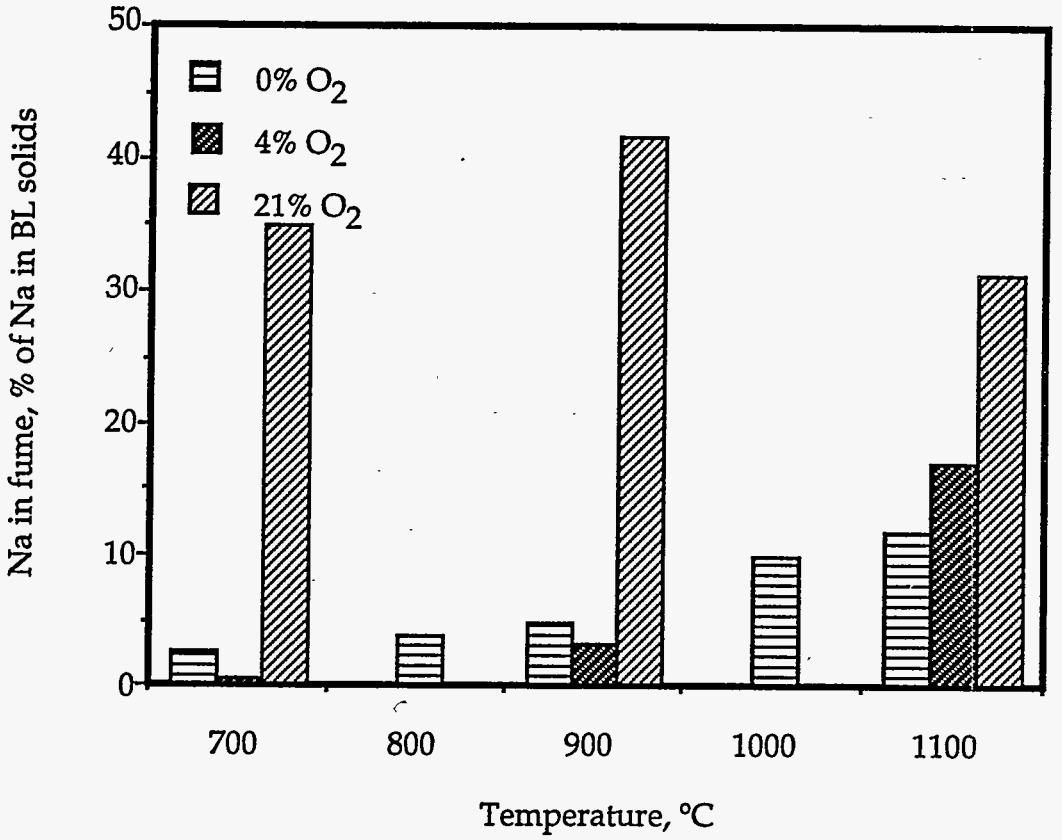

Figure IV.B.25. Sodium yield as fume as measured by the post-cyclone filter catch versus furnace temperature and furnace oxygen concentration for 100 μm dry black liquor particles pyrolyzed or burned for 0.5 seconds.

Table IV.B-11. Fume generated and sodium in fume for laminar entrained-flow reactor experiments at 700-1100°C, 0-21% O_2

Temperature °C	Residence Time, s	Furnace O_2 Content, %	Fume, Weight % BL Solids[1]	Na in Fume, % of Na in BL Solids
700	0.80	0.00	2.80	2.45
700	0.80	4.00	0.30	0.45
700	0.80	21.00	17.32	34.90
800	0.75	0.00	4.04	3.75
900	0.70	0.00	3.73	4.65
900	0.70	4.00	1.81	3.15
900	0.70	21.00	19.48	41.70
1000	0.65	0.00	8.26	9.85
1100	0.60	0.00	7.53	11.55
1100	0.60	4.00	9.01	16.95
1100	0.60	21.00	17.05	31.30

Figure IV.B-25 shows the yield of inorganic fume in these experiments. The fume yield at lower oxygen contents and furnace temperatures was relatively low, less than 3% of the black liquor solids mass. The mass of sodium per gram of black liquor solids in these fume particles increased rapidly with temperature. The yield of fume and of sodium as fume increased both with increasing furnace oxygen concentration and with increasing furnace temperature. For particles burned in air, 30-40% of the sodium in the black liquor solids was collected as fume.

The composition of the fume collected in these experiments was rich in K- and Cl-rich at lower reactor temperatures and oxygen contents. For particles reacted at 700-900°C in N_2 and 4% O_2 (Figures IV.B-26 – IV.B-27), the fume collected was only about 1% of the black liquor solids mass, or 2-3% of the inorganic in the black liquor solids. These fume particles were relatively rich in K and Cl. At higher temperatures and oxygen contents, the mass of K and Cl volatilized increased (Figures IV.B-26 – IV.B-28), but the amount of sodium volatilized increased even more rapidly. The net result was lower K/Na and Cl/Na ratios in the fume particles collected at the higher temperatures and oxygen contents.

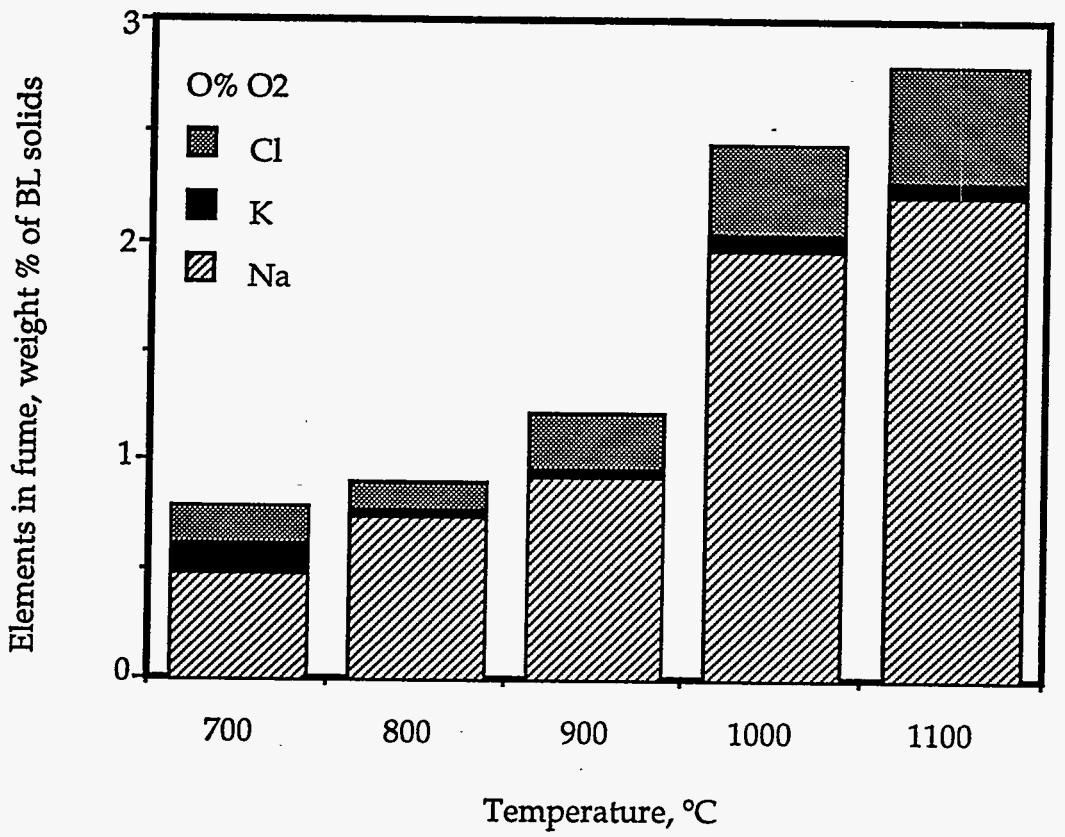

Figure IV.B.26. The amounts of Na, K, and Cl released during pyrolysis of 100 μm dry black liquor particles in N_2 in a laminar entrained-flow reactor, 0.5 s residence time.

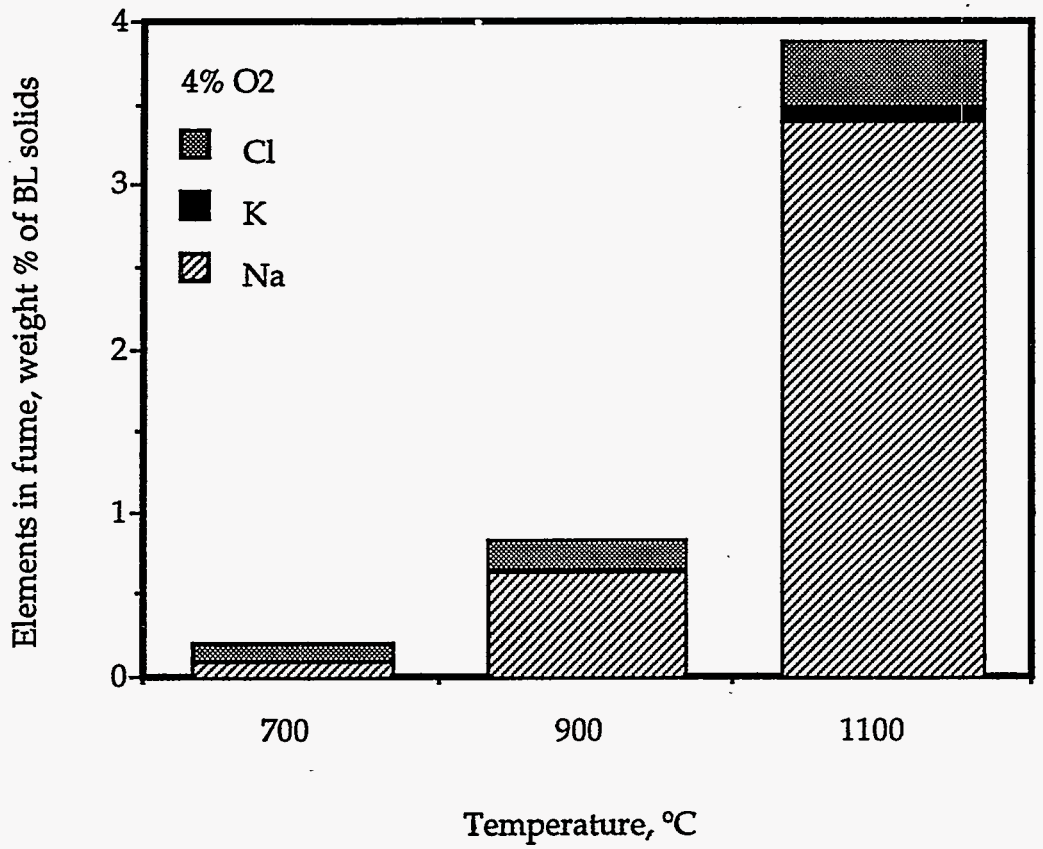

Figure IV.B.27. The amounts of Na, K, and Cl released during combustion of 100 μm dry black liquor particles in 4% O_2/96% N_2 in a laminar entrained-flow reactor, 0.5 s residence time.

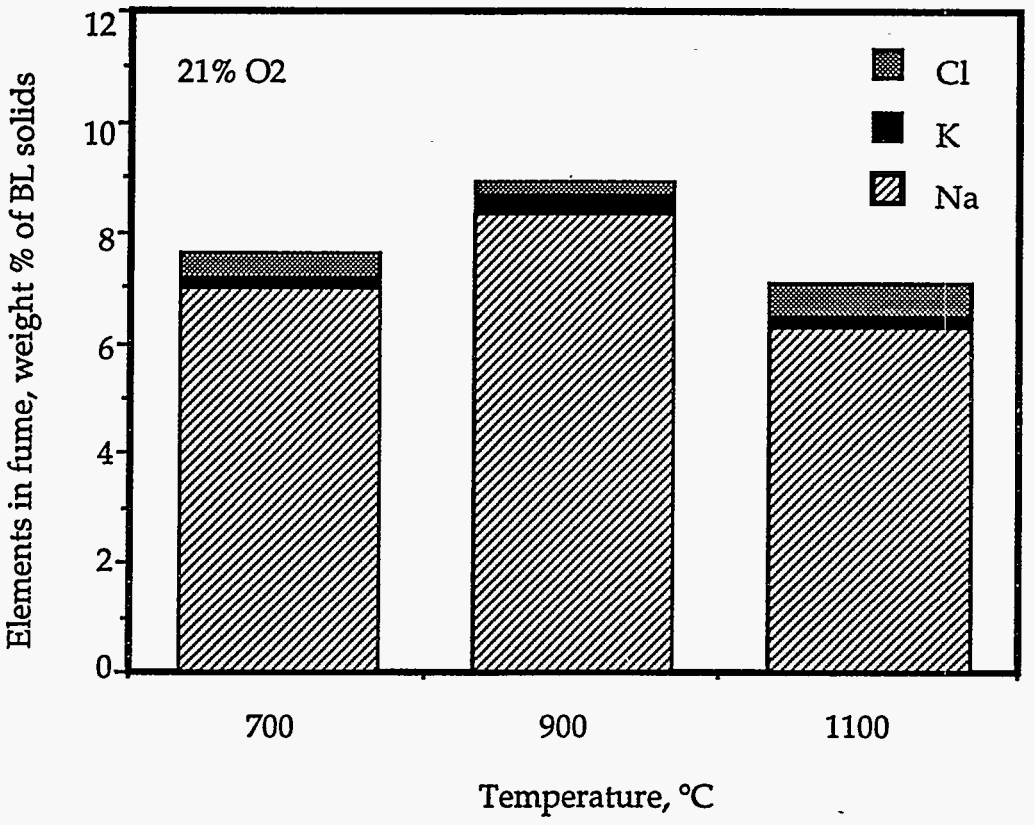

Figure IV.B.28. The amounts of Na, K, and Cl released during combustion of 100 μm dry black liquor particles in 21% O_2/79% N_2 in a laminar entrained-flow reactor, 0.5 s residence time.

Interpretation

A. Na Release During Devolatilization

The experimental data on sodium release during devolatilization of black liquor particles fall into two categories. In all studies with single droplets of the size typically burned in recovery boilers, a significant loss of Na from the droplets, 10-30% of the Na in the black liquor at temperatures from 500-900°C, was reported in several studies (Volkov et al., Verrill et al., Frederick and Hupa) including this work. Fume particles were not collected or measured in any of these experiments.

In experiments with smaller particles (laminar entrained-flow reactor and grid heater experiments), there was little or no Na loss at lower temperatures, 700°C and below. The experiments of McKeough et al. (1995) showed clearly no Na loss. The LEFR experiments conducted in this study showed that less than 3% of the Na in black liquor solids was collected as sub 3 micron fume at 700°C in either N_2 or low oxygen content environments. Further, the inorganic fume collected at 700°C was mainly NaCl and KCl (Figures IV.B.26 – IV.B.28), suggesting that fume formation at these low temperatures may be due mainly to vaporization of these salts.

The greater loss of Na from the larger droplets during devolatilization may be due to ejection of small liquor particles during drying and devolatilization and/or shedding of fragments of black liquor char as the particles react as suggested by Verrill et al. (1994). Convective transport of atomically or finely dispersed mineral matter has been shown to be an important mechanism of release of non-volatile metals in coal combustion. Baxter et al. (1990) showed, for example, that titanium, which exists in coal as complexes with oxygen or as organically bound Ti and is essentially nonvolatile, is lost by convective transport from coal particles during devolatilization. The amount of Ti loss depended upon the heating rate. For 75-106 and 106-125 μm coal particles heated at 10^4 K/s, there was no loss of Ti. At 10^5 K/s, 3-4% of the Ti originally in the coal particles was lost from the residue, while at 5×10^5 K/s, 10-20% of the Ti was lost from the residue. The heating rates employed by Baxter et al. are much higher than those encountered by black liquor droplets except at the external surface. However, the organic matter in black liquor is much more volatile than that of coal, and may enhance physical ejection or shedding of small particles from pyrolyzing or burning droplets.

Physical ejection could account for the particles in the diameter range 1-30 microns that were reported by Verrill and Nichols (1994). Kauppinen et al. (1993), who measured the size distribution of fine particles from black liquor combustion in the gases from both recovery boilers and a laboratory entrained flow reactor, reported a bimodal distribution, with peaks in the range 0.1-1 μm and 1-30 μm. The smaller particles were clearly fume particles but the larger ones may have been formed by ejection of particles from burning droplets or other mechanisms of breakup of burning black liquor droplets.

Another possible mechanism for Na release while devolatilization is occurring is the reduction of Na_2CO_3, releasing Na vapor. This reaction is very temperature sensitive as indicated by the high activation energy (244 kJ/mol) reported by Li and van Heiningen (1990). Their rate equation predicts that very little sodium would be volatilized by Na_2CO_3 reduction at 700-800°C but that the Na loss from Na_2CO_3 reduction could be significant at 900°C. The data of Volkov et al. (1980) in Figures 1 and 2 suggests that at typical recovery furnace temperatures the Na release mechanism may be the same over the entire droplet burning time. This may mean that the exterior surface devolatilizes rapidly and in effect loses sodium via Na_2CO_3 reduction by char carbon even when most of the droplet mass is still devolatilizing.

We therefore suggest that there are three mechanisms of sodium loss from black liquor particles during the ***devolatilization*** stage of black liquor:

1. Vaporization of NaCl, forming sub-micron fume particles. This can occur at the lower temperatures at which many of the sodium release experiments were conducted.

2. Ejection or shedding of small liquor particles or char fragments from droplets during drying and devolatilization. These would form particles larger than the typical 0.1-1 μm fume particles.

3. Reduction of Na_2CO_3 by char carbon during devolatilization. This would occur to a significant extent only at higher furnace temperatures, where droplets are charred on the outside while still devolatilizing on the inside, and where temperatures are high enough for Na_2CO_3 reduction to occur rapidly.

The relative importance of each of these depends upon the temperature of the gases very near the particle and the particle heating rate.

B. Na Release During Char Burning and Gasification

The data strongly supports Na_2CO_3 reduction as the source of Na fume during char burning. The work of Li and van Heiningen (1990) showed that reduction of sodium carbonate in black liquor char can account for the loss of sodium from char. The experimental results for char reactions obtained in this study are consistent with mechanism.

An important question with respect to recovery boilers is how important is suppression of Na_2CO_3 reduction by CO or CO_2. Li and van Heiningen (1990) indicated that Na volatilization from black liquor char could be suppressed completely in the presence of CO at 800°C and below. Our data indicates that suppression occurs with either CO or CO_2 at 800°C and below but not at higher temperatures.

To evaluate this, we first examine possible pathways for reduction of Na_2CO_3. These include

$$Na_2CO_3 + 2C \rightleftarrows 2\,Na + 3\,CO \quad (1)$$

$$2\,Na_2CO_3 + C \rightleftarrows 4\,Na + 3\,CO_2 \quad (2)$$

$$Na_2CO_3 + C \rightleftarrows 2\,Na + CO + CO_2 \quad (3)$$

$$Na_2CO_3 + 1/4\,Na_2S \rightleftarrows 2\,Na + CO_2 + 1/4\,Na_2SO_4 \quad (4)$$

Reaction 3 is the sum of reactions 1 and 2.

The equilibrium sodium vapor partial pressures, calculated for each of these reactions at two different CO and CO_2 partial pressures, are shown in Table IV.B-12. These results show two important points. The first is that the equilibrium sodium vapor partial pressure from the reduction of Na_2CO_3 with carbon is much greater than that obtained by reduction with Na_2S. The second point is that the equilibrium sodium vapor partial pressure increases rapidly with temperature, and can exceed 1 bar at temperatures obtained in recovery boilers. When the sodium vapor partial pressure exceeds 1 bar, suppression by CO and CO_2 in effect no longer occurs, since the local sodium vapor pressure cannot exceed the combustor (atmospheric) pressure.

The data on inhibition by CO and CO_2 of Na_2CO_3 reduction indicates that inhibition occurs at 800°C and below but not at higher temperatures. The data available are summarized in Table IV.B-13.

Sodium loss from the single droplets at 800°C and below may have been from shedding or physical ejection of small particles as discussed earlier. Otherwise, CO and CO_2 apparently suppress sodium volatilization at 800°C and below but not at higher temperatures.

The mechanism of reduction of alkali metal carbonates and reoxidation of the resulting reduced surface groups has been investigated in the context of alkali metal catalyzed gasification of carbon. Sams and Shadman (1986) proposed the following multi-step mechanism for the reduction of alkali metal carbonates (shown here for Na_2CO_3):

$$Na_2CO_3 \xrightarrow{C} (\text{-}CO_2Na) + (\text{-}CONa) \quad (5)$$

$$(\text{-}CO_2Na) + C \rightleftarrows (\text{-}CNa) + CO_2 \quad (6)$$

$$(\text{-}CO_2Na) + C \rightleftarrows (\text{-}CONa) + CO \quad (7)$$

$$(\text{-}CONa) + C \rightleftarrows (\text{-}CNa) + CO \quad (8)$$

$$(\text{-}CNa) \rightarrow Na_{(v)} \quad (9)$$

Table IV.B-12. Equilibrium sodium vapor partial pressures versus temperature for reactions 1-4 at various CO and CO_2 partial pressures.

Temperature	Na_2CO_3 Reduction			
	by Carbon			by Na_2S
	Rxn 1	Rxn2	Rxn 3	Rxn 4
0.1 bar CO, 0.1 bar CO_2				
1000	.834	.00129	.0111	8.36×10^{-5}
1100	19.6	.0128	.104	.000706
1200	293	.0906	1.34	.00438
1.0 bar CO, 1.0 bar CO_2				
1000	.0093626	.000229	.000788	2.64×10^{-5}
1100	.219	.00227	.0104	.000223
1200	3.27	.0161	.0947	.00138
1.0 bar CO, 0.0001 bar CO_2				
1000	.00933	.229	.0788	.00264
1100	.219	2.27	1.042	.0223
1200	3.27	16.1	9.47	.138
0.0001 bar CO, 0.0001 bar CO_2				
1000	9320	.229	7.88	.00264
1100	219,000	2.27	104	.0223
1200	3.27×10^{-6}	16.1	947	.138

Table IV.B-13. Summary of experimental data on inhibition by CO and CO_2 of Na_2CO_3 reduction.

Temperature	Gas Composition (total pressure)	Result	Study
≤800°C	10-12% CO, 0-20% CO_2 in He (1 bar)	No carbonate reduction or Na volatilization in thermo-balance experiments	Li and van Heiningen (1990)
≤800°C	10-40% CO_2 (1-30 bar)	No Na volatilization in thermobalance experiments	Frederick et al. (1993)
800°C	This study	Reduction in Na volatilized from char particles	This study
900°C	12% CO	No reduction in Na volatilized from single droplets	This study
1000°C	20% CO_2, 10% CO, 20% $H_2O_{(v)}$, 10% He in N_2	No reduction in Na volatilized in LEFR measurements	This study
600, 900°C	N_2	No Na volatilization at 600°C; large losses at 900°C	McKeough et al. (1994)
600°C	5% CO or 20% CO_2	Na loss from black liquor droplets was significant at both temperatures	Verrill et al. (1994)
900°C	5% CO		

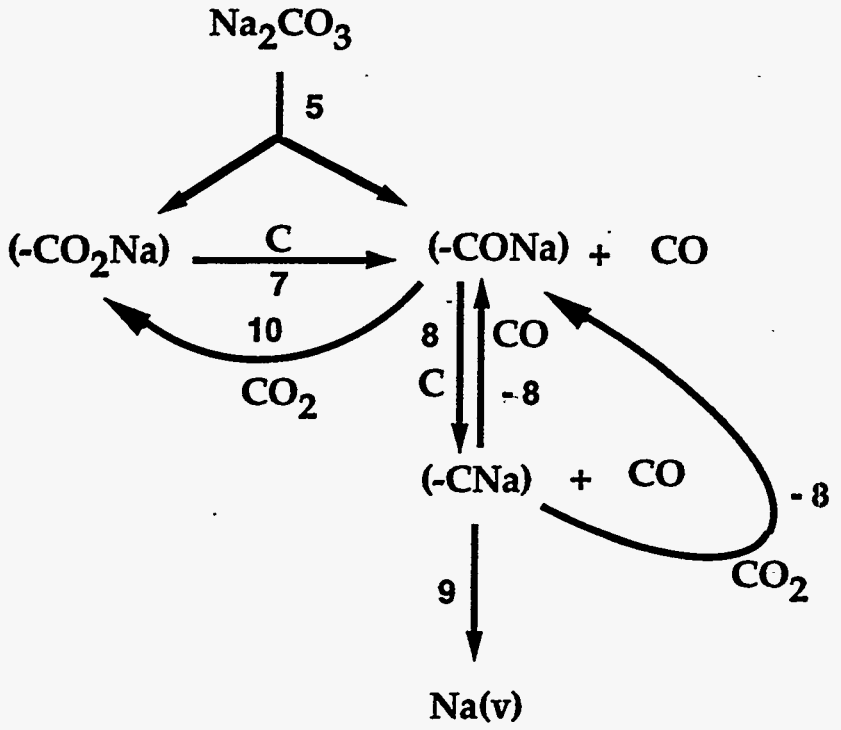

Figure IV.B-29. Reaction path diagram for Na_2CO_3 reduction and Na volatilization in black liquor char.

There is currently no data available on the effects of CO and CO_2 partial pressures on the rate of Na_2CO_3 reduction, and it is not known whether reaction 9 is reversible. These are part of ongoing work at Oregon State University on the kinetics of Na_2CO_3 reduction in black liquor chars.

References

Baxter, L.L., Mitchell, R.E., and Fletcher, T.H. (1990), "Experimental Determination of Mineral Matter Release During Coal Devolatilization," *Proc. Seventh Ann. Intl. Pittsburgh Coal Conference*, pp. 62-71, September 10-14.

Borg, A., Teder, A., and Warnqvist, B. (1974), *Tappi*, 57(1):126-129.

Cameron, J.H. *(1988), Chem. Eng. Comm.*, 59:243-257.

Frederick, W.J. (1990), Combustion Processes in Black Liquor Recovery: Analysis and Interpretation of Combustion Rate Data and an Dngineering Design Model. US DOE Report DOE/CE/40637-T8 (DE90012712), March.

Frederick, W.J. and Hupa, M. (1994b), "The Effects of Temperature and Gas Composition on Swelling of Black Liquor Droplets During Devolatilization," *J. Pulp Paper Sci.* (October)

Frederick, W.J., Hupa, M., Stenberg, J., Hernberg, R. (1994a), "Optical Pyrometric Measurements of Surface Temperatures During Black Liquor Char Burning and Gasification," accepted for publication in the December issue of *Fuel.*

Frederick, W.J., Hupa, M., and Uusikartano, T. (1994c), "Volatiles and Char Carbon Yields During Black Liquor Pyrolysis," *Bioresource Technology*, 48:59-64.

Frederick, W.J., Wåg, K., and Hupa, M. (1993), "Rate and Mechanism of Black Liquor Char Gasification with CO_2 at Elevated Pressures," *Ind. Eng. Chem. Research*, 32(8):1747-1753.

Hyöty, P., Hupa, M., Skrifuars, B.-J., and Karki, R. (1989), *Proc. 1989 TAPPI-CPPA Intl. Chem. Recovery Conf.*, TAPPI Press, Atlanta, p. 169.

Kauppinen, E.I., Mikkanen, P., Jokiniemi, J.K., Iisa, K., Boonsongsup, L., Sinquefield, S.A., and Frederick, W.J. (1993), "Fume Particle Characteristics and Their Reactions with SO_2 at Kraft Recovery Boiler Conditions," *Proc. 1993 TAPPI Engineering Conf.*, TAPPI Press, Atlanta, pp. 369-376.

Levenspiel, O. (1972), *Chemical Reaction Engineering*, 2nd ed., John Wiley & Sons, New York.

Li, J. and van Heiningen, A.R.P. (1990), *Tappi Jl.*, 73(12):213-219.

McKeough, P., Arpiainen, V., Venelampi, E., and Alén, R. (1994), *Paperi ja Puu*, 76(10):650-656.

Pejryd, L. and Hupa, M. (1984), "Bed and Furnace Gas Compositions in Recovery Boilers – Advanced Equilibrium Calculations," *Proc. 1984 TAPPI Pulping Conf.*, San Francisco, November.

Sams, D.A. and Shadman, F. (1986), *AIChE Jl.*, 32(7):1132-1137.

Söderhjelm, L., Hupa, M., and Noopila, T. (1989), *J. Pulp and Paper Science*, 15(4):J117-J122.

Verrill, C.L. (1992), "Inorganic Aerosol Formation During Black Liquor Droplet Combustion," PhD Thesis, The Institute of Paper Science and Technology, Atlanta.

Verrill, C.L., Grace, T.M., and Nichols, K.M. (1994), "The Significance of Sodium Release During Devolatilization Fume Formation in Kraft Recovery Boilers," accepted for publication in the *Jl. Pulp Paper Sci.*

Verrill, C.L. and Nichols, K.M. (1994), "Inorganic Aerosol Formation During Black Liquor Drop Combustion," *AIChE Symp. Ser.*, 90(302):55-72.

Volkov, A.D., Evseev, O.D., Ibatullina, R.I. Dravolina, E.I., Meszhvuz (1980), Sb. Nauchn. Tr. Ser. Khim. Teknol. Tsellyul. no. 7, 72-5, Institute of Paper Chemistry translation to English.

IV.C SULFUR RELEASE

IV.C.1 Sulfur Release During Pyrolysis of Single Black Liquor Droplets

Summary

The onset and rate of sulfur release rate from black liquor droplets during devolatilization can be measured using the experimental method developed here. Sulfur release is a decomposition reaction that starts when decomposition of the organic fraction of black liquor begins. The rate is dependent on the temperature of the furnace in which the droplets are devolatilized. It is not greatly affected by the initial droplet mass in the range studied (10-70 mg).

The rate of sulfur release is influenced by both chemical kinetics and the rate of heat transfer to the black liquor droplet. Heat transfer becomes more important as temperature increases, and dominates above 700°C. In most regions of a recovery boiler, therefore, the rate of sulfur release will be controlled by the rate of heat transfer.

The amount of sulfur released during pyrolysis has been shown earlier to go through a maximum with furnace temperature. Our data indicates that the amount released is not strongly dependent on initial droplet size. The maximum in release rate with furnace temperature can be explained qualitatively in terms of competing release and recapture mechanisms; this concept remains to be tested quantitatively.

An empirical model for predicting the rate and total amount of sulfur released during devolatilization of black liquor droplets has been developed based on experimental data from this and other studies. In this model, the rate of sulfur release is proportional to the rate of carbon release, while the total amount of sulfur released is a fraction of the total sulfur in black liquor and depends only on furnace temperature.

Introduction

Kraft black liquor contains typically 4-8% sulfur which comes from the pulping chemicals. It is present in several forms:

- sulfur which is organically bound to the dissolved wood fragments as a result of the pulping reactions,
- sulfide ion (S^{2-}), a residual active pulping chemical,
- thiosulfate ($S_2O_3^{2-}$) and sulfate (SO_4^{2-}) which result from oxidation of Na_2S, makeup chemicals, and incomplete conversion of sulfur compounds to Na_2S during recovery, and
- elemental sulfur and sulfite ion, SO_3^{2-}, which may be present if they are added as makeup chemicals or as spent liquor from NSSC pulping.

Sulfur release from black liquor during pyrolysis has been a subject of several studies using a variety of different experimental ways. Brink et al. (1970), Li and van Heiningen (1991), and Faix et al. (1990) used slow pyrolysis techniques to identify the major sulfur species released during pyrolysis. In these studies hydrogen sulfide (H_2S), methyl mercaptan (CH_3SH) and dimethyl sulfide ($(CH_3)_2S$) were found to be the major sulfur containing gaseous compounds.

Experiments to determine which sulfur compounds in black liquor are the main contributors to sulfur gas formation have been made by several researchers. Douglass and Price (1968) found that $S_2O_3^{2-}$, S^{2-} and elemental sulfur are the main sources of sulfur gases under slow pyrolysis conditions. Very little sulfur was released from SO_4^{2-} or SO_3^{2-}. Strohbeen and Grace (1982) confirmed the findings for $S_2O_3^{2-}$, S^{2-}, SO_4^{2-} and SO_3^{2-}; they did not use elemental sulfur in their experiments. Harper (1989) obtained similar results in flash pyrolysis experiments. No other studies of the effect of elemental sulfur on sulfur release during pyrolysis have been reported.

In earlier studies, the total amount of sulfur released at different temperatures was dependent on the experimental procedure and influenced mainly by heating rate. In batch pyrolysis studies at low heating rates (~ 0.1°C/s) the amounts released were almost constant over the temperature range 400°C-1000°C (Brink et al., 1970). At higher heating rates (~ 100°C/s), total sulfur release went through a maximum between 400 and 700°C (Brink et al., 1970; Clay et al., 1985, 1987). In flash pyrolysis experiments (heating rates ~ 1000°C/s) Harper obtained a maximum in sulfur release at 480°C. Harper also made experiments with pyrolysis of single droplets (heating rates ~ 100°C/s) at 665°C. He found that sulfur release was not strongly dependent on droplet size, increasing by about 25% over the range 7 mg - 30 mg (2.1-3.4 mm) droplets.

Cantrell et al. (1986) measured sulfur release rates from black liquor droplets at 1090°C in oxidizing conditions (~ 100°C/s heating rates). In their experiments the main factor affecting sulfur release was droplet size. Sulfur release varied from about 80% of the total sulfur for small (1.3 mm, 1.6 mg) droplets to 10% for large (4 mm, 47 mg) droplets. Increasing the dry solids content decreased the amount of sulfur released. A change in O_2 content had essentially no affect on the amount of sulfur released, nor did addition of emulsified sulfur or sodium sulfate. Sulfur release rates typically about 1.2 mg sulfur g BLS^{-1} s^{-1} were observed for droplets burning in air/nitrogen mixtures. The rate was independent of the oxygen content of the gas phase.

While the information on sulfur release during black liquor pyrolysis is extensive, it is not adequate for modeling of sulfur release during black liquor droplet combustion or gasification. For this purpose, data on sulfur release rates under pyrolysis conditions, i.e. with no oxygen present, are needed. Prior to this work, no such data have been reported.

The objective of this work was to obtain rate and total yield data on sulfur release as a function of droplet size and temperature under pyrolysis conditions. In this chapter we present our results on the rate of sulfur release from black liquor during pyrolysis and an analysis of the overall mechanism of sulfur release as a function of pyrolysis temperature.

Results and Discussion

Sulfur Release Rate

Figure IV.C.1-1 shows the rate of sulfur release versus time for nine experiments at temperatures from 350°C to 500°C. The data are for droplet sizes of approximately 16 mg, 40 mg and 57 mg. At the lower temperatures, 350°C and 400°C, the sulfur release rate is relatively slow. A maximum in sulfur release rate occurs at the beginning of the experiment and usually two but sometimes even three peaks are observed later in the experiment. With larger droplets the second and third peak appear later than with small ones. At 400°C the peaks for small droplets are already so close to each other that it is difficult to distinguish them from each other. However larger droplets still have clearly separated peaks. At 500°C the peaks are not clearly separated; they appear as a broadening of the first peak for larger droplets but are not visible for smaller droplets. At 600°C the rate of sulfur release is so fast that it seems to be independent of droplet size. The extended time scale in Figure IV.C.1-1 is a result of the gas residence time in the reactor, oxidizer, and samples lines. Pyrolysis times are much shorter, in the order of 3-10 seconds at these conditions.

There are two possible explanations for the multiple peaks in the sulfur release versus time curves. The first is that different sulfur compounds release sulfur at different rates. While this may account for the effect, it is not likely the whole explanation since droplet size has a large effect on the number of peaks observed and the distance between them. A second and perhaps complementary factor is that sulfur may be released nonuniformly as the droplets are heated. The temperature of the droplets are not uniform during pyrolysis, and the nonuniformity would be expected to increase with increasing droplet size. Therefore the degree of pyrolysis would be expected to be less uniform with larger droplets than with smaller ones. This could account for the multiple peaks in sulfur release for larger droplets, and would be stochastic in nature.

Release of Reduced and Oxidized Sulfur Gases

Experiments were performed to examine the distribution between oxidized and reduced state of the sulfurous gases that are evolved during the pyrolysis process. Two sets of experiments were done at 700°C. In the first set the SO_2 converter was kept at 800°C but no oxygen was added in the pyrolysis gases entering the converter. In the second set of experiments the converter was run as normally with 1% O_2 at 800°C. In the second set all the reduced sulfurous gases were oxidized to SO_2, thereby the sum of all sulfurous gases was measured. The SO_2 produced during the pyrolysis was given by the measurement with no oxygen in the converter. The reduced sulfur gases was calculated as the difference between the two measurements. The result is shown in Figure IV.C.1-2.

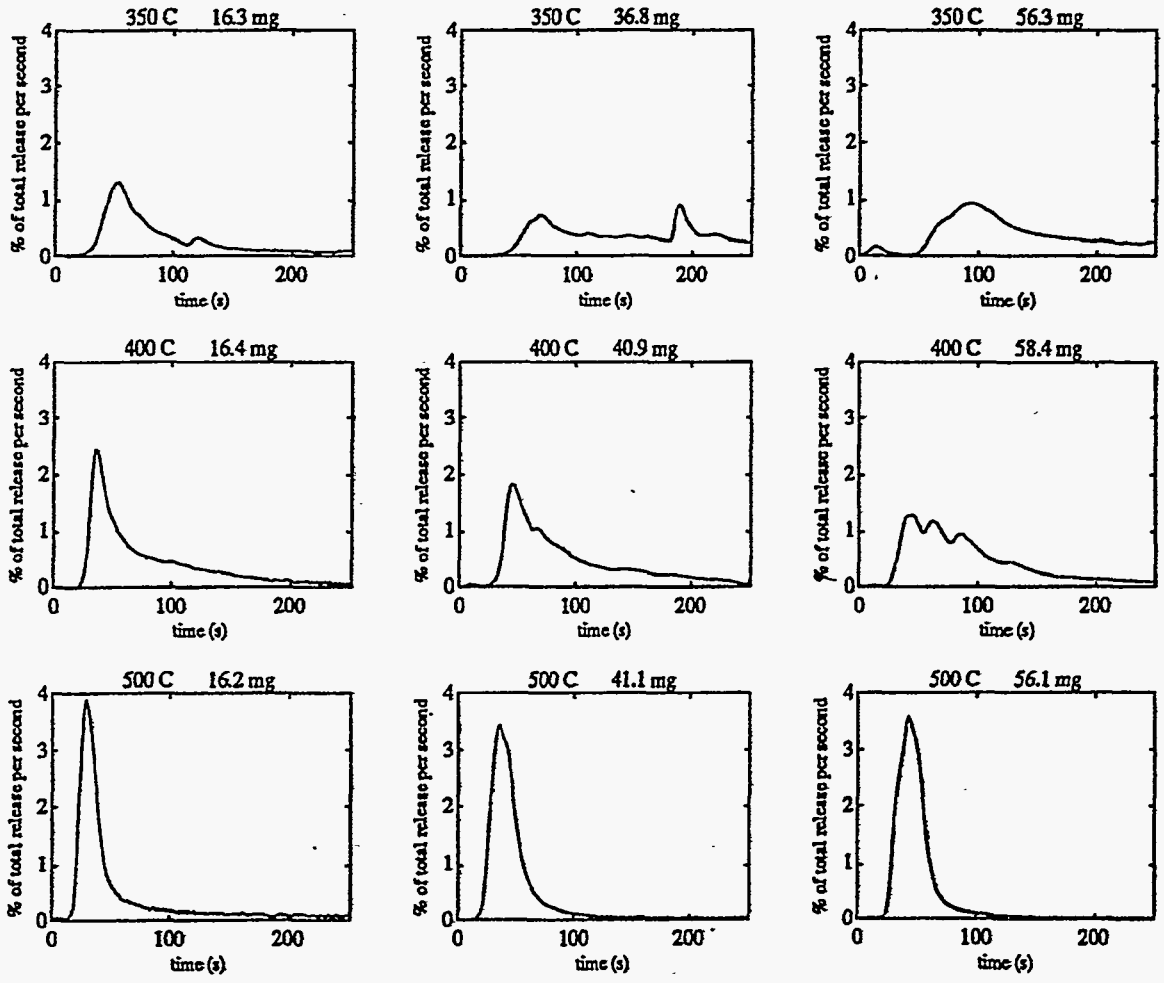

Figure IV.C.1-1. Rate of sulfur release versus time for nine experiments at temperatures from 350°C to 500°C. The data are for droplet sizes of approximately 16 mg, 40 mg and 57 mg.

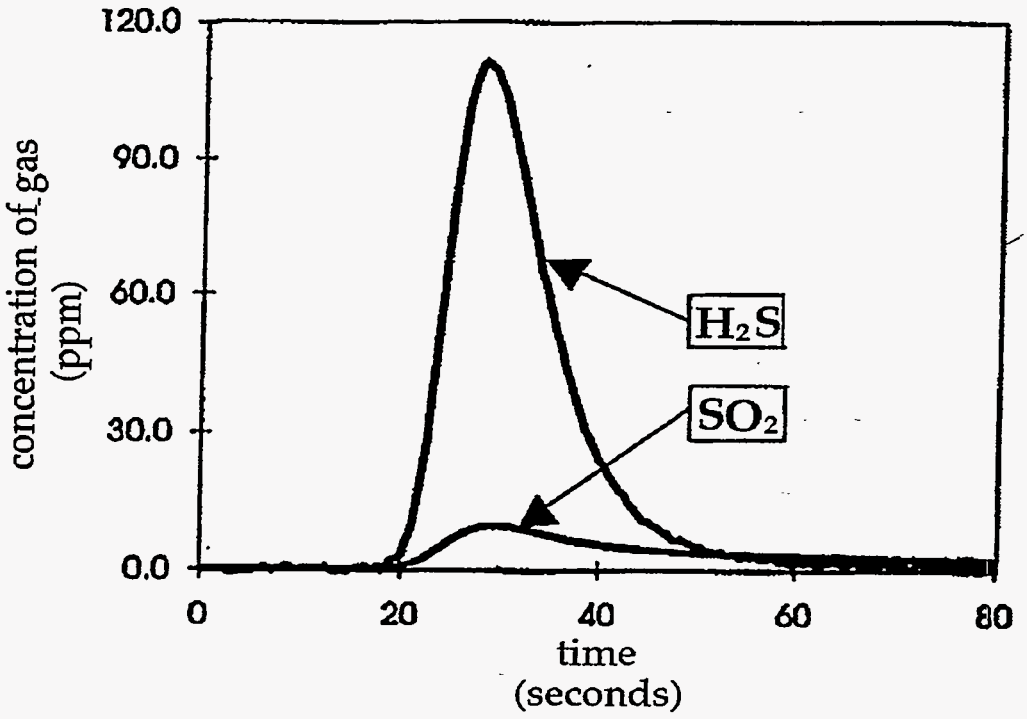

Figure IV.C.1-2. Release of sulfurous gases during pyrolysis of black liquor A at 700°C for 180 seconds in nitrogen atmosphere.

To account for all the initial sulfur, the char was also analyzed for sulfur content. The distribution of the sulfur in the gas phase and in the char is given in Table IV.C.1-1. The balance of both sulfur and carbon in the experiments did not close – at 700°C, 20% of the sulfur and 36% of the carbon were unaccounted. The unaccounted part is partly caused by a conversion of about 90-95% of the reduced sulfur gases to SO_2, but may also be because of unaccounted sulfur compounds in tar or particulates. Tar would be the most probable reason for the unaccounted part of the carbon. The amount of SO_2 released during the experiments is probably due to a reaction mechanism proposed by Strohbeen and Grace (1982). Sufficient amounts of CO_2 needed for this reaction was found in the pyrolysis gases.

Table IV.C.1-1. Distribution of sulfur during pyrolysis experiments at 700°C.

Source	700°C % of Initial Sulfur	900°C % of Initial Sulfur
In char	47.5	44.7
As SO_2	5.5	7.1
As reduced sulfur gases, H_2S, CH_3S, CH_3S_2, etc.	26.5	63.6
Total measured	79.5	115.4
Unaccounted	20.5	-15.4

In earlier studies by Feuerstein et al. (1967) and Brink et al. (1967, 1970), SO_2 has not been found in the off gases from pyrolysis of black liquor. Also, Li and van Heiningen did not find any SO_2 during slow pyrolysis of black liquor in a TG apparatus. Strohbeen and Grace (1982) found small amounts of SO_2 during pyrolysis of $Na_2S_2O_3$, Na_2SO_3 and Na_2SO_4 with organic compounds. Clay et al. (1987) only measured the total reduced sulfur with gas chromatography and did not report if there was SO_2 or not. Faix et al. (1990) found SO_2 in the same quantities as H_2S during slow pyrolysis of an alkaline sulfite anthraquinone/methanol (ASAM) waste liquor in a thermogravimetric-mass spectrometer (TG-MS) apparatus. In coal pyrolysis SO_2 has been found in the pyrolysis products.

Figures IV.C.1-3 and IV.C.1-4 shows the integrated sulfur release rate curves at several temperatures as well as the residence time curve from Figure IV.C.1-2. It is evident that at the lower temperatures (Figure IV.C.1-3), the rate of sulfur release, indicated by the slopes of the curves, increases with increasing temperature. Also, the rates are significantly slower than the rate of sulfur gas transport with the bulk gas. This means that the rate of sulfur release which we measured is indicative of the chemical and/or thermal processes involved in pyrolysis.

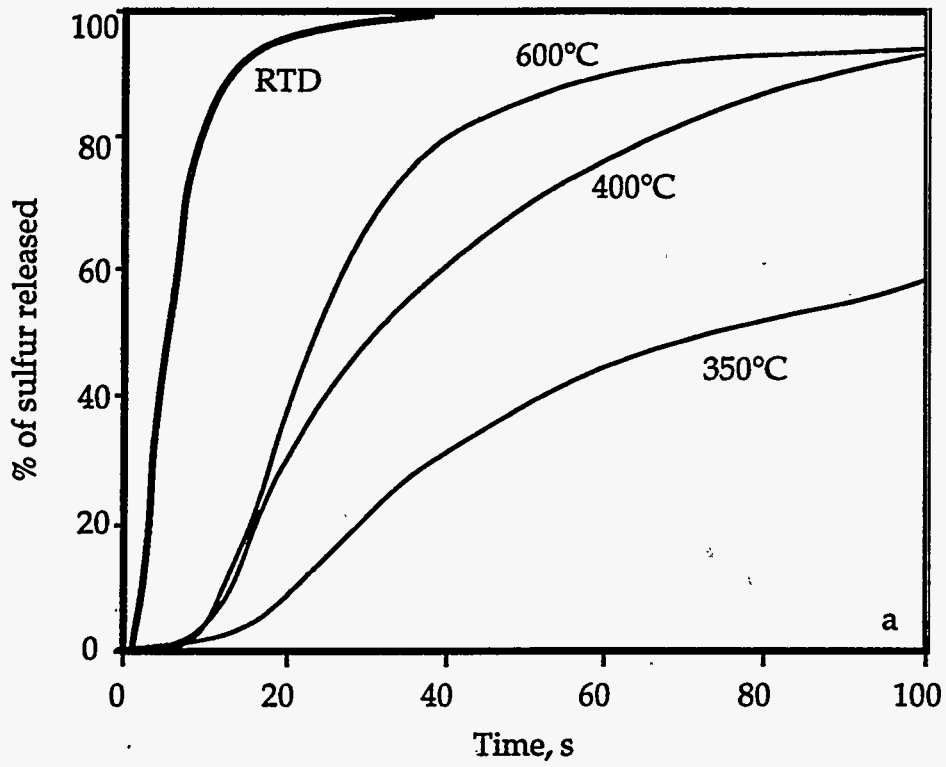

Figure IV.C.1.3. Integrated sulfur release curves (350-600°C) and residence time distribution curve.

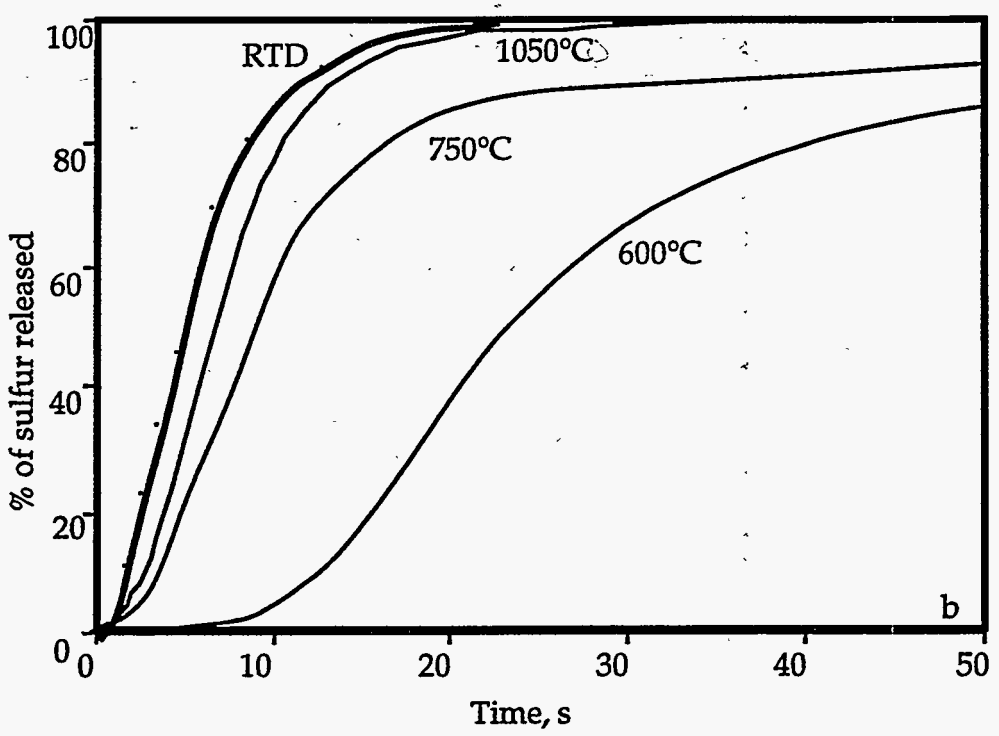

Figure IV.C.1-4. Integrated sulfur release curves (600-1050°C) and residence time distribution curve.

At higher temperatures (Figure IV.C.1-4), however, the sulfur release rate curves fall very close to the residence time distribution curve. At furnace temperatures of 750°C to 1050°C, the curves are very close to each other, especially for the first half of the sulfur release. This suggests that the rate of sulfur release is faster than the measured rate.

Onset of Sulfur Release

In the experiments the droplets were assumed to be resting on the quartz wool pad in the pyrolysis reactor before pyrolysis began. It is further assumed that the droplets dried completely before the sulfur release began. To test this latter assumption, a numerical model for drying of black liquor droplets (Frederick, 1990) has been used to calculate the drying times for the droplets. The calculated drying times for the droplets in furnace temperatures 350-600°C are compared in Figure IV.C.1-5 with the experimentally measured times for the onset of sulfur release. Figure IVC.1-5 shows that sulfur release almost never begins before the droplets have dried. Although the time to first sulfur release data are somewhat scattered, it is clear that sulfur release begins when the pyrolysis reactions begin, and not during drying.

Duration of Sulfur Release

The time to 50% conversion ($t_{50\%}$) of an irreversible chemical process is a convenient parameter for characterizing the temperature dependency of its overall kinetics because as long as the kinetic mechanism is independent of temperature, then the relative magnitude of $t_{50\%}$ depends only on the rate constant and not the chemical factors which influence rate (Levenspiel, 1972). In this study, we define $t_{50\%}$ as the time required for release of half of the sulfur which is ultimately released from the droplet. We obtained $t_{50\%}$ by integration of the sulfur release rate curves first to get the total amount of sulfur released in each experiment, and then to determine the time at which half of that sulfur had been released.

The $t_{50\%}$ data are plotted for each temperature as function of droplet size in Figure IV.C.1-6. At lower temperatures there is a strong dependency of $t_{50\%}$ on droplet size, but it decreases with increasing temperature until there is no effect of droplet size at 600°C.

The $t_{50\%}$'s for 10 and 30 mg droplets are shown in an Arrhenius plot in Figure IV.C.1-7. The $t_{50\%}$'s are slightly lower for the smaller droplets at lower temperatures, but the data are coincident at temperatures above 600°C. The slope of the overall data apparently changes slope, becoming less steep above 700°C.

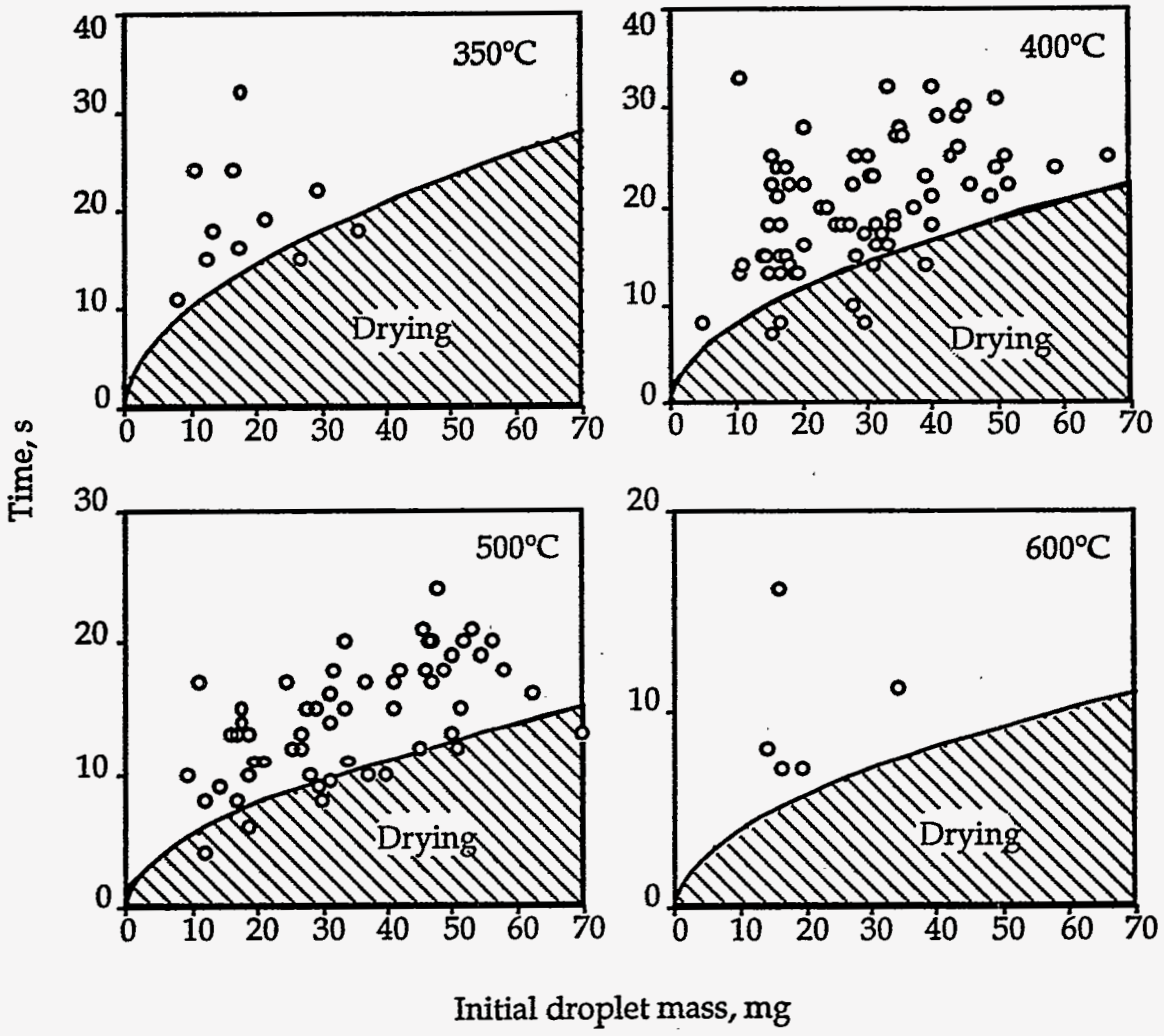

Figure IV.C.1-5. The time to onset of sulfur release at four temperatures for black liquor droplets pyrolyzed in N_2. The data points indicate the experimentally observed times to first appearance of sulfur, corrected for the residence time in the oxidizer and sample lines. The curves are the calculated times to onset of devolatilization, separating the drying (shaded area) and devolatilization (unshaded) stages.

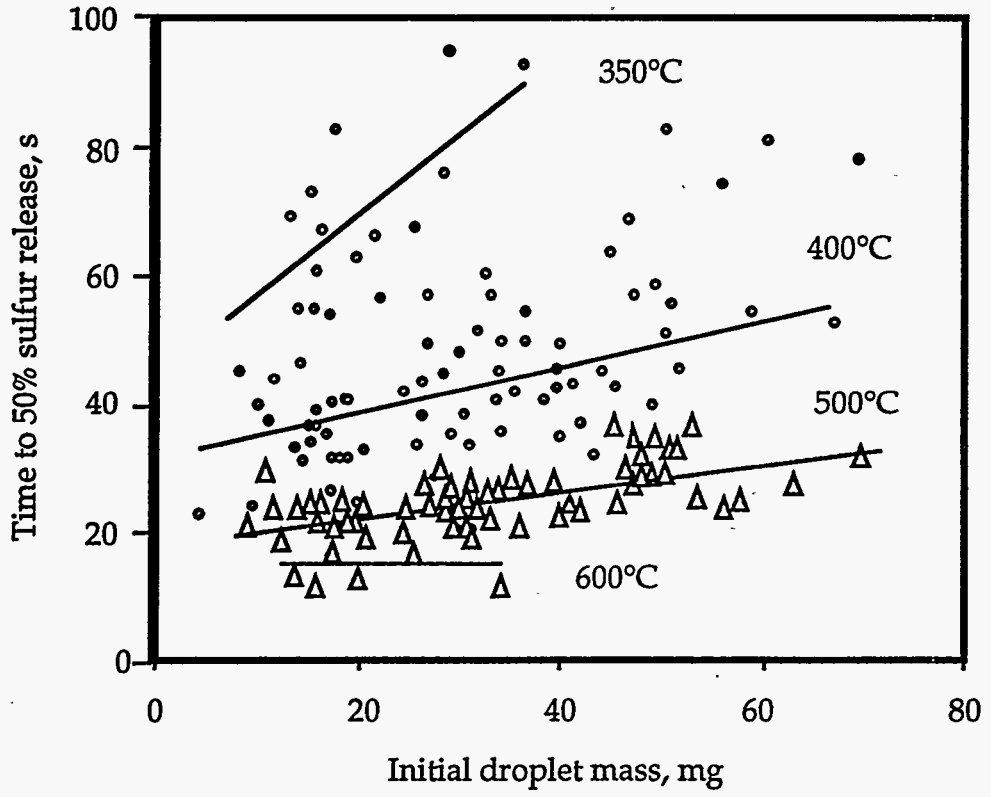

Figure IV.C.1-6. Time to 50% Conversion of the Sulfur Release Process Versus Initial Droplet Mass, 350-600°C.

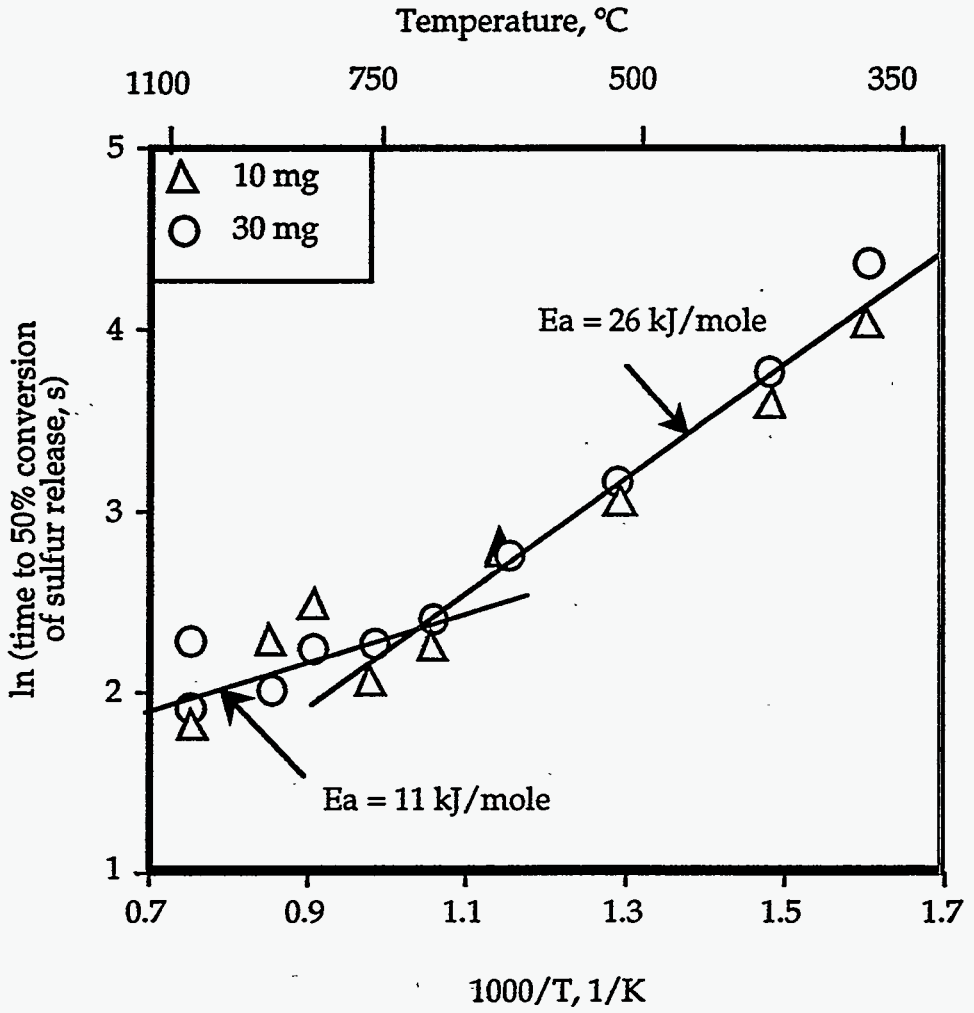

Figure IV.C.1-7. Activation energy plot for the sulfur release data from 10 and 30 mg droplets.

We estimated the apparent activation energy from the slope of the data between 350°C and 675°C in Figure IV.C.1-7 to be 26 kJ/mole. This is higher than expected for heat- or mass-transfer or diffusion controlled rate processes but is low for a chemical kinetic controlled process. At the higher temperatures, the apparent activation energy changes to 11 kJ/mole. This is the same value of apparent activation energy that one obtains for heat transfer to the pyrolyzing droplets (see Appendix IV.C.1-A). This result suggests that the rate is influenced by both heat transfer and chemical kinetics at lower temperatures but becomes dominated by heat transfer as temperature increases. In recovery boilers, the temperatures are high enough so that sulfur release is controlled by the rate of heat transfer to the black liquor droplets. This is consistent with results for pyrolysis of black liquor reported earlier (Frederick, 1990).

Total Sulfur Release

Figure IV.C.1-8 shows the data on total sulfur loss from black liquor droplets during devolatilization. The data include those obtained in this work together with data of Brink et al. (1970) and Clay et al. (1985, 1987). Brink's data are for droplets sprayed into a hot gas environment, while Clay's data are for single droplets suspended in a hot radiant environment with a low gas flow past the particle. The trends in the yield of total sulfur gas are both qualitatively and quantitatively very similar: an increase with increasing temperature at low temperatures, a maximum near 600°C, and a decrease as temperature increases further. The data also seem to fall into two groups: the higher sulfidity Finnish liquors and the lower sulfidity American liquors. Harper's (1989) flash pyrolysis data, for soda liquors to which Na_2S or $Na_2S_2O_3$ had been added, follow a similar trend, with a maximum in total sulfur release between 400 and 500°C. The two curves in Figure IV.C.1-8 are fitted to data from Finnish and American liquors.

Our preliminary results indicate that droplet mass has little effect on total sulfur release. Figure IV.C.1-9 shows the total sulfur released versus initial (wet) droplet mass for the 400°C experiments. The trend seems to be similar at other temperatures in the range studied. The scatter in the data in Figure IV.C.1-9 is common in our lower temperature experiments but decreases with increasing furnace temperature. The variation in total sulfur release is similar to that reported by others in similar experiments (Harper, 1989; Clay et al., 1987).

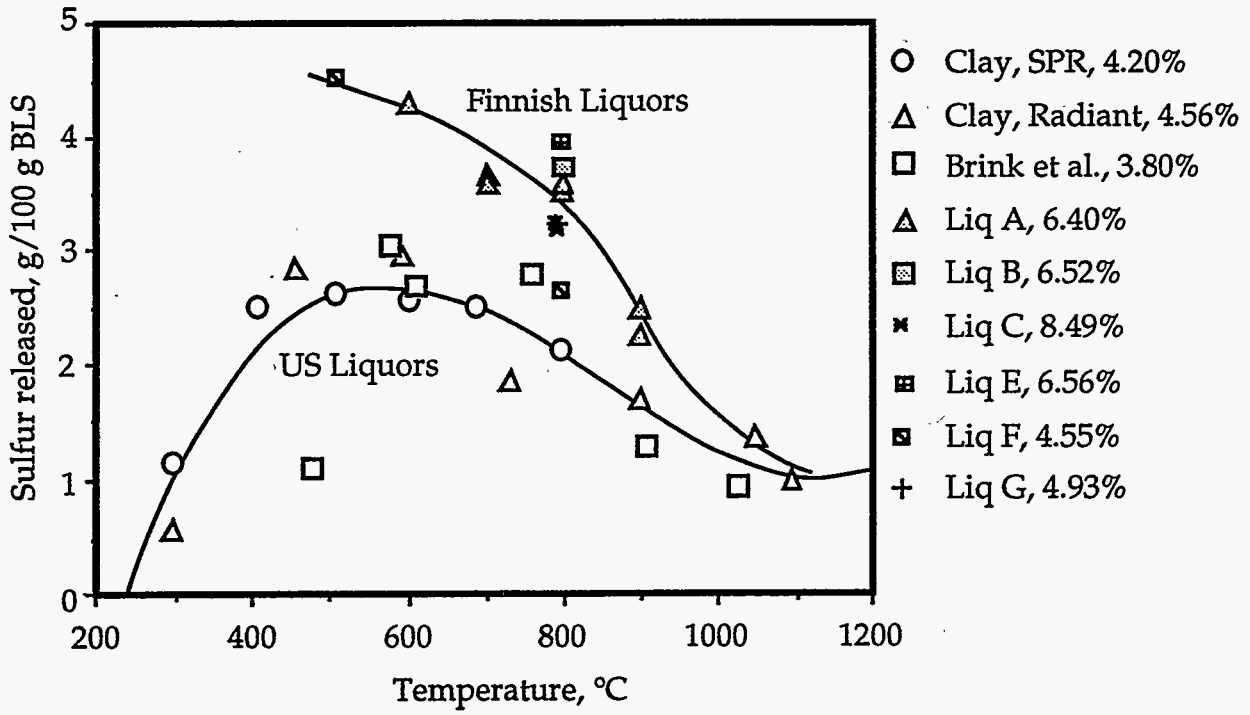

Figure IV.C.1-8. Total sulfur released during devolatilization of black liquor droplets. Data are from this study as well as from Brink et al. (1970) and Clay et al. (1985, 1987).

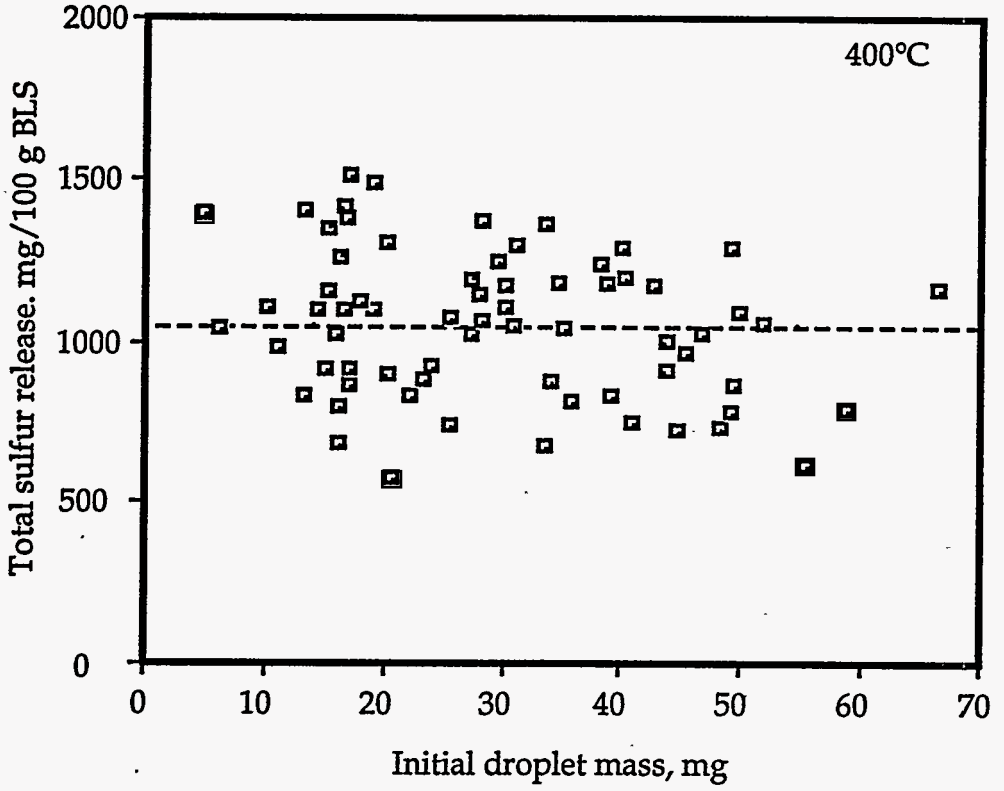

Figure IV.C.1-9. Total sulfur released versus droplet mass for droplets pyrolyzed at 400°C. The solid line indicates the mean value.

Sulfur Release During Pyrolysis

Analysis of the rate of release of sulfur- and carbon-containing gases showed that sulfur is released during the first moments of pyrolysis of black liquor at about the same relative rate as, or slightly faster than carbon is. Figure IV.C.1-10 shows the fraction of sulfur released during pyrolysis versus the fraction of carbon released during pyrolysis for three liquors, A,B and C. The values are calculated from the char analysis. Experiments were done on liquor A at temperatures 700 to 900°C. At lower temperatures, 700°C and 800°C, a greater fraction of the sulfur is released than for carbon from liquor A. At 900°C the amount of sulfur released is of the same magnitude as the carbon release. Carbon release has increased slightly from 800°C but the amount sulfur released has decreased by about 30%. At this temperature the sulfur recapture reactions starts to dominate and sulfur is thermodynamically favored in the condensed phase (Backman and Hupa, 1990).

Two other liquors, B and C, were also tested. Liquor B is a virgin liquor and liquor C is the corresponding "as fired" liquor from the same mill, containing the recirculated particulate from the electrostatic precipitators (ESP). The amount of dust added increases the Na content of black liquor by about 10%. Usually the particulates contain over 90-95% Na_2SO_4 and the rest Na_2CO_3. The increased sulfur in liquor C therefore originates from Na_2SO_4 and the lower carbon content is because of the diluting effect of the recirculated dust which is almost entirely Na_2SO_4. The fractional release of sulfur and carbon for liquor B was about the same as for liquor A. Liquor B had about the same amount of sulfur and carbon as liquor A.

Table IV.C.1-2. Elemental analysis of black liquors in pyrolysis experiments.

Black Liquor Name	Dry Solids (DS)	Sodium in DS	Sulfur in DS	Carbon in DS	Molar Ratio of C/S
A	76.10%	19.12%	6.40%	31.41%	13.1
B	74.20%	19.74%	6.52%	33.05%	13.5
C	78.60%	21.56%	8.49%	27.32%	8.6

The release of carbon from liquor C was about the same as for liquor B. With the addition of precipitator dust there was no increase of the organic carbon, only a small increase of the relative total amount of carbon in the black liquor due to the Na_2CO_4. The sulfur release decreased about 30%. The added Na_2SO_4 has been reported to be stable during pyrolysis and not contribute to sulfur release (Strohbeen and Grace, 1982; Douglass and Price, 1968). The decrease, Figure IV.C.1-11 is therefore a cause of the relative increase of the stable inorganic sulfur, Na_2SO_4.

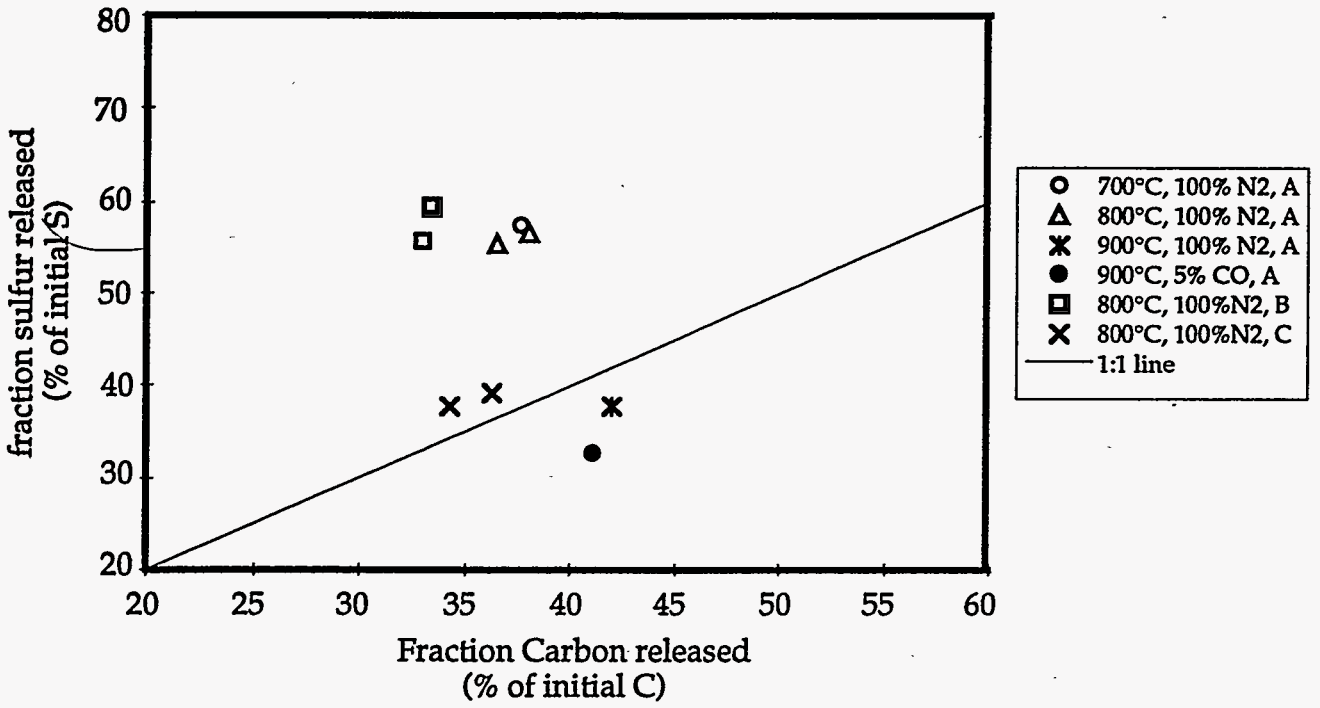

Figure IV.C.1-10. Fraction of sulfur released vs fraction of carbon released for 15 seconds pyrolysis of black liquors A, B and C in inert atmosphere at 700-900°C.

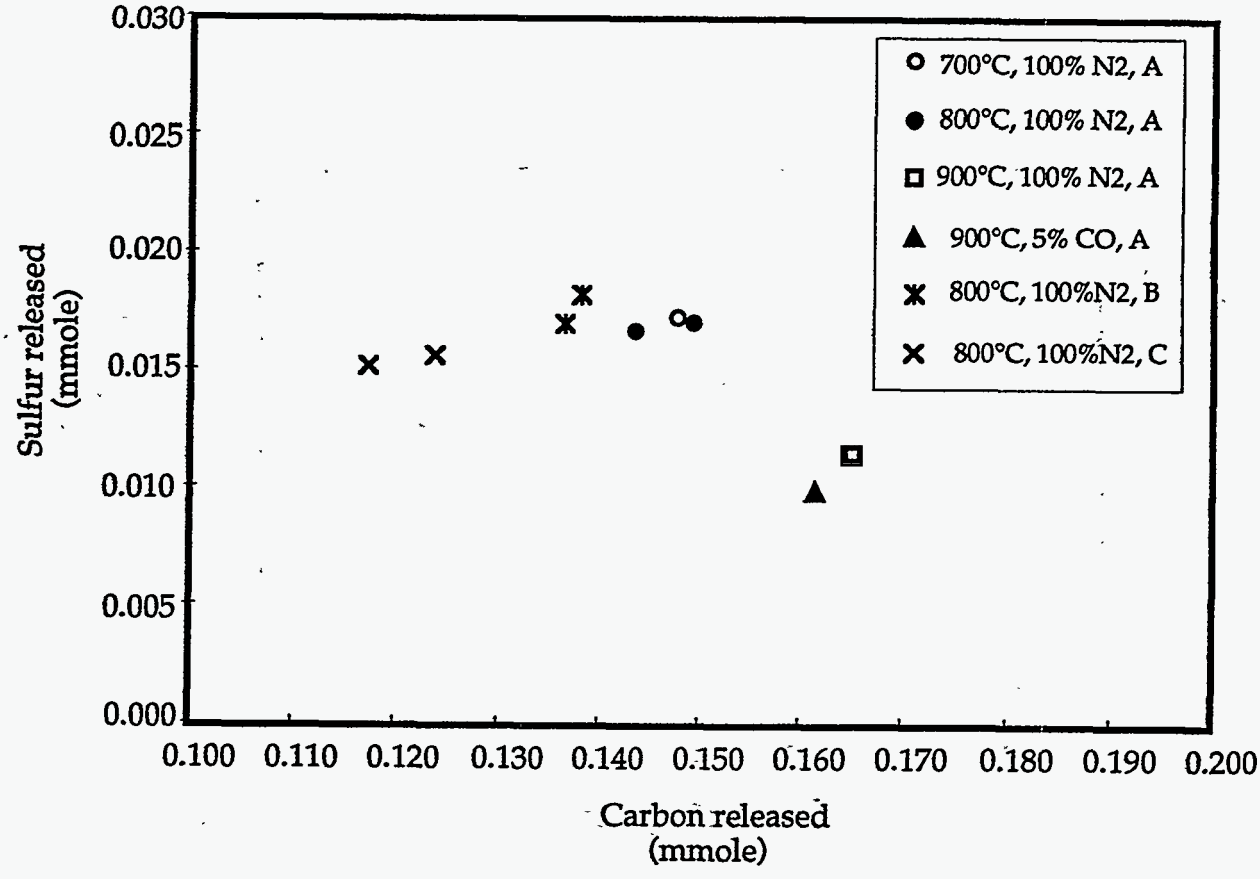

Figure IV.C.1-11. Amount in moles of sulfur released vs amount of carbon released for 15 seconds pyrolysis of black liquors A, B and C in inert atmosphere at 700-900°C.

Figure IV.C.1-11 shows the release of sulfur versus the release of carbon on a molar basis. The figure shows that the amount of sulfur and carbon release is about the same for all three liquors at 800°C. The initial sulfur and carbon content does not have a great influence on the amounts released. The small difference in the amounts of sulfur released from liquors B and C shows that the added Na_2SO_4 and Na_2CO_3 collected from the electrostatic precipitator do not increase the amount of sulfur released. Na_2SO_4 does not release any sulfur during the pyrolysis, but shows rather a slightly decreasing effect on sulfur release. Na_2SO_4 has earlier also been shown not to release any sulfur during pyrolysis (Strohbeen and Grace, 1982; Douglass and Price, 1968).

Figure IV.C.1-12 shows the molar ratio between carbon and sulfur released during pyrolysis as function of temperature. The ratio between carbon and sulfur in the pyrolysis gases is between 7 and 8 at temperatures of 800°C and lower. In the black liquor the molar ratio is about 13.5 for liquors A and B and 8.6 for liquor C, Table IV.C.1-2. At 900°C the molar ratio in the pyrolysis gases increased to about 15. This is due to the decreased amount of sulfur released (Figure IV.C.1-11). There was no substantial change in the amount of carbon release between 800°C and 900°C. Figure IV.C.1-12 also shows data from the experiments where the black liquor droplets were held longer times, 180 seconds, in the reactor in inert atmosphere. The longer residence time does not influence the carbon to sulfur release ratio, even at 900°C.

The gas composition during devolatilization may have an effect on the amount of sulfur released. Figure IV.C.1-13 compares data on sulfur release from black liquor during devolatilization taken at different furnace temperatures and gas concentrations. These data suggest that there is no difference in sulfur loss during devolatilization in N_2 versus other gases for CO_2 and water vapor partial pressures not exceeding 0.05 bar. The droplets were inserted in the furnaces for 15 seconds which is longer than the time required for complete devolatilization at these temperatures, so that some of the sulfur loss may have occurred during the char reactions stage. The times corresponding to completion of the drying and devolatilization stages for 15 mg droplets at the same initial dry solids content (76.1%) are approximately as shown in Table IV.C.1-3. These are based on the droplet combustion time models of Frederick (1990).

Table IV.C.1-3. Estimated times for completion of drying and devolatilization of black liquor droplets.

Temperature, °C	Elapsed time, s, for		
	Drying	Devol	Sum, s
700	3.7	4.9	8.6
800	2.9	3.0	5.9
900	2.1	2.1	4.2

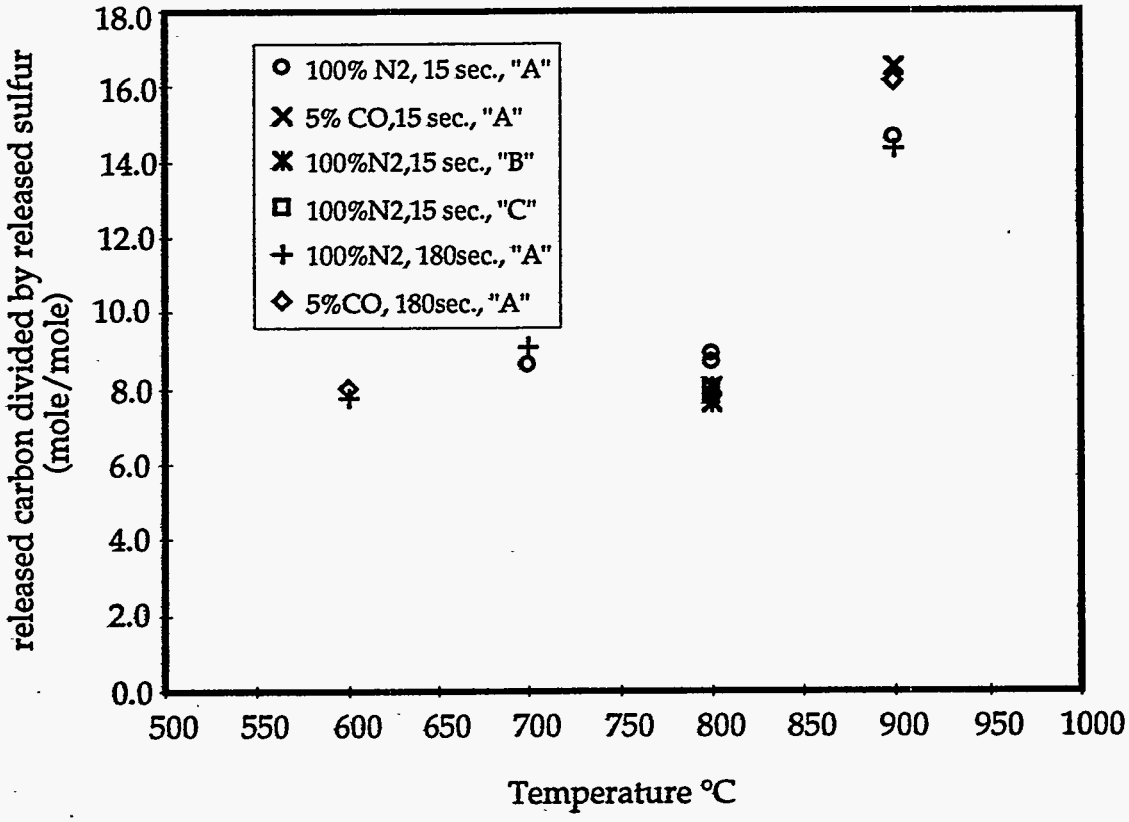

Figure IV.C.1-12. Molar ratio of sulfur to carbon for pyrolysis of black liquors A, B and C in inert atmosphere for 15 or 180 seconds at 600-900°C.

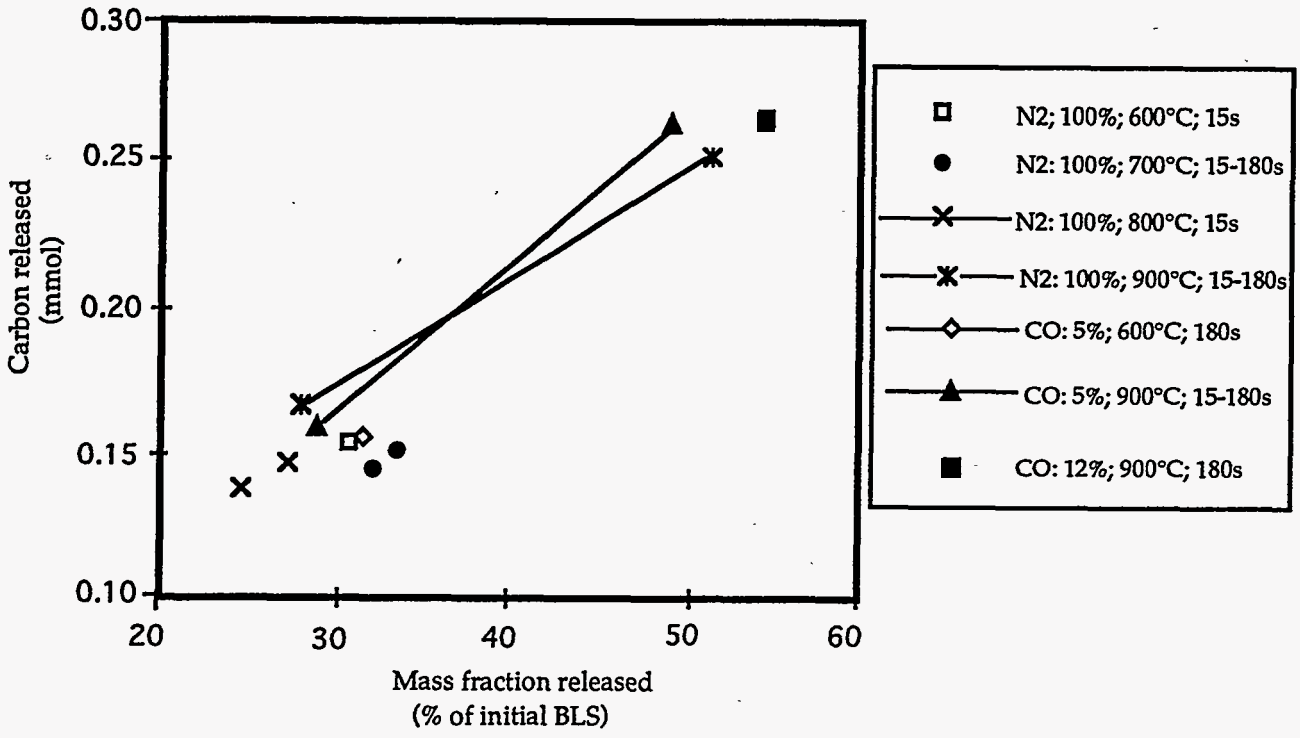

Figure IV.C.1-13. Sulfur retained in the char for droplets of liquor A inserted for 15 seconds in gas environments of different temperatures and gas compositions.

At higher CO_2 and water vapor partial pressures, the presence of both of these gases increased the loss of sulfur from char even at these relatively short reaction times (Table IV.C.1-4).

Table IV.C.1-4. The fraction of the sulfur originally in black liquor that was retained in the char 15 seconds after the black liquor droplet was inserted into a 900°C furnace containing the following gases and the balance N_2. Data are for Liquor A.

Mole fraction of gases in N_2			Fraction of sulfur retained in char
CO	CO_2	H_2O	
0.011	0.104		0.49
	0.10	0.05	0.47
0.04	0.113		0.49
0.05	0.05	0.10	0.25
0.10	0.05	0.05	0.25
	0.10	0.10	0.45
0.10	0.10	0.10	0.33
0.10	0.10	0.10	0.46

The average sulfur retained for liquor A in experiments where the CO_2 or H_2O content of the gases did not exceed 5% is shown in Table IV.C.1-5. These data were obtained in the Åbo Akademi droplet/flow reactor. The sulfur retained increases with increasing reactor temperature as was discussed earlier, in Section IV.C.1. We use these values of sulfur in the char at the end of devolatilization to find by difference the sulfur loss during char reactions for droplets that remained in the reactor for longer residence times. The results are included in Tables IV.C.2-4 to IV.C.2-6.

Table IV.C.1-5. The average sulfur retained for liquor A in experiments where the CO_2 or H_2O content of the gases did not exceed 5%.

Temperature, °C	Sulfur retained in char, % of sulfur originally in the black liquor solids
600	33.0
700	43.0
800	44.3
900	62.1±3.4

Effect of Reaction Time on Sulfur Release

Experiments to determine the effect of exposure time in an inert atmosphere on sulfur release were performed. The experiments were done in either N_2 or in mixtures of N_2 and CO. Figure IV.C.14 shows the carbon release for different duration times and temperatures. The points in the lower left corner are for 15 seconds duration and the points in the upper right corner is for 180 seconds duration. The two lines in the figure shows the data points that has the duration of 15 and 180 seconds with the same temperature and gas composition. The CO points (triangles) shows that, compared to the N_2 experiment (diamonds), there is a minor increase in carbon release for the 180 s duration time. A shorter line for 700°C (open squares) shows that there is no further release of carbon at 180 seconds duration for that temperature. At 800°C only measurements with 15 seconds duration where made. It showed a slightly lower release of carbon than at 900°C but about the same as at 700°C.

The sulfur release is plotted against mass fraction released for the same experiments as above in Figure IV.C.15. There is a clear trend of the temperature dependency on sulfur release. Lower temperature, down to 600°C, shows a higher sulfur release. The duration time of 180 seconds at 700°C does not give a increased sulfur release.

At 900°C the increase of sulfur release after the first 15 seconds is essential, the released amount of sulfur reaches the same level as at 700 and 800°C.

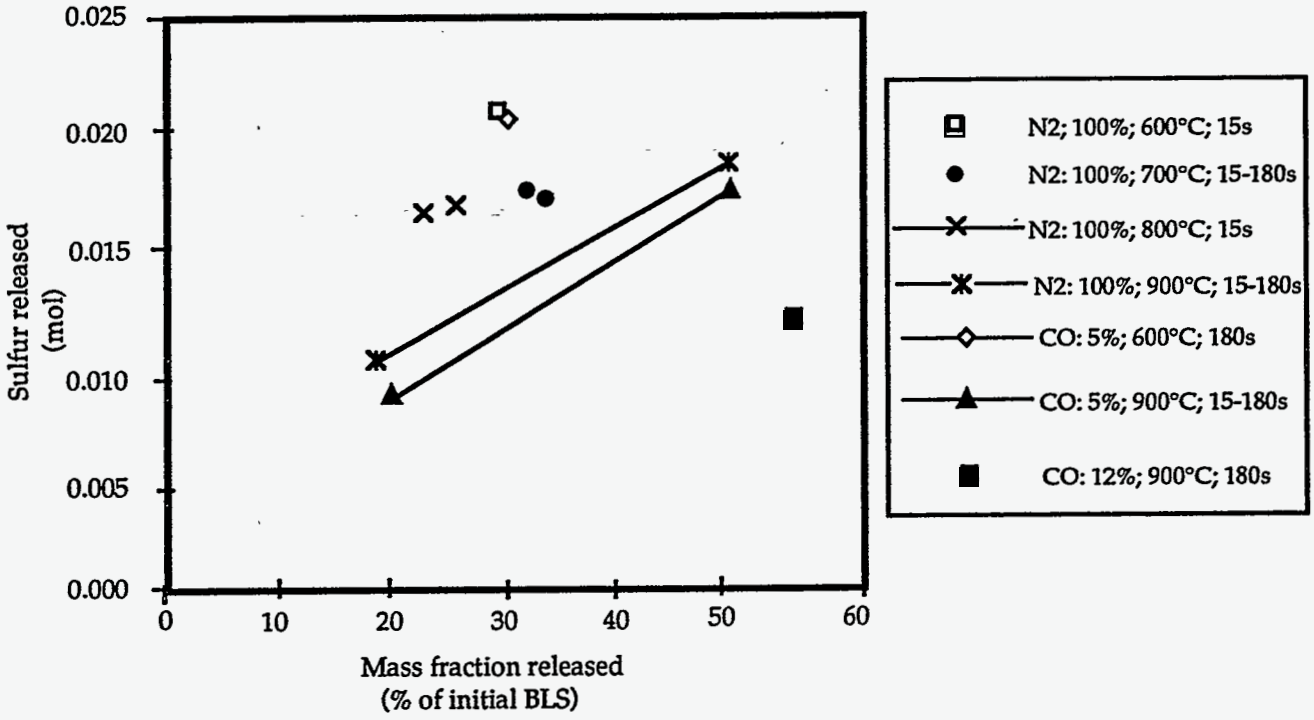

Figure IV.C.1-14. Carbon released in moles as function of residual char for pyrolysis of black liquor A at 600-900°C in inert gas atmosphere.

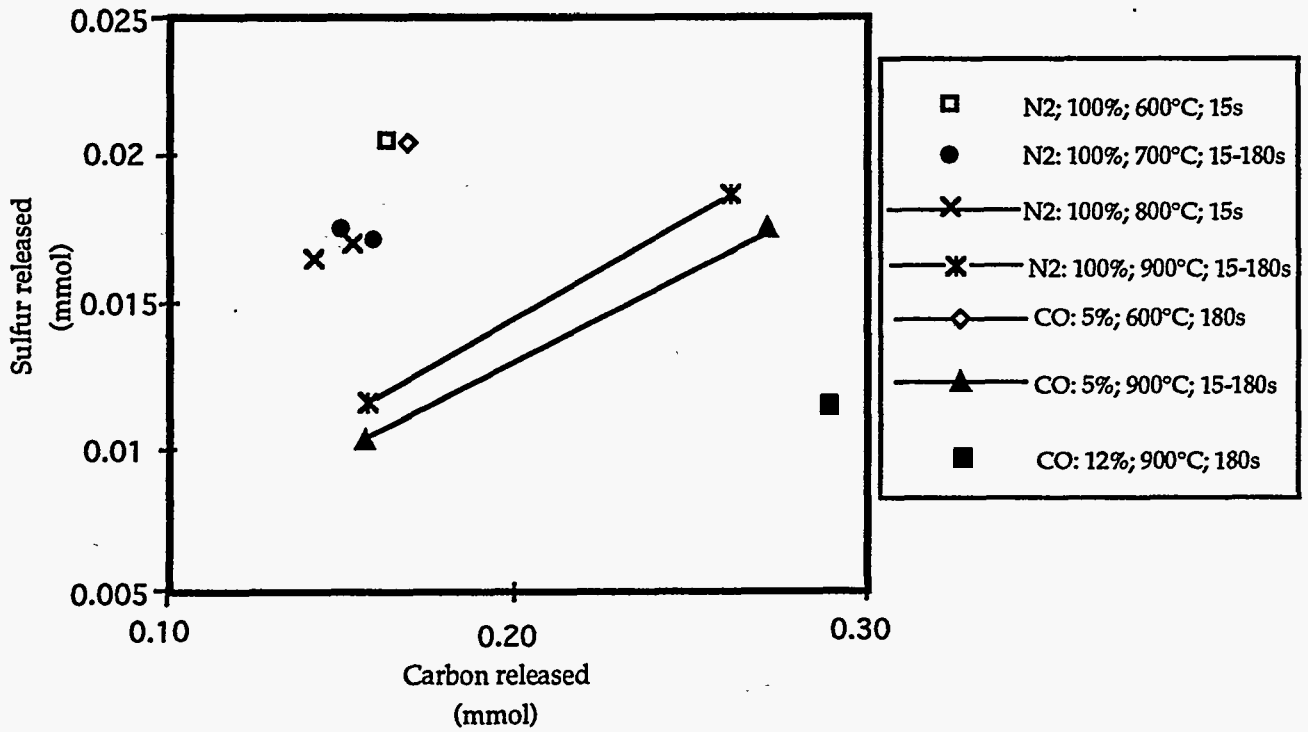

Figure IV.C.1-15. Sulfur released in moles as function of released mass fraction for pyrolysis of black liquor A at 600-900°C in inert gas atmosphere.

Total Sulfur Released During Devolatilization

In Figure IV.C.1-8 we saw that the amount of sulfur released from black liquor droplets during devolatilization goes through a maximum between 600°C and 800°C. The total amount released was greater for those liquors with higher total sulfur contents, but otherwise depended only on the temperature of the furnace in which devolatilization occurred.

The data from Figure IV.C.1-8 is replotted in Figure IV.C.1-16 as the fraction of the sulfur in black liquor that is released during devolatilization. When plotted this way, the data, while somewhat scattered, fall along a single curve with a maximum at about 700°C. Correlations that fit this data are as follows:

for 250°C < T < 1018°C

$$S_{vol} = -163.27 + 0.9171\,T - 1.150 \times 10^{-3}\,T^2 + 4.283 \times 10^{-7}\,T^3$$

for T > 1018°C

$$S_{vol} = 458.85 \exp(-2.666 \times 10^{-3}\,T)$$

where S_{vol} is the percentage of sulfur in black liquor that was volatilized and T is the furnace temperature in °C.

Table IV.C.1-6. Possible sulfur species products during devolatilization.

Form of Sulfur in Black Liquor	Sulfur Species Formed During Devolatilization	Temperature at Which Formation Becomes Important	Reference
Organic sulfur	H_2S, mercaptans, sulfides, disulfides	200°C	22
Na_2S	H_2S COS	320°C 350°C	4, 22
$Na_2S_2O_3$	Na_2S, S	275°C	4, 5
Na_2SO_4	Na_2S	610°C	22, 35
Na_2SO_3	Na_2S, Na_2SO_4	600°C	15
S	H_2S		2

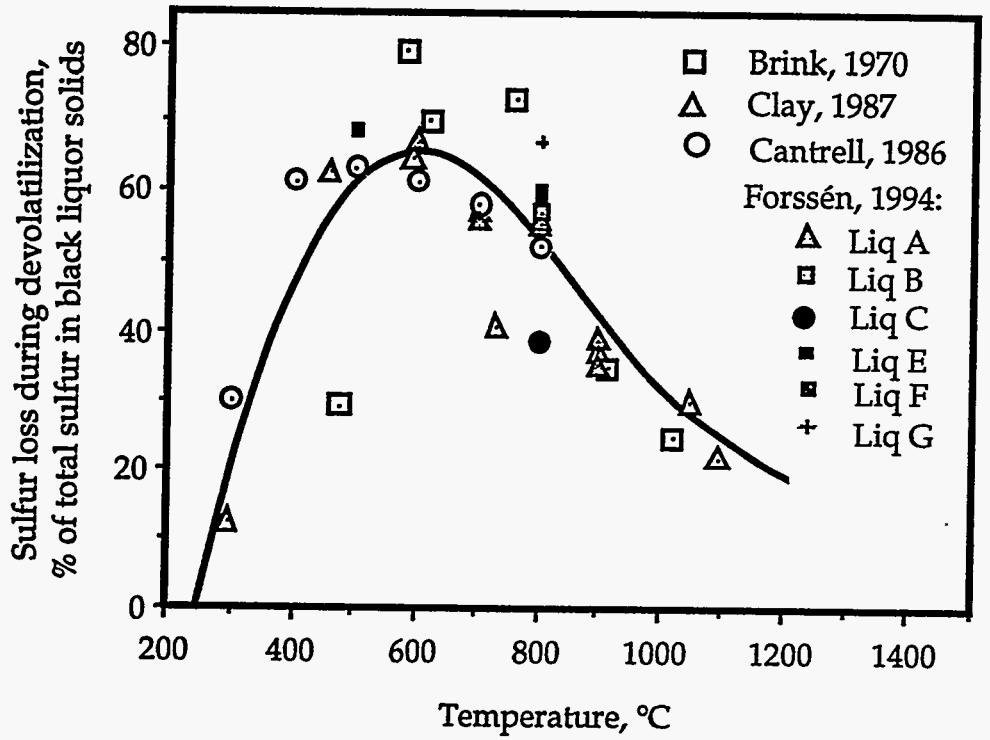

Figure IV.C.1-16. Data from Figure IV.C.1-8 replotted as fraction of total sulfur in black liquor that was released during devolatilization versus temperature.

Based on data presented earlier in this report, one would expect that the total amount of sulfur released during devolatilization of black liquor would depend on the composition of the sulfur species in black liquor. The explanation for why sulfur species composition is not an important variable here may be as follows:

1. Sulfur release from thiosulfate and sulfide follow very similar patterns (Harper, 1989). Since thiosulfate is formed from sulfide during pulping and oxidation of black liquor, the sum of these two species plus organic sulfur is approximately the sulfide in white liquor. While sulfidities vary from mill to mill, the variation is within the range of scatter of the data of Figure IV.C.1-16.

2. The range of variation of sulfur as sulfate versus other sulfur species in black liquor is not greater than the scatter observed in the data of Figure IV.C.1-16.

The Mechanism of Sulfur Release

The general trend of sulfur release data at high heating rates is consistent with other known information regarding black liquor pyrolysis. For example, thermodynamic calculations indicate that sulfur conversion to gases is favored at temperatures below 600°C, but increasingly prefers the condensed phase above 600°C (Figure IV.C.1-17).

Another key factor is that pyrolysis yield increases with increasing temperature (Frederick and Hupa, 1993). This means that more of the organic sulfur is volatilized at higher temperatures. It also means that the residue contains more inorganic material and less carbon or organic.

The inorganic compounds in black liquor do not all yield volatile sulfur upon heating: Na_2S, and $Na_2S_2O_3$ do, Na_2SO_3, and Na_2SO_4 do not. The decomposition temperature for $Na_2S_2O_3$ is 330°C (Dearnaley et al., 1983), so it contributes to sulfur release only above that temperature. For Na_2SO_3, the corresponding temperature is 600°C. Finally, Na_2SO_4 is reduced to Na_2S, but this occurs at an appreciable rate only above 600°C; below this, it contributes nothing to sulfur release; above it, the Na_2S formed can contribute to sulfur release.

Finally, Na_2CO_3 can act as a sulfur recapture agent (Bachman et al., 1985; Kimura and Smith, 1987). Na_2CO_3 begins to melt at 762°C in mixtures with Na_2S and may react more rapidly with gaseous sulfur species as temperature increases.

These observations are consistent with an overall process of sulfur release which involves competing release and recapture mechanisms. The release mechanisms include formation of sulfur gases during pyrolysis of organic matter, decomposition of inorganic sulfur compounds, and reaction of inorganic sulfur compounds with CO_2 or water vapor. The sulfur capture mechanism is probably the reaction of a melt containing Na_2CO_3 with sulfur gases before they escape from the black liquor droplet or char particle.

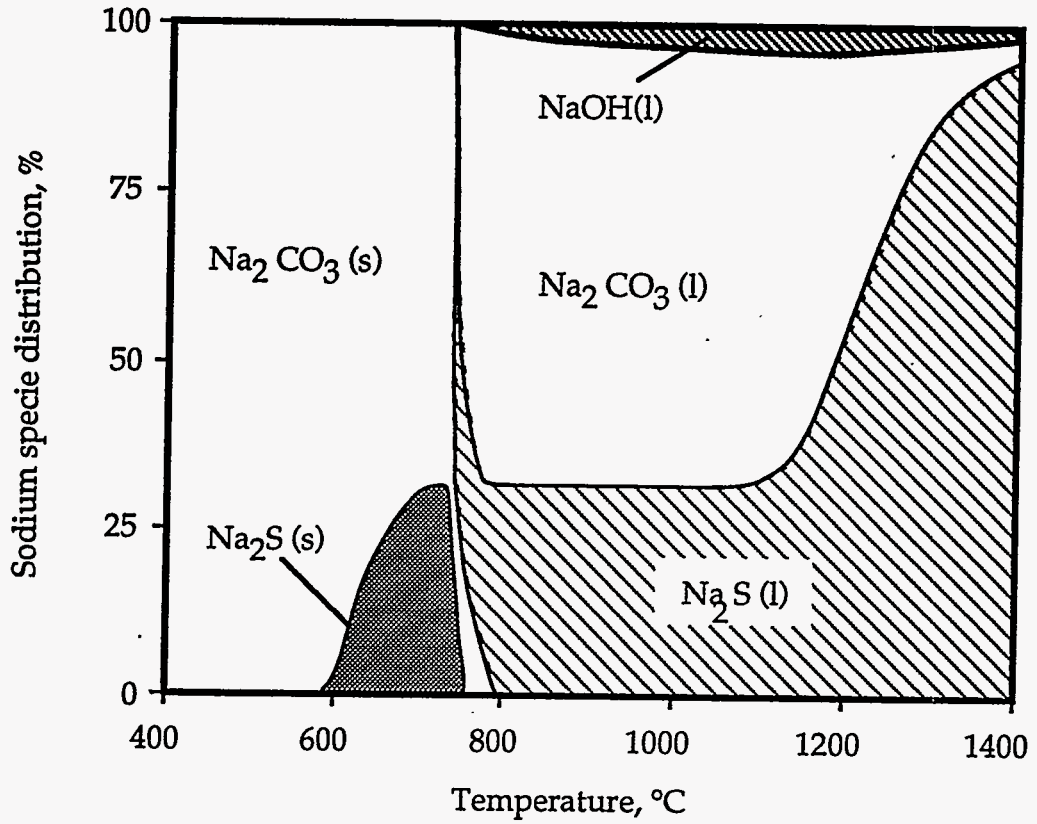

Figure IV.C.1-17. Calculated equilibrium distribution of condensed Na and S species for pyrolysis of black liquor (from Backman and Hupa, 1990).

These competing mechanisms can account for the trends in sulfur release with temperature (Figure IV.C.1-16) as follows:

- Below 500°C, the kinetic processes which release sulfur gases dominate over those which capture sulfur gases. Sulfur release increases with temperature below 500°C because the conversion of organic matter to pyrolysis gases increases with increasing temperature. This results in an increase the conversion of organic sulfur to gases. Also, thiosulfate may begin to decompose and contribute sulfur gases above 330°C. Below 600°C, sulfur is thermodynamically favored in the gas phase, so there is no driving force for the recapture of sulfur gases in the condensed phase.

- Above 700-750°C, the sulfur gas capture mechanisms start to dominate. Sulfur is thermodynamically favored in the condensed phase, Figure IV.C.1-17, so there is a driving force for recapture of sulfur gases by Na_2CO_3, and the rate of the capture reactions increases with temperature. Although sulfur is thermodynamically favored in the condensed phase above 600°C, the rate of sulfur gas capture by Na_2CO_3 may be slow below the melting point.

- At the plateau region at intermediate temperatures there is of a tradeoff between the sulfur release and recapture mechanisms.

The basis for this mechanism, i.e. a balance within each pyrolyzing droplet between sulfur release and recapture with recapture becoming increasingly dominant as temperature increases, was suggested earlier by Clay et al. (1987). This mechanism is consistent with the observed effect of temperature on sulfur release as well as with other observations of black liquor pyrolysis, but obviously requires more direct verification. The actual mechanisms for release and recapture of sulfur are currently under investigation.

References

Backman, R. and Hupa, M. (1990), "Gasification of black liquor at elevated pressures. Thermodynamic analysis," *Combustion Chemistry Research Group Report 90-10,* Abo Akademi University, Turku, Finland.

Backman, R., Hupa, M., and Uusikartano, T. (1985), "Kinetics of sulphation of sodium carbonate in flue gases," *Proc. 1985 Int'l. Recovery Conf.*, New Orleans, pp. 445-450, April.

Brink, D.L., Thomas, J.F., Feuerstein, D.L. (1967), *Tappi*, 50(6):276

Brink, D.L., Thomas, J.F., and Jones, K.H. (1970), *Tappi Jl.*, 53(5):837-843.

Calkins, W.H. (1985), "Determination of organic sulfur-containing structures in coal by flash pyrolysis experiments," *Energy and Fuels*, 1(1):59-64.

Cantrell, J.G., Clay, D.T., and Hseih, J.S. (1986), "Sulfur release and retention during combustion of kraft black liquor," *Chemical Engineering Technology in Forest Products Processing*, B. Crowell, editor, AIChE For. Prod. Div., Vol. 2, pp. 31-40.

Clay, D.T., Grace, T.M., Kapheim, R.J., Semerjian, H.G., Macek, A., and Charagundla, S.R. (1985), "Fundamental study of black liquor combustion. Report No. 1 - Phase 1," US DOE Report DOE/CE/40637-T1 (DE85013773), January.

Clay, D.T., Lien, S.J., Grace, T.M., Macek, A., Semerjian, H.C., Amin, N., and Charagundla, S.R. (1987), "Fundamental studies of black liquor combustion. Report No. 2," US DOE Report DE88005756, January.

Dearnaley, R.I., Kerridge, D.H., and Rogers, D.J. (1983), *Inorg. Chem.* 22:3242.

Douglass, I.B. and Price, L. (1968), *Tappi Jl.*, 51(10):465-467.

Faix, O., Jakab, E., Fuchs, K., Patt, R., Till, F., and Székely, T. (1990), *Paperi ja Puu*, 72(3):239-247.

Feuerstein, D., Thomas, J., and Brink, D.L. (1967), *Tappi*, 50(6):258-262.

Frederick, W.J. (1990), "Combustion processes in black liquor recovery: analysis and interpretation of combustion rate data and an engineering design model," US DOE Report DOE/CE/40637-T8 (DE90012712), March.

Frederick, W.J., Forssén, M., Hupa, M., and Hyöty, P. (1992), "Sulfur and sodium volatilization during black liquor pyrolysis." 1992 TAPPI - CPPA International Chemical Recovery Conference, Seattle, June 7-11.

Frederick, W.J. and Hupa, M. (1993), "Combustion parameters for black liquor," US DOE Report DOE/CE/40936-T1 (DE94007502), April.

Harper, F.D. 1989, "Sulfur release during the pyrolysis of kraft black liquor," PhD thesis, The Institute of Paper Chemistry, June.

Kimura, S. and Smith, J.M. (1987), *AIChE Jl.*, 33:1522.

Levenspiel, O. (1972), *Chemical Reaction Engineering*, 2nd ed., John Wiley & Sons, New York.

Li, J. 1989, "Rate processes during gasification and reduction of black liquor char," PhD thesis, McGill University, October.

Li, J. and van Heiningen, A.R.P. (1991), *Tappi Jl.*, 74(3):237-239.

Strohbeen, D.T. and Grace, T.M. (1982), *Tappi Jl.*, 65(10):125-126.

IV.C.2 Sulfur Release During Char Burning

During char burning, a significant amount of sulfur can be released. The mechanism of sulfur release during char burning is the reaction Na_2S with CO_2 and water vapor to form H_2S and COS. When water vapor is present, the rate of H_2S formation is much faster than that of COS. Under conditions of interest in recovery boilers, H_2S formation during char burning is much more important than COS formation.

The rate of H_2S and COS formation are both strongly affected by chemical equilibrium. The equilibria for both reactions favor more sulfur release at lower furnace temperatures and less at high temperatures. At conditions typical in recovery boilers, conversion of char sulfur to gases would not be complete but would be greater in colder regions. In low temperature gasification of black liquor, all of the Na_2S in the char may be converted to H_2S.

The rate of conversion of char sulfur to gases is controlled by both equilibrium and mass transport effects at temperatures of interest in recovery boilers. The reactions of Na_2S with water vapor and CO_2 are rapid, and within a char particle, H_2S and COS are at their equilibrium partial pressures. Because the equilibria increasingly favor Na_2S rather than H_2S and COS as furnace temperature increases, the partial pressure of these gases within the char particle decreases as temperature increases. For a given H_2S or COS partial pressure within the particle, the overall rate of sulfur gas release is then dependent on the rate at which it diffuses from the particle and is transported away from it.

The rate of H_2S release is also apparently influenced by the rate of sulfate reduction as well as reactions of H_2S with other gas species, forming, e.g., SO_2 or CS_2. Sulfate reduction is slow relative to H_2S formation and can limit the availability of Na_2S, thereby limiting the rate of H_2S production. Reactions of H_2S with other gas species can increase the H_2S concentration gradient, thereby increasing the rate of transport of H_2S and the overall rate of sulfur release. Further work is needed to confirm and quantify these effects.

Introduction

In Section IV.C.1, we showed that much of the sulfur release during black liquor combustion or gasification occurs during devolatilization. However, sulfur release continues to occur from char during char burning, gasification, and even during heating in non-reactive gases. In this chapter, we review existing data and present new experimental results on sulfur release during char reactions. The mechanisms of sulfur release during char reactions are discussed, and kinetic rate equations are presented.

An important point to remember is that the rate of sulfur release is much faster and potentially the total amount of sulfur released much greater during devolatilization than during char reactions. Typically 20-60% of the sulfur is released in 2-5 seconds during devolatilization of typical black liquor droplets. By contrast, the sulfur lost during char reactions is 20-50% in 30-200 seconds. The relative importance of these two stages to the total sulfur release therefore depends largely on what happens in the char bed.

Review of Available Data

All of the previous data reported on sulfur release during char reactions was obtained under gasification conditions. Durai-Swamy et al. (1991) presented data on sulfur reduction and release obtained during black liquor reforming with steam in a fluidized bed pilot plant reactor at 565-625°C. They analyzed the gases from their reactor for H_2S, COS, CH_3SH, $(CH_3)_2S$, and SO_2 using gas chromatography, and the bed material and cyclone catch for sulfate, sulfide, and total sulfur content. The results are summarized in Table IV.C.2-1. They found that nearly 90% of the sulfur recovered in their studies was converted to H_2S, with less than 1% of the sulfur recovered as COS and no CH_3SH detected. The remaining sulfur measured was as Na_2SO_4 in the reactor or cyclone catch. Both devolatilization and char reactions occurred in their reactor and some of the sulfur release occurred during devolatilization. However, the total sulfur converted to H_2S in their experiments exceeded the maximum conversion during pyrolysis (see Figure IV.C.1.16), and the additional sulfur released must have occurred during char gasification.

Table IV.C.2-1. Typical sulfur species distribution in gasifier products from two different Douglas fir kraft liquors. Data are from Durai Swamy et al., 1991.

Run	1/24/90	2/23/90	3/7/90
Liquor	1	2	1
Sulfur outputs, % of sulfur input in black liquor			
H_2S	76.8	63.2	135
COS	0.5	1.0	0.2
CH_3SH	0.0	0.0	0.0
Solid residues	—	8.8	16.3
Total sulfur recovered	—	72.9	152
% of recovered sulfur as gas	—	88.0	89.2

In carbon gasification experiments, Whitty (1993) reported the data in Table IV.C.2-2 on the loss of sulfur from black liquor char when the char was first heated in N_2 and subsequently gasified in 17% water vapor, 83% N_2 at 650°C, 10 bar. The carbon content is also shown, and both are expressed as weight % of the original char mass. Neither the sulfur gases nor the sulfur species in the char were analyzed. These data show that there is a significant loss of sulfur both during heating in N_2 and gasification in water vapor at this temperature.

Table IV.C.2-2. Sulfur release data during heating of black liquor char and during gasification with water vapor (from Whitty, 1993).

	Sulfur, wt%	Carbon, wt%
Original char	4.85	31.47
Heated in N_2 for 45 minutes	2.67	27.76
Heated in N_2 for 6.7 minutes and then gasified for 51.7 min (to complete gasification of the fixed carbon)	1.34	5.22

Li (1989) and Li and van Heiningen (1994) investigated the mechanism of sulfur release during gasification of black liquor char with CO_2 and water vapor. The measurements were made in a thermobalance. For gasification with CO_2 at 675-750°C and CO_2 partial pressures of 0.05-0.2 bar, they found that nearly all of the sulfur released was as COS. At relatively low CO_2 partial pressures and high temperatures (e.g., below 0.11 bar CO_2 at 725°C but at least to 0.2 bar CO_2 at 750°C) his data agreed with a model that assumed that the COS concentration within the pores of the char was at thermodynamic equilibrium and that the rate of COS release was controlled by film mass transfer. This model did not satisfactorily estimate the overall rate of COS formation at lower temperatures and higher CO_2 partial pressures where the overall rate may have been influenced by chemical kinetics as well. Li indicated that the overall stoichiometry of COS formation would be

$$Na_2S_{(s,l)} + 2CO_2 \Rightarrow Na_2CO_{3(s,l)} + COS \qquad \text{(IV.C.2-1)}$$

Li's analysis suggested that at low CO partial pressures (0.01-0.05 bar), S_2 would also be an intermediate product, subsequently reacting with CO as an alternate path to COS formation, i.e.

$$2\,Na_2S + 4\,CO_2 \Rightarrow S_2 + 2\,Na_2CO_3 + 2\,CO \qquad \text{(IV.C.2-2)}$$

$$S_2 + 2\,CO \Rightarrow 2\,COS \qquad \text{(IV.C.2-3)}$$

However, the CO partial pressures in recovery boilers are too high for reaction IV.C.2-2 to be important in COS production. COS can also react with CO_2 to produce SO_2 and CO. While Li observed no SO_2 formation in his experiments, this is probably important at higher temperatures and could increase the COS production rate.

Li and van Heiningen (1994) also reported that H_2S was the only sulfur species released during gasification of black liquor char with water vapor in the presence of H_2 at 600-700°C. This indicates that COS formation may not be important in recovery boilers. The range of water vapor and H_2 partial pressures in these measurements were 0.068-0.15 bar and 0.01-0.15 bar,

respectively. They indicated that the overall stoichiometry of H_2S formation under these conditions would be

$$Na_2S + H_2O + CO_2 \Rightarrow Na_2CO_3 + H_2S \qquad \text{(IV.C.2-4)}$$

and they interpreted the results of his kinetic studies as follows:

- H_2S formation in kraft char is an equilibrium process that depends upon the partial pressures of H_2S, CO_2 (both increase it) and H_2 (which decreases it).
- The water gas shift reaction probably determines the gas composition in the vicinity of the char surface (i.e. within the pores of the char particles).
- Since the rate of carbon gas formation is the rate of gasification, the rate of H_2S release is directly proportional to the rate of carbon gasification. This condition applies to Li and van Heiningen's experimental data but not to recovery boilers where CO_2 and water vapor are both always present.

Li and van Heiningen found that the fraction of Na_2S in black liquor char that had been converted to H_2S at the point when gasification was complete decreased with increasing temperature as shown in Figure IV.C.2-1. This indicates that the rate of Na_2S conversion to H_2S became slower relative to the rate of carbon conversion as temperature increased.

Their data also showed a maximum in the rate of Na_2S conversion to H_2S at 650°C. This suggests that either equilibrium is involved, i.e., as in a decreasing driving force for H_2S formation with increasing temperature, or series or parallel reactions. The latter is less likely because there is only one product sulfur gas (H_2S) found.

Data from the Åbo Akademi Single Droplet/Flow Reactor

In Chapter IV.C.1, the effect of furnace temperature and gas concentration was on sulfur release from black liquor during devolatilization was compared in Figure IV.C.1-3. These data suggested that there is no difference in sulfur loss during devolatilization in N_2 versus other gases for CO_2 and water vapor partial pressures not exceeding 0.05 bar. However, at higher CO_2 and water vapor partial pressures, the presence of both of these gases increased the loss of sulfur from char even at these relatively short reaction times. The effect of gas composition on sulfur release during devolatilization that was presented in Table IV.C.1-5 is included here as well since it must be subtracted from the sulfur release data from combined pyrolysis and char reaction experiments.

At higher CO_2 and water vapor partial pressures, the presence of both of these gases increased the loss of sulfur from char even at these relatively short reaction times (Table IV.C.1-5).

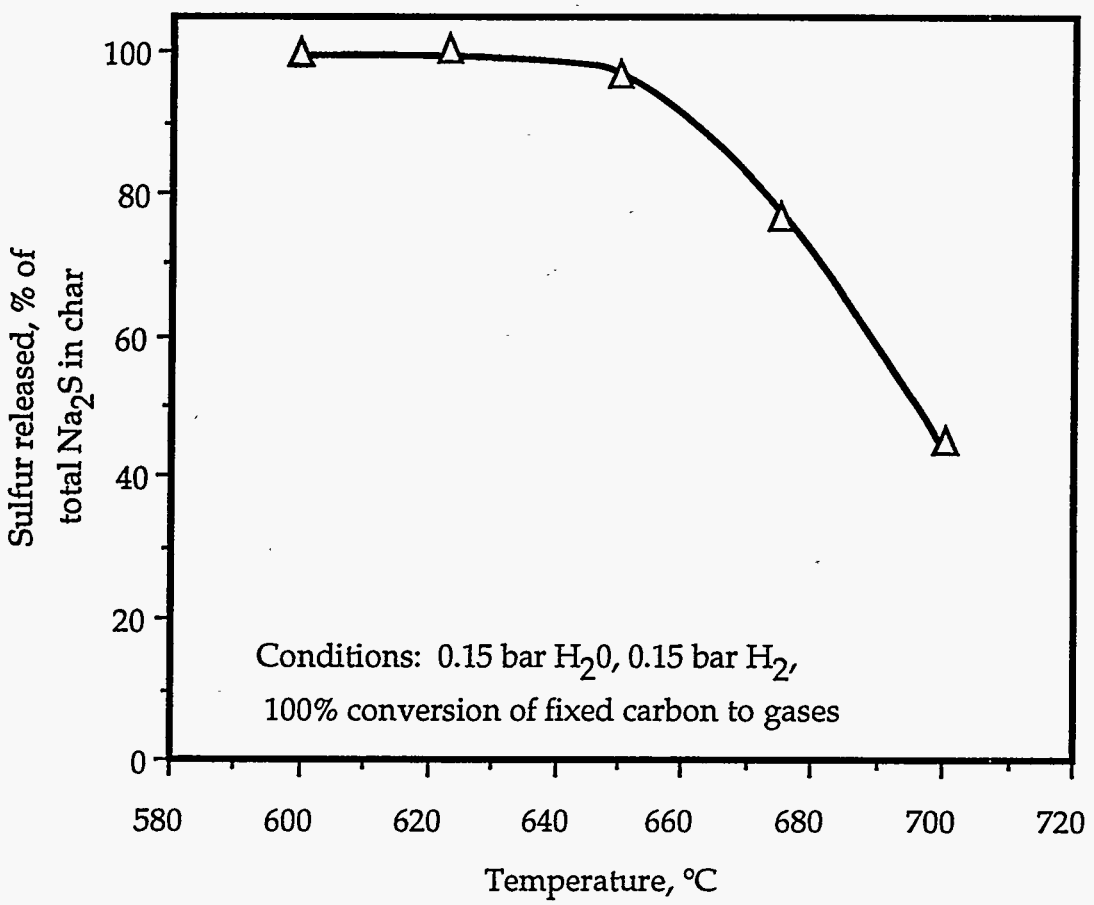

Figure IV.C.2-1. Percentage of the sulfur in black liquor char that is converted to gases during char gasification with water vapor at temperatures between 600 and 700°C. Data are from Li and van Heiningen (1994).

Table IV.C.1-5. The fraction of the sulfur originally in black liquor that was retained in the char 15 seconds after the black liquor droplet was inserted into a 900°C furnace containing the following gases and the balance N_2. Data are for Liquor A.

Mole fraction of gases in N_2			Fraction of sulfur retained in char
CO	CO_2	H_2O	
0.011	0.104		0.49
	0.10	0.05	0.47
0.04	0.113		0.49
0.05	0.05	0.10	0.25
0.10	0.05	0.05	0.25
	0.10	0.10	0.45
0.10	0.10	0.10	0.33
0.10	0.10	0.10	0.46

The average sulfur retained for liquor A in experiments where the CO_2 or H_2O content of the gases did not exceed 5% is shown in Table IV.C.2-3. These data were obtained in the Åbo Akademi droplet/flow reactor. The sulfur retained increases with increasing reactor temperature as was discussed earlier, in Section IV.C.1. We use these values of sulfur in the char at the end of devolatilization to find by difference the sulfur loss during char reactions for droplets that remained in the reactor for longer residence times. The results are included in Tables IV.C.2-4 to IV.C.2-6.

Effect of CO

Table IV.C.2-4 contains data for the sulfur retained in char for black liquor droplets heated in CO/N_2 mixtures, obtained in the Åbo Akademi droplet/flow reactor. There seems to be a greater sulfur loss during the char reactions stage at 900°C and above, although the last data point does not agree well with the others. It is possible that CO is converted to CO_2 via an alkali metal-catalyzed reverse Boudouard reaction and the CO_2 converts Na_2S in the char to COS.

Table IV.C.2-3. The average sulfur retained for liquor A in experiments where the CO_2 or H_2O content of the gases did not exceed 5%.

Temperature, °C	Sulfur retained in char, % of sulfur originally in the black liquor solids
600	33.0
700	43.0
800	44.3
900	62.1±3.4

Table IV.C.2-4. Sulfur retained in char for black liquor droplets heated in CO/N_2 mixtures (Åbo Akademi droplet/flow reactor).

Temperature °C	CO partial pressure, bar	Reaction time, s		Sulfur retained in char	Sulfur loss during char reactions
		Black liquor	Char		
600	0.039	180[1]		32.9%	0.1%
800	0.116	15[2]	20	42.9%	0.4%
900	0.040	180[1]		27.0%	35.1%
900	0.116	15[2]	20	45.5%	16.6%
900	0.116	15[2]	100	41.1%	21.0%
900	0.116	180[1]		60.0%	2.1%

[1]Droplets were inserted into the hot reactor at the temperature indicated and remained there for the time indicated.
[2]Droplets were inserted into the hot reactor for 15 seconds and then removed through a N_2 quench and cooled. They were subsequently reinserted int the reactor for the time indicated in the "Char" column.

Effect of CO_2

Table IV.C.2-5 contains data for the sulfur retained in char for black liquor droplets heated in CO_2/N_2 mixtures, obtained in the Åbo Akademi droplet/flow reactor. The data show that the sulfur loss during char gasification with CO_2 is low at temperatures below 700°C and moderate (~10-20%) at higher temperatures. The sulfur loss during char gasification generally increases with increasing temperature, CO_2 partial pressure, and reaction time.

Effect of Water Vapor

Table IV.C.2-6 contains data for the sulfur retained in char for black liquor droplets heated in water vapor/N_2 mixtures, obtained in the Åbo Akademi droplet/flow reactor. These data show that the sulfur loss during char gasification with H_2O generally increases with increasing temperature, H_2O partial pressure, and reaction time.

Effect of O_2

Table IV.C.2-7 contains data for the sulfur retained in char for black liquor droplets heated in O_2/N_2 mixtures, obtained in the Åbo Akademi droplet/flow reactor. These data show that the sulfur loss during char combustion with O_2 is low at temperatures of 800°C and below except at higher O_2 partial pressures. The sulfur loss is much higher at 900°C, about 50% at moderate O_2 partial pressures. The sulfur loss during char gasification generally increases with increasing O_2 partial pressure and reaction time. The effect of O_2 may in fact be due to the CO_2 partial pressure created at the particle surface during char burning.

Comparison of the Data from This Study with Li and van Heiningen's Data

In the data reported here, the sulfur release at 600-700°C was very low, usually within the uncertainty of the data. The amount of sulfur released generally increases with temperature, and there seems to be a threshold between 700-800°C where sulfur release begins to increase rapidly. Also, reaction time is more important than gas concentration in determining sulfur release. More sulfur was released from droplets in O_2/N_2 than in other gases, but this could be a result of higher particle temperatures for those burned in O_2/N_2 mixtures. Overall, these results suggest some kinetic influence and a non-gas reaction.

The effect of temperature on the data reported here does not agree with that reported by Li (1989). Li found a decrease in sulfur release as temperature increased, while the data reported here generally indicates the opposite. The main differences in the experimental conditions are between the experiments reported here and those of Li and van Heiningen's are:

Table IV.C.2-5. Sulfur retained in char for black liquor droplets heated in CO_2/N_2 mixtures (Åbo Akademi droplet/flow reactor).

Temperature °C	CO_2 partial pressure, bar	Reaction time, seconds		Sulfur retained in char	Sulfur loss during char reactions
		Black liquor	Char		
600	0.015	100		36.8%	-3.8%
600	0.045	180		26.3%	6.7%
650	0.116	15	200	42.6%	0.4%
750	0.116	15	200	35.7%	8.3%
800	0.015	100		32.5%	11.8%
900	0.005	100		50.5%	11.6%
900	0.015	100		51.3%	10.8%
900	0.045	180		41.2%	20.9%
900	0.050	15	20	45.6%	16.5%
900	0.050	15	100	41.7%	20.4%

Table IV.C.2-6. Data for sulfur retained in char for black liquor droplets heated in water vapor/N_2 mixtures (Åbo Akademi droplet/flow reactor).

Temperature °C	H_2O partial pressure, bar	Reaction time, seconds		Sulfur retained in char	Sulfur loss during char reactions
		Black liquor	Char		
700	0.150	15	100	37.0%	6.0%
800	0.150	15	15	46.2%	-1.9%
800	0.150	15	100	31.9%	12.4%
900	0.150	15	15	41.8%	20.3%

Table IV.C.2-7. Data for sulfur retained in char for black liquor droplets heated in O_2/N_2 mixtures (Åbo Akademi droplet/flow reactor)

Temperature °C	O_2 partial pressure, bar	Reaction time, seconds		Sulfur retained in char	Sulfur loss during char reactions
		Black liquor	Char		
600	1%	130		33.8%	-0.8%
650	7%	15	200	40.9%	2.1%
700	1%	130		46.0%	-3.0%
700	7%	15	20	48.0%	-5.0%
800	1%	130		47.3%	-3.0%
800	4%	10	200	41.8%	2.5%
800	4%	20	200	54.8%	-10.5%
800	4%	20	200	36.3%	8.0%
800	7%	15	20	28.8%	15.5%
900	1%	130		30.0%	32.1%
900	4%	15	20	10.3%	51.8%
900	7%	15	20	14.2%	47.9%

1. Li and van Heiningen's chars were pre-reduced, so the only sulfur species that they contained was Na_2S. The sulfur species in the chars used in this study were determined by the initial sulfur species distribution in the black liquor and the reactions that occurred during devolatilization and char burning. It is unlikely that the only sulfur species present after devolatilization would have been Na_2S.

2. The temperature range for the data reported here was higher than Li and van Heiningen's, 600-900°C versus 600-700°C for H_2S and 675-750°C for COS. Also, our experiments involved molten rather than solid sodium salt species at 800°C and above.

3. The reaction times for the data reported here were generally shorter than in Li and van Heiningen's experiments.

The rate of sulfate reduction may be an important factor in explaining the differences between our data and Li and van Heiningen's. Sulfate reduction proceeds very slowly at

600-700°C (Li and van Heiningen, 1992) but significant reduction can occur in the time frame of our experiments at higher temperatures (Cameron and Grace, 1985). The increase in the amount of sulfur released from char with increasing furnace temperature in our experiments may be because much more sulfide was formed at the higher temperatures and therefore available to be converted to H_2S by water vapor and CO_2.

Another important factor in explaining the differences between our data and Li's is that H_2S may react to form SO_2, CS_2, or other sulfur gas species. Removal of H_2S by chemical reaction would increase its concentration gradient near or within the particle. This would increase the rate of transport of H_2S from the particle and therefore increase the overall rate of sulfur release from the particles.

A third factor is the effect of temperature on the rate of gasification of carbon and the reduction of Na_2CO_3. Conversion of Na_2S to H_2S requires both CO_2 and water vapor as reactants. In our experiments with water vapor at 900°C, gasification proceeds rapidly at 900°C, producing CO, and Na_2CO_3 is reduced at an appreciable rate, producing CO and possibly CO_2. Recent data obtained in a separate study at Oregon State University (Frederick, 1994) indicates that the char is a very effective catalyst for the water gas shift reaction,

$$CO + H_2O \; <=> \; CO_2 + H_2$$

so that CO_2 would certainly be available along with water vapor to react with Na_2S at 900°C and above. In Li and van Heiningen's experiments, the temperatures were too low for appreciable Na_2CO_3 reduction and gasification proceeds much more slowly. The CO_2 partial pressure would therefore probably be lower within the particles in Li's experiments, contributing to a slower rate of H_2S formation.

In summary, it is clear that the data reported earlier by Li and van Heiningen do not fully account for the rate of release of sulfur from black liquor droplets at higher temperatures. A better understanding of the chemistry and physical processes involved in sulfur release is needed. This work is now under way.

References

Cameron, J. H. and Grace, T.M. (1985), "Kinetic Study of Sulfate Reduction with Kraft Black Liquor Char," *Ind. Eng. Chem. Fundamentals*, 24(4): 443.

Durai-Swamy, K., Mansour, M.N., Warren, D.W. (1991), "Pulsed Combustion Process for Black Liquor Gasification," US DOE Report DOE/CE/40893-T1 (DE92003672), February.

Li, J. and van Heiningen, A.R.P. (1992), "Kinetics of Solid State Reduction of Sodium Sulfate by Carbon," *Proc. 1992 TAPPI-CPPA Intl. Chem. Recovery Conf.*, TAPPI Press, Atlanta, p. 531-538.

Li, J. and van Heiningen, A.R.P. (1994), "The Rate Process of H_2S Emission During Steam Gasification of Black Liquor Char," *Chem. Eng. Sci.*, 49(24):4143-4151.

Li, J. (1989), "Rate Processes During Gasification and Reduction of Black Liquor Char," PhD thesis, McGill University, October.

Whitty, K.J. (1993), "Gasification of Black Liquor Char with H_2O under Pressurized Conditions," MS Thesis, Åbo Akademi University.

IV.D MODELING OF SODIUM AND SULFUR RELEASE

IV.D.1 Sodium Release During Devolatilization

The best current model for sodium release during devolatilization is that sodium is vaporized during devolatilization only by Na_2CO_3 reduction. Sodium release from black liquor droplets does occur by fragmentation of the droplets. The limit data available with which to estimate the amount of sodium in these fragments is shown in the inset of Figure IV.B-7. This data was obtained from droplets that were exposed to a hot furnace environment for ten seconds which is longer than the time to complete devolatilization, so the sodium loss resulting from by Na_2CO_3 reduction during that period was subtracted to obtain the sodium loss by fragmentation. The results, for temperatures 700-1000°C, are shown in Table IV.D.1-1. Except for the point at 1000°C, these results suggest that the loss of sodium from the droplets during devolatilization as char fragments is 13-14% of the sodium initially in the droplets. The lower value at 1000°C may be because substantial sodium was volatilized from the charred outer droplet surface while devolatilization was still under way within the droplet at this highest experimental temperature.

Table IV.D.1-1. Estimation of sodium loss from black liquor droplets via Na_2CO_3 reduction versus via fragmentation.

Furnace Temperature °C	Na lost in 10 seconds at the indicated temperature, % of Na in BLS		
	Total	From Na_2CO_3 Reduction	From Fragmentation
700	13.0	0.0	13.0
800	14.6	0.5	14.1
900	16.4	3.4	13.0
1000	20.0	13.1	6.9

These results are based on data from a relatively limited number of liquors. Results from on-going research at Åbo Akademi University, the Technical Research Centre of Finland, and Oregon State University may provide additional insight into the question of sodium release during devolatilization.

IV.D.2 Sodium Release During Char Burning and Gasification

Char Burning

Sodium release during char burning can result from the reduction of Na_2CO_3 to elemental sodium, and from vaporization of NaCl.

The rate of sodium vapor generation via Na_2CO_3 reduction during char burning is controlled by a combination of kinetic, pore diffusion, and gas-phase transport. The kinetic rate of Na_2CO_3 reduction in black liquor char reported by Li and van Heiningen (1990) is described by IV.D.2-1.

$$\frac{d[Na_2CO_3]}{dt} = 10^9 [Na_2CO_3] \exp\left[\frac{-244000}{RT}\right] \qquad \text{(IV.D.2-1)}$$

Inhibition of reduction by CO or CO_2 is neglected at recovery furnace temperatures.

Transport effects commonly play an important role gas-solid reactions particles as large as black liquor droplets. In the case of sodium volatilization via Na_2CO_3 reduction, the sodium vapor, once formed, must diffuse to the particle surface and be transported across the boundary layer to the bulk gas. These processes are illustrated in Figure IV.D-1.

Transport processes can slow the overall rate of sodium vaporization by acting as resistances in series with the kinetic rate "resistance". They may also slow the reaction itself by increasing the sodium vapor partial pressure at the reaction sites if reaction 9 is reversible.

Estimation of film mass transfer effects is straightforward in the case of burning black liquor droplets (Frederick, 1990), and for reacting gases (CO_2, $H_2O_{(v)}$) diffusing into char particles, the effect of intraparticle diffusion can be handled by a Thiele modulus-based effectiveness factor (Levenspiel, 1972). In the case of Na_2CO_3 reduction, however, the reaction product diffuses from the particle and Na_2CO_3 reduction, if reversible, may be slowed by the presence of sodium vapor. The combined effects of diffusion of a product from a reversible reaction out of a large particle remains to be modeled. This is a part of our continuing work on Na_2CO_3 reduction.

We recommend the following method for estimating the rate of sodium volatilization during char burning.

The overall rate of sodium release from black liquor char is

$$\frac{1}{R_{Na}} = \frac{1}{R_{mNa}} + \frac{1}{\eta_i R_{cNa}} \qquad \text{(IV.D.2-2)}$$

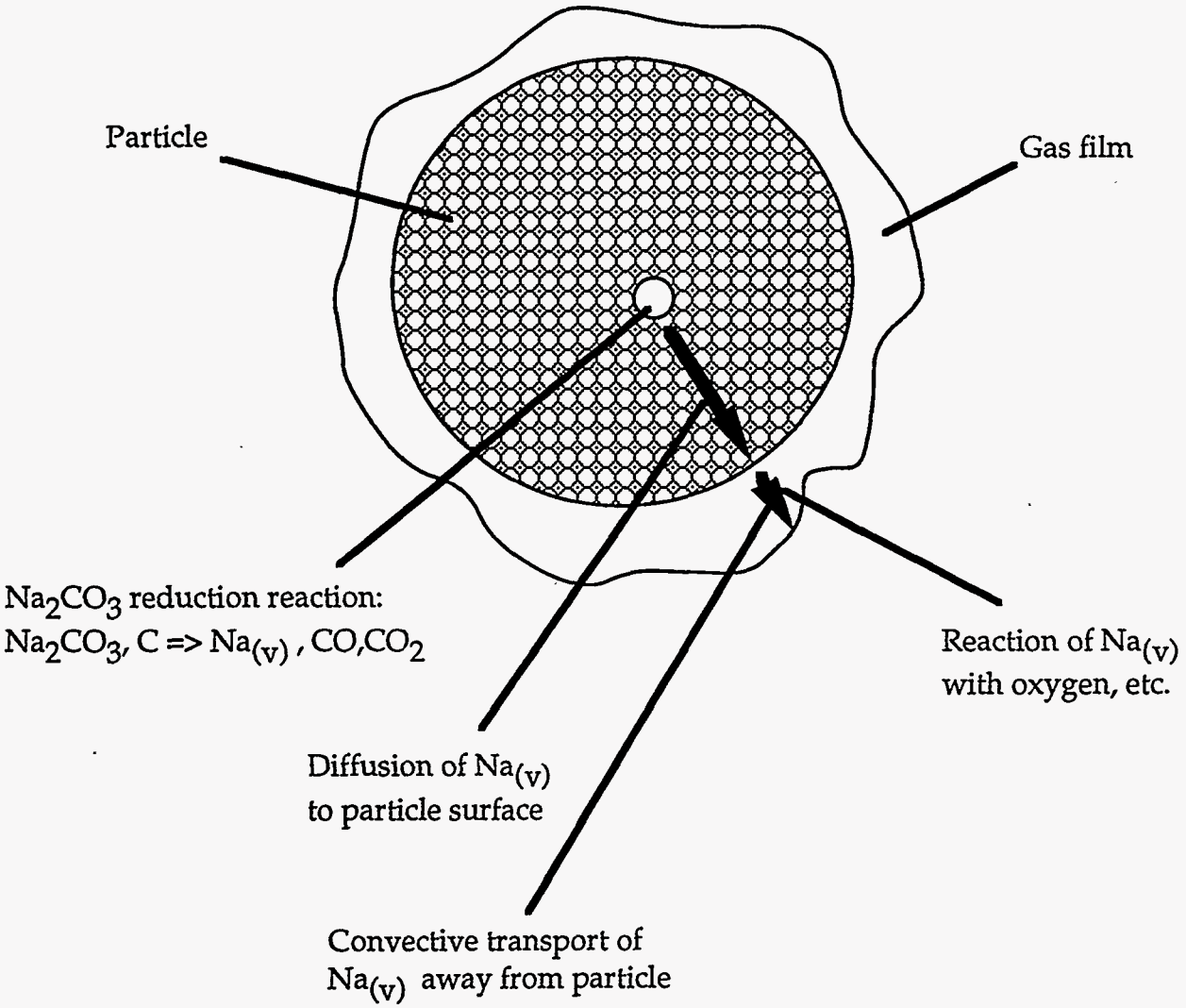

Figure IV.D-1. Transport processes involved in volatilization of sodium from char particles.

In equation IV.D.2-2,

$$R_{mNa} = k_{Na} A_p C_{Na} \qquad \text{(IV.D.2-3)}$$

where R_{mNa} is the moles of sodium vapor transferred per second, A_p is the external surface area of the particle, and C_{Na} is the concentration of the gas species of interest in the bulk gas. The gas film mass transfer coefficient is estimated from a Sherwood number correlation which accounts for both free and forced convection effects (Treybal, 1981).

$$Sh = \frac{k_g D}{D_p} = 2 + 0.569\,(Gr\,Sc)^{0.25} + 0.347\,(Re\,Sc^{0.5})^{0.62} \qquad \text{(IV.D.2-4)}$$

The effectiveness factor, η_i, in equation IV.D.2-2 accounts for the rate-limiting effect of intraparticle diffusion on the overall rate R_i (Levenspiel, 1989). It is estimated from the Thiele modulus as

$$\eta_i = \frac{\tanh(M_{Ti})}{M_{Ti}} \qquad \text{(IV.D.2-5)}$$

where the Thiele modulus is estimated as

$$M_{Ti} = \frac{D}{6}\left[\frac{k_i}{D_i}\right]^{1/2} \qquad \text{(IV.D.2-6)}$$

k_i, the apparent first order rate constant, is calculated as

$$k_i = \frac{R_{ci}}{V_p C_i} \qquad \text{(IV.D.2-7)}$$

The density of black liquor char particles is very low ($\approx$ 30-50 kg/m^3) during char burning, so that the diffusivity of the reacting gases within the char particles can be assumed to be the same as in the bulk gas. The diffusivity for each gas is assumed to be proportional to the absolute temperature to the 1.75 power.

Predictions of the rate of sodium volatilization from black liquor droplets during char burning are compared with experimental data in Figures IV.D-2 – IV.D-5. The data are from four different experimental systems, and for char particle sizes from 300 μm to 9 mm (initial black liquor particles/droplets 100 μm and 2-3 mm). The agreement between the predictions and experimental data is very good over the entire range.

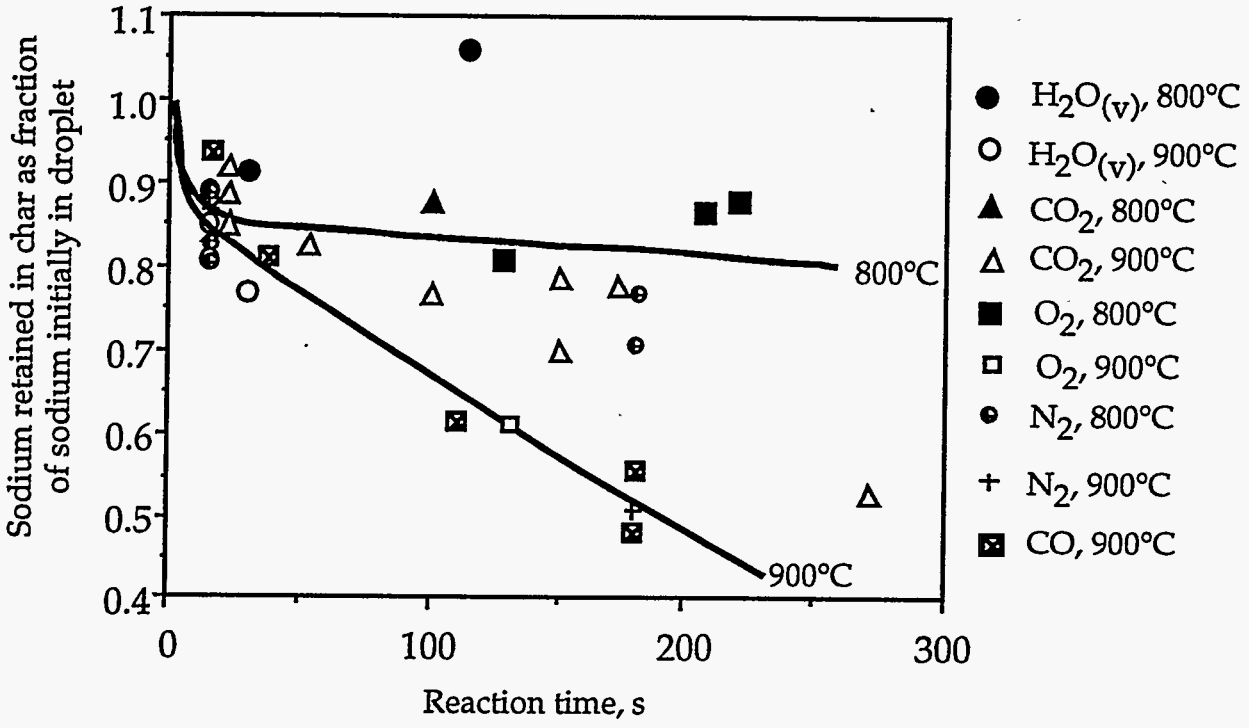

Figure IV.D-2. Comparison of experimental and predicted sodium volatilization during char pyrolysis, burning, and gasification. Data are from the Åbo Akademi University single particle/stagnant gas reactor. Gas concentrations were as follows: $H_2O_{(v)}$: 1-15%; CO_2: 1-14%; O_2: 1-7%; CO: 4-12%.

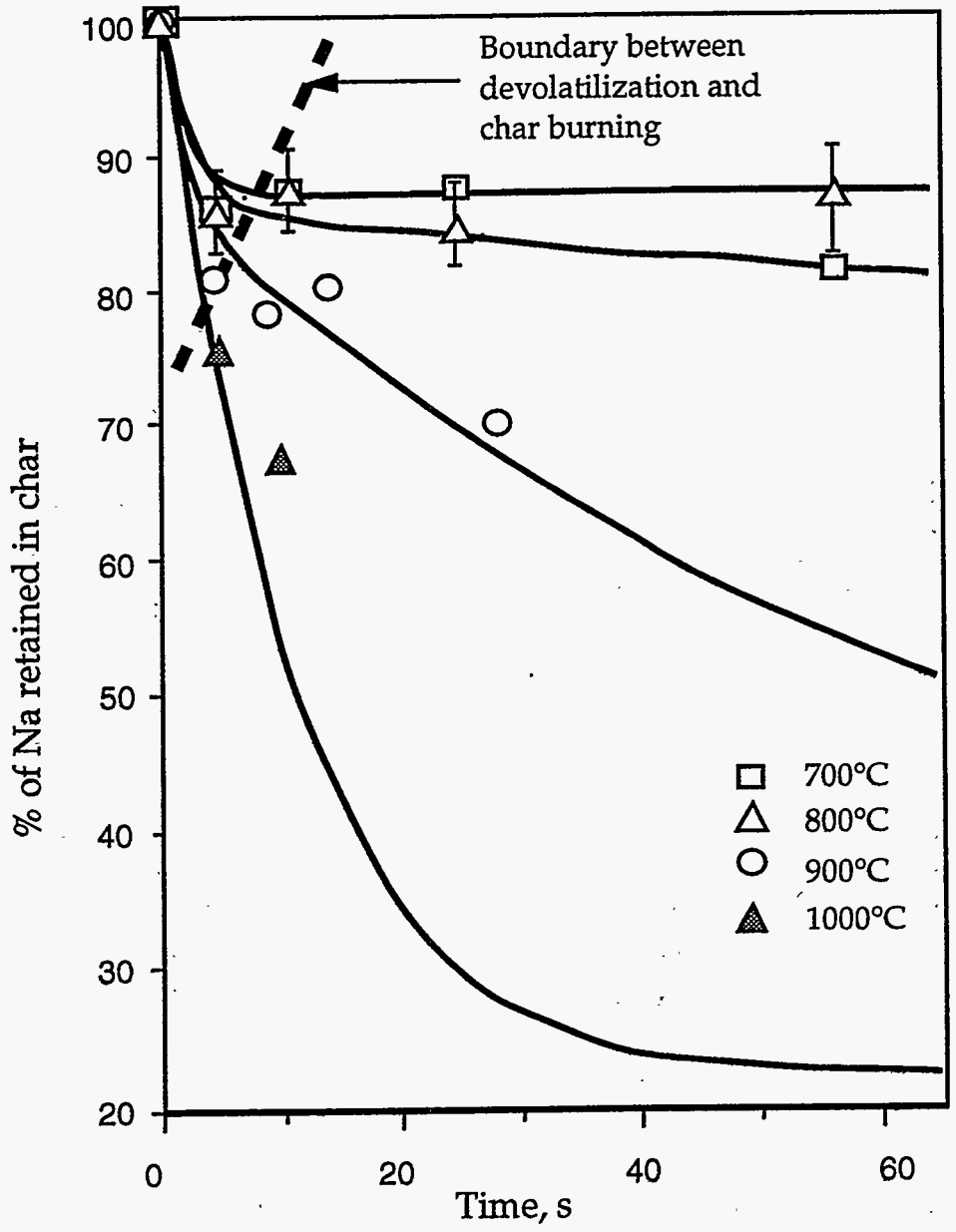

Figure IV.D-3. Comparison of experimental and predicted sodium volatilization during char pyrolysis and burning. Data are from the Åbo Akademi University single particle/stagnant gas reactor.

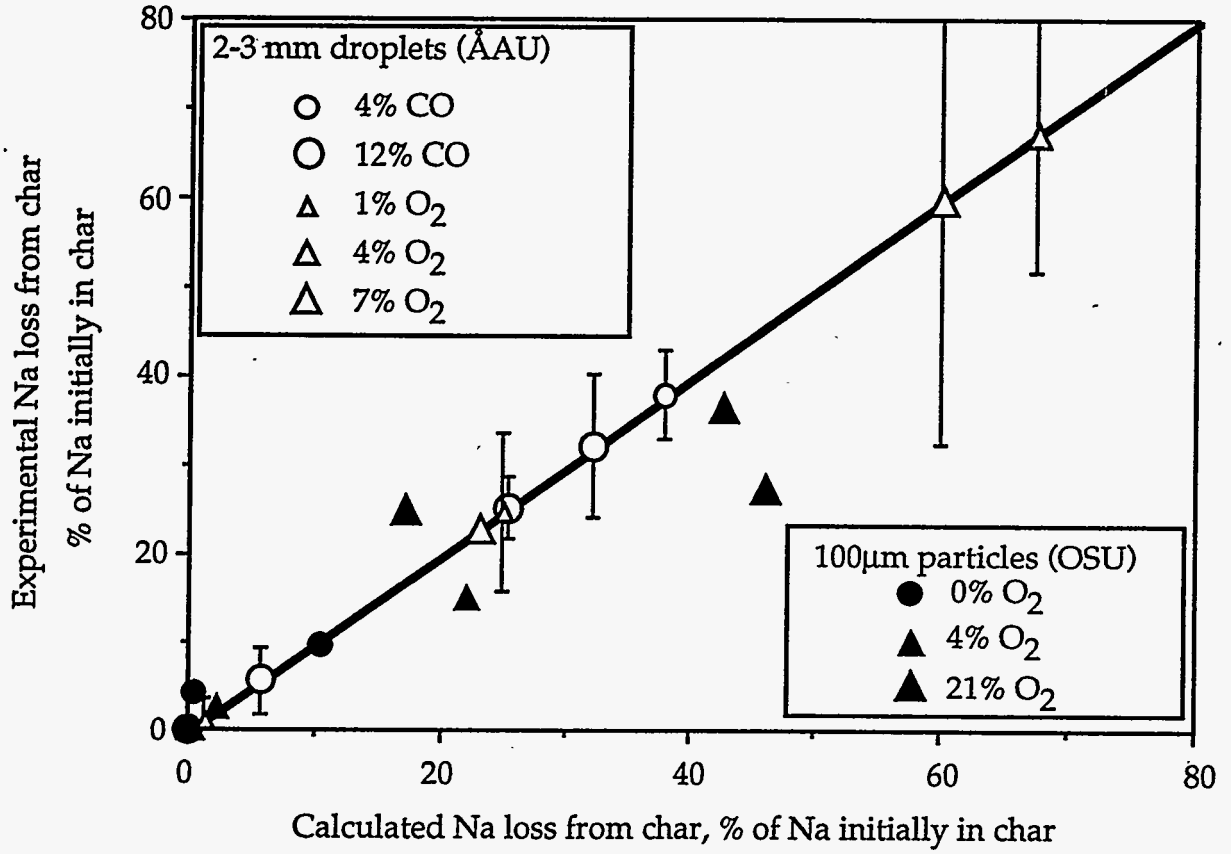

Figure IV.D-4. Comparison of experimental and predicted sodium volatilization during char pyrolysis and burning.

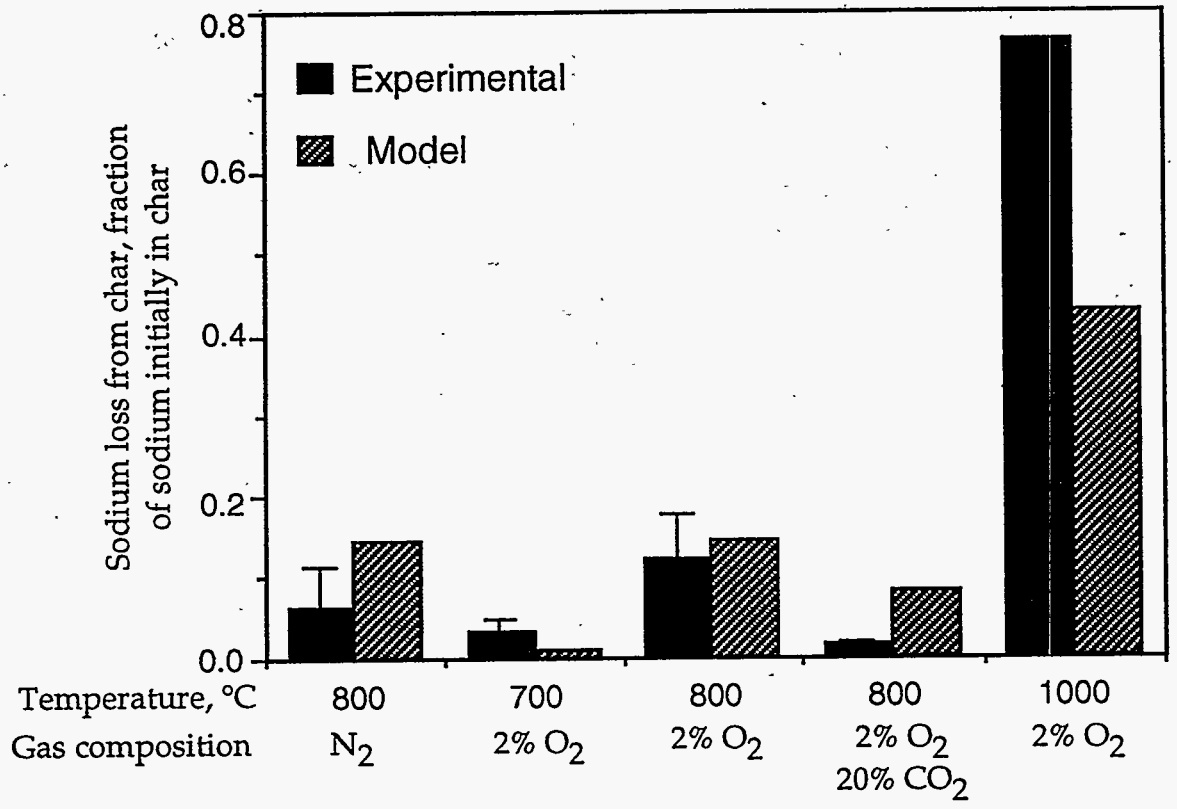

Figure IV.D-5. Comparison of experimental and predicted sodium volatilization during char pyrolysis and burning. Data are from the Åbo Akademi University fume reactor.

IV.D.3 Sulfur Release During Devolatilization

As was shown in Section IV.C.1, the fraction of the total sulfur in black liquor that is lost during devolatilization is the same for all liquors for which data is available and depends only on the furnace temperature. The sulfur loss is estimated from the data in Figure IV.C.1.17. Correlations that fit this data are as follows:

for 250°C < T < 1018°C,

$$S_{vol} = -1.63.27 + 0.9171\,T - 1.150 \times 10^{-3}\,T^2 + 4.283 \times 10^{-7}\,T^3 \qquad \text{(IV.D.3-1)}$$

for T > 1018°C,

$$S_{vol} = 458.85 \exp\left(-2.666 \times 10^{-3}\,T\right) \qquad \text{(IV.D.3-1)}$$

where S_{vol} is the percentage of sulfur in the black liquor that was volatilized and T is the furnace temperature in °C.

In modeling sulfur release during devolatilization, the rate of sulfur release is proportional to the rate of carbon release, while the total amount of sulfur released is a fraction of the total sulfur in black liquor that depends only on furnace temperature.

IV.D.4 Sulfur Release During Char Burning and Gasification

In the presence of both CO_2 and water vapor, the rates of H_2S and COS release when both are mass transfer limited are given by

$$\frac{d_{Ni}}{dt} = k_g A_{ext} [C_i]_{eq} \qquad \text{(IV.D.4-1)}$$

where

N_i = moles of species i (H_2S or COS)

kg = mass transfer coefficient

A_{ext} = external surface area of the char particle

$[C_i]_{eq}$ = equilibrium concentration of species i (H_2S or COS) at the existing partial pressures of CO_2 and water vapor

The equilibrium partial pressures of H_2S and COS are calculated from the equilibrium expressions as

$$[COS]_{eq} = \frac{K_{COS} P_{CO2}^2}{RT} \qquad \text{(IV.D.4-2)}$$

where

$$K_{COS} = \frac{P_{COS}}{P_{CO2}^2} = \exp(-16.0739 + 12307/T) \qquad \text{(IV.D.4-3)}$$

and

$$[H_2S]_{eq} = \frac{K_{H2S} P_{H2O} P_{CO2}}{RT} \qquad \text{(IV.D.4-4)}$$

where

$$K_{H2S} = \frac{P_{H2S}}{P_{H2O} P_{CO2}} = \exp(-16.4674 + 16507/T) \qquad \text{(IV.D.4-5)}$$

and concentrations are in mol/m^3, pressures in bar, and temperatures in K.

This model predicts that the rate of COS release decreases with increasing temperature because the equilibrium P_{COS} decreases. It might account for the higher sulfur release observed in colder lower furnaces in recovery boilers, although the rate of sulfur release becomes much slower than that the predicted H_2S release rate at realistic furnace temperatures.

Preliminary rate models for both H_2S and COS formation from black liquor char particles have been developed, based on these equilibria and the transport considerations discussed in Section IV.D.2. They give reasonable predictions of the rates of H_2S and COS formation from char particles when compared with the limited data available for black liquor char particles. Modification of the models to account more rigorously for diffusion of H_2S and COS from the particles remains to be completed, and additional data is needed to better test these models.

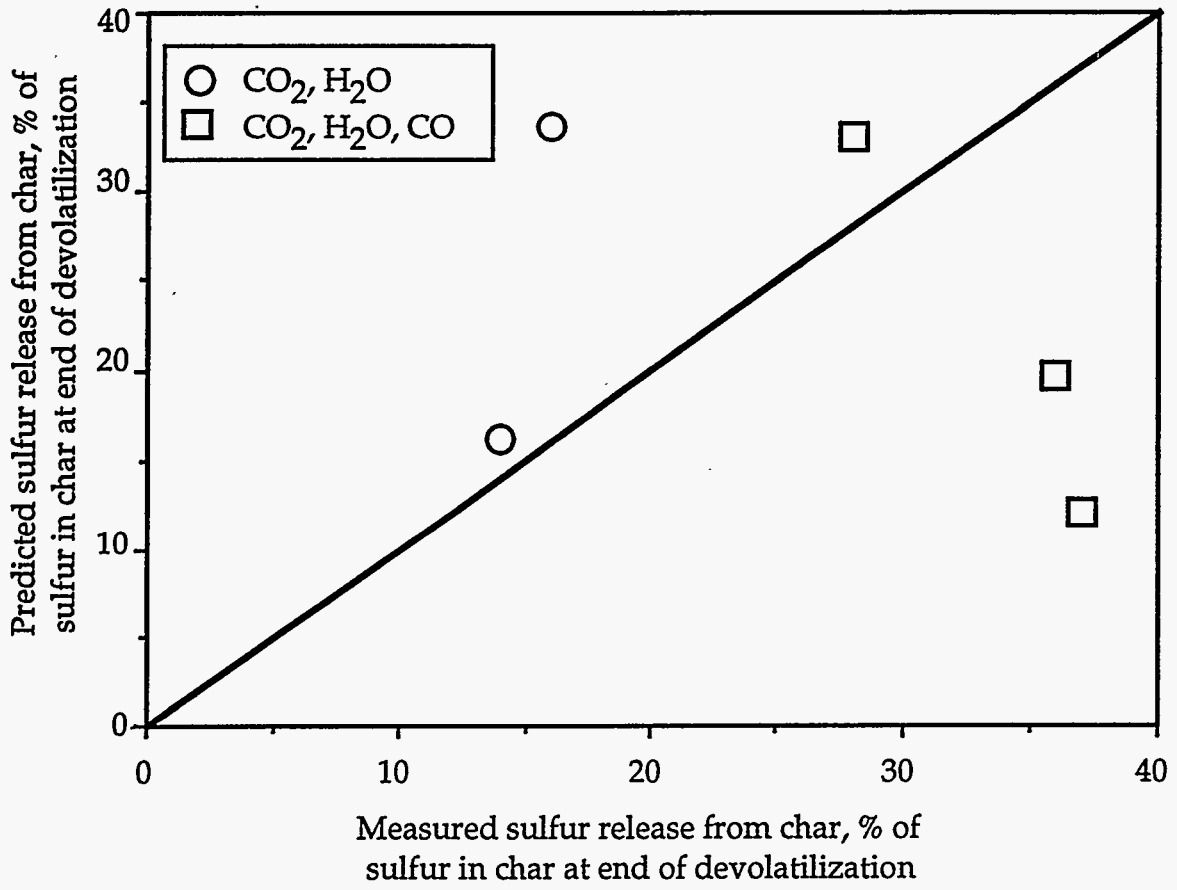

Figure IV.D.6. Comparison of measured and predicted sulfur loss during char burning and gasification. Data are from the Åbo Akademi University single particle/flow reactor. Particle temperatures were calculated using the procedure described in Section IV.A.1 of this report.

References

Levenspiel, O., *Chemical Reaction Engineering*, Second edition, John Wiley & Sons, New York (1972).

Levenspiel, O., *Chemical Reactor Omnibook,* OSU Bookstores, Corvallis, Oregon, 1989.

Li, J. and van Heiningen, A.R.P., *Tappi Jl.*, 73(12):213-219 (1990).

Treybal, R.E., *Mass Transfer Operations*, Third edition, .McGraw-Hill Book Company, New York, 1981.

V.A ANALYSIS OF SO_2 CAPTURE BY NA_2CO_3 AT KRAFT RECOVERY BOILER CONDITIONS

Summary

The reaction of SO_2 with Na_2CO_3 is important in the capture of sulfur gases in black liquor combustion. There has been relatively little information available on the rate of sulfation of Na_2CO_3.

The reaction of Na_2CO_3 with SO_2 in the presence of oxygen, with products are Na_2SO_4 and CO_2, has been studied by several investigators. Published data on the sulfation of solid Na_2CO_3 are available but no data were found on the reactions of molten Na_2CO_3 with SO_2. The data for sulfation of solid Na_2CO_3 were fitted with appropriate gas-solid reaction models. The rate of sulfation of Na_2CO_3 is mainly controlled by intraparticle diffusion in the temperature range 120-700°C and the diffusion process is probably solid-state diffusion. Based on the intraparticle diffusion rate, the residence time of solid fume particles in a recovery furnace is too short for any substantial sulfation to take place. Thus almost all of the sulfation of Na_2CO_3 has to take place in the molten phase.

The rates of sulfation of both Na_2CO_3 and NaCl in solid particles is too slow at conditions in the boiler and generator banks to account for significant SO_2 capture. This implies that nearly all of the sulfation of fume particles in recovery boilers occurs as reactions in the gas phase or before the particles solidify. This conclusion is supported by experimental data obtained from operating recovery boiler. The rates are fast enough, however, to account for significant sulfation of Na_2CO_3 and NaCl in boiler tube deposits.

Introduction

In black liquor combustion, sulfur dioxide may be captured by the sulfation of sodium carbonate. The reaction is

$$Na_2CO_3\,(s,l) + \frac{1}{2}O_2 + SO_2 \rightarrow Na_2SO_4\,(s,l) + CO_2 \qquad \text{(V.A-1)}$$

The SO_2 capture may occur by both liquid and solid Na_2CO_3.

Sulfation of Na_2CO_3 is also important in other applications. The injection of dry $NaHCO_3$ can be used in the flue gas desulfurization (FGD) system to capture sulfur compounds in flue gas from coal-fired boilers (Keener and Davis, 1984). The decomposition of $NaHCO_3$ to Na_2CO_3 takes place at 270°C but it is known partially at temperature as low as 100°F. In addition, Na_2CO_3 is also a candidate for flue gas desulfurization systems, and an understanding of the sulfation of Na_2CO_3 is important in this application as well.

Sulfation of Na_2CO_3

The sulfation of Na_2CO_3 has been studied by several researchers. The objectives and conditions of each study were different. Backman, Hupa, and Usikartano (1985), Maule and Cameron (1989), Keener and Davis (1984) and Lloyd-George (1985) studied this reaction in the presence of oxygen whereas Smith and Kimura (1987) and Butler and Waites (1981) studied in the absence of oxygen. The condition of interest for sulfation of Na_2CO_3 for kraft recovery boilers is in the presence of oxygen.

Data on the kinetics of the SO_2-Na_2CO_3 reaction in the presence of oxygen have been reported by Backman et al. (1985), Maule and Cameron (1989) and Keener and Davis (1984). All of these studies were made at temperatures below the melting point of Na_2CO_3.

Figure V.A-1 compares the reaction rates as reported in these three studies. There is considerable discrepancy in the rates reported - they differ by as much as a factor of more than 100 when compared at the same temperature.

In understanding and modeling the sulfation of fume particles and deposits in recovery boilers, it is important to be able to predict reliably the rate of sulfation of Na_2CO_3. There is too great a difference in the rate data reported in these three studies for use in modeling and interpreting sulfation rates in recovery boilers. Two of the objectives of this part of the work, therefore, were to determine whether these data are consistent and if a single rate relationship could be developed to predict the rate of sulfation of fume particles and deposits in recovery boilers.

Analysis of the Existing Rate Data

Both the materials and the gas concentrations used in the studies varied considerably as shown in Table V.A-1. Keener and Davis (1984) used a relatively porous commercial grade Na_2CO_3 of sizes 20-200 μm. Backman et al. (1985) used 55 μm particles that had been presintered by heating at 600°C for 12 hours to minimize the effect of sintering on the reaction rate during sulfation. Maule and Cameron (1989) generated submicron Na_2CO_3 particles from a Na_2CO_3/Na_2S melt.

In interpreting their data, Backman et al. (1985) had determined the chemical reaction rate based on the initial rate. Maule and Cameron (1989) had used the shrinking unreacted core model (Levenspiel, 1972) to determine the chemical reaction kinetics. The shrinking unreacted core model describes gas-solid reactions when the porosity of the unreacted solid is very small. In the model, the reaction is assumed to start at the surface of the solid and to proceed at a sharp interphase between the unreacted core and the porous product layer which is formed on the outer surface of the particles.

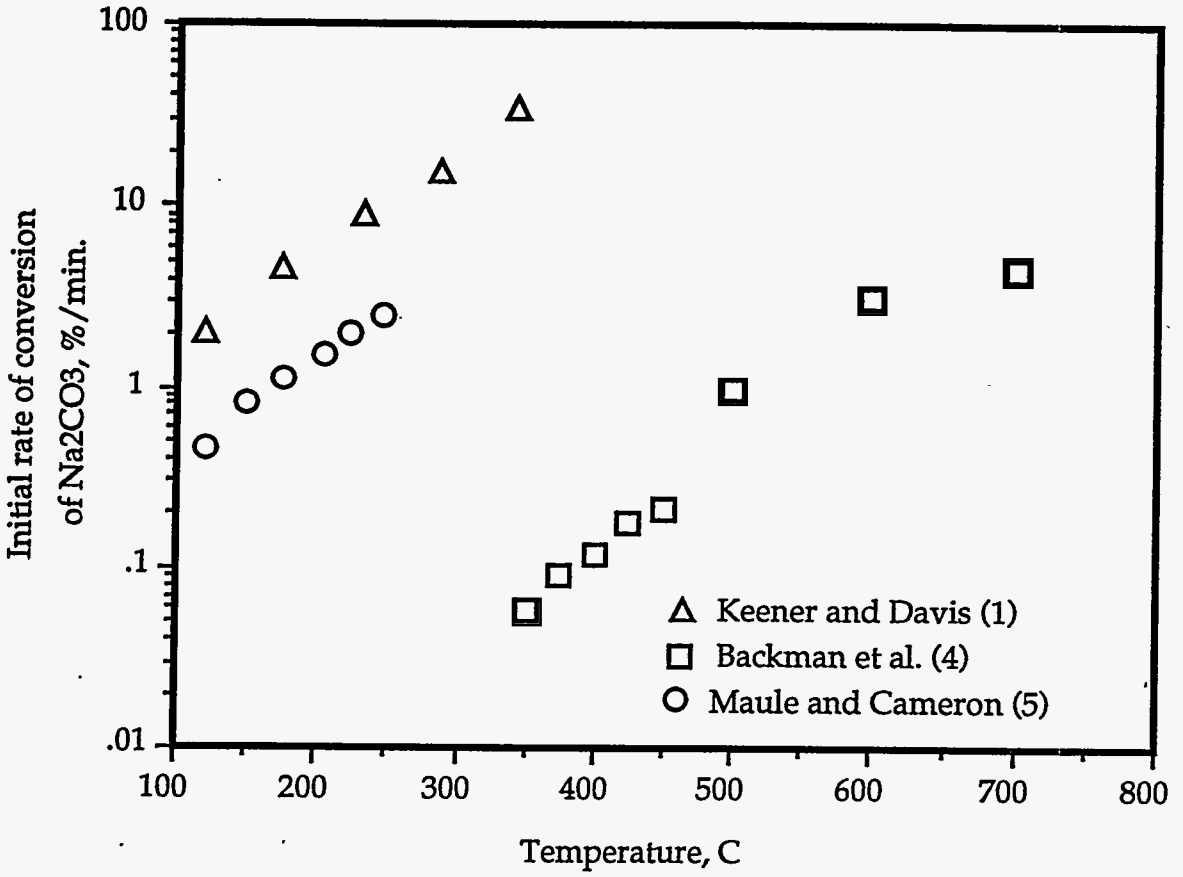

Figure V.A-1. Initial rates of sulfation of Na_2CO_3 as reported by Backman et al. (1985), and as estimated from Keener and Davis (1984), and Maule and Cameron (1989). The particle characteristics and gas compositions for these three studies are included in Table V.A-1.

Table V.A-1. Experimental conditions employed in previously reported Na_2CO_3 sulfation studies.

	Keener and Davis (1984)	Backman et al. (1985)	Maule and Cameron (1989)
Particle size, μm	20, 90, 200	55	0.25-1.0
Temperature, °C	121-344	350-700	120-246
Specific surface area, m^2/g	1.72 (20 μm)	0.132	6.56
	1.25 (90 μm)		
	0.91 (200 μm)		
Ratio of total to external surface area	14.3 (20 μm)	3.03	1.71
	46.9 (90 μm)		
	75.8 (200 μm)		
SO_2, %	2.45	1-5	0.25-0.43
O_2, %	4.9	5-20	0.34-2.15

The activation energies of the chemical reaction reported by Backman et al. (1985) and Maule and Cameron (1989) were 65 kJ/mol and 23 kJ/mol respectively. Diffusion through the product layer seemed to be important at higher conversions in both of the studies. Keener and Davis (1984) presented data at different temperatures but they did not determine chemical reaction or diffusion rates.

We wanted to determine the chemical reaction and the diffusion rates from all of the studies and compare them. We determined the chemical reaction rates from the initial rates as well as both the chemical reaction and the product layer diffusion rates using the shrinking unreacted core model for Backman et al. (1985) and Maule and Cameron (1989) data. An example of the fit of the shrinking unreacted core model is shown in Figure V.A-2.

For Keener and Davis (1984) data, the materials used were porous and the reaction rate depend strongly on the particle size. It seemed that the initial reaction rate was limited by both gas diffusion in the pores and chemical reaction. The general model for gas solid reaction developed by Ishida and Wen (Wen, 1968; Ishida and Wen, 1968; Froment and Bischoff, 1979) was used to fit the Keener and Davis (1984) data to determine the chemical reaction and the diffusion rate. This model is an intermediate between the shrinking unreacted core model and the homogeneous model. The homogeneous model describes a gas-solid reaction which the reaction occurs homogeneously throughout the solid to produce a gradual variation in solid reactant concentration in all parts of the particle. This general model accounts for both

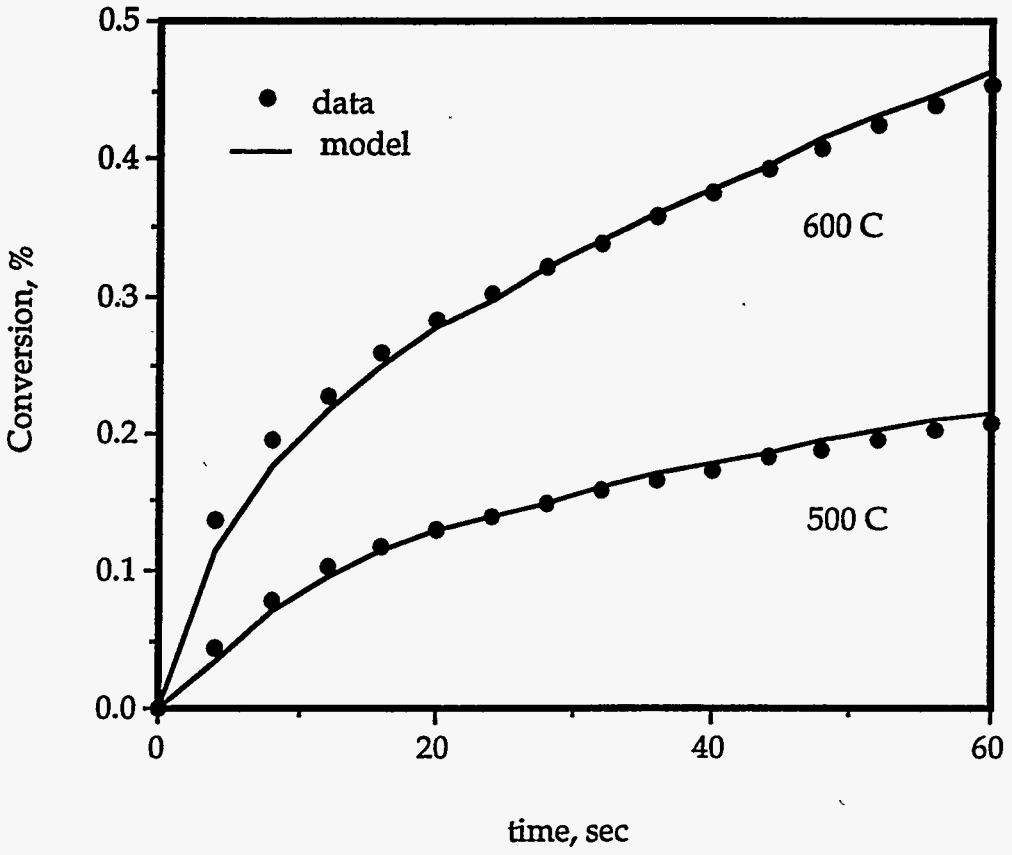

Figure V.A-2. The fit with shrinking unreacted core model with both chemical and diffusion control with Backman et al. (1985) data at 500 and 600°C.

considers that the reaction is faster near the surface than in the interior of the particle, and that after a certain time the solid reactant near the surface will be completely exhausted forming an inert product layer. The shrinking unreacted core model and the homogeneous model are also special cases of this model.

In the initial rate analysis we assumed that the total surface area of the particles was available for the reaction, not only the external surface area of the particles. We accounted for this by dividing the initial rates (moles/s) by the ratio of the total surface area of the particles (m^2/particle). The total surface area was calculated from the specific surface areas reported in each study (Table V.A-1). The chemical reaction rate constants thus determined are presented in Figure V.A-3. The agreement of these studies is improved. The range of variation was reduced by an order of magnitude when compared with the data in Figure V.A-1.

Temperature Dependence

The activation energies of both the chemical reaction kinetics and the product layer diffusion were determined. An example of the Arrhenius plots used in the activation energy determinations is presented in Figure V.A-4. The activation energies are presented in Table V.A-2.

Table V.A-2. The activation energies of the chemical reaction and product layer diffusion in the sulfation of Na_2CO_3.

Study	Chemical Reaction, E_a	Diffusion, E_a
Backman et al. (4)	67 kJ/mol	98 kJ/mol
Keener and Davis (1)	66 kJ/mol	51 kJ/mol
Maule and Cameron (5)	25 kJ/mol	37 kJ/mol

The agreement between the activation energies of the chemical reaction rates from the two methods is excellent. The activation energies from the study of Maule and Cameron (1989) were, however, considerably lower for both of the processes. Maule and Cameron (1989) used very fine particles which sintered together during the sulfation. The sintering reduced the reaction rate at higher temperature and thus diminished the activation energy. This is a possible reason why they got lower activation energy of reaction than others. The data of Maule and Cameron (1989) may be relevant for fume particles in deposits in which sintering is important. However, the data may not be applicable for sulfur capture by fume particles in-flight.

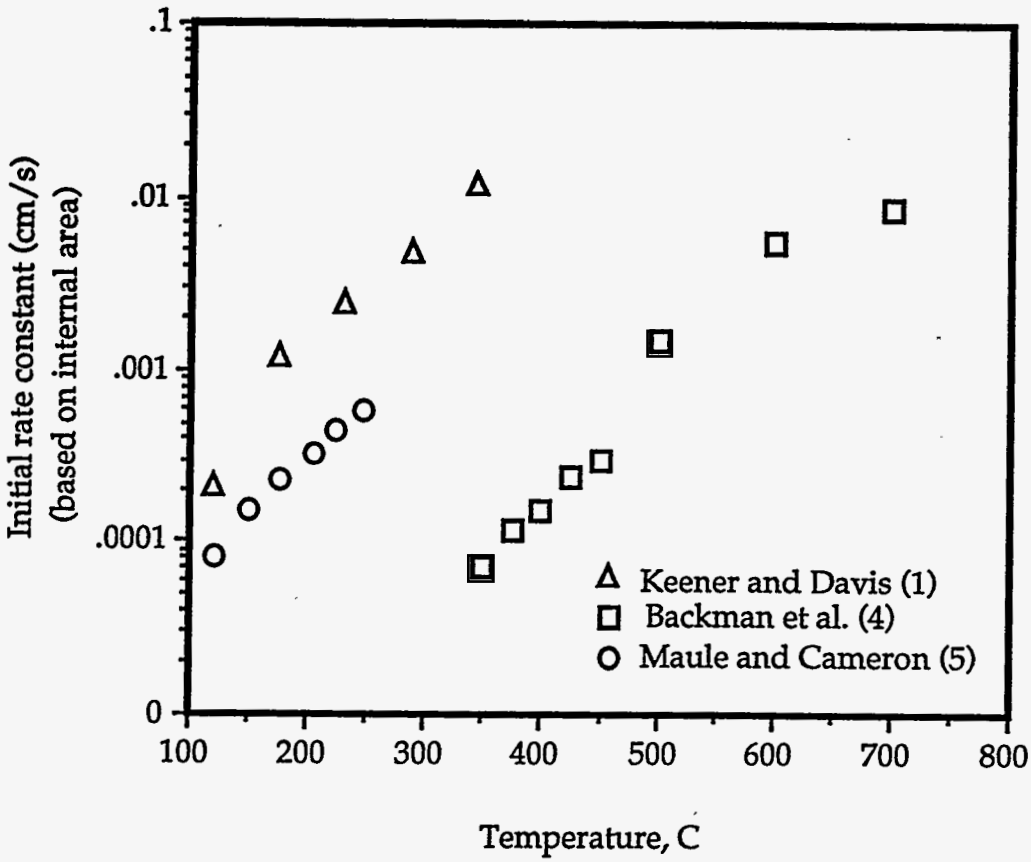

Figure V.A-3. The chemical reaction rate coefficients determined from the initial rate data for the sulfation of Na_2CO_3.

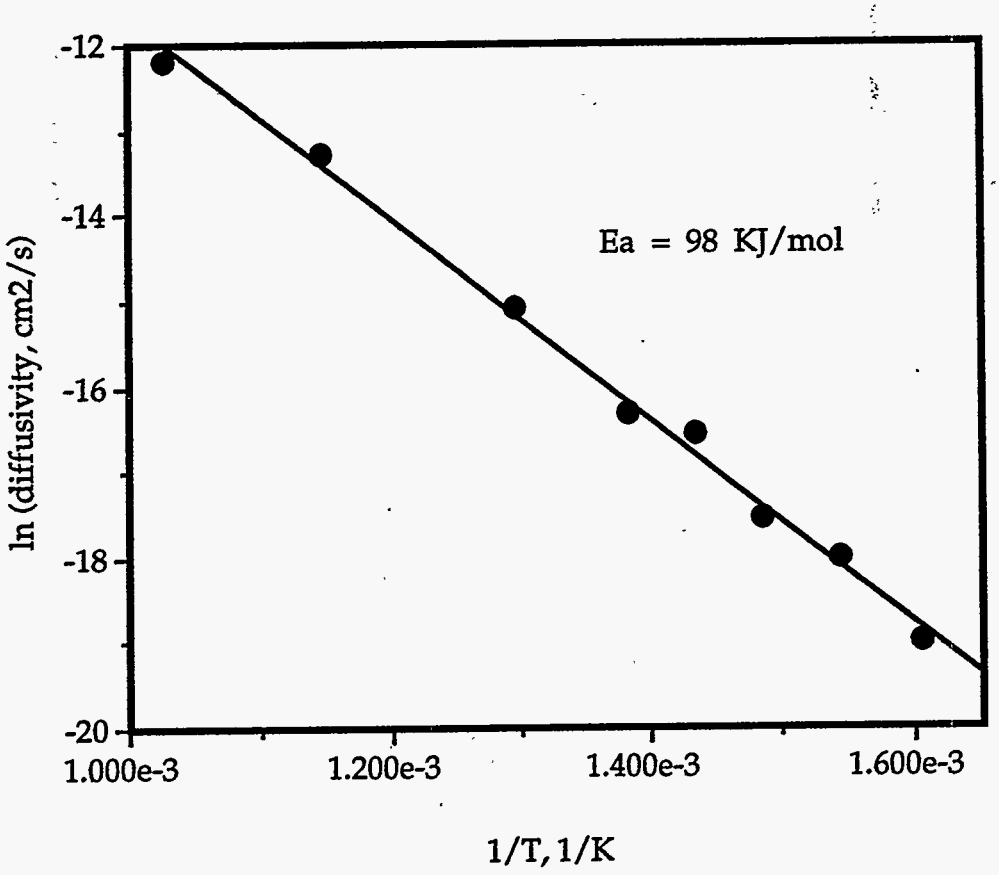

Figure V.A-4. Arrhenius plots for the effective diffusivity through Na_2SO_4 product layer from Backman et al. (1985) data.

Based on the shrinking unreacted core modelling, the major limiting step of this reaction was diffusion through the product layer (Boonsongsup, 1993). The apparent activation energy of diffusion process was very high in all of the studies and was as high as 98 KJ/mol for the Backman et al. (1985) data. All of the activation energy values are too high for bulk gas diffusion or Knudsen diffusion which have activation energies of the order of 10 and 3 kJ/mol at these temperatures. The high apparent activation energy of the product layer diffusion process suggests that the diffusion may be solid state diffusion. Iisa et al. reported that the rate of sulfation of $CaCO_3$ was also controlled by solid state diffusion (Iisa, Hupa, and Yrjas, 1992).

A further support for the hypothesis that the diffusion process is not gas phase diffusion comes from the dependence of the diffusion rate on the gas concentration. If the diffusion had been gas phase diffusion, the diffusion rate would have been a linear relationship of the concentration of the diffusing gas component. The diffusion was a linear function of neither the SO_2 or O_2 gas concentration (Boonsongsup, 1993). Based on these two reasons - the high apparent activation energy of diffusion and that SO_2 and O_2 are not the diffusing species - the diffusion of this reaction is most likely solid state diffusion.

The apparent activation energy of the product layer diffusion determined from the data of Keener and Davis was again approximately one half of the activation energy from Backman et al. data. If the rate in the study of the Keener and Davis was limited by both solid state and gas phase diffusion in the pores, the method would give one half of the true activation energy of the solid state diffusion process. The assumption of both pore diffusion and solid state diffusion control in the Keener and Davis (1984) study is supported by the fact that the diffusion rate from Keener and Davis (1984) data was considerably higher than in the other studies (Boonsongsup, 1993).

Conversion of Na_2CO_3 in Fume Particles to Na_2SO_4

We used the kinetics data calculated to predict the conversion of Na_2CO_3 to Na_2SO_4 in recovery boilers. Product layer diffusion was assumed to be the limiting process in the calculations. The diffusion rate determined from the study of Backman et al. (1985) was used. The calculation is based on assumption that the particles had become 50% sulfated in the molten stage. The temperature profile of Na_2CO_3 particle that was used in the calculation are shown in Figure V.A-5.

The conversions calculated are in Figures V.A-6 and V.A.-7. Figure V.A.-6 shows the conversion of 1 a μm particle at different SO_2 concentrations whereas Figure V.A.-7 shows the conversion at 300 ppm of SO_2 for different particle sizes.

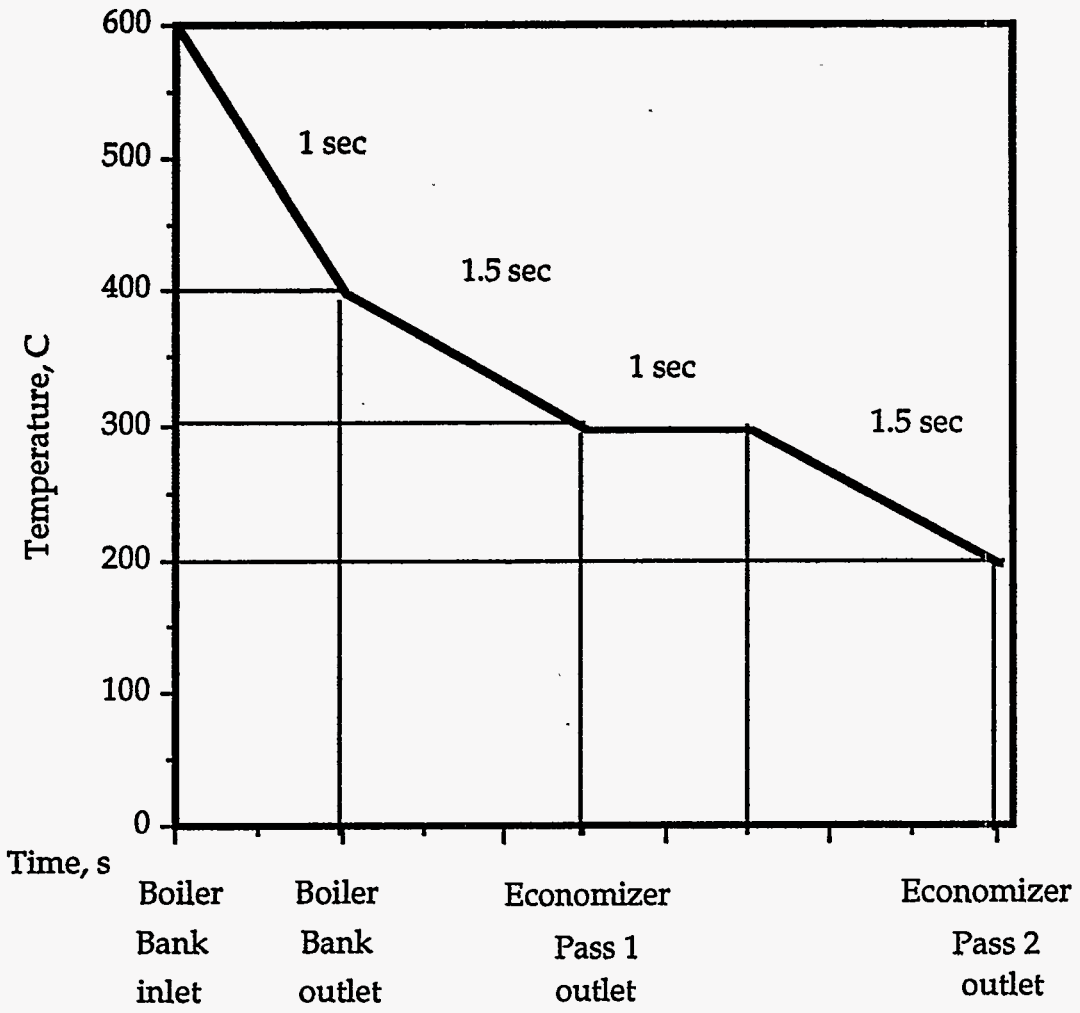

Figure V.A-5. The residence time and temperature used in the calculation of the sulfation of in-flight Na_2CO_3 particles.

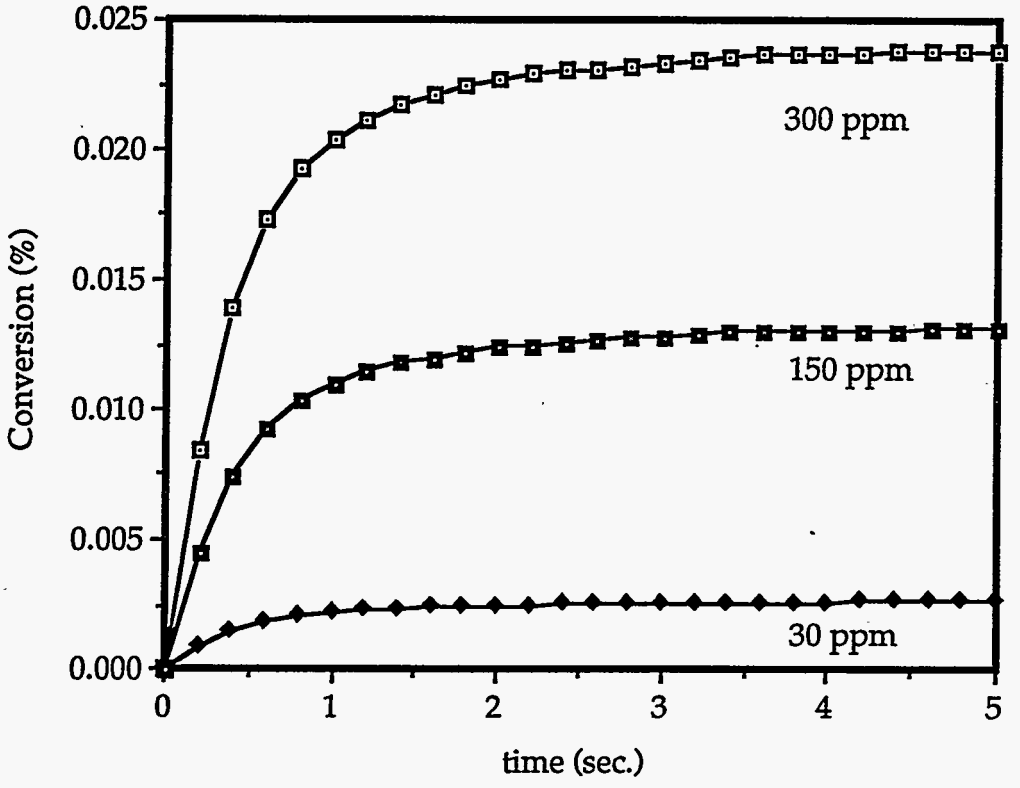

Figure V.A-6. The conversion of Na_2CO_3 to Na_2SO_4 of a 1 μm particle at 30, 150 and 300 ppm of SO_2.

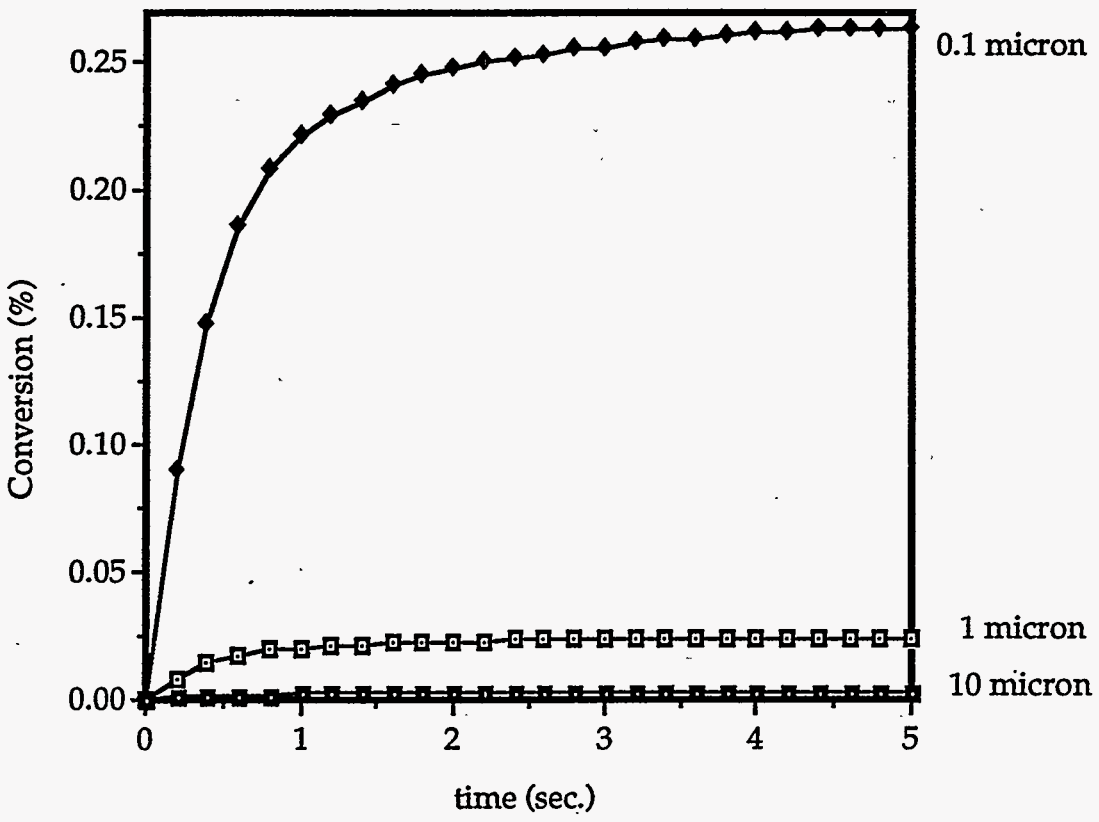

Figure V.A-7. The conversion of Na_2CO_3 to Na_2SO_4 at 300 ppm of SO_2 for 1, 10, and 100 μm particles.

The conversions to $NaSO_4$ were very low: only 0.16% conversion for a 0.1 μm particle at 300 ppm of SO_2. Based on this result, it was concluded that the conversion of solid fume particles to Na_2SO_4 in-flight is too slow to be important. This suggests that the sulfation of fume particles in-flight occurs in the molten phase, i.e., before the boiler bank. The residence time for Na_2CO_3 in deposits is much higher than the residence time for in-flight solid fume particles, hours to weeks versus seconds. Thus sulfation of Na_2CO_3 is fast enough to account for significant sulfation of Na_2CO_3 in these deposits.

Implications

From the results of sulfation of both Na_2CO_3 and NaCl, SO_2 capture in solid particles is not significant in the boiler and generator banks. This implies that nearly all of the sulfation of fume particles in recovery boilers occurs as reactions in the molten phase or before the particles solidify. Figure V.A-8 shows data on SO_2 concentration in a boiler from Babcock and Wilcox company. The SO_2 concentration was measured from boiler bank entrance, superheater entrance and boiler stack. It shows that there is no change in SO2 concentration between the boiler bank inlet and stack, but that there is a significant change across the superheater. This agrees very well with the data of sulfation of solid Na_2CO_3 and NaCl.

The rates of sulfation of both Na_2CO_3 and NaCl in solid particles are fast enough, however, to account for significant sulfation of Na_2CO_3 and NaCl in deposits from heat transfer surface in recovery boilers.

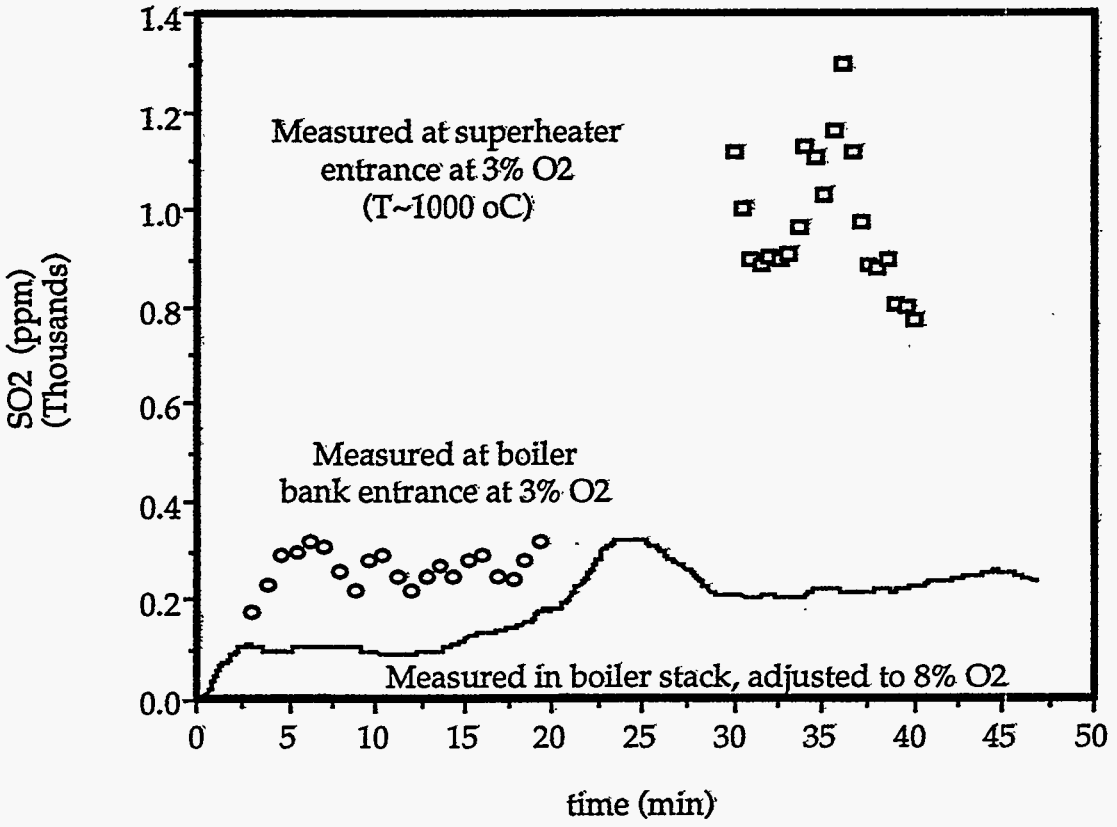

Figure V.A-8. SO_2 concentration in boiler from Babcock and Wilcox Company at boiler bank entrance, superheater entrance and boiler stack.

References

Anderson, A. (1984), "Mechanism for Forming Hydrogen Chloride and Sodium Sulfate from Sulfur Trioxide, Water and Sodium Chloride," *J. Am. Chem. Soc.*, 106(21): 6262-6265

Backman, R., Hupa, M., and Usikartano, T. (1985), "Kinetics of Sulphation of Sodium Carbonate in Flue Gases," Proc. 1985 International Chemical Recovery Conference, TAPPI Press, Atlanta.

Boonsongsup, L. (1993), "SO_2 Capture and HCl Release at Kraft Recovery Boiler Conditions," M.S. thesis, Oregon State University.

Butler, F. and Waites, I. (1981), "A Thermoanalytical Study of the Reaction Between Gaseous Sulfur Dioxide and Solid Sodium Carbonate," 2nd European Symposium on Thermal Analysis, pp. 310-314.

Fielder, W., Stearns, C. and Kohl, F. (1984), "Reaction of NaCl with Gaseous SO_3, SO_2 and O_2," *J. Electrochem. Soc.*, 131(10):2414-2417.

Froment, G.F. and Bischoff, K.B. (1979), *Chemical Reactor Analysis and Design*, p. 201-207, John Wiley & Son.

Henriksson, M. and Warnqvist, B. (1979), "Kinetics of Formation of HCl(g) by the Reaction Between NaCl(s) and SO_2, O_2, and H_2O(g)," *Ind. Eng. Chem. Process*, Des. Dev. 18(2):249-254.

Iisa, K., Hupa, M. and Yrjas, P. (1992), "Product Layer Diffusion in the Sulphation of Calcium Carbonate," Twenty-Fourth (International) Symposium on Combustion, Sydney, Australia, July 5-10.

Ishida, M. and Wen, C.Y. (1968), "Comparison of Kinetic and Diffusional Models for Solid-Gas Reactions," *AIChe J.*, 14(2):311-317.

Keener, T. and Davis, W. (1984), "Study of the Reaction of SO_2 with $NaHCO_3$ and Na_2CO_3," *J. Air Pollution Control Assoc.*, 34:651-654.

Kimura, S. and Smith, J. (1987), "Kinetics of the Sodium Carbonate-Sulfur Dioxide Reaction," *AIChe J.*, 33(9):1522-1532.

Kirk-Othmer, *Encyclopedia of Chemical Technology*, 3rd Edition, Volume 12, p. 996, John Wiley & Sons.

Levenspiel, O. (1972), *Chemical Reaction Engineering*, 2nd Edition, p. 361-373, John Wiley & Son.

Lloyd-George, I. (1985), "The Sulfation of Sodium Carbonate: The Significance of Pyrosulfate, Potassium, and Chloride," M.S. thesis, University of Toronto.

Maule, G. and Cameron, J. (1989), "Reaction of Na_2CO_3 Fume Particles with SO_2 and O_2," IPC Technical Paper Series, Number 317, January.

Wen, C.Y. (1968), "Noncatalytic Heterogeneous Solid Fluid Reaction Models", *J. Ind. and Engr. Chem.*, 60(9):34-54.

V.B KINETICS OF SULFATION OF SOLID NACL AT COMBUSTION CONDITIONS

Summary

The sulfation of NaCl was studied in a fixed bed reactor in the temperature range 400-600°C where NaCl, Na_2SO_4, and their mixtures are solids. Under the experimental conditions employed, diffusion and mass transfer did not influence the overall rate and true kinetic data were obtained. The rate of sulfation of NaCl was very slow for solid NaCl, with only 0.5-1.0% of the NaCl converted to HCl in three hours at the experimental conditions employed. The rate was not strongly temperature dependent, with an activation energy of 17.3 kJ/mol. The rate of reaction depends on the partial pressure of SO_2 but not in the partial pressure of O_2 and H_2O for the range of conditions of $0.3\% < P_{SO2} < 1.1\%$, $3\% < P_{O2} < 11\%$, $0.5\% < P_{H2O} < 20\%$ and $400°C < T < 600°C$. The adsorption of SO_2 (g) on the surface of NaCl was determined to be the rate limiting step of this reaction.

The rate of sulfation of NaCl in solid particles is too slow at conditions in the boiler and generator banks to account for significant SO_2 capture and HCl release in that part of the boiler. The rate is fast enough, however, to account for significant sulfation of NaCl in boiler tube deposits.

Introduction

The reaction of SO_2 with NaCl in the presence of water vapor and oxygen is shown in Equation V.B-1. This reaction is important in the capture of sulfur gases in black liquor combustion and in purging of chlorides from the soda cycle in kraft pulp mills. It produces HCl emissions which, in addition to detrimental environment effects, can cause corrosion in the boiler.

$$NaCl\,(s,l) + \frac{1}{2}SO_2 + \frac{1}{4}O_2 + \frac{1}{2}H_2O \rightarrow HCl + \frac{1}{2}Na_2SO_4\,(s,l) \qquad \text{(V.B-1)}$$

The kinetics of reaction 1 have been studied by few researchers. In one study, Henriksson and Warnqvist (1979) measured the rate of sulfation of NaCl in the presence of O_2 and water vapor. Their experimental procedure involved placing Al_2O_3 boats which contained NaCl into a long Al_2O_3 tube within an electrically heated tube furnace. The temperature range studied was from 500 to 800°C which included both the solid and molten regions for NaCl and Na_2SO_4 mixtures. The rate of conversion exhibited an unexpected flow dependence, i.e. the rate of reaction first increased and then decreased with increasing gas flow rate. This may have resulted from mass transfer effects in the experimental apparatus. Henriksson and Warnqvist reported that the reaction was 0.5 order with respect to SO_2 partial pressure and also 0.5 order with respect to O_2 partial pressure, but that it was independent of water vapor partial pressure. An unexpected temperature dependence, i.e. the rate of reaction decreased with increasing

temperature below 500°C, was also observed in this study. The chemical reaction was reported to be the rate limiting step of this reaction although this was not consistent with the observed effect of flow rate on the reaction rate. The following mechanism of this reaction was also suggested: SO_2 and O_2 are adsorbed on the NaCl surface and then react together to form SO_3 (ads). The SO_3 (ads) reacts with adsorbed water and NaCl to form HCl and Na_2SO_4 with the intermediates H_2SO_4 (ads) or $NaHSO_4$ (ads).

In the second study, Fielder et al. (1984) followed this reaction in SO_3-SO_2 mixtures by suspending a sample inside a quartz tube from a sensitive electrobalance. A Pt catalyst was used to produce the desired concentration of SO_3 in a SO_2-O_2 mixture. High pressure mass spectrometric sampling techniques were used to analyze the gaseous reactant compositions and to identify the gaseous products. The temperature range studied was from 100 to above 650°C. Different products were formed on the NaCl surface at different ranges of temperature under anhydrous conditions, i.e. water less than 20-40 ppm. Fielder et al. (1984) also studied the sulfation of NaCl in the presence water vapor between 400-450°C. The products were Na_2SO_4 and HCl instead of Cl_2. This reaction were first order with respect to SO_3 and also first order with respect to water vapor. The overall rate of reaction was reported to be controlled by the chemical reaction step.

From these two previously studies, almost all of the Fielder et al. (1984) were for anhydrous conditions. The effect of SO_2 on the reaction was not clarified because of the presence of SO_3 in the gas mixture. The data in this study were reported as total weight of sample gained versus time. These data could not be transformed to conversion versus time data based on the information available in the paper and the temperature dependence of the reaction rate in each range of temperature was not reported in this study. Thus no kinetics could be obtained from their data. For the Henriksson and Warnqvist (1979) study, the results were dependent on the gas flow rate and an unexpected temperature dependence was observed below 500°C. It was concluded that more reliable kinetic data were needed for this reaction.

Experimental

A flow diagram for the experimental system used in these experiments is shown in Figure V.B-1. The kinetics of sulfation of NaCl were measured in a fixed bed reactor consisting of a vertical quartz tube (2 cm ID) inside a tube furnace. The reaction was constructed of quartz glass to avoid uncontrolled catalytic oxidation of SO_2 to SO_3 at high temperature on metallic parts. The NaCl used in these experiments was prepared by grinding reagent grade NaCl, sieving, and collecting fractions in the size range of 63-90, 90-125 and 125-250 μm particles. The total surface area of NaCl particles, obtained from BET analysis with N_2 gas, were, respectively, 0.289, 0.181 and 0.134 for the 63-90, 90-125 and 125-250 μm particles. The NaCl was placed on a fritted quartz glass support in the center of the reactor. The operating temperature was measured by a thermocouple inserted into the NaCl bed.

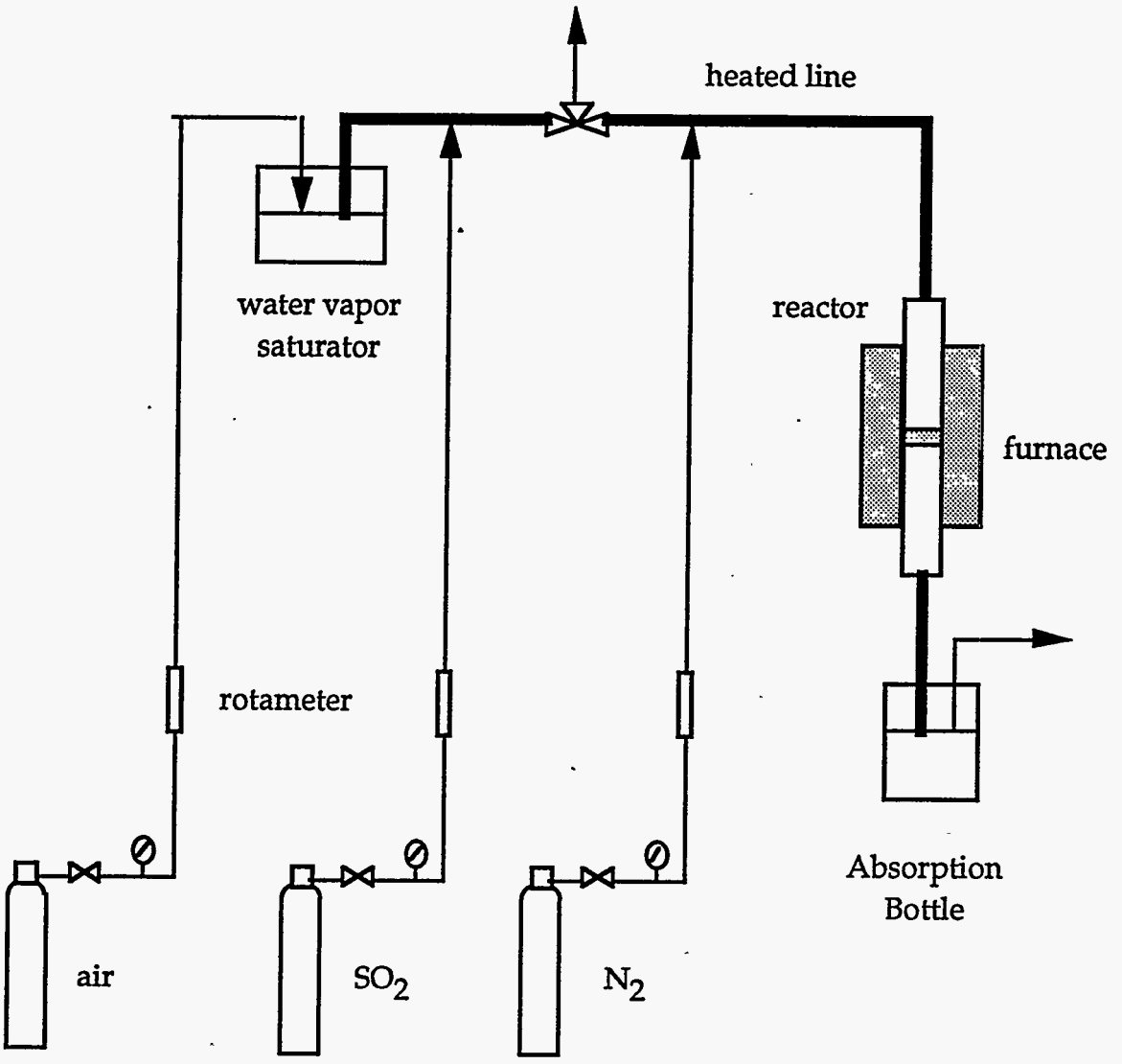
heated line
water vapor
saturator
reactor
furnace
rotameter
Absorption
Bottle
air
SO_2
N_2

Figure V.B-1.

The kinetic studies were conducted by passing a mixture of SO_2, O_2, water vapor, and N_2 over preheated NaCl samples. The water vapor concentration was controlled by saturating an air stream with water vapor at constant temperature prior to mixing it with SO_2.

The rate of reaction was monitored by absorbing the HCl generated in deionized water and measuring the chloride ion concentration with a specific ion electrode. The product gas lines from the reactor were heated to prevent HCl and water vapor from condensing in them. A typical experiment was run for 3 hours and the absorbed HCl was measured every 30 minutes.

A preliminary test was made to determine whether all of the HCl generated in the reactor would be absorbed in a single absorption bottle. A gas containing 1% HCl with the balance N_2 was passed through two adsorption bottles in series. At flow rates less than 15 cm^3/sec, 98% of the chloride input was collected in one bottle.

The residual solid products from several runs were sent to the Weyerhaeuser Company analytical laboratory in Tacoma, Washington, for sodium, chloride and sulfate analysis. The conversion of NaCl was calculated from both the residual solid composition and the product gas analysis. The comparison is shown in Table V.B-1. The conversions calculated from both methods agree very well.

Results and Discussion

Gas Flow Rate Effect

Initial experiments were run to determine the operating conditions at which external mass transfer through the gas boundary would be negligible. The conversion rates at 500°C for different flow rates are shown in Figure V.B-2. The conversion rate increased with an increase in flow rate below 10 cm^3/s (20°C, 1 atm) and was constant above this gas flow rate. This result implies that external mass transfer through the gas boundary is negligible at total gas flow rates above 10 cm^3/s. Based on the experimental results obtained in this study, the external mass transfer effect at 600°C was negligible at total flow rates of 15 cm^3/s (20°C, 1 atm) and above (Boonsongsup, 1993). To ensure that this would not affect the reaction at temperatures below 600°C, the experimental data were obtained at a total flow rate 15 cm^3/s (20°C, 1 atm).

Particle Size Effect

Particles of different sizes, 125-250, 90-125 and 63-90 μm, were used to evaluate whether intraparticle diffusion was important. The conversion versus time data for different particle sizes is shown in Figure V.B-3. Chemical kinetic rates (mol/m^2.atm.min) of different particle sizes, based on total surface area, were calculated to determine the effect of porosity (Boonsongsup, 1993). The results, in Table V.B-2, show that the kinetic rates different particle sizes were almost the same. This implies that intraparticle diffusion has no significant effect on the measured rate.

Table V.B-1. Comparison of the degree of conversion obtained by the residual solid analysis and the gas analysis. The results are expressed as percent conversion of the NaCl charged to the reactor.

Run No.	Residual Solid Analysis (%)	Gas Analysis (%)
10	0.64	0.61
14	0.83	0.81
20	0.41	0.43

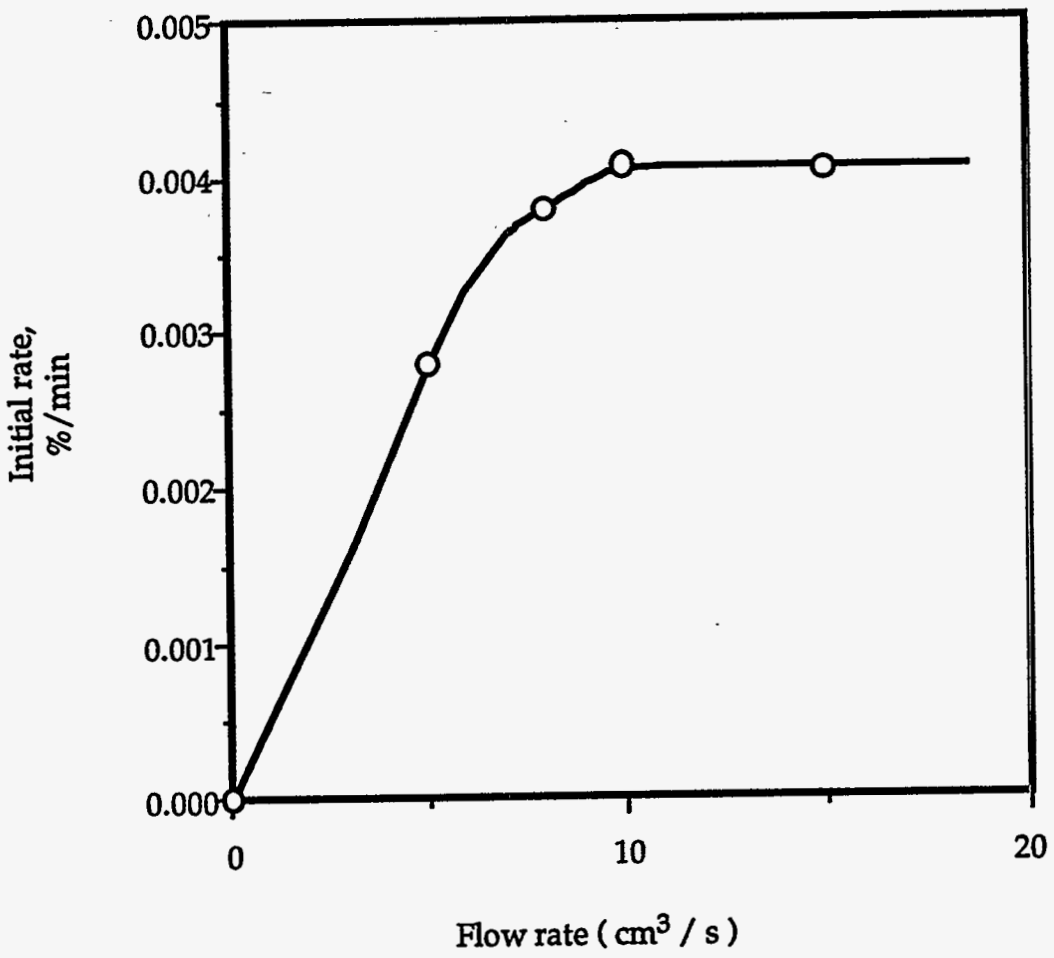
0.005
0.004
0.003
0.002
0.001
0.000
Initial rate, %/min
0
10
20
Flow rate (cm3 / s)

Figure V.B-2

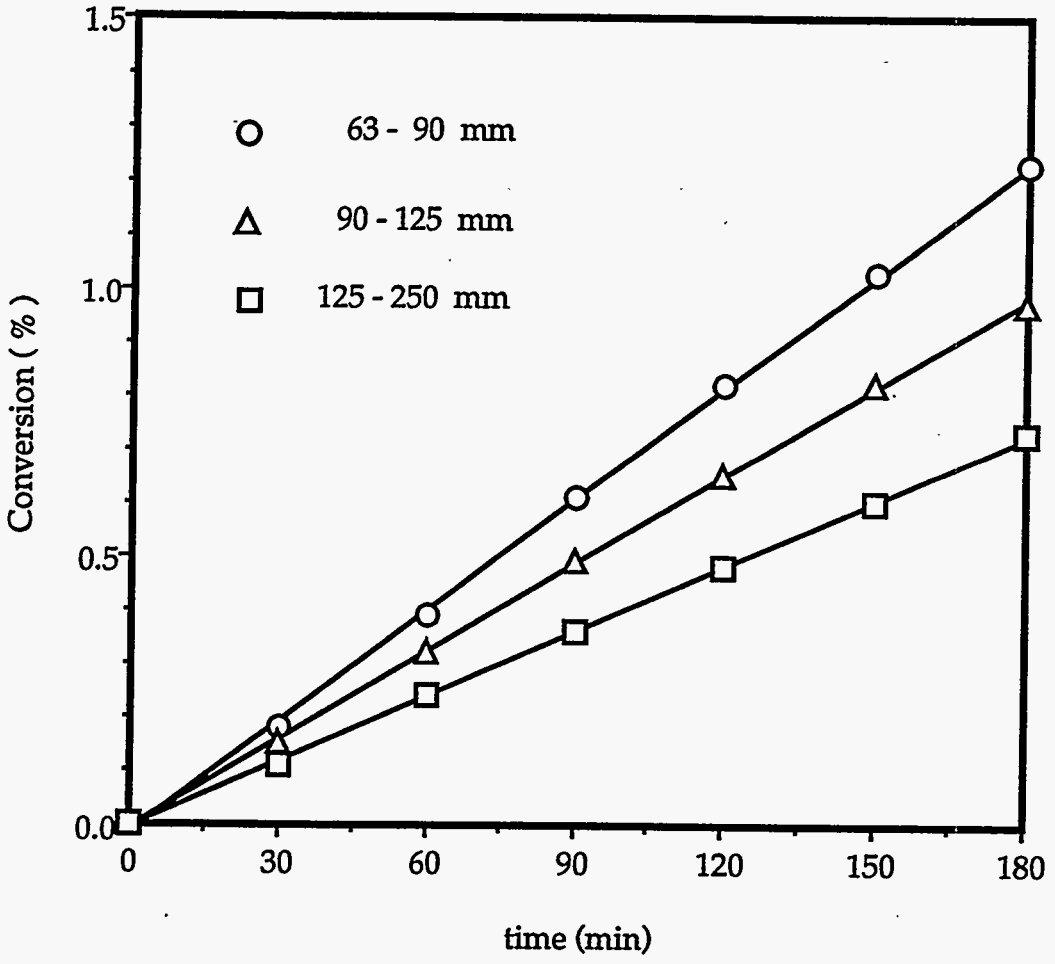
1.5
1.0
0.5
0.0
Conversion (%)
63 - 90 mm
90 - 125 mm
125 - 250 mm
0
30
60
90
120
150
180
time (min)

Figure V.B-3.

Table V.B-2. Comparison of total surface areas and rate constants of different particle sizes at flow rate of 15 cm^3/s (20°C, 1 atm) total flow rate, 500°C, 0.3% SO_2, 5% O_2, 10% H_2O, and 2 g of NaCl.

Particle Size Range (μm)	Total Surface Area (m^2/g)	Rate Constant ($mol/m^2.atm.min$)
63-90	0.289	1.53×10^{-3}
90-125	0.181	1.21×10^{-3}
125-250	0.134	1.21×10^{-3}

Temperature Effect

The conversion versus time data for the sulfation of NaCl at different temperatures from 400-600°C are shown in Figure V.B-4. The rate of SO_2 capture by NaCl was not strongly temperature dependent, increasing by slightly more than a factor of two over the temperature range 400-600°C.

The reaction rate increased with temperature throughout the temperature range studied. An Arrhenius plot of the rate constant is shown in Figure V.B-5. The activation energy of reaction was determined to be 17.3 KJ/mol which was quite low for a chemical kinetic-controlled process. The low activation energy suggests that a physical process such as adsorption or desorption was the rate-controlling step.

The unexpected temperature dependence observed in Henriksson and Warnqvist (1979) study was not detected in our experiments. It could have been the result of liquid sodium pyrosulfate formation as suggested by Lloyd-George (1985) in his investigation of the sulfation of Na_2CO_3. In the presence of liquid sodium pyrosulfate, the mechanism of sulfation may change and give a higher kinetic rate because the reaction is gas-liquid reaction instead of gas-solid. The temperature range in which liquid sodium pyrosulfate was stable depends on the SO_3 concentration. This range was 350-550°C in the Lloyd-George (1985) study. The SO_3 in those experiments was formed by oxidation of SO_2 (20%), catalyzed by the metallic parts in experimental apparatus; the SO_3 concentration were not reported. In our study the high temperature parts of the equipment were non-metallic so no oxidation of SO_2 to SO_3 should have occurred. Thus there was no possibility of sodium pyrosulfate formation at these conditions. An other possibility is that the sintering effect observed by Backman et al. (Backman, Hupa, and Uusikartano, 1985) in his study of the sulfation of Na_2CO_3 decreased the reaction rate. The available surface area of the Na_2CO_3 was reduced by sintering more at higher temperatures. The available surface area during sulfation was therefore lower at higher reaction temperatures and this caused a decrease in the overall reaction rate at higher temperatures.

SO_2 Concentration Effect

The SO_2 concentration range studied was from 0.3-1.1%. The conversion versus time data for different SO_2 concentrations are shown in Figure V.B-6. These data show that the rate increases more rapidly with increasing SO_2 partial pressure at lower SO_2 partial pressure than at higher SO_2 partial pressure.

The data in Figure V.B-6 were analyzed further to find the reaction order with respect to SO_2. To find this reaction order, the logarithm of the chemical kinetic rate was plotted against the logarithm of the SO_2 concentration as shown in Figure V.B-7. The chemical kinetic rate increased with SO_2 concentrations and was less dependent on SO_2 concentration at higher SO_2 concentrations. The slope of this curve, which was the order of the reaction with respect to SO_2, decreased from 0.67 at the lowest SO_2 concentrations used to 0.16 at the highest. The nonlinear dependence of the rate on SO_2 concentration in Figure V.B-7 indicates that the rate is not first order in SO_2 but that SO_2 is involved in the rate limiting step of the reaction.

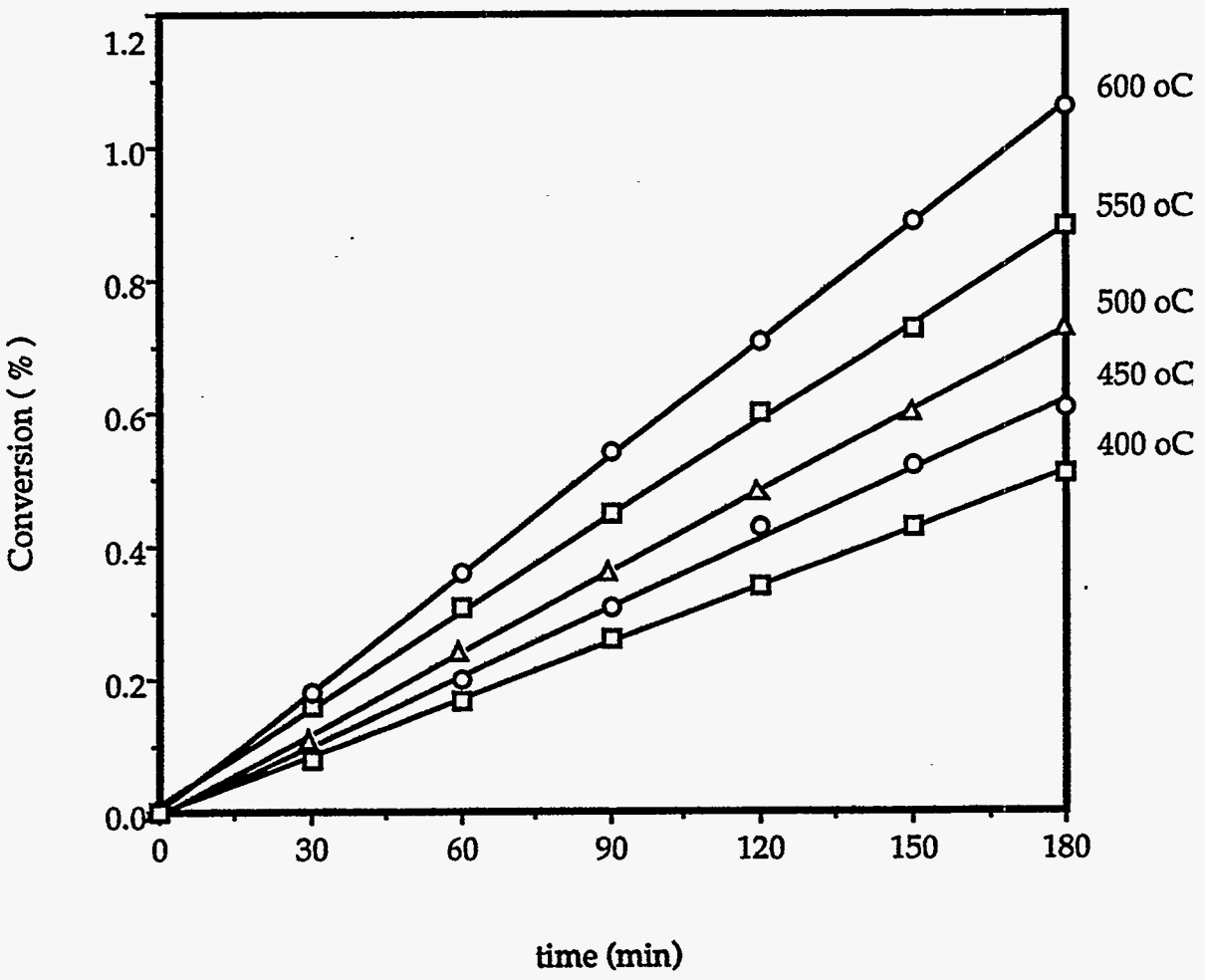
1.2
1.0
0.8
0.6
0.4
0.2
0.0
Conversion (%)
0
30
60
90
120
150
180
time (min)
600 oC
550 oC
500 oC
450 oC
400 oC

Figure V.B-4.

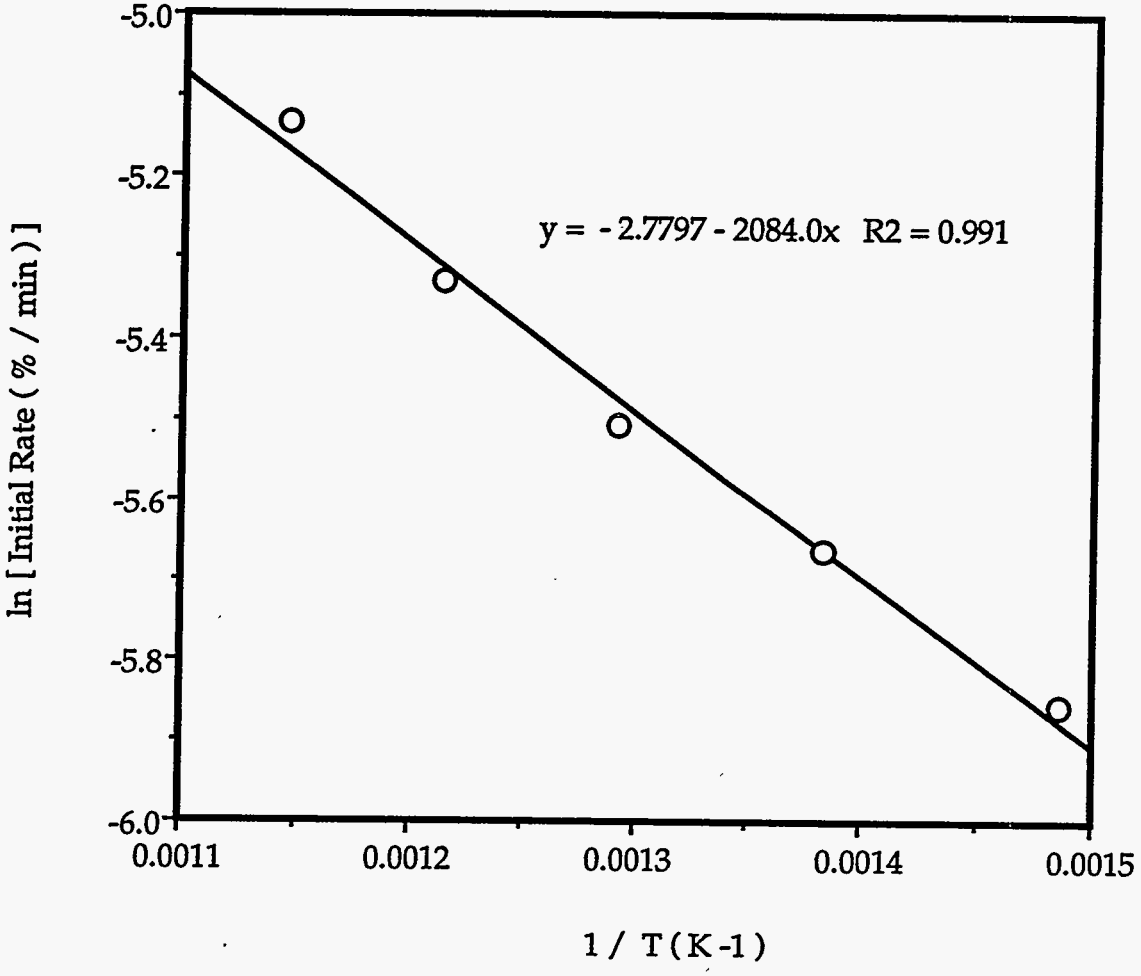
-5.0
-5.2
-5.4
-5.6
-5.8
-6.0
ln [Initial Rate (% / min)]
y = - 2.7797 - 2084.0x R2 = 0.991
0.0011
0.0012
0.0013
0.0014
0.0015
1 / T (K -1)

Figure V.B-5.

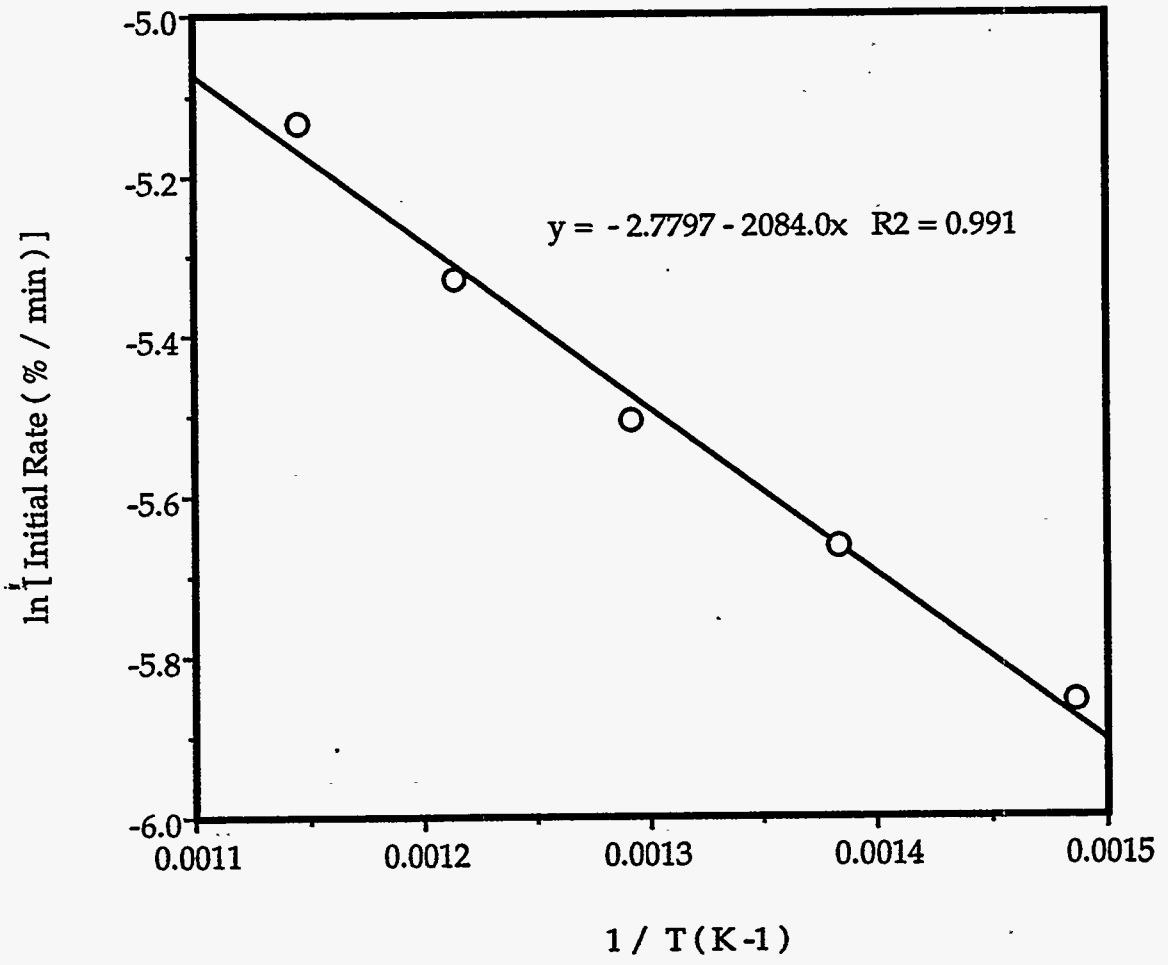
-5.0
-5.2
-5.4
-5.6
-5.8
-6.0
y = - 2.7797 - 2084.0x R2 = 0.991
ln [Initial Rate (% / min)]
0.0011
0.0012
0.0013
0.0014
0.0015
1 / T (K -1)

Figure V.B-6.

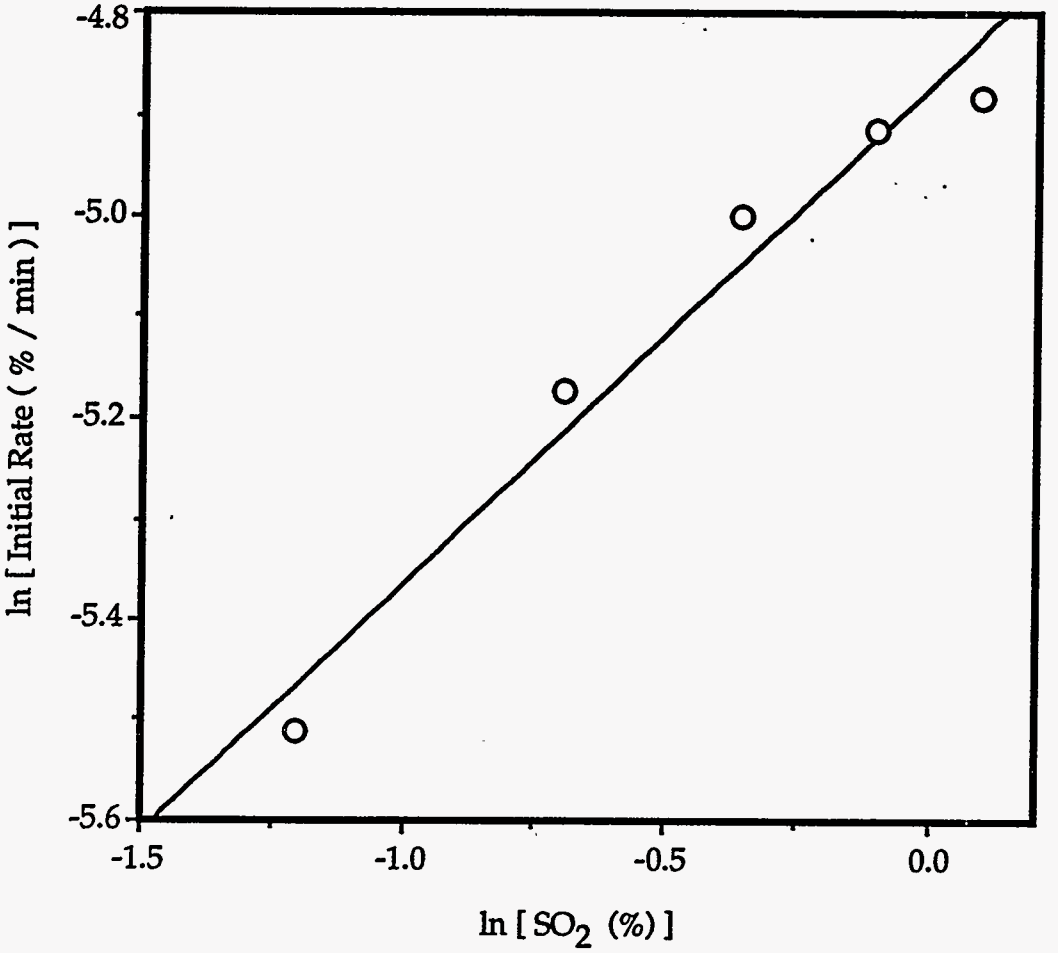

Figure V.B.-7.

H_2O and O_2 Concentration Effects

The O_2 and H_2O (v) concentration ranges studied were from 3-11% and from 0.5-20%, respectively. The conditions of these studies were 15 cm^3/s (20°C, 1 atm) total gas flow rate, 500°C, 0.3% SO_2, 5% O_2 or 10% H_2O and 2 g of 125-250 μm NaCl. The reaction rate was independent of O_2 and H_2O concentration at the conditions employed. It indicated that oxygen and water vapor were involved in a fast reaction step which did not control the overall rate of reaction.

Proposed Mechanism

The mechanism of the sulfation of NaCl by SO_2 in the absence of SO_3 was suggested by Henriksson and Warnqvist (1979). The mechanism is shown below:

$$SO_2\ (g) \Leftrightarrow SO_2\ (ads)$$

$$O_2\ (g) \Leftrightarrow O_2\ (ads)$$

$$H_2O\ (g) \Leftrightarrow H_2O\ (ads)$$

$$SO_2\ (ads) + \frac{1}{2} O_2\ (ads) \rightarrow SO_3\ (ads)$$

$$SO_3\ (ads) + H_2O\ (ads) \rightarrow H_2SO_4\ (ads)$$

$$H_2SO_4\ (ads) + NaCl\ (s) \rightarrow HCl\ (g) + NaHSO_4\ (ads)$$

$$NaHSO_4\ (ads) + NaCl\ (s) \rightarrow Na_2SO_4\ (s) + HCl\ (g)$$

In this mechanism, SO_2 (g), O_2 (g) and H_2O (g) are first adsorbed on the surface of NaCl and then SO_2 (ads) reacts with O_2 (ads) to form SO_3 (ads). H_2O (ads) reacts with SO_3 (ads) to form H_2SO_4 (ads). The products, Na_2SO_4 and HCl, are obtained from the reaction between H_2SO_4 (ads) and NaCl.

From the results of our experiments, the apparent activation energy of the overall reaction was quite low which is consistent with a physical adsorption-desorption process as the rate-controlling step in this reaction. From the gas concentration effects, SO_2 was involved in the rate limiting step of this reaction whereas O_2 and H_2O were not. From these two results, the rate limiting step of this reaction should be the adsorption-desorption of SO_2 (g) on the surface of NaCl. Additional support for this conclusion was that the chemical kinetic rate increased with increasing SO_2 concentration and was less dependent at higher SO_2 concentrations. This is also Langmiur adsorption type behavior (Fronment and Bischoff, 1979).

Reaction Rate Analysis

The overall rate of reaction was limited by chemical kinetics at the conditions investigated in this study. It implied that the adsorption of SO_2 (g) on the surface of NaCl controls the overall rate of reaction. Thus the overall rate of reaction can be approximated by the rate of adsorption of SO_2 (g) which can be described by a Langmuir isotherm. The model is based on the assumption that the surface is energetically ideal and that forces of interaction between adsorbed species are negligible. The adsorption rate is assumed to be proportional to the partial pressure of the adsorbed species and the fraction of the solid surface unoccupied. The resulting rate equations is then :

$$-r_{SO2} = S' \frac{k P_{SO2}}{1 + K_1 P_{SO2} + K_2 P_{O2} + K_3 P_{H2O}} \qquad \text{(V.B-2)}$$

where

r_{SO2} = rate of deformation of SO_2, mol/min.

k = reaction rate constant, $mol/m^2.min.atm$

P_{SO2} = partial pressure of SO_2, atm

S' = internal surface area, m^2/g

K_1 = adsorption equilibrium constant of SO_2, atm^{-1}

K_2 = adsorption equilibrium constant of O_2, atm^{-1}

K_3 = adsorption equilibrium constant of H_2O, atm^{-1}

$$K = K_o \exp [Q/RT] \qquad \text{(V.B-3)}$$

where

Q = heat of adsorption

If K_2P_{O2} and K_3P_{H2O} are much less than 1 and K_1P_{SO2} this reaction rate will be:

$$-r_{SO2} = S' \frac{k P_{SO2}}{1 + K_1 P_{SO2}} \qquad \text{(V.B-4)}$$

from the overall reaction stoichiometry, $2r_{SO2} = r_{NaCl}$

so that

$$2S' \frac{kP_{SO2}}{1 + K_1 P_{SO2}} = \frac{1}{M} \frac{dX}{dt} \qquad \text{(V.B-5)}$$

or

$$\frac{2S'M}{(dX/dt)} = \left(K_1/k\right) + (1/k) \frac{1}{P_{SO2}} \qquad \text{(V.B-6)}$$

In Figure V.B-8 the plot between 2S'M/(dX/dt) and $1/P_{SO2}$ is linear which shows good agreement between this model and the data. The values of K_1 and k at 500°C, calculated from the plot in Figure V.B-8, are 172 atm^{-1} and 1.21×10^{-3} $mol/m^2.atm.min$, respectively. Thus the kinetic rate equation of this reaction at 500°C was:

$$r = -r_{NaCl} = r_{HCl} = -2 r_{SO2} = S' \frac{2.42 \times 10^{-3} P_{SO2}}{1 + 172 P_{SO2}} \qquad \text{(V.B-7)}$$

References

Backman, R., Hupa, M., and Uusikartano, T. (1985), "Kinetics of Sulphation of Sodium Carbonate in Flue Gases," Proc. 1985 International Chemical Recovery Conference, TAPPI Press, Atlanta.

Boonsongsup, L. (1993), "SO_2 Capture and HCl Release at Kraft Recovery Boiler Conditions", M.S. thesis, Oregon State University.

Fielder, W., Stearns, C. and Kohl, F. (1984), "Reaction of NaCl with Gaseous SO_3, SO_2 and O_2," *J. Electrochem. Soc.*, 131(10):2414-2417.

Fronment, G.F. and Bischoff, K.B. (1979), "Chemical Reactor Analysis and Design", p. 201-207, John Wiley & Son.

Henriksson, M. and Warnqvist, B. (1979), "Kinetics of Formation of HCl(g) by the Reaction Between NaCl(s) and SO_2, O_2, and H_2O(g)," *Ind. Eng. Chem. Progress*, Des. Dev. 18(2):249-254.

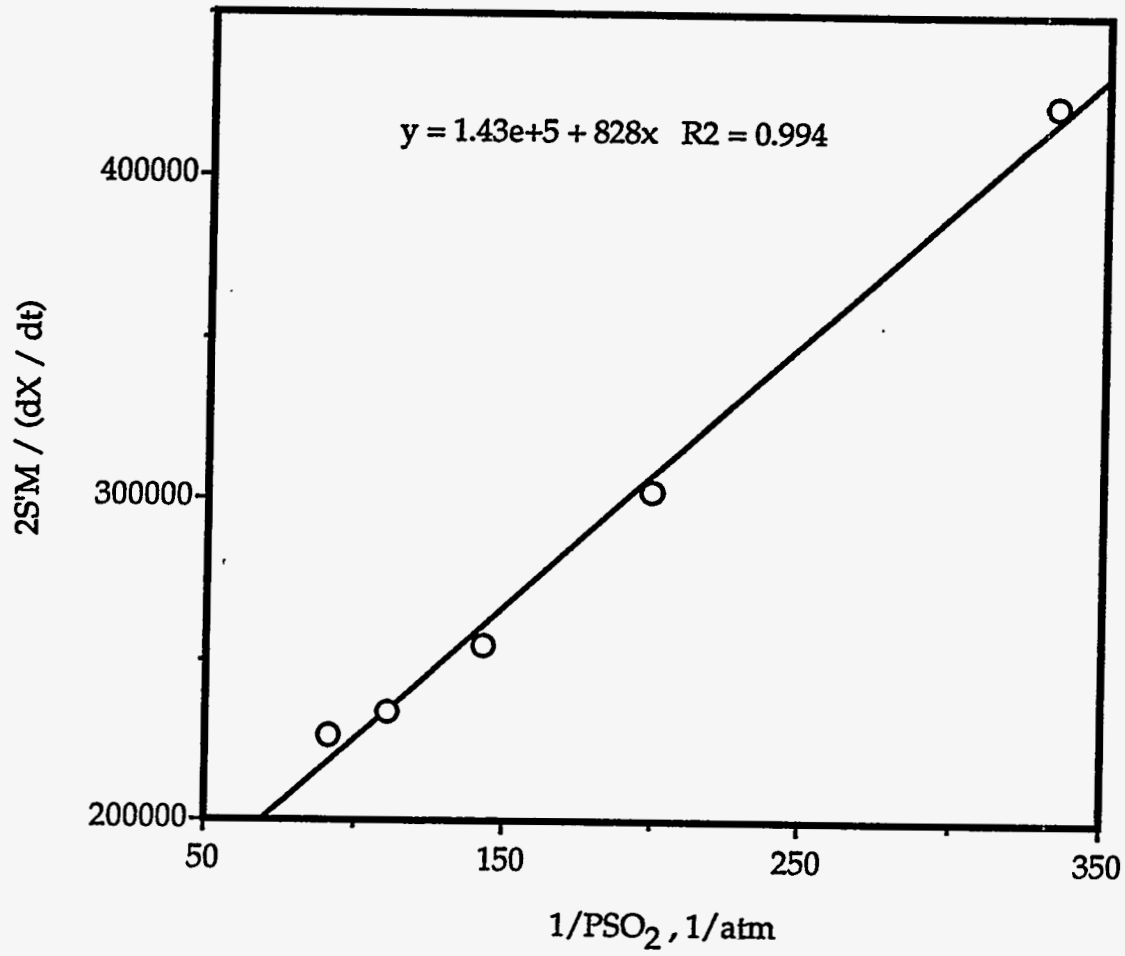
y = 1.43e+5 + 828x R2 = 0.994
400000
300000
200000
2S'M / (dX / dt)
50
150
250
350
1/PSO2 , 1/atm

Figure V.B-8.

Kirk-Othmer, *Encyclopedia of Chemical Technology*, 3rd Edition, Volume 12, p. 996, John Wiley & Sons.

Lloyd-George, I. (1985), "The Sulfation of Sodium Carbonate: The Significance of Pyrosulfate, Potassium, and Chloride," M.S. thesis, University of Toronto,

Appendix 1. Single Droplet Pyrolysis, Combustion, and Gasification Data from the Åbo Akademi University Single Droplet Reactors

File: Table IV.A.1.2

Printed: 10/3/95 at 10:28 PM

				Conditions							Experimental				Analysis								Results			
					Gases						Reactor		Rxn time		gas		char						Content in char % of ini species			
Date	T	BL name	Dry solids	nbr of drps	N2	CO	CO2	H2O	O2		Vid eo	Sulf ur	Pyro lysis	Char burn	S	C	Na	S	C	STD pyr.	Rxn time	Masses ini.	aft.pyr	char	Na	S	C	Char
-	C	-	%	pcs	%	%	%	%	%		-	-	sec	sec						-	s	mg	mg	mg	%	%	%	%
7.Jan	500	AA 048		1	100%							X	180		X	X		X	X									73%
8.Jan	500	AA 048		5	100%							X	180		X	X		X	X							31%	84%	75%
9.Jan	500	AA 048		10	100%							X	180		X	X		X	X							32%	81%	73%
10.Jan	800	AA 048		7	100%							X	180		X	X		X	X							40%	50%	55%
24.Feb	900	Tamp 3		7	95%		5%				X		2				X				2.0	18.1	11.4		82%			82%
24.Feb	900	Tamp 3		8	95%		5%				X		4				X				4.0	17.9	8.8		83%			64%
24.Feb	900	Tamp 3		7	95%		5%				X		8				X		X		8.0	18.2	7.7		74%			55%
24.Feb	900	Tamp 3		2	95%		5%				X		12				X				12.0	16.1	5.6		74%			45%
24.Feb	900	Tamp 3		3	95%		5%				X		14				X				14.0	18.6	6.2		71%			44%
24.Feb	900	Tamp 3		1	95%		5%				X		16				X				16.0	19.5	6.7		65%			45%
26.Feb	1000	Tamp 3		7	95%		5%				X		2				X				2.0	17.2	8.9		83%			68%
26.Feb	1000	Tamp 3		7	95%		5%				X		4				X				4.0	17.9	7.9	0.0	80%			58%
26.Feb	1000	Tamp 3		7	95%		5%				X		8				X		X		8.0	18.5	5.9	0.0	60%		14%	42%
2.Mar	750	Tamp 3		4	95%		5%				X		2				X								87%			105%
2.Mar	750	Tamp 3		4	95%		5%				X		4				X								83%			82%
3.Mar	900	Tamp 3		4	95%	5%					X		4				X								80%			59%
3.Mar	900	Tamp 3		4	95%	5%					X		2 s				X								85%			76%
3.Mar	900	Tamp 3		4	95%	5%					X		4 s				X								73%			59%
3.Mar	900	Tamp 3		4	95%	5%					X		8 s				X		X						72%			55%
4.Mar	750	Tamp 4		7	95%		5%				X		6															
4.Mar	750	Tamp 4		4	95%		5%				X		8															
4.Mar	900	Tamp 4		7	95%		5%				X		4															
4.Mar	900	Tamp 4		7	95%		5%				X		8															
10.Mar	1000	Tamp 4		7	95%		5%				X		3.5															
11.Mar	1000	Tamp 4		7	95%		5%				X		4															
12.Mar	750	Tamp 4		7	95%		5%				X		16															
12.Mar	750	Tamp 4		7	95%		5%				X		32				X				32.0	19.3	4.8		52%			33%
17.Mar	900	Tamp 4		5	95%		5%				X		4															
17.Mar	900	Tamp 4		8	95%		5%				X		16															
20.Mar	750	Tamp 3		7	95%		5%				X		16				X				16.0	19.0	7.8		77%			54%
27.Mar	750	Tamp 3		7	95%		5%				X		8				X				8.0	18.4	7.2		79%			51%
30.Mar	900	Tamp 3		7	99%				1%		X		2				X								82%			
30.Mar	900	Tamp 3		7	99%				1%		X		4				X				4.0	17.9	8.8		77%			53%
1.Apr	900	Tamp 3		7	99%				1%		X		8				X								77%			53%
2.Apr	750	Tamp 3		7	99%				1%		X		4				X								88%			
2.Apr	750	Tamp 3		7	99%				1%		X		8				X								77%			
7.Apr	750	Tamp 3		7	99%				1%		X		2				X								76%			
8.Apr	900	Tamp 4		7	99%				1%		X		4				X								46%			
8.Apr	900	Tamp 4		7	99%				1%		X		4				X								78%			
15.Apr	600	Tamp 4		6	100%							X	190		X	X												71%
16.Apr	600	Tamp 4		10	100%							X	180		X	X	X	X	X		182.2	18.0	0.0	9.6	75%	33%	60%	70%
27.Apr	900	Tamp 4		5	100%							X	180		X	X												49%
28.Apr	900	Tamp 4		10	100%							X	180		X	X	X	X	X		177.9	18.1	0.0	6.6	51%	41%	36%	48%
29.Apr	600	Tamp 4		8	96%		5%					X	180		X		X	X	X		177.3	18.4	0.0	9.9	77%	26%	61%	71%
5.May	900	Tamp 4		8	96%		5%					X	180		X		X	X	X		179.8	18.1	0.0	7.3	53%	41%	22%	53%
6.May	900	Tamp 4		6	96%	4%						X	180		X		X	X	X		179.7	17.4	0.0	6.5	49%	27%	41%	49%
7.May	600	Tamp 4		6	96%	4%						X	180		X						179.7	18.6	0.0	9.9	69%	33%	59%	69%
8.May	600	Tamp 4		8	99%				1%			X	130		X	X	X	X	X		144.3	17.9	0.0	9.8	71%	34%	61%	71%

File: Table IV.A.1.2

Printed: 10/3/95 at 10:28 PM

Date	T	BL name	Dry solids	Conditions: nbr of drps	Gases: N2	CO	CO2	H2O	O2	Experimental: Reactor Vid eo	Reactor Sulf ur	Rxn time Pyro lysis	Rxn time Char burn	Analysis: gas S	gas C	char Na	char S	char C	STD pyr.	Rxn time	Masses ini.	Masses aft.pyr	Masses char	Results: Content in char % of ini species Na	S	C	Char
-	C	-	%	pcs	%	%	%	%	%	-	-	sec	sec						-	s	mg	mg	mg	%	%	%	%
11.May	900	Tamp 4		10	99%				1%		X	130		X	X	X	X	X		130.7	17.8	0.0	5.0	62%	30%	12%	37%
12.May	800	Tamp 4		8	96%				4%		X	10	200	X	X	X	X	X		#DIV/0!	17.7	0.0	7.0	87%	42%	16%	52%
13.May	800	Tamp 4		4	93%				7%		X	10	200	X	X												
13.May	800	Tamp 4		4	93%				7%		X	20	200	X	X												
14.May	800	Tamp 4		7	88%		12%				X	10	200	X		X											
15.May	950				100%																						
20.May	750	Tamp 4		5	88%		12%				X	15	200	X		X	X	X		#DIV/0!	17.9	0.0	9.0	78%	36%	47%	66%
20.May	950	Tamp 4		3	88%		12%				X	15	200	X													
21.May	650	Tamp 4		8	88%		12%				X	15	200	X		X	X	X		201.6	17.5	0.0	9.8	82%	43%	63%	74%
25.May	650	Tamp 4		8	93%				7%		X	15	200	X	X	X	X	X		#DIV/0!	18.3	0.0	9.0	81%	41%	45%	65%
26.May	950	Tamp 4		8	93%				7%		X	15	200	X	X												
2.Jun	950	Tamp 4		8	88%		12%				X	15	200	X													
3.Jun	900	Tamp 4		6	67%			33%		X		2															
3.Jun	900	Tamp 4		6	67%			33%		X		5				X	X	X		5.0	17.8	0.0	7.9	83%	58%	35%	58%
4.Jun	900	Tamp 4		6	67%			33%		X		8				X	X	X		8.0	17.8	0.0	6.8	75%	49%	16%	51%
5.Jun	700	Tamp 4		6	67%			33%		X		2															
5.Jun	700	Tamp 4		6	67%			33%		X		5				X	X	X		5.0	16.9	0.0	10.2	85%	58%	69%	79%
8.Jun	700	Tamp 4		6	67%			33%		X		8				X	X	X		8.0	18.4	0.0	9.3	76%	49%	49%	66%
9.Jun	800	Tamp 4		5	100%						X	15		X	X	X	X	X		15.0	18.4	0.0	10.4	81%	44%	62%	74%
9.Jun	800	Tamp 4		5	100%						X	15		X	X	X	X	X		15.0	17.2	0.0	9.9	83%	45%	64%	76%
12.Jun	900	Tamp 4		10	86%		14%				X	15		X		X	X	X		15.0	17.7	0.0	9.8	85%	48%	54%	73%
6.Jul	700	Tamp 4		8	80%			20%		X		4															
6.Jul	700	Tamp 4		8	80%			20%		X		8															
7.Jul	700	Tamp 4		8	80%			20%		X		12															55%
8.Jul	900	Tamp 4		8	80%			20%		X		4															
9.Jul	900	Tamp 4		8	80%			20%		X		8				X	X	X		12.0	18.5	0.0	6.4	72%	50%	20%	50%
9.Jul	900	Tamp 4		8	80%			20%		X		12				X	X	X		8.0	17.7	0.0	6.7	70%	49%	10%	43%
20.Jul	900	Tamp 4		8	89%				11%		X	180		X	X	X	X	X									
21.Jul	900	Tamp 4		8	81%		19%				X	180		X													
22.Jul	800	Sunila		8	100%						X	180		X	X	X	X	X		184.4	17.9	0.0	7.7	71%	41%	50%	67%
23.Jul	800	Kaukas		8	100%						X	180		X	X	X	X	X		186.0	18.1	0.0	8.2	77%	33%	55%	66%
25.Aug	800	Sunila		8	96%				4%		X	20	200	X	X	X	X	X		208.3	16.6	0.0	5.4	88%	55%	13%	50%
27.Aug	800	Kaukas		8	96%				4%		X	20	200	X	X	X	X	X		204.9	17.6	0.0	5.7	88%	36%	12%	47%
28.Aug	900	Tamp 4		8	99%				1%		X	20	130	X	X												
16.Sep	900	Tamp 4		8	88%		12%				X	15	130	X													
17.Sep	900	Tamp 4		8	88%		12%				X	15	30	X													
18.Sep	900	Tamp 4		8	88%		12%				X	8		X													
18.Sep	900	Tamp 4		8	88%		12%				X	16		X													
21.Sep	900	Tamp 4		8	100%						X	15		X	X	X	X	X		18.4	17.7	0.0	10.3	87%	61%	57%	71%
21.Sep	900	Tamp 4		5	100%						X	180		X	X												
22.Sep	900	Tamp 4		8	95%		5%				X	15		X		X	X	X		15.4	18.5	0.0	10.6	85%	61%	53%	69%
23.Sep	900	Tamp 4		8	95%		5%				X	15	100	X		X	X	X									
24.Sep	900	Tamp 4		8	95%		5%				X	15	20	X		X	X	X		20.1	17.7	0.0	9.2	76%	42%	46%	63%
24.Sep	900	Tamp 4		4	95%		5%				X	15	100	X		X	X	X		100.0	18.5	0.0	6.7	72%	39%	16%	44%
25.Sep	700	Tamp 4		8	93%				7%		X	15	20	X	X	X	X	X		20.0	18.0	10.5	8.2	83%	44%	24%	55%
28.Sep	800	Tamp 4		8	93%				7%		X	15	20	X	X	X	X	X		20.0	17.7	10.6	4.3	55%	27%	9%	30%
29.Sep	900	Tamp 4		8	93%				7%		X	15	20	X	X	X	X	X		20.0	17.3	9.4	2.1	27%	13%	4%	15%
30.Sep	900	Tamp 4		8	96%				4%		X	15	20	X	X	X	X	X		20.0	18.1	10.4	1.6	20%	10%	3%	11%

File: Table IV.A.1.2

Printed: 10/3/96 at 10:28 PM

	Conditions									Experimental				Analysis						Results							
					Gases					Reactor		Rxn time		gas		char							Content in char % of ini species			
Date	T	BL name	Dry solids	nbr of drps	N2	CO	CO2	H2O	O2	Vid eo	Sulf ur	Pyro lysis	Char burn	S	C	Na	S	C	STD pyr.	Rxn time	Masses ini.	aft.pyr	char	Na	S	C	Char
-	C	-	%	pcs	%	%	%	%	%	-	-	sec	sec						-	s	mg	mg	mg	%	%	%	%
1.Oct	800	Tamp 4		8	99%				1%		X	130		X	X	X	X	X		130.0	18.1	0.0	7.9	81%	47%	24%	53%
2.Oct	700	Tamp 4		8	99%				1%		X	130		X	X	X	X	X		130.0	17.7	0.0	9.5	88%	46%	56%	65%
6.Oct	900	Tamp 4			99%		2%				X	180		X		X	X	X									
7.Oct	900	Tamp 4			99%		2%				X	100		X		X	X	X		100.0	17.6	0.0	7.1	79%	51%	23%	49%
8.Oct	600	Tamp 4			99%		2%				X	100		X		X	X	X		100.0	17.4	0.0	9.8	88%	37%	65%	69%
8.Oct	800	Tamp 4			99%		2%				X	100		X		X	X	X		100.1	18.3	0.0	9.2	78%	33%	57%	61%
19.Oct	700	Tamp 4			100%						X	15		X	X	X	X	X		15.1	18.2	0.0	10.2	87%	43%	62%	68%
20.Oct	700	Tamp 4			100%						X	180		X	X												
21.Oct	700	Tamp 4			100%						X	180		X	X	X	X	X		180.1	17.9	0.0	9.9	86%	44%	61%	67%
22.Oct	900	Tamp 4			95%	5%					X	15		X		X	X	X		15.0	18.0	0.0	10.5	94%	67%	59%	71%
23.Oct	900	Tamp 4			88%	12%					X	180		X		X	X	X		180.0	18.2	0.0	6.6	55%	60%	33%	44%
26.Oct	900	Tamp 4			88%	12%					X	15	20	X		X	X	X		20.0	17.8	10.0	9.0	81%	45%	49%	62%
27.Oct	900	Tamp 4			95%	5%				X		15				X	X	X		15.0	18.2	0.0	7.9	88%	65%	24%	53%
28.Oct	900	Tamp 4			95%		5%			X		15		X		X	X	X		15.0	18.7	0.0	6.5	90%	61%	12%	42%
30.Oct	900	Tamp 4			70%	10%	10%	10%		X		15		X	X	X	X	X		15.0	17.8	0.0	6.0	78%	46%	13%	41%
2.Nov	800	Tamp 4			88%	12%					X	15	20	X		X	X	X		20.0	18.3	10.6	10.2	96%	43%	59%	68%
3.Nov	900	Tamp 4			88%	12%					X	15	100	X		X	X	X		100.0	18.1	10.5	7.9	62%	41%	42%	53%
5.Nov	900	Tamp 4			89%	1%	10%				X	15		X	X	X	X	X		15.0	17.8	0.0	9.9	87%	49%	50%	67%
6.Nov	900	Tamp 4			85%	4%	11%				X	15		X	X	X	X	X		15.0	17.8	0.0	9.9	88%	49%	49%	67%
7.Nov	900	Tamp 4			100%		1%				X	15		X		X	X	X		15.0	17.7	0.0	9.9	89%	49%	50%	68%
10.Nov	900	Tamp 4			100%		1%				X	100		X		X	X	X		100.0	18.3	0.0	7.5	70%	51%	37%	50%
13.Nov	900	Tamp 4			85%			15%			X	15		X	X	X	X	X		15.0	18.1	0.0	8.4	81%	47%	28%	56%
14.Nov	800	Tamp 4			85%			15%			X	15		X	X	X	X	X		15.0	17.9	0.0	10.0	88%	41%	56%	68%
17.Nov	800	Tamp 4			85%			15%			X	100		X	X	X	X	X		100.0	17.9	0.0	4.1				
18.Nov	700	Tamp 4			85%			15%			X	100		X	X	X	X	X		100.0	17.9	0.0	9.2	83%	35%	47%	62%
18.Nov	800	Tamp 4			85%			15%			X	15	100	X	X	X	X	X		100.0	18.2	10.8	6.3	106%	32%	12%	42%
23.Nov	800	Tamp 4			85%			15%			X	15	15	X	X	X	X	X		15.0	18.1	10.4	10.0	91%	46%	54%	67%
23.Nov	900	Tamp 4			85%			15%			X	100		X	X												
25.Nov	900	Tamp 4			85%			15%			X	15	15	X	X	X	X	X		15	18.19	10.54	8.763	77%	42%	34%	58%
26.Nov	900	Tamp 4			85%			15%			X	15	100	X	X												
27.Nov	700	Tamp 4			85%			15%			X	15	100	X	X	X	X	X		100.0	18.0	10.5	9.7	87%	37%	45%	65%
30.Nov	900	Tamp 4			95%			5%			X	15		X	X	X	X	X		15.0	17.9	0.0	9.9	89%	59%	50%	68%
2.Dec	900	Tamp 4			85%		10%	5%			X	15	20	X	X	X	X	X		20.0	18.2	10.7	9.5	86%	39%	42%	63%
3.Dec	900	Tamp 4			85%		10%	5%			X	15		X	X	X	X	X		15.0	18.4	0.0	10.2	88%	47%	48%	68%
4.Dec	900	Tamp 4			75%		10%	15%			X	15		X	X	X	X	X		15.0	17.9	0.0	9.3	89%	45%	39%	63%
5.Dec	800	Tamp 5A			100%						X	15		X	X	X	X	X		15.0	17.8	0.0	9.7	89%	45%	67%	73%
6.Dec	800	Tamp 5B			100%						X	15		X	X	X	X	X		15.0	17.8	0.0	10.5	87%	62%	66%	75%
8.Dec	800	Tamp 5A			100%						X	15		X	X	X	X	X		15.0	17.4	0.0	9.4	88%	41%	67%	73%
9.Dec	800	Tamp 5B			100%						X	15		X	X	X	X	X		15.0	18.2	0.0	10.7	87%	61%	64%	75%
10.Dec	900	Tamp 4			99%			1%			X	15		X	X	X	X	X		15.0	18.7	0.0	10.1	85%	58%	45%	65%
11.Dec	900	Tamp 4			70%	10%	10%	10%			X	15		X	X	X	X	X		15.0	18.0	0.0	8.7	85%	29%	35%	58%
15.Dec	900	Tamp 4			80%	10%	5%	5%			X	15		X	X	X	X	X		15.0	18.4	0.0	9.2	82%	24%	38%	61%
16.Dec	900	Tamp 4			80%	5%	10%	5%			X	15		X	X	X	X	X		15.0	18.1	0.0	9.3				63%
17.Dec	900	Tamp 4			80%	5%	5%	10%			X	15		X	X	X	X	X		15.0	18.0	0.0	9.0	83%	25%	39%	61%

Appendix 2. Calculation Program for Gas Temperature in the Åbo Akademi University Single Droplet/Flow Reactor

```
C       doetemp.for
C**********************************************************************
C   Temperature profile for AAU reactor (11/29/93 KW)
C   Modifications for Nitrogen
C   Last modified: 3/8/95
C**********************************************************************
C   Program for numerical integration of a differential heat transfer
C   equation by the Runge-Kutta method.
C**********************************************************************
C
C   Parameter:
C   pi = 3.1415927
C
C   Integer variables:
C   flag = Nusselt equation indicator, -
C
C   Real variables (double precision)
C   answer = temperature at 20cm from inlet, K
C   v = volume flow at inlet of reactor, l/h
C   ro = gas density, kg/m3
C   m = mass flow through furnace, kg/hr
C   T1 = temperature of inlet stream, K
C   Told,Tnew = loop variable for temperature during integration, K
C   Ts = temperature of furnace, K
C   Tf = wall film temperature, K
C   L = length of furnace, m
C   Lold,Lnew = loop variable for length during integration, m
C   D = diameter of tube, m
C   cp = heat capacity of gas, J/(kg K)
C   u = viscosity of gas, kg/(m s)
C   uwall = viscosity of gas at wall temperature, kg/(m s)
C   k = thermal conductivity of gas, J/(m hr K)
C   h = local heat transfer coefficient, J/(m2 hr K)
C   step = step size of integration, -
C   K1,K2,K3,K4 = Runge-Kutta variables during integration, -
C
        integer flag
        double precision pi,m,T1,Ts,L,D,Told,Lold,ro,v,answer
        parameter(pi=3.1415927)
        common m,D,L,T1,Ts,flag
        open(1,file='doetemp.dat',status='unknown')
        WRITE(*,*) 'UNIFORM WALL TEMPERATURE SOLUTION'
        write(*,*)
        write(*,*)
     &  'Nu number for intermediate ducts with laminar flow'
        write(*,*) 'Give volume flow of inlet stream in l/h'
        read(*,*) v
        write(*,*) 'Give inlet density of gas in kg/m3'
        read(*,*) ro
        m=ro*v/1000.0/3600.0
        write(*,*) 'Mass flow at inlet',m,' kg/s'
        write(*,*) 'Give inlet temp of cold stream in K'
        read(*,*) T1
        write(*,*) 'Give inlet temp of hot stream in K'
        read(*,*) Ts
C       Length of drop tube reactor
        L=0.45
C       Diameter of drop tube reactor
        D=0.02
        call RUNGE(Told,Lold,answer)
        write(*,88) 'R-K   method gives T at 20cm of tube =',
     +  answer-273,' C'
        write(*,88) 'Reactor temperature =',Ts-273,' C'
88      format(A40,F10.1,A4)
```

```
      END
C
C     This subroutine integrates the differential heat balance
C     equation using the fourth order Runge-Kutta method.
C
      SUBROUTINE RUNGE(Told,Lold,answer)
      integer flag
      double precision cp,u,uwall,k,h,step,pi,m,D,T1,Ts,Told,Tnew
      double precision K1,K2,K3,K4,Re,Pr,L,Lnew,Lold,test,answer,Nu
      parameter(pi=3.1415927,step=0.01)
      common m,D,L,T1,Ts,flag
      Lold=0.01
      Told=T1
      write(*,98) 'L','T/C','RePrDL+','RePrDL','Re','T/Ts','u/uwall'
      write(1,98) 'L','T/C','RePrDL+','RePrDL','Re','T/Ts','u/uwall'
C
C*******Beginning of loop**********************************
200   continue
      call EVAL(Ts,Told,cp,u,uwall,k)
      Re=4*m/pi/D/u
      Pr=u*cp/k
C     Local Nusselt number for intermediate ducts with laminar flow
      Nu=1.86*(Re*Pr*D/L)**0.33*(u/uwall)**0.14
     +  *(Told/Ts)**0.25
      h=k/D*Nu
c      write(*,*) 'h(rk) ',h
      K1=pi*D*h*(Ts-Told)/(m*cp)
      K2=pi*D*h*(Ts-Told+.5*step*K1)/(m*cp)
      K3=pi*D*h*(Ts-Told+.5*step*K2)/(m*cp)
      K4=pi*D*h*(Ts-Told+step*K3)/(m*cp)
      Tnew=Told+step/6.*(K1+2.*K2+2.*K3+K4)
      Lnew=Lold+step
      if (Lnew.gt.0.19.and.Lnew.lt.0.21) then
       answer=Tnew
      endif
      if (Lnew.lt.L) then
       Told=Tnew
       Lold=Lnew
     write(*,99) Lold,Told-273.15,(Re*Pr*D/L)**0.33*(u/uwall)**0.14,
    + Re*Pr*D/L,Re,Told/Ts,u/uwall
     write(1,99) Lold,Told-273.15,(Re*Pr*D/L)**0.33*(u/uwall)**0.14,
    + Re*Pr*D/L,Re,Told/Ts,u/uwall
c       write(2,*) Lold,',',Told,','
       goto 200
C*******End of loop************************************************
      else
       return
      endif
98    format(A6,7A10)
99    format(F6.2,7F10.4)
      END

C
C     This subroutine evaluates thermal conductivity, heat capacity,
C     and viscosity.
C
      subroutine EVAL(Ts,Told,cp,u,uwall,k)
      double precision Ts,Told,cp,u,uwall,k,Tf
C     Data for N2 units k(W/mK) cp(kJ/kgK) u(Pa s)
      k=(33.7175*log(Told)-169.9859)*1e-3
      cp=(-2.7762e-10*Told**3+6.8451e-7*Told**2-3.1917e-4*Told+
     +  1.0799)*1000.0
      u=(19.93717*log(Told)-95.45063)*1.e-6
      uwall=(19.93717*log(Ts)-95.45063)*1.e-6
```

```
return
END
```

Appendix 3. Calculation Program for Particle Temperature in the Åbo Akademi University Single Droplet/Flow Reactor

St	Input----	Name---	Output---	Unit-----	Comment----------
					Program for calculating the particle temperature in the AAU convective-flow reactor Gas properties for 100% N2 Last modified: 3/8/95 KW
		dT	49.78	K	Temp diff between furnace and particle
	473	Tini		K	Initial gas temp
	973	Tfur		K	Furnace wall temp
	832.45	Tgas		K	Gas temp (317l/h 200C inlet) 900C: 709.1C 982.25K 800C: 633.9C 907.05K 700C: 559.3C 832.45K
		Tp	923.2	K	GUESS PARTICLE TEMPERATURE
		Tf	877.8	K	Particle film temp (for SC and DiffCO2
	.00001	po2		bar	O2 partial pressure
	.1	pco2		bar	CO2 partial pressure
	0	pco		bar	CO partial pressure
	.05	ph2o		bar	H2O partial pressure
	0	ph2		bar	H2 partial pressure
	.00029774	Carb		mol/part	C initially in particle for 18mg drop 900C: 0.15735 mmol C 800C: 0.174556 mmol C 700C: 0.1914 mmol C
	1.392801	Aint		m2	Internal surface area for 18mg drop 900C: 0.7364 m2 800C: 0.8169 m2 700C: 0.89577 m2
		rO2	3.614E-10	mol/s	O2 kinetic rate
		rCO2	1.3425E-7	mol/s	CO2 kinetic rate
		rH2O	9.5646E-7	mol/s	H2O kinetic rate
		Rreduc	9.4743E-7	mol/s	C converted by sulfate reduction
	.18	SO4			SO4/Na2 mole ratio
	3.1415927	pi			Archimedes' constant
	10	Mult			Rate multiplier
		dHrtot	674.98547	J/mol	Total heat of reaction
		dHrO2	-176.1085	J/mol	O2 heat of reaction
		dHrCO2	-13.09559	J/mol	CO2 heat of reaction
		dHrH2O	-154.1331	J/mol	H2O heat of reaction
		dHrRed	1018.3227	J/mol	Sulfate reduction heat of reaction
		HfO2	196.46919	J/mol	O2 heat of formation
		HfCO	81.673349	J/mol	CO heat of formation
		HfCO2	16.89506	J/mol	CO2 heat of formation
		HfC	159.54723	J/mol	C heat of formation
		HfH2	156.10225	J/mol	H2 heat of formation
		HfH2O	232.36149	J/mol	H2O heat of formation
		HfNa2S	84.908382	J/mol	Na2S heat of formation
		HfNa2SO	-1244.91	J/mol	Na2SO4 heat of formation
		Qg	.00135276	W	Heat generation by reaction
		Qc	2.9937058	W	Heat transfer by convection
		Qr	2.9950585	W	Heat transfer by radiation
		wini	.28028777	m/s	Flow speed at inlet of reactor
		w	.47792676	m/s	Flow speed at particle
		nyini	3.4551E-5	m2/s	Viscosity at inlet of reactor
		ny	8.8078E-5	m2/s	Viscosity of gas in bulk
		nys	9.5866E-5	m2/s	Viscosity of gas in film
		nyratio	.91876035		Viscosity ratio
	8.8055E-5	Vini		m3/s	Volume flow at inlet of reactor

				200:25->200C: 5.55e-5 -> 8.8055e-5m3/s
				400:25->200C: 1.11e-4 ->
	V	.00015015	m3/s	Volume flow at particle
	mini	6.3521E-5	kg/s	Gas mass flow
	kgO2	.10293633	m/s	O2 mass transfer coefficient
	kgCO2	.08510711	m/s	CO2 mass transfer coefficient
	kgH2O	.13916395	m/s	H2O mass transfer coefficient
	nygas		m2/s	Kinetic viscosity of gas
	O2byMT	4.6872E-9	mol/s	O2 mass transfer rate
	CO2byMT	3.8753E-5	mol/s	CO2 mass transfer rate
	H2ObyMT	3.1684E-5	mol/s	H2O mass transfer rate
	CO2	.00014639	mol/m3	O2 concentration
	CCO2	1.4638964	mol/m3	CO2 concentration
	CH2O	.73194818	mol/m3	H2O concentration
.02	D		m	Tube diameter
.761	S0			Solids content
.000028	m		kg	Initial droplet mass
	dens	1490.889	kg/m3	
	Dp	.00995041	m	Swollen particle diameter
	Vp	5.1585E-7	m3	Particle volume
	Aext	.00031105	m2	Particle external surface area
	L	.0016584	m	Characteristic length
	h	106.02814	W/m2/K	Convective heat transfer coefficient
.5	f			Fraction of saturated smelt
.5	Pore			Porosity (0.5 or 0.95(Wu))
.000015	Prsz		m	Pore diameter (0.000015 or 600e-10Wu)
5.6703E-8	SB		W/m2/K4	Stefan-Boltzmann constant
	k	.15566929	W/m/K	Local apparent thermal conductivity
	Nu	6.7773396		Nusselt number
.73	Pr			Prandtl number
	Reini	162.24728		Reynolds number at inlet
	Re	108.52324		Reynolds number at particle
	ScO2	.6337339		O2 Schmidt number
	ScCO2	.81539203		CO2 Schmidt number
	ScH2O	.42657943		H2O Schmidt number
	ROO2	4.6872E-9	mol/s	C depletion by O2 gasification
	ROCO2	1.3358E-7	mol/s	C depletion by CO2 gasification
	ROH2O	9.1843E-7	mol/s	C depletion by H2O gasification
	DiffO2	1.3898E-4	m2/s	O2 diffusivity
	DkO2	3.9076E-5	m2/s	Knudsen diffusivity of O2
	DeffO2	7.6252E-6	m2/s	Effective diffusivity of O2
	DiffCO2	1.0802E-4	m2/s	CO2 diffusivity
	DkCO2	3.3324E-5	m2/s	Knudsen diffusivity of CO2
	DeffCO2	6.3669E-6	m2/s	Effective diffusivity of CO2
	DiffH2O	2.0648E-4	m2/s	H2O diffusivity
	DkH2O	5.2101E-5	m2/s	Knudsen duffusivity of H2O
	DeffH2O	1.0401E-5	m2/s	Effective diffusivity of H2O
	THO2	.3077		O2 Thiele modulus
	THCO2	.06728		CO2 Thiele modulus
	THH2O	.1837		H2O Thiele modulus
	EFFO2	.9696		O2 effectiveness factor
	EFFCO2	.9985		CO2 effectiveness factor
	EFFH2O	.9889		H2O effectiveness factor

BiO2	22.39	O2 Biot number (mass transfer)
BiCO2	22.17	CO2 Biot number (mass transfer)
BiH2O	22.19	H2O Biot number (mass transfer)

```
================== RULE SHEET ================================================
! Rule-------------------------------------------------------------------------
  dT=Tfur-Tp
  L=Dp/6
  dens=(0.997+.649*S0)*1000
! m=dens*pi/6*(Dp/3)^3
  Dp=(m/dens/pi*6)^0.333*3
  Vp=3.1415927*Dp^3/6
  Aext=3.1415927*Dp^2
  Nu=2+0.6*Re^0.5*Pr^0.333 "Falling drop
  Nu=2+(0.4*Re^0.5+0.06*Re^0.667)*Pr^0.4*nyratio^0.25 "Whitaker equation
  k=(1-f)*(0.05+4*Pore*Prsz*SB*Tp^3)+0.26*f "Merriam equation
  h=Nu*k/Dp
  rO2=9.5e6*Aint*po2*Carb*exp(-33950/1.987/Tp)
  rCO2=63.0e9*pco2/(pco2+3.4*pco)*Carb*exp(-30070/Tp)
  rH2O=2.56e9*ph2o/(ph2o+1.42*ph2)*Carb*exp(-25300/Tp)
  Rreduc=Mult*2620*SO4/(0.0011+SO4)*Carb*exp(-29200/1.987/Tp)
  Qg=(RO2+ROCO2+ROH2O+Rreduc)*dHrtot
  Qc=h*Aext*(Tp-Tgas)
  Qr=Aext*SB*(Tfur^4-Tp^4)
  Qr=Qg+Qc
  dHrtot=dHrO2+dHrCO2+dHrH2O+dHrRed
  dHrO2=HfCO-HfC-HfO2/2
  dHrCO2=2*HfCO-HfCO2-HfC
  dHrH2O=HfCO+HfH2-HfC-HfH2O
  dHrRed=HfNa2S+4*HfCO-HfNa2SO4-4*HfC
  HfO2=(-9679.104+29.95744*Tp+.2092*Tp^2+167360/Tp)/1000
  HfH2O=(-251770.9+29.99928*Tp+0.535552*Tp^2-33472/Tp)/1000
  HfH2=(-8110.091+27.27968*Tp+0.163176*Tp^2-50208/Tp)/1000
  HfCO=(-119348.1+28.40936*Tp+0.205016*Tp^2+46024/Tp)/1000
  HfCO2=(-409930.4+44.1412*Tp+0.451872*Tp^2+853536/Tp)/1000
  HfC=(-2106.402+0.108784*Tp+0.1947024*Tp^2-0.579484e-5*Tp^3+148113.6/Tp)/1000
  HfNa2S=(-397616.4+90.02294*Tp+0.468608*Tp^2)/1000
  HfNa2SO4=(-1427155+197.4011*Tp)/1000
  Re=w*D/ny
  Reini=wini*D/nyini
  w=V/(3.1415927*D^2/4)
  wini=Vini/(3.1415927*D^2/4)
  mini=Vini*28/(82.06e-6*Tini)/1000
  V=mini*82.06e-6*Tgas/28.9*1000
  nyini=5.6026e-11*Tini*Tini+7.5776e-8*Tini-1.3826e-5
  ny=5.6026e-11*Tgas*Tgas+7.5776e-8*Tgas-1.3826e-5
  nys=5.6026e-11*Tf*Tf+7.5776e-8*Tf-1.3826e-5
  nyratio=ny/nys
  nygas=-8.7664e-5+2.0989e-7*Tf
  Tf=Tgas+abs(Tp-Tgas)/2
  DiffO2=0.000018*(Tf/273)^1.75
  DiffCO2=DiffO2*1.378/1.773
  DiffH2O=DiffO2*2.634/1.773
  kgO2=DiffO2/Dp*(2+0.6*Re^0.5*ScO2^0.333) "Re < 325
  kgCO2=DiffCO2/Dp*(2+0.6*Re^0.5*ScCO2^0.333)
  kgH2O=DiffH2O/Dp*(2+0.6*Re^0.5*ScH2O^0.333)
  ScO2=ny/DiffO2
  ScCO2=ny/DiffCO2
  ScH2O=ny/DiffH2O
  CO2=po2/82.06e-6/Tgas
  CCO2=pco2/82.06e-6/Tgas
  CH2O=ph2o/82.06e-6/Tgas
  O2byMT=kgO2*pi*Dp^2*CO2
  CO2byMT=kgCO2*pi*Dp^2*CCO2
```

```
* H2ObyMT=kgH2O*pi*Dp^2*CH2O
* THO2=Dp/6*sqrt(abs(rO2)/Vp/DiffO2/CO2)
* THCO2=Dp/6*sqrt(abs(rCO2)/Vp/DiffCO2/CCO2)
* THH2O=Dp/6*sqrt(abs(rH2O)/Vp/DiffH2O/CH2O)
* EFFO2=tanh(THO2)/THO2
* EFFCO2=tanh(THCO2)/THCO2
* EFFH2O=tanh(THH2O)/THH2O
C 1/ROO2=1/O2byMT+1/(EFFO2*abs(rO2))
* ROO2=O2byMT
* 1/ROCO2=1/CO2byMT+1/(EFFCO2*abs(rCO2))
* 1/ROH2O=1/H2ObyMT+1/(EFFH2O*abs(rH2O))
* BiO2=kgO2*L/DeffO2
* BiCO2=kgCO2*L/DeffCO2
* BiH2O=kgH2O*L/DeffH2O
* DeffO2=Pore^2*1/(1/DiffO2+1/DkO2)
* DeffCO2=Pore^2*1/(1/DiffCO2+1/DkCO2)
* DeffH2O=Pore^2*1/(1/DiffH2O+1/DkH2O)
* DkO2=9700*Prsz/2*sqrt(Tp/32)/10000 "cm2/s /10000 => m2/s
* DkCO2=9700*Prsz/2*sqrt(Tp/44)/10000 "cm2/s /10000 => m2/s
* DkH2O=9700*Prsz/2*sqrt(Tp/18)/10000 "cm2/s /10000 => m2/s
```

Appendix 4. Calculation Program for Thermocouple Temperature in the Åbo Akademi University Single Droplet/Flow Reactor

VARIABLE SHEET

St	Input----	Name---	Output---	Unit-----	Comment----------
					Program for calculating the thermo-couple temperature for AAU convective flow reactor Gas assumed 100% N2 Last modified: 2/7/95 KW
		dT	53.765645	K	Temp diff between furnace and TC
		Pr	.75690844		Prandtl number
		Nu	3.7664778		Nusselt number
		Re	16.11382		Reynolds number at particle
	.0027	Dp		m	Thermocouple diameter
		Tp	719.23436	K	Guess TC temperature
	.85	em			Emissivity of thermocouple
	300	Tini		K	Initial gas temp
	773	Tfur		K	Furnace wall temp
	657.85	Tgas		K	Gas temp (calc for 100% N2) Tgas has to be recalc'd for this case becase gas enters at 25C; Tgas lower
		Tf	688.54218	K	Particle film temp (for SC and DiffC(
		Qc	.0987306	W	Heat transfer by convection
		Qr	.0987306	W	Heat transfer by radiation
		w	.38739029	m/s	Flow speed at particle
	.02	D		m	Tube diameter
		ny	.00006491	m2/s	Kin viscosity gas surrounding partic
	.0000555	Vini		m3/s	Volume flow at inlet of reactor 200l/h: 5.55e-5m3/s 317l/h: 8.805e-5
		V	.0001217	m3/s	Volume flow at particle
		mini	6.5379E-5	kg/s	Mass flow at reactor inlet
		Vp	1.0306E-8	m3	Particle volume
		Aext	2.2902E-5	m2	Particle external surface area
		L	.00045	m	Characteristic length
		h	70.229028	W/m2/K	Convective heat transfer coefficient
		k	.05034369	W/m/K	Local apparent thermal conductivity
	5.6703E-8	SB		W/m2/K4	Stefan-Boltzmann constant
		my	3.3921E-5	kg/m/s	Dynamic viscosity at film temp
		myw	.00003483	kg/m/s	Dynamic viscosity at bulk
		cp	1.0940337	kJ/kg/K	Specific heat capacity of gas

```
================== RULE SHEET ==============================================
 Rule-------------------------------------------------------------------------
 dT=Tfur-Tp
 L=Dp/6
 Vp=3.1415927*Dp^3/6
 Aext=3.1415927*Dp^2
 Nu=2+0.6*Re^0.5*Pr^0.333 "21.7 Nu=5.0 (Ranz&Marshall 1952 in Scott Fogler 10-
 Nu=0.37*Re^0.6 "12.8 Nu=2.8 (Kreith 7.7)
 Nu=2+(0.4*Re^0.5+0.06*Re^0.666)*Pr^0.4*(my/myw)^0.25 "19.7 Nu=4.5 (Kreith 7.9
 Nu=0.51*Re^0.5*Pr^0.36 "11.7 Nu=2.6 (Zukauskas 7.3)
 Pr=cp*myw/k*1000
 k=-1.25e-6*Tp^2+2.425e-2*Tp+48.8 "Conductivity of Ni(s)
 k=(33.7175*ln(Tf)-169.9859)/1000 "Conductivity of N2(g)
 h=Nu*k/Dp
 Qc=h*Aext*(Tp-Tgas)
 Qr=em*Aext*SB*(Tfur^4-Tp^4)
 Qc=Qr
 Re=w*Dp/ny
 w=V/(3.1415927*D^2/4)
 mini=Vini*29/(82.06e-6*Tini)/1000
 V=mini*82.06e-6*Tgas/29*1000
 ny=5.6026e-11*Tf*Tf+7.5776e-8*Tf-1.3826e-5 "kinematic viscosity (m2/s)
 Tf=Tgas+abs(Tp-Tgas)/2
 my=(19.93717*ln(Tgas)-95.45063)*1e-6
 myw=(19.93717*ln(Tf)-95.45063)*1e-6
 cp=-2.7762e-10*Tf^3+6.8451e-7*Tf^2-3.1917e-4*Tf+1.0799
```

REACTOR TEMPERATURE PROFILE PROGRAM

```
C   TREACTOR.FOR
C*****************************************************************
C   Temperature profile for AAU reactor (11/29/93 KW)
C   Modifications for Nitrogen
C   Last modified: 3/8/95
C*****************************************************************
C   Program for numerical integration of a differential heat transfer
C   equation by the Runge-Kutta method.
C*****************************************************************
C
C   Parameter:
C   pi = 3.1415927
C
C   Integer variables:
C   flag = Nusselt equation indicator, -
C
C   Real variables (double precision)
C   answer = temperature at 20cm from inlet, K
C   v = volume flow at inlet of reactor, l/h
C   ro = gas density, kg/m3
C   m = mass flow through furnace, kg/hr
C   T1 = temperature of inlet stream, K
C   Told,Tnew = loop variable for temperature during integration, K
C   Ts = temperature of furnace, K
C   Tf = wall film temperature, K
C   L = length of furnace, m
C   Lold,Lnew = loop variable for length during integration, m
C   D = diameter of tube, m
C   cp = heat capacity of gas, J/(kg K)
C   u = viscosity of gas, kg/(m s)
C   uwall = viscosity of gas at wall temperature, kg/(m s)
C   k = thermal conductivity of gas, J/(m hr K)
C   h = local heat transfer coefficient, J/(m2 hr K)
C   step = step size of integration, -
C   K1,K2,K3,K4 = Runge-Kutta variables during integration, -
C
      integer flag
      double precision pi,m,T1,Ts,L,D,Told,Lold,ro,v,answer
      parameter(pi=3.1415927)
      common m,D,L,T1,Ts,flag
      open(1,file='doetemp.dat',status='unknown')
      WRITE(*,*) 'UNIFORM WALL TEMPERATURE SOLUTION'
      write(*,*)
      write(*,*)
     & 'Nu number for intermediate ducts with laminar flow'
      write(*,*) 'Give volume flow of inlet stream in l/h'
      read(*,*) v
      write(*,*) 'Give inlet density of gas in kg/m3'
      read(*,*) ro
      m=ro*v/1000.0/3600.0
      write(*,*) 'Mass flow at inlet',m,' kg/s'
      write(*,*) 'Give inlet temp of cold stream in K'
      read(*,*) T1
      write(*,*) 'Give inlet temp of hot stream in K'
      read(*,*) Ts
C     Length of drop tube reactor
      L=0.45
C     Diameter of drop tube reactor
      D=0.02
      call RUNGE(Told,Lold,answer)
```

```
      write(*,88) 'R-K   method gives T at 20cm of tube =',
     +  answer-273,' C'
      write(*,88) 'Reactor temperature =',Ts-273,' C'
88    format(A40,F10.1,A4)
      END
C
C     This subroutine integrates the differential heat balance
C     equation using the fourth order Runge-Kutta method.
C
      SUBROUTINE RUNGE(Told,Lold,answer)
      integer flag
      double precision cp,u,uwall,k,h,step,pi,m,D,T1,Ts,Told,Tnew
      double precision K1,K2,K3,K4,Re,Pr,L,Lnew,Lold,test,answer,Nu
      parameter(pi=3.1415927,step=0.01)
      common m,D,L,T1,Ts,flag
      Lold=0.01
      Told=T1
      write(*,98) 'L','T/C','RePrDL+','RePrDL','Re','T/Ts','u/uwall'
      write(1,98) 'L','T/C','RePrDL+','RePrDL','Re','T/Ts','u/uwall'
C
C*******Beginning of loop************************************
200   continue
      call EVAL(Ts,Told,cp,u,uwall,k)
      Re=4*m/pi/D/u
      Pr=u*cp/k
C     Local Nusselt number for intermediate ducts with laminar flow
      Nu=1.86*(Re*Pr*D/L)**0.33*(u/uwall)**0.14
     +  *(Told/Ts)**0.25
      h=k/D*Nu
c      write(*,*) 'h(rk) ',h
      K1=pi*D*h*(Ts-Told)/(m*cp)
      K2=pi*D*h*(Ts-Told+.5*step*K1)/(m*cp)
      K3=pi*D*h*(Ts-Told+.5*step*K2)/(m*cp)
      K4=pi*D*h*(Ts-Told+step*K3)/(m*cp)
      Tnew=Told+step/6.*(K1+2.*K2+2.*K3+K4)
      Lnew=Lold+step
      if (Lnew.gt.0.19.and.Lnew.lt.0.21) then
       answer=Tnew
      endif
      if (Lnew.lt.L) then
       Told=Tnew
       Lold=Lnew
      write(*,99) Lold,Told-273.15,(Re*Pr*D/L)**0.33*(u/uwall)**0.14,
     + Re*Pr*D/L,Re,Told/Ts,u/uwall
      write(1,99) Lold,Told-273.15,(Re*Pr*D/L)**0.33*(u/uwall)**0.14,
     + Re*Pr*D/L,Re,Told/Ts,u/uwall
c       write(2,*) Lold,',',Told,','
       goto 200
C*******End of loop*************************************************
      else
       return
      endif
98    format(A6,7A10)
99    format(F6.2,7F10.4)
      END

C
C     This subroutine evaluates thermal conductivity, heat capacity,
C     and viscosity.
C
```

```
      subroutine EVAL(Ts,Told,cp,u,uwall,k)
      double precision Ts,Told,cp,u,uwall,k,Tf
C     Data for N2 units k(W/mK) cp(kJ/kgK) u(Pa s)
      k=(33.7175*log(Told)-169.9859)*1e-3
      cp=(-2.7762e-10*Told**3+6.8451e-7*Told**2-3.1917e-4*Told+
     + 1.0799)*1000.0
      u=(19.93717*log(Told)-95.45063)*1.e-6
      uwall=(19.93717*log(Ts)-95.45063)*1.e-6
      return
      END
```

Appendix 5. Analysis Procedures for Total Carbon, Total Sulfur, Sodium, and Carbonate, Sulfate, Sulfite, Sulfide, and Thiosulfate Ions in the Åbo Akademi University Experiments

Analyses for carbon, sulfur, carbonate, sulfate, sulfite, sulfide, thiosulfate, and sodium in residues from single droplet experiments at Åbo Akademi University were made at Analytische Laboratorien, Fritz-Pregl-Strasse 24, D-5270 Gummersbach, Germany, Phone: 0 22 63/50 36, Fax: 0 22 63/56 89.

The analytical procedures used were as follows.

- **Carbon:** A Carhomat 12 ADG analyzer, produced by Wosthoff oHG Corporation, Bochum, Germany was used for the carbon analysis. The test samples were burned at 1350°C in an oxygen stream and pumped into the measuring cell. The cell contained a NaOH solution of known electrical conductivity. The CO_2 produced from combustion of carbon in the samples was absorbed, and the change in electrical resistance of the cell contents was used to determine the amount of CO_2 absorbed.

  References:

  Malissa, H., *Mikrochim. Acta* (Wien), 1957, p. 553

  Bartscher, W., Schmidts, W., *Z. Anal. Chem.* 203, 168 (1964).

- **Sulfur:** A Sulmohomat 12 ADG analyzer, produced by Wosthoff oHG Corporation, Bochum, Germany was used for the sulfur analysis. The test samples were burned in a porcelain boat at 1350°C in an oxygen stream with V_2O_5 as an oxidation catalyst. The gases were pumped into the measuring cell which contained a solution of H_2O_2 and dilute sulfuric acid of known electrical conductivity. SO_2 produced from combustion of the samples was absorbed, oxidized to SO_3, and the change in electrical resistance of the cell contents was used to determine the amount of SO_3 absorbed.

- **Carbonate:** CO_2 was evolved by addition of HCl, and the analysis procedure described in the carbon analysis procedure was used to measure the CO_2 produced.

- **Sulfate:** Gravimetric analysis as $BaSO_4$, DIN 38405 - D 5.

- **Sulfite:** Evolution of SO_2, oxidation to SO_3, and analysis as described in the procedure for sulfur analysis.

- **Sulfide:** Evolution of H_2S, absorption, and measurement with an ion specific electrode.

- **Thiosulfate:** iodometric titration, DIN 38405 - D 15.

- **Sodium:** sodium was dissolved with a sulfuric/phosphoric acid mixture and analyzed by flame photometry.

Appendix 6. Estimation of the Apparent Activation Energy for Heat Transfer to Pyrolyzing Black Liquor Droplets

The apparent activation energy for pyrolyzing black liquor droplets was calculated from the average apparent overall heat transfer coefficients versus temperature. The instantaneous apparent overall heat transfer coefficient, $h_{app}(t)$, is defined by the overall heat transfer rate equation

$$q(t) = h_{app}(t)\Delta T(t) \qquad \text{(A.6-1)}$$

where q(t) is the instantaneous rate of heat transfer to the droplet during pyrolysis and $\Delta T(t)$ is the difference in temperature between the surroundings and the droplet. h_{app} includes the contributions of the radiative and convective heat transfer to the droplet surface as well as convective heat transfer within the droplet.

q(t) was calculated using a heat transfer-based pyrolysis model; details of the model and the computer code are presented elsewhere (Frederick et al, 1992). The model requires as input the droplet mass, initial solids content, the average dry solids mass fraction at the onset of devolatilization, the maximum swollen volume during pyrolysis, the relative gas/particle velocity, the gas temperature, and the effective temperature of the radiant environment. The following experimentally based correlations for the average dry solids mass fraction at the onset of devolatilization (S_i) and the maximum swollen volume during pyrolysis (SV_{max}) were used in the calculations:

$$S_i = 2.055 - 0.00236T + 10^{-6}T^2 \qquad \text{(A.6-2)}$$

$$SV_{max} = 255 - 0.175T \qquad \text{(A.6-3)}$$

where SV_{max} has units of cm^3/g dry black liquor solids and T is in °C. Both correlations apply in the range 600-1200°C (Frederick and Hupa, 1993).

The $h_{app}(t)$ values calculated this way varied by less than 32% over the pyrolysis period, so a linear average was used to average apparent overall heat transfer coefficient, h_{app}.

The apparent activation energy for pyrolyzing black liquor droplets was calculated from a plot of the ln (h_{app}) versus the reciprocal of the absolute furnace temperature (Figure A.6-1). The values obtained were 11-12 kJ/mole decreasing slightly with increasing initial droplet mass.

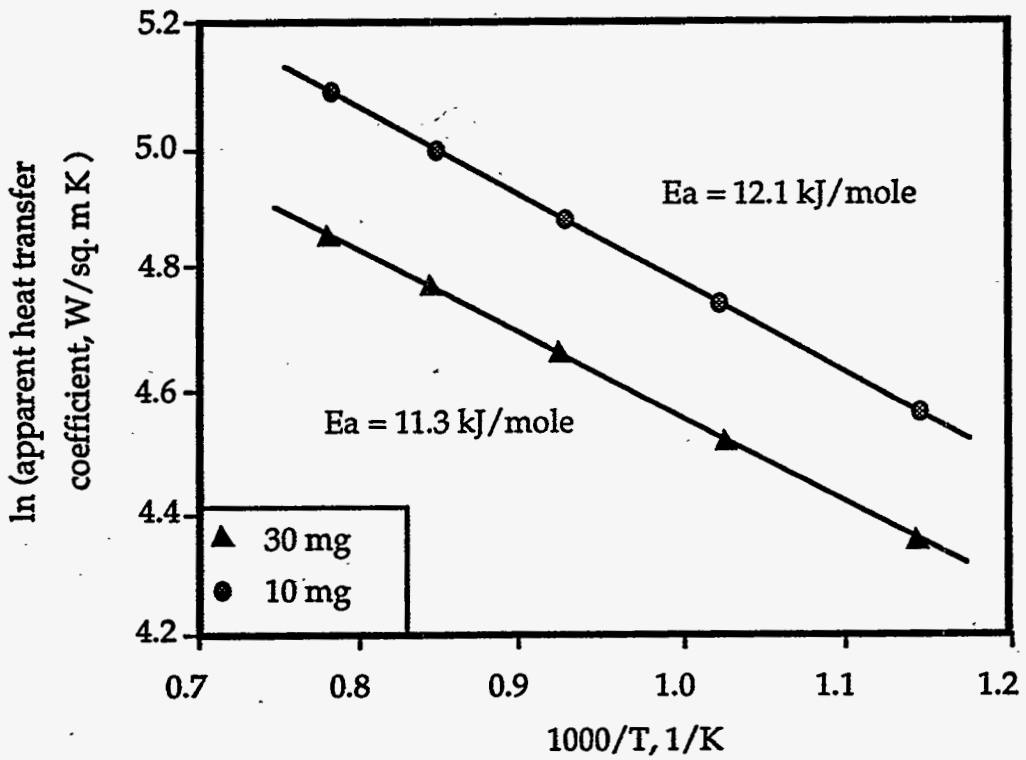

Figure A.6-1. Estimation of the Apparent Activation Energy for Pyrolyzing Black Liquor Droplets.

☆U.S. GOVERNMNET PRINTING OFFICE: 1996 - 750-195/20011